⑫

AFWAL-TR-80-2090
Part III

WATER INGESTION INTO AXIAL FLOW COMPRESSORS

PART III Experimental Results and Discussion

Purdue University
School of Mechanical Engineering
West Lafayette, Indiana 47907

October 1981

TECHNICAL REPORT AFWAL-TR-80-2090, PART III
Final Report for Period 15 December 1977 - 30 June 1981

AD A114830

DTIC
SELECTED
MAY 24 1982
E

82 05 24 026

Project Engineer
LARRY E. CRAWFORD
Compressor Research Group

WALKER H. MITCHELL
Chief, Technology Branch

FOR THE COMMANDER

JAMES M. SHIPMAN, MAJOR, USAF
Deputy Director
Turbine Engine Division
Aero Propulsion Laboratory

SECURITY CLASSIFICATION OF THIS PAGE (When Data Entered)

REPORT DOCUMENTATION PAGE	READ INSTRUCTIONS BEFORE COMPLETING FORM

1. REPORT NUMBER	2. GOVT ACCESSION NO.	3. RECIPIENT'S CATALOG NUMBER
AFAPL-TR-80-2090, Part III	AD-A114 830	

4. TITLE (and Subtitle)	5. TYPE OF REPORT & PERIOD COVERED
WATER INGESTION INTO AXIAL FLOW COMPRESSORS Part III: EXPERIMENTAL RESULTS AND DISCUSSION	Final Report 15 Dec. 1977 - 30 June 1981
	6. PERFORMING ORG. REPORT NUMBER

7. AUTHOR(s)	8. CONTRACT OR GRANT NUMBER(s)
S.N.B. Murthy, T. Tsuchiya, C.M. Ehresman and D. Richards	F33615-78-C-2401

9. PERFORMING ORGANIZATION NAME AND ADDRESS	10. PROGRAM ELEMENT, PROJECT, TASK AREA & WORK UNIT NUMBERS
Purdue University School of Mechanical Engineering West Lafayette, IN 47907	Project No. 3066 Task No. 306604

11. CONTROLLING OFFICE NAME AND ADDRESS	12. REPORT DATE
Air Force AERO PROPULSION LABORATORY, Air Force Wright Aeronautical Laboratories Air Force Systems Command, WPAFB, Ohio 45433	October 1981
	13. NUMBER OF PAGES

14. MONITORING AGENCY NAME & ADDRESS(if different from Controlling Office)	15. SECURITY CLASS. (of this report)
NASA-Lewis Research Center 21000 Brookpark Road Cleveland, Ohio 44135	
	15a. DECLASSIFICATION/DOWNGRADING SCHEDULE Unclassified

16. DISTRIBUTION STATEMENT (of this Report)

Approved for Public Release; Distribution Unlimited.

17. DISTRIBUTION STATEMENT (of the abstract entered in Block 20, if different from Report)

18. SUPPLEMENTARY NOTES

19. KEY WORDS (Continue on reverse side if necessary and identify by block number)

Water Ingestion	Gas Turbine Performance
Axial-Flow Compressors	Gas Turbine Control
Distortion	Two-Phase Flow
Water Vapor Effects	Droplet-Laden Gas Flow
Turbo-Machinery	

20. ABSTRACT (Continue on reverse side if necessary and identify by block number)

The subject of air-water mixture flow in axial compressors of jet engines is of practical interest in two contexts of water ingestion: during take-off from rough runways with puddles of water and during flight through rain storms. The change in the compressor performance in turn produces changes in the performance of other components and of the engine as a whole. During the current investigation, (i) an analysis of the effects of water ingestion into a compressor has been carried out leading to the development of a predictive ....Continued

DD FORM 1473 EDITION OF 1 NOV 65 IS OBSOLETE
S/N 0102-LF-014-6601

SECURITY CLASSIFICATION OF THIS PAGE (When Data Entered)

20. continued...

code, the PURDU-WICSTK program and (ii) a series of tests have been carried out on a small test compressor with mixtures of gases (containing methane gas to simulate steam) and with air-water droplet mixtures. The experimental results have been compared with predictions. It is concluded that the basic effects of water ingestion into compressors arise through (a) blockage, (b) distortion and (c) heat and mass transfer processes, the changes in blade aerodynamic performance being relatively small. In the case of a compressor of small mass flow and pressure ratio and high operating speed, increased quantities of water ingestion give rise to large quantities of water in the tip region. When the pressure ratio and air mass flow are large and the operating speed is correspondingly small, there arises a possibility of water evaporation, especially towards the hub, which gives rise to changes in gas phase mass flow and temperature. The changes in compressor performance are large at high speeds and high flow rates; there also arises a change in the surge characteristics. In light of the nature of changes produced by water ingestion, a preliminary analysis has been carried out on the possible changes in engine performance.

Accession For		
NTIS GRA&I	☒	
DTIC TAB	☐	
Unannounced	☐	
Justification		
By		
Distribution/		
Availability Codes		
Dist	Avail and/or Special	
A		

DTIC
COPY
INSPECTED
2

FOREWORD

This final report presents the results of research undertaken at Purdue University under Air Force Contract No. F33615-78-C-2401. The effort was sponsored by the Aero Propulsion Laboratory, Air Force Wright Aeronautical Laboratories, Air Force Systems Command, Wright-Patterson Air Force Base, Ohio, under Project 3066, Task 306604 and Work Unit 30660454, with Mr. Larry E. Crawford, AFAPL/TBC, as Project Engineer.

Two earlier publications of direct relevance to the project are as follows:

   i) "Water Ingestion into Axial Flow Compressor," Report No. AFAPL-TR-76-77, August, 1976; and

   ii) "Analysis of Water Ingestion Effects in Axial Flow Compressors," Report No. AFAPL-TR-78-35, June, 1978.

The research reported in the current report pertains to a further development of a prediction code for the performance of an axial compressor with water ingestion, experimental studies on a small engine-driven axial compressor with water ingestion and an analysis of the results.

The final report consists of three parts, Part I entitled Analysis and Predictions, Part II entitled Computational Program and Part III entitled Experimental Results and Discussion. Each part is presented in a separate volume.

Dr. Bruce A. Reese, currently Chief Scientist at the Arnold Engineering Development Center, Arnold Air Force Base, who was Professor and Head, School of Aeronautics and Astronautics, Purdue University, up to June 30, 1979, participated in the conduct of research from January, 1978 until June 30, 1979.

The Drive Engine and the Test Compressor provided by the Air Force for the experimental studies under this project were manufactured by the Detroit Diesel Allison of Indianapolis. They refurbished the units during this program under a subcontract. In that work and in a variety of ways the DDA and several of their personnel have been most helpful in the investigation.

iii

TABLE OF CONTENTS

TABLE OF CONTENTS (continued)

TABLE OF CONTENTS (continued)

LIST OF FIGURES

x

xii

xv

LIST OF TABLES

NOMENCLATURE

Symbol

A	pipe cross-sectional area
C	over pressure ratio
D_o	water droplet nominal diameter
N	rotor speed
$N/\sqrt{\theta}$	corrected rotor speed
$\dot{m}$	mass flow rate
$\dfrac{\dot{m}\sqrt{\theta}}{\delta}$	corrected mass flow rate
P_{01}	stagnation pressure at compressor inlet
P_{01}/P_{02}	stagnation pressure ratio
T_{01}	stagnation temperature at compressor inlet
T_{02}/T_{01}	stagnation temperature ratio
TRRF	temperature rise ratio factor (defined by Eq. 5.1)
U_{tip}	rotor speed at blade tip section
V_g	gas phase velocity
V_l	liquid phase velocity
V_z	axial velocity
W_s	saturation specific humidity (lb_m, vapor/lb_m, dry air)
W_s^*	saturation specific humidity (lb_m, vapor/lb_m, mixture)
x_{CH4}	methane content (mass fraction)
x_v	vapor content (mass fraction)

Symbol

x_w	water content (mass fraction)
$x_{w,o}$	water content at compressor inlet

Greek Letters

α	void fraction
γ	ratio of specific heats
ΔP_{meas}	measured differential pressure between gas stagnation pressure and static pressure
ΔP_g	difference between gas phase stagnation pressure and static pressure
ΔT_o	rise in stagnation pressure
δ	corrected pressure (p/p_{ref})
η	adiabatic efficiency
θ	corrected temperature (T/T_{ref})
ρ_g	density of gas phase
ρ_l	density of liquid phase
τ	equivalent temperature ratio
ϕ	flow coefficient
ϕ_o	flow coefficient at compressor inlet
ψ	equivalent pressure ratio

Subscript

A	pertaining to air flow
D	pertaining to design value
G	pertaining to gas phase
g	pertaining to gas phase
H	pertaining to hub section of a blade
l	pertaining to liquid phase

xxii

Subscripts

M	pertaining to air-water mixture flow
M	pertaining to mean section of · blade
ref	pertaining to reference conditions
o	pertaining to stagnation value
1	pertaining to compressor inlet
2	pertaining to compressor outlet

SUMMARY

A series of tests with (a) air flow, (b) air-methane mixture flow and (c) air-water droplet mixture flow has been conducted with a Test Compressor consisting of the axial portion of the T-63 engine compressor driven with a T-63 engine. The results of these tests have been presented in the form of overall performance changes at different operating speeds. The test results have been compared with predictions obtained utilizing the PURDU-WICSTK program. While the predictions seem to yield the general trend of experimental results, further advances are required in (a) the modeling of droplet centrifuging and droplet heating processes and (b) the measurement of flow properties in a two phase flow in the environment of a compressor. A discussion is also presented on the effects of water ingestion on an aircraft gas turbine engine.

CHAPTER I

INTRODUCTION

Water ingestion into an aircraft gas turbine arises due to two circumstantial reasons:

    (1) wheel-generated spray clouds entering the engine inlet during take-off and landing from a rough runway with puddles of water; and

    (2) rain, occasionally mixed with hail, entering the engine inlet during various parts of a flight in a rain storm.

A number of studies (Refs. 1-6) have shown that adverse effects can arise in engine performance due to such ingestion of water at engine inlet, when the engine has been designed for operation with air flow. In particular the engine may surge and may suffer blow-out or unsteadiness in the main burner or the after-burner. Simple corrective steps, such as resetting the throttle, have generally been ineffective in overcoming the problems of loss of power and nonsteady behaviour of the engine. In the case of wheel-spray ingestion, it has again become clear that basic changes in engine installation may be necessary in relation to inlets and landing wheels.

In the current investigation, there is no particular emphasis on the precise cause for the presence of water at the engine inlet. Water is assumed to enter the compressor along with air in droplet form. The droplet (nominal) diameters may be in the range of 20 to 1,300 microns. The water content by weight may be in the range of 2.5 to 15.0 per cent. In case of rain through which an aircraft may have to fly (Refs. 7-9) the droplet sizes may be of the order of 100 to 1,500 microns, although 3,000 micron size droplets have also been reported (Fig.1.1). On the

other hand, 15.0 per cent of water by weight is probably to be consider-
ed as a large amount of ingestion into the inlet, corresponding to
flight through storm conditions. Under such extreme conditions there
may also be hail and snow ingestion into the engine. However, only
water ingestion effects are examined here.

A comprehensive investigation of the problem of water ingestion
into engines during flight should take into account details of the
engine, its installation and the engine and aircraft conti 's. In the
current investigation attention is focussed on the engine.

Furthermore, it is felt that the response of the compressor in the
engine to water ingestion plays a determining and crucial role in the
response of the engine as a whole in view of two considerations.
   (1) The compressor receives the ingested water directly and, as a
        rotating machine, is most strongly affected by the ingested
        water, and also changes the "state of water" before the
        fluid enters the burner.
   (2) The compressor performance most directly affects the operating
        point of the engine under steady and transient state conditions.*
However, the compressor performance is affected by the presence of an
inlet through the changes in the flow field introduced by it, especially
the distortion of the compressor inlet flow field. While noting such
strong interaction between the inlet and the compressor flow fields, the

---

* It may be pointed out that the operating point of an engine is
determined by the matching between all of the components of the engine.
Thus, the swallowing capacity of the turbine and nozzle, for example
in a simple jet engine, at a given engine speed and turbine entry temperature,
determine the engine operating point on the compressor map. However, any
changes in the compressor outlet conditions affect the engine operating
point most directly with a given turbine and nozzle. In particular, during
water ingestion, the compressor map becomes completely changed, causing
at least a change in the surge margin for a possible operating point and,
in extreme cases, a total mismatch between the components. Even with a
turbine and nozzle that have variable-area capability, it may become
necessary to regulate the compressor outlet conditions independently.

most important aspect of the problem of water ingestion into an engine is still considered to be that pertaining to changes in the compressor performance itself.

In the case of turbofan engines, the air-water mixture upon entering the inlet becomes divided between the fan and the compressor. In particular cases, the compressor stream may have a different water content and droplet size distribution from that of the compressor stream in the absence of a fan. The effects of water ingestion are important both in the fan and the core engine compressor, although, perhaps, more so in the latter. When there is an after-burner in the fan stream or when a "mixing" nozzle is employed, water ingest n into the fan stream may, however, become critically important.

From practical operational and design points of view, the effects of water ingestion in a compressor are as follows:
  (1) changes in temperature ratio, pressure ratio and efficiency of the compressor;
  (2) changes in surge line and operating line, and therefore the surge margin under given operating conditions;
  (3) blade deformation and erosion due to impact of droplets;
  (4) blade and casing deformation due to differential thermal expansion under transient conditions;
  (5) oscillation of pressure ratio and flow, and
  (6) changes in dynamic loading including aero-elastic effects.

For given entry conditions, the response of the compressor is determined by the following:
  (1) compressor geometry;
  (2) blade loading;
  (3) machine rotational speed; and
  (4) parameters of the engine of which the compressor is a part.
The latter pertain to engine matching and should include not only the steady state performance parameters but also the mechanical, aero-dynamic and thermal inertia of the various components of the engine

under transient conditions. It should be noted that in particular
cases, the engine components may include a fan, an after-burner or a
second nozzle as part of the engine.

In establishing the response of a compressor to water ingestion,
it seems therefore useful to divide the total problem into two parts.

(1) The compressor as a machine itself; and

(2) The compressor as a part of the engine system.

In that fashion, one can separate the problems associated with engine
matching (steady or transient) from those dependent upon the design
of the compressor itself. Once the latter have been understood in
detail, the engine as a whole may be studied from a system point of
view. This is the approach adopted in the current investigation, since
it is also especially convenient in conducting experimental studies.

A number of parameters pertaining to the air-water mixture entering
a compressor during water ingestion are the following:

(1) amount of water approaching and actually entering a blade row
     as a fraction of the total mass flow of fluid entering
     compressor;

(2) form in which water is present, film and droplets;

(3) temperature and pressure of air, temperature of water and
     temperature of machine;

(4) vapor content;

(5) turbulence; and

(6) distortion, radial and circumferential.

Water vapor is always present in air-water mixtures ingested into
an engine. The water vapor content changes in the compressor because of
changes in pressure and temperature and because of transfer processes
between the two phases. In particular, in a multi-stage compressor of
large pressure ratio, there is a possibility of some of the water
reaching local saturation temperature and undergoing a phase change due
to boiling causing addition of large quantities of vapor to the gas phase.

It will be observed that each of the afore-mentioned six parameters changes after each blade row and the cumulative changes are therefore especially significant in a multi-stage machine. Furthermore, both time-dependent changes during sudden and sporadic ingestion, as well as steady state changes that may arise in conducting a laboratory experiment, need consideration. Thus, a detailed study of this problem should result in the determination and verification of methods for establishing (a) the changes in the performance of a compressor with water ingestion and (b) the changes in the state of fluid between the inlet and the outlet of the compressor. Such a study requires investigations both on a single row of blades (stationary and rotating) as well as on a unit with several rows of blades, under steady, transient, and distorted flow conditions. The latter is a means of establishing the response of a blade row to the flow generated by a preceding row. Furthermore, in order to examine the occurrence and effects of phase change in a blade row, the entry conditions to the blade row have to be selected such that they are suitable for such phase change. In a multi-stage compressor of large pressure ratio, there is, of course, a considerable change in air temperature at design conditions.

However, at this stage there are still considerable problems in conducting detailed measurements of two-phase flows in rotating machinery. It has therefore been felt in this investigation that one should aim at establishing overall performance changes and fluid flow changes in a compressor for given entry conditions of state of the two-phase fluid. Once such overall changes are established and related to verifiable models for performance prediction, it is felt one can proceed to more detailed measurements and modeling.

For a given compressor, the variables of interest during water ingestion are the following:
   (1) speed of the machine;
   (2) throttle setting;
   (3) stagnation pressure;
        temperature of air and water;

(5)   amount of water as a fraction of total mixture flow;

(6)   droplet size and number density distribution, and

(7)   vapor content.

The variables (3) to (7) have a spanwise and circumferential distribution at compressor inlet, which may or may not be uniform.

The overall performance parameters of a compressor with two-phase flow are the following:

(I)   pressure ratio, temperature ratio and efficiency;

(2)   changes in total water content and droplet size across the compressor; and

(3)   changes in vapor content across the compressor.

Each of these varies along the span of a compressor blade. Both the measurements and prediction of these are beset with considerable difficulties at this time. In particular the determination of water and vapor content and of droplet size distribution requires further advances in instrumentation, data acquisition and data processing.

On establishing and demonstrating predictive methods for the estimation of such overall performance parameters for a compressor, an analysis can be carried out for an engine operating with water ingestion. Under steady conditions, the equilibrium running of a simple engine depends upon the following parameters:

(1)   ambient conditions;

(2)   compressor operating characteristics
      with air-water droplet mixture flow;

(3)   turbine inlet temperature; and

(4)   turbine and nozzle area.

Regarding the latter, a fixed geometry thrust nozzle with a constant area turbine restricts the number of variables for equilibrium running of a simple engine to a single parameter, namely fuel flow. In a variable geometry engine which permits changes in area of the turbine and the thrust nozzle, one can select, at least in principle, three variables independently for equilibrium running: engine speed, compressor mass flow and turbine entry temperature.

An analysis of steady state equilibrium running of an engine with water ingestion can be expected to reveal the following:

(1) whether equilibrium running is feasible under a given set of operating conditions,

(2) changes in surge margin, and

(3) effect of fuel scheduling and bleed of working fluid.

The latter, along with other aspects of engine operation, is dependent upon the type of engine control incorporated in the system.

Even when attention is focussed on the performance of a compressor by itself, several aspects of the performance may come to light only when it is operated as a part of an engine. However, if engine matching and its effect on compressor performance are not included, one can test a compressor as a separate unit by driving it, for example, with an aerodynamically-independent drive engine. This has been the basis for experimental studies in the current investigation.

1.1 Objectives and Scope of the Investigation

The principal objectives of the present investigation are as follows:

(1) Establishment and demonstration of a predictive method for the calculation of the performance of an isolated compressor driven by an external drive unit and operating with air-water mixture flow; and

(2) Obtaining and correlating experimental data on a multistage compressor with air-water mixture flow.

In the calculation of performance, the vapor content of the air-water mixture is taken into account, both initial humidity and changes in vapor content due to phase change. The changes in vapor content were not measured during the experiments.

The other objectives of the present investigation are as follows:

(1) Determination of the manner in which engine performance becomes affected by water droplet ingestion into the engine compressors; and

(2) Providing a review of instrumentation suitable in compressors.

1.1.1 Analytical-Predictive Investigations

The analytical-predictive investigations are divided into two parts; (1) investigation on the performance of a compressor with water ingestion, and (2) analysis of a simple gas turbine engine with water ingestion.

Part I: Performance of Compressor with Water Ingestion

The analytical-predictive investigations on performance of compressor with water ingestion are divided into three parts:

(1) Setting up the general aero-thermodynamic equations for compressor with air-water mixture flow and deduction of a one-dimensional model.

(2) Establishing one-dimensional models for the estimation of performance of a compressor in four limiting cases as follows:

   (i)   Ingestion of mixtures of gases directly into a compressor at inlet, without water droplets.

   (ii)   Ingestion of small droplets that can be assumed to follow gas motion and hence absorb angular momentum.

   (iii)   Ingestion of large droplets that can be assumed to move with equal probability in all directions and that cause a loss of compressor performance due to drag forces acting on them; and

   (iv)   Injection of water with sudden phase change into steam at an appropriate stage in the compressor.

(3) Adapting and exercising a three-dimensional streamline computer code, the UD-0300 computer code (Ref.10), for the case of direct ingestion of mixtures of gases into a compressor.

Part II: Analysis of Gas Turbine Engine with Water Ingestion

The objectives of Part II are as follows:

(1) Establishing a model for steady state engine matching with water ingestion; and

(2) Establishing a model for calculation of flight performance with water ingestion.

1.1.2. Experimental Investigation

The experimental investigations have been conducted on a specially built Test Compressor. The experimental investigations may be divided into the following three parts:

(1) Tests with air as the working fluid;

(2) Tests with air-methane mixture as the working fluid; and

(3) Tests with air-water droplet mixture as the working fluid.

The Air Force System Command has provided the Test Compressor and a T-63 Drive Engine for the experimental investigations. The predictive methods developed for estimating compressor performance with two phase flow have also been employed to calculate the performance of the Test Compressor.

Details regarding the Test Compressor and Drive Engine are provided in Appendix 1 to this Report.

The Test Compressor, it will be observed, has several limitations:

(1) the annulus and the blade heights are small and only overall performance parameters at one or at most two radial locations at the exit plane can be measures; and

(2) the overall pressure and temperature ratios, even at design point, are too small to cause evaporation of more that 2.5 per cent of water (by weight) although the inlet temperature is raised to as high a value as 185° (85°C).

The Test Compressor has a plastic coating that is not expected to withstand a temperature of over 200°F (about 90°C). Plans were made for preheating the air up to about 140°F (60°C) but tests with such preheating could not be undertaken in view of an explosion in the air supply line.

Accordingly, the Test Compressor has been tested at inlet temperatures in the range of 70°F to 100°F (about 20°C to 40°C). Such inlet temperatures do not cause water evaporation within the Test Compressor. The test program has therefore been conducted in two parts:

(1) With a mixture of gases to simulate air-stream mixture flow corresponding to (a) high humidity in the air and (b) operation of a compressor with air-stream mixture following complete evaporation of water, and

(2) With air-water droplet mixture flow.

In examining the effects of presence of water vapor on a compressor performance, it is clear that another gas, such as methane, can be substituted for water vapor so long as the desired similarity laws with respect to Reynolds and Mach numbers, are satisfied. A comparison of properties for steam and methane is presented in Table 1.1. In view of the similar properties, experimental studies have been undertaken in this investigation utilizing air-methane mixtures.

The tests with air-water droplet mixtures have been conducted utilizing the following variables: mixture temperature, mixture composition and droplet size.

1.1.3 Measurements and Predictions

The results of the experimental investigation have been compa ed with prediction from models from the point of view of examining selected assumptions introduced in the models. It is clear that in view of limitations on the feasibility of measurements and the nature of assumptions introduced in modeling, comparison of analytical predictions with experimental results is restricted to certain overall performance parameters, in particular, the effects of mechanical-aero-thermodynamic interactions are established indirectly from overall compressor performance parameters and changes in water and vapor content.

TABLE 1.1

COMPARISON OF PROPERTIES FOR STEAM AND METHANE

	Steam	Methane
Chemical Formula	H_2O	CH_4
Molecular Weight	18.016	16.043
Specific Heat at Constant Pressure		
$\quad$ (Btu/lbm-^{O}F)	0.445**	0.531*
$\quad$ (kJ/kg-^{O}C)	1.863**	2.223*
Ratio of Specific Heats*	1.329**	1.304*
Enthalpy Increase		
$\quad$ (Btu/lbm)	62.70+	69.96+
$\quad$ (kJ/kg)	145.84+	162.73+

*pressure = 1 atm; temperature = 78^OF (26^OC)

** pressure = 1 atm; temperature = 212^OF (100^OC)

+ pressure ratio, P_{02}/P_{01} = 2.6; T_{01} = 68^OF (20^OC)

1.1.4 Measurement Techniques

A brief review of instrumentation suitable for use in axial flow compressors and cascades operating with two phase fluid flow has been undertaken.

Two important overall performance parameters in compressors are the stagnation pressure ratio and the stagnation temperature ratio. A probe for the measurement of stagnation pressure in two phase flow has been developed. Its possible use in a compressor flow field has been examined. However, such a special probe has not been utilized in the current investigation.

1.1.5 Engine Performance

The engines considered are those that have been designed for air flow through the inlet. Engines in which there may be injection of water at gas flow part locations beyond the compressor or in other stream such as fan ducts or after-burners are not under consideration. Specifically water ingestion effects have been examined in the case of simple turbo-jet and turbo-fan engines that have originally been designed for air flow operation only. Thus (a) the adverse flow effects due to water ingestion and (b) possible methods of mitigating such effects are of interest.

The response of an engine to water ingestion depends upon the following:
    (a) component geometrical constraints;
    (b) component performance characteristics; and
    (c) nature of control incorporated into the engine.

The performance characteristics that are of major interest are the following:
    (a) Changes in component performance characteristics due to water injection, in particular the compressor;
    (b) Changes in operating characteristics of engine under conditions of equilibrium running;

(c) Changes in surge margin; and

(d) Limiting conditions of operation.

The foregoing have been analyzed in order to establish general performance trends without reference to specific engine configurations.

It may be noted that, because of the aero-thermo-mechanical processes arising on account of water ingestion, one may also expect, at least in extreme cases, aero-elastic processes becoming significant. However, the manner in which flutter, for example may be altered during two phase flow in compressors is not included for study in the current investigation.

1.2 Effects of Water Ingestion

The two critical factors during water ingestion may be said to be the following: (a) the aero-thermo-mechanical processes associated with two phase flow and (b) the centrifugal action on droplets in the compressor. The first of these includes droplet disintegration and evaporation processes. The latter gives rise to a change in gas phase mass flow as well as reduction in gas phase temperature. The centrifugal action introduces a radial distortion in the flow and fluid properties, and the distortion changes in every stage of a multistage compressor. In particular, the spanwise distribution of the composition and properties of the fluid, in terms of air, water vapor and water droplets (both content and size distribution), undergoes changes continuously along the compressor flow path. The effects (a) and (b) should be examined in a compressor in relation to the following:

(i) Formation of a water film in the tip region, that may flow into the diffuser;

(ii) Possibility of choking hub sections and stalling tip sections with redistributed gas and liquid phase mass flow; and

(iii) Nonuniform distribution of water vapor in the radial direction.

The foregoing will in turn affect engine performance depending

upon engine-matching and the type of control in the engine.

In order to reduce the effects of water ingestion, one can consider the following in order of increasing complexity.

(i) Bleeding of gas or liquid phase flow at appropriate locations in the compressor;

(ii) Resetting stator blades;

(iii) Modifying engine control; and

(iv) Introduction of variable geometry nozzle and (also) turbine.

The results of some preliminary studies on bleeding and also gas injection have been reported in Ref. 11.

1.2.1. Relation to Other Two-Phase Flow Problems in Turbo-Machinery

The current investigation deals with air-water droplet mixture ingestion into engines. On the other hand there has also been considerable interest in the problem of dust particle ingestion into engines (Refs. 12-13). In the latter case the principal interest is in erosion of blades and nozzles, although there is some loss in aerodynamic performance.

It is generally considered that the solid particulates may agglomerate but not disintegrate during dust ingestion. Furthermore the heat and mass transfer processes between the two phases are considered negligible.

Solid particulates are also of interest in certain rocket motor nozzle and plume flows (Refs. 14-16). In this case, in addition to erosion and particulate drag effects it is generally necessary to take into account heat and mass transfer processes, as well as condensation, solidification and other phase change processes. However, in this case there is not strong centrifugal action, although there may be some swirl in the flow.

The low pressure stages of a steam turbine (Refs. 17-19) may

operate, as is well known, with steam-water droplet mixture, the droplets arising through condensation. However, in this case, while erosion, loss of aerodynamic performance, and consequences of strong centrifugal action are important, one does not have the problems of stalling and surging. A compressor is prone to surging and the surge margin with respect to operating line when it is part of an engine is an extremely important parameter in engine operation. Hence the problem of water ingestion into an engine compressor attains a level of complexity and significance much larger than the two phase flow problem in steam turbines. One should also note that a turbine is basically a nozzle, while a compressor flow (both past a blade and through a blade passage) involves diffusion and complicated blade wake interactions.

The current investigation does not take into account geometrical changes in a compressor because of, say, differential contraction of rotor and casing upon water ingestion. In general one can expect a change in clearance between rotor and stator. If a compressor has been designed with optimum clearance, one has to examine both aerodynamic and mechanical effects caused by changes in clearance. This aspect of water ingestion should be examined in relation to the general problems of gas flow path integrity (Ref. 20).

While nonsteady state operation is not considered in the current investigation, one of the most important aspects of water ingestion into compressors and engines is transient state operation. The aero-thermo-mechanical interactions including differential contraction of casing and rotor under transient conditions are significant in evolving various means of reducing the effects of water ingestion.

Finally, it is recognized that the entry conditions into a compressor are not uniform radially and circumferentially. The effects of distortion with respect to pressure, temperature, velocity and turbulence continue to be a subject of concern even with air flowing alone (Ref. 21). During water ingestion, one can expect, in general, distortion both at entry and to the compressor and at entry to each stage. The sensitivity

of an engine to water ingestion should include consideration of inlet
distortion with regard to water content and water droplet size distri-
bution. This problem has been entirely neglected in the current investi-
gation. It may be pointed out that even under uniform inlet flow
conditions, radial distortion, of course, arises within the compressor
due to centrifuging and heat and mass transfer processes.

1.3 Implications of Models

The models derived in the current investigation may be divided into
four groups:
  (i)   Model for the calculation of stage performance with air flow.
  (ii)   Model for droplet motion across a blade row.
  (iii) Model for centrifuging of water, and
  (iv)   Model for heat and mass transfer processes, including droplet
         disintegration.

Experimental investigations have been conducted in order to
determine overall compressor performance changes for chosen initial and
operating conditions. A comparison between predictions and measurements
therefore yields no detailed verification of the models. It is in any
case doubtful if detailed verification of all aspects of the models can
be obtained even if one attempted additional measurements.

The performance of a compressor stage with two phase flow depends
upon the following parameters:
  (i)   geometrical design of blade and blade passage,
  (ii)   spacing between blade rows,
  (iii) leading and trailing edge geometry,
  (iv)   casing geometry,
  (v)   rotor and stator blade junctions,
  (vi)   incoming flow conditions, and
  (vii) operating speed and throttle setting.

The foregoing determine (a) the stage work input, (b) the states

of gas and liquid phases, (c) the efficiency of compressor, (d) the redistribution of water and vapor and (e) limiting condition of steady state operation of compressor. When the compressor is part of an engine, the operating characteristics of all other components of the engine and of the engine as a whole are also determined by the compressor design and initial conditions. It is clear that while the models developed can be employed to determine the performance of any compressor under a set of reasonable operating conditions, there is need to establish relations that can be employed to scale the performance of a compressor with respect to design, initial and operating conditions. Such scaling laws have to be based on characteristic lengths, characteristic times, and blade, blade passage and blade row characteristics of the compressor and, when the compressor is part of an engine, the characteristics of other components such as diffuser, burner, turbine and nozzle. Under certain assumptions an attempt has been made to establish scaling laws for both a compressor and a simple jet engine.

1.4 Outline of the Report

The final report is being issued in three parts:

    Part I: Analysis and Predictions

    Part II: Computational Program; and

    Part III: Experimental Results and Discussion

This Report constitutes Part III of the Final Report. Chapter I is the introduction. Chapters II, III, and IV are devoted to describing the experimental studies and the test data obtained. The final Chapter, V, presents a discussion of the experimental and theoretical results and also summarizes the conclusions of the investigation. A few recommendations have also been made for future studies.

CHAPTER II

THE TEST INSTALLATION

The Test Installation consisted of the following:

(1) The 6-stage Test Compressor that was driven by the Drive Engine by an interconnection between the engine power turbine and the Test Compressor through a gear box: Details regarding this part of the Installation have been given in Section 2.1.

(2) The Test Compressor Air Supply System: Details regarding this part of the Installation have been given in Section 2.2.

(3) The methane-injection system for undertaking tests with air-methane mixture flow: Details regarding this part of the Installation have been given in Section 2.3.

(4) The water-injection system for undertaking tests with air-water droplet mixture flow: Details regarding this part of the Installation have been given in Section 2.4.

The Test Installation included instrumentation and data acquisition systems that may be divided broadly into two groups.

(1) Operation related instrumentation, and

(2) Instrument for testing of the Test Compressor

Details regarding these have been provided in Section 2.5 and 2.6 respectively.

2.1 Drive Engine and Test Compressor Installation

The Drive Engine and the Test Compressor have been described in Appendix 1 of this Report. A photograph of the Drive Engine and Test Compressor assembly is provided in Figure 2.1.

The Drive Engine and Test Compressor installation consisted of the following:

    (1) The assembly mounted on a test bed structure, located securely on the floor of the test cell.

    (2) The inlet and exhaust ducting for the Drive Engine and the Test Compressor; and

    (3) The fuel and oil supply system.

The Drive Engine operated with the ambient air in the test cell. The test cell had adequate ventilation for air supply. The Drive Engine exhaust was removed through the roof of the test cell by means of exhaust ducting. The exhaust ducting was in two parts and connected symmetrically to the outlet of the power turbine.

The Test Compressor had provision for operation with either (a) atmospheric air, or (b) the laboratory air supply. In both cases, the air was brought to a plenum chamber from which the air was supplied by ducting to the Test Compressor. Details regarding the air supply system have been given in Section 2.2. The Test Compressor discharge was connected to a throttle valve for the regulation of air flow through the compressor. The compressed air was then removed from the test cell through compressor exhaust ducting. The method of regulating air flow through the Test Compressor by means of the throttle valve has been described further in Section 2.2.

The fuel and oil supply systems have been described in detail in Appendix 1 to this Report. Their systems were located in a corridor directly north of the test cell.

The fuel employed for the Drive Engine was Jet A fuel. The fuel flowed from the storage tank into the test cell by gravity. The fuel supply to the Drive Engine was then governed by a fuel govenor assembly connected to the power turbine shaft of the Drive Engine.

A dedicated combustor was employed to heat a part of the laboratory air that could be mixed with cold air as and when desired. The

combustor, referred to as the laboratory air heating combustor (_AHC),
was operated with methanol fuel and was located within the test cell
next to the Drive Engine. However, as stated earlier, the air heater
has not been utilized in the current investigation on the Test Com-
pressor, although the air heater itself has been tested to determine
its operational characteristics.

Both the Jet A and the methanol systems were located in the afore-
mentioned north corridor of the test cell, and comprised the fuel
supply system. The oil employed was Mobil II Jet Engine Oil. The oil
supply system consisted of two independent systems. One system supplied
oil to the Drive Engine and the hydraulic system. The other system was
for the Test Compressor. The oil supply tanks, heat exchangers and filters,
comprising the oil supply system, were located, as stated earlier, in the
north corridor of the test cell.

The fuel and oil supply and return lines passed through openings
in the test cell wall which forms one wall of the corridor.

2.1.1 Operating of the Test Compressor

The general procedure for the operation of the Test Compressor at
a particular speed and mass flow has been described in Appendix 1 to
this Report.

2.2 Test Compressor Air Supply System

The Test Compressor could be operated with either (a) atmospheric
air or (b) the laboratory air supply. In the latter case, provision
existed for regulating the pressure and temperature of the air supplied.
The pressure was regulated by means of pressure regulators. The temp-
erature was regulated by mixing air that was heated in the laboratory
air heating combustor (LAHC) with cold laboratory supply air.

The Test Compressor air supply system has been shown schematically
in Figure 2.2. When the 3.0 in. laboratory air supply valve (LASV) was

closed and the 10.0 in. atmospheric air valve (ATAV), admitting atmos-
pheric air to the plenum chamber, was opened, the Test Compressor
operated with atmospheric air. On the other hand, when the ATAV was
closed and the LASV was opened, the Test Compressor operated with the
laboratory air supply. The LASV and the ATAV were both Posi-Seal model
SDN butterfly valves. The LASV was equipped with an electric operator
modulating control; thus the amount of valve opening could be set
precisely and measured. The ATAV was equipped with an operator control
for on-off service only.

A drawing (dimensioned elevation) of the air supply starting from
the plenum chamber to the Test Compressor has been presented in Figure
2.3. The ducting consisted of the following:

(1) A straight section that incorporated the flow metering
section.

(2) A 180^0 turn followed by a straight section and a second 180^0
turn.

(3) An expander section of entry diameter equal to 8.0 in., and
outlet diameter equal to 16.0 in., and a length of 15.0 in.
This section incorporated a concentric cone of base diameter
6.0 in., that was supported by four thin spikes. Thus the
air was not permitted to "stream through" the expander section
into the Test Compressor.

(4) An injector section of 16.0 in. internal diameter and 8.0 in.
length consisted of a gas injector ring or water injection
ring. Details regarding these rings have been provided in
Sections 2.3 and 2.4. The gas injection ring was also suit-
able for use as a connecting ring during tests with air flow.
It was replaced by the water injection ring during tests with
air-water mixture flow.

(5) A bell-mouth section that was designed for smooth contraction
of flow into the Test Compressor.

(6) The Test Compressor entry section consisting of two straight
duct sections (with appropriate flanges) that were connected

by a flexible hose utilizing adjustable clamps. In this manner, the Test Compressor was mechanically "isolated" from the air supply system upstream.

(7) The Test Compressor discharge section connected to a throttle valve and the compressed air exhaust ducting.

The air from the plenum chamber thus flowed through the air flow metering section and then after passing through the ducting entered the expander section. Following this, provision existed for injection of either (a) another gas or (b) water into the air stream. The working fluid then flowed through a bell-mouth section into the straight entry section of the Test Compressor.

The bell-mouth section was designed for smooth flow of air or another working fluid. Details regarding the design of the bell-mouth have been given in Appendix 2 of this Report.

The Test Compressor throttle valve, located in the discharge section of the Test Compressor, has been described in Appendix 3 of this Report.

2.2.1 Laboratory Air Supply System

The laboratory air supply system may be divided into two parts:

(i)   The general air supply system that supplied air from the Air Supply System of the Thermal Sciences and Propulsion Center to a location on the roof of the Propulsion Laboratory building in which was located the test cell used in the current project; and

(ii)   the air supply system within the test cell.

The general air supply system to the test cell has been described in Appendix 4 of this Report. It consisted of (a) a low pressure air supply system and (b) a high pressure air supply system.

The laboratory air supply system within the test cell is shown schematically in Figure 2.4.

The low pressure air supply was utilized, as shown in Figure 2.4, for the following purposes in the test cell:

(1) Operation of the many air-actuated valves in the test instal-
lation.

(2) Controlling the opening of the dome regulators in conjunction
with Grove hand loaders.

(3) Cooling the vibration transducer on the Drive Engine turbine
during and after a test run.

(4) Maintaining the Test Compressor labyrinth seal pressure at a
design value of 5.0 p.s.i.

(5) Operation of pump to fill the fuel tanks (for the Drive Engine
and the LAHC) from the fuel storage drums.

(6) Pressurizing the methanol fuel tank, and

(7) Atomizing the LAHC fuel.

The high pressure air was utilized, as shown in Figure 2.4, to supply "conditioned" air to the Test Compressor through the Plenum Chamber. The main air supply line passed over the roof of the Propulsion Laboratory, as stated earlier. The line was connected to the test cell through a Jamesburg model 6800-3600G FOKOO AA (remotely operated) air valve, known as the High Pressure Air Supply Valve (APASV). Downstream of this valve, the air supply line was divided into two branches, as shown in Figure 2.4 by thick lines. One branch supplied air to the laboratory air heater combustor (LAHC) and the other branch supplied primary or "diluent" air. The heated air from the LAHC could be mixed with the diluent air in a desired proportion in the downstream ducting and the mixed air supplied to the plenum chamber and eventually to the Test Compressor. The LAHC air supply and the primary air supply were controlled by Grove Powerreactor regulators, model 31 1B and model 21 2B, respectively, in conjunction with Grove hand loaders. Downstream of the regulators, burst diaphragms, B.S. and B type were located in

order to prevent damage to the test installation, should the regulators
fail. The primary and the LAHC air supplies then entered the test cell.

Each branch of the air flow was equipped for the measurement of
flow rate with a standard orifice, an orifice entry pressure gauge, a
differential pressure gauge for measurement of the pressure drop across
the orifice plate and an Omega type K thermocouple. The temperature
was read on the Omega model 402A-K-F digital read-out meter located in
the laboratory air supply control panel.

The air supply system was designed with four valves, as shown in
Figure 2.4, such that the plenum chamber could be supplied with either
(a) cold air or (b) "conditioned" air obtained by mixing heated air
from the LAHC and the cold air. The heated air from the LAHC could be
used only to the extent desired. The mixed air could also be used only
to the extent desired. It is obvious that the Test Compressor under
given operating conditions (speed and throttle setting) would allow
only a particular mass flow to pass through. Provision was, therefore,
made in the system to supply a large air flow from the laboratory air
supply system and to dump the "unused" air into the atmosphere.

2.2.2 Operation of the Air Supply System

The operation of the laboratory air supply system has been
described in Appendix 4 of this Report.

2.3 Methane Injection System

One of the series of tests planned originally for the Test Com-
pressor was to utilize air-steam mixtures as the working fluid with
different content of steam in different mixtures. A water boiler was
to be utilized for the generation of steam. However, no boiler could
be found at Purdue University that was suitable for location at the
Propulsion Laboratory. Accordingly, as stated in Chapter I, it was

decided to conduct a limited number of tests with air-methane mixtures.
Methane was considered as an acceptable substitute for steam. Test
Compressor performance obtained with air-methane mixtures would differ
from those that would have been obtained with air-steam mixtures to
the extent of differences in molecular weight and ratio of specific
heats, although the general trends in performance changes would be the
same compared to performance with air as the working fluid.

2.3.1 Methane Injection Ring

As stated in Section 2.1, the air supply system of the Test Com-
pressor was designed with a gas injector ring upstream of the bell-
mouth section, Figure 2.3. Methane was injected, when desired, through
injectors located in the gas injection ring.

A drawing of the gas injector ring is presented in Figure 2.5.

The injector ring consisted of a closed annular chamber of length
equal to 8.0 in., and inner and outer diameters of 16.0 in., and 24.0
in., respectively. The ring was provided with a 0.75 in. diameter pipe
connection for supply of methane (or another injected gas) and a 0.25
in. diameter tube connection for venting the annular chamber. Sixteen
gas injectors were located symmetrically in the ring around the circum-
ference of the inner wall. Each gas injector consisted of a 1.50 in.
diameter body with a 1/16 in. diameter hole in its center. The methane
injector design is illustrated in Figure 2.6 and a photograph of an
injector is provided in Figure 2.7.

2.3.2 Methane Supply System

Methane was supplied to the methane injection ring utilizing the
methane gas supply system, illustrated schematically in Figure 2.8. It
may be observed that provision was made in the system for the venting
of the entire system with nitrogen so as to meet the safety requirements.

During every test with air-methane mixture, the nitrogen supply line was left open during the test and for several minutes following the test.

The methane gas employed was commercial grade methane. In view of a simultaneous supply of nitrogen, the air-methane mixture was invariably depleted in oxygen proportion compared to air.

The amount of methane gas supplied to the injection ring (and hence injected into the air stream entering the Test Compressor) was measured by means of a choking flow nozzle in conjunction with a Gould model PMB22-50 differential pressure transducer and an Omega type K thermocouple. The temperature and pressure were read on a digital indicator (Daytronic model 9615) and a digital read-out meter (Data Tech model 73-100), respectively.

The nitrogen flow rate was not measured.

The methane gas injection system has been described in detail in Appendix 5 of this Report.

2.3.3 Operation of Methane Injection System

The procedure for operation of the methane gas injection and nitrogen purge system has been given in Appendix 5 of this Report.

2.4 Water Injection System

The water injection system was required to inject, as uniformly as possible, a predetermined quantity of water into the air stream entering the Test Compressor.

The water injection system consisted of the following:
(1) A water injection ring with 16 injector locators distributed uniformly over the circumference of the ring; the injectors could be located in the injector locators, when desired.

(2) The water supply and distribution system.

(3) Water drains located in the bell-mouth and at the exit plane of the Test Compressor; these were designed to remove any water that flowed along the wall and tended to settle down due to gravity at the lowest points in the two afore-mentioned locations.

2.4.1 Water Injection Ring

As stated in Section 2.1, the air supply system of the Test Compressor was designed with a water injection ring that could be assembled upstream of the bell-mouth section, Figure 2.3. Water was injected when desired through injectors located in the water injection ring. A drawing of the water injection ring is presented in Figure 2.9. The design of the injector locator has been illustrated in Figure 2.17; a photograph of the injector locator is given in Figure 2.11.

Two types of injectors were employed for injecting water into the air stream, both of them manufactured by Spraying Systems Co. of Illinois:

(1) No. ¼ LNG-¼ LNNG atomizing nozzle: droplet sizes were expected to range, according to manufacturer's specifications, from 10 to 100 microns with 50 per cent of droplets, by volume, occupied by droplets under 90 microns in size.

(2) No. 1/8 GI-1/8 GGI Full Jet nozzle: droplet sizes were expected to range, according to manufacturer's specifications, from 300 to 2,000 microns with 50 per cent of droplets, by volume, occupied by droplets under 600 microns in size.

The injector locators were designed so as to permit the injectors to be located either flush with the inner surface of the injector ring or a short distance inwards.

2.4.2 Water Supply and Distribution System

The water supply and distribution system consisted of the following:

(1) Water softener and filter section,

(2) Water pump and drive,

(3) Water flow measurement section, and

(4) Water distribution system.

The water supply system is shown schematically in Figure 2.12. The water distribution scheme has been illustrated in Figure 2.13. A photograph of the water distribution system has been presented in Figure 2.14.

Water employed for injection was from the main supply to the Propulsion Laboratory. The water was softened by a Culligan Mark 5 water softener and then filtered by a 25 and 5 micron filter unit.

In order to maintain a desired value of pressure of water, an electrically driven water pump (named the Aurora model G4TS-BF turbine pump) was employed. Referring to Figure 2.12, when the pump functioned, water circulated through the flow regulating valve (FRV) at all times. The pressure, and thus the flow rate to the test cell, were regulated thus by the amount of opening of the FRV. A shut-off valve (SOV), when closed, permitted the water to flow into the test cell.

The water flow rate was measured by a rotometer in the flow line. The rotometer employed was a Brooks model 1110-08H2G1A rotometer with a range of 0.078 to 0.78 gallon per minute. When the pump was operating and the shut-off valve (SOV) was closed, the flow rate could be regulated by opening the FRV by the desired amount. The SOV also served the purpose of preventing the possibility of water hammer on the rotometer.

The water distribution system was designed so as to permit 4, 8,
or all of the 16 injectors (located symmetrically over the water
injection ring) to be supplied with water at equal values of pressure.
As seen in Figures 2.13 and 2.14, water was supplied to the small surge
tank of the water distribution system at the desired pressure by means
of 1.0 in. diameter PVC pipe. Water from the surge tank was then
branched out into four parts, each connected to a distributor with
four outlets leading to four injectors. Thus the four distributors
together supplied sixteen injectors, the outlets from any one distribu-
tor supplying four injectors located symmetrically on the injector ring.

Each of the four branches had a remotely-operated solenoid valve,
the Atkomatic model AAD 3200 valve, between the surge tank and the
distributor. When the solenoid valve in any branch was opened, water
was supplied to the distributor in that branch and hence to the four
injectors connected to the four outlets from that distributor. Care
was taken in the design of the distribution system and in locating it
in relation to the water injection ring such that (a) equal pressure
was ensured at the injectors and (b) no dribbling of water would occur
through the injectors after the solenoid valves were shut down.

The type of water spray obtained in the injection ring was a func-
tion of the type of injector employed and the water pressure. The
amount of water injected could be varied by selecting the number of
injectors fed during a test.

2.4.3 Special Provisions for Drainage of Water in the Air Flow System

It was felt that a part of the water that was injected into the
air stream would impact the wall of the bell-mouth section and collect,
by gravity, at the lowest point of that section. In order to determine
the amount of water that entered the test compressor during a test with
water injection, it was necessary to subtract the amount of water so

collected in the bell-mouth section from the amount of water injected. Accordingly a drain was located in the bell-mouth section to remove the water collected, and subsequently to measure it.

At the exit of the Test Compressor, it was considered important to remove all of the water from the air-water mixture so that none of that water would enter the air flow throttle valve located in the discharge section of the Test Compressor. Accordingly, two drains were incorporated, one immediately at the exit of the Test Compressor and another in the turning section following the Test Compressor. The turning section was also stuffed with plastic wool in order to ensure as complete a capture of water as feasible. The drain locations have been shown schematically in Figure 2.15.

A provision was made to measure the water collected from the drains at the exit plane of the Test Compressor so as to permit a further balance of mass of water injected. However, such a mass balance would require a careful measurement of change in humidity (or water vapor content) across the Test Compressor and that of water that escaped with the air flow through the air throttle valve. It was found later during the tests that the measurement of water collected at the exit of the Test Compressor did not serve any useful purpose in view of the large amounts of water that tended to escape with the air flow.

2.4.4 Operation of the Water Injection System

The procedure for operating the water injection system has been given in Appendix 6 to this Report.

2.5 Instrumentation for System Operation

The instrumentation for system operation may be divided broadly into the following:

(i)   Drive Engine and Test Compressor operation (Section 2.5.1);

(ii)   Methane injection system operation (Section 2.5.2); and

(iii) Water injection system operation (Section 2.5.3).

2.5.1 Instrumentation for Drive Engine and Test Compressor Operation

2.5.1.1 Flow Rate of Primary Air Supply and the Laboratory Air Heater Combustor (LAHC) Supply

(1) Pressure at entry to orifice employed for the measurement of air flow: Ashcroft 0-100 psig pressure gauge.

(2) Differential pressure across orifice: ITT Barton 0-100 psig differential pressure gauge.

(3) Temperature of air at entry to orifice: Thermocouple and Omega model 402A-K-F digital readout meter.

2.5.1.2 Laboratory Air Heater Combustor Inlet and Outlet Conditions

(1) Combustor fuel pressure and combustor fuel nozzle air pressure: Ashcroft 0-600 psig differential pressure gauge.

(2) Combustor outlet temperature: Omega model NBI CAIN-140-6 type K thermocouple assembly and digital readout meter as in 2.5.1.1 (3).

2.5.1.3 Mixed Air Temperature

(1) Primary air temperature: Thermocouple assembly and readout meter as in 2.5.1.2 (2).

(2) Mixed air temperature: Thermocouple assembly and readout meter as in (1) above.

(3) Power turbine speed: Standard Electric Company 0-50,000 rpm indicator.

(4) Gas producer turbine temperature: Omega model 4035K 2000 thermocouple readout meter.

(5) Compressor and turbine vibration: CEC type 4-125-001
vibration transducers and Wave Labs Co. model WL-950
vibration meter.

2.5.1.4 Laboratory Air Supply System

(1) Opening of 5 Posi-Seal butterfly valves: Honeywell model
MS3 analog gauges.

2.5.1.5 Air Flow Metering Nozzle

The air flow into the Test Compressor, whether obtained from the
atmosphere or from the laboratory air supply system, was measured, as
stated earlier by means of an air flow metering nozzle located in the
straight duct section following the plenum chamber. Two nozzles were
employed, one for the measurement of low rates of air flow (obtained in
the range of Test Compressor speeds of 50-70 per cent design speed) and
another for larger flow rates (obtained in the range of Test Compressor
speeds of 70-100 per cent design speed). Details concerning the noz-
zles are provided in Appendix 4 to this Report.

The following instrumentation was employed with the nozzles:
(1) Pressure at entry to flow measurement nozzle: Gould model
PA822-100 thin film strain gauge pressure transducer and
Northrup Co. model R-820-1 strip chart recorder and manometer.
(2) Differential pressure across nozzle: Gould model PM822
differential pressure transducer and Leeds strip chart
recorder as in (1) above.

2.5.1.6 Drive Engine

(1) Oil pressure into the engine and scavenge oil pressure: U.S.
Gauge Co. 0-200 psig pressure gauge.

(2) Gas producer speed: Standard Electric Time Company 0-80,000 rpm indicator.

(3) Power turbine speed: Standard Electric Company 0-50,000 rpm indicator.

(4) Gas producer turbine temperature: Omega model 4035K 2000 thermocouple readout meter.

(5) Compressor and turbine vibration: CEC type 4-125-001 vibration transducers and Wave Labs Co. model WL-950 vibration meter.

2.5.1.7 Test Compressor

(1) Oil pressure into the Test Compressor: U.S. Gauge Co. 0-200 psig pressure gauge.

(2) Test Compressor speed: deduced from the Drive Engine power turbine speed using a value of gear speed ratio equal to 0.119676.

(3) Test Compressor vibration: CEC type 4-125-001 transducer and the vibration meter stated under 2.5.1.5 (5).

(4) Test Compressor air flow throttle valve setting: controlled by a remotely operated electric motor and measured by a standard rule.

2.5.2 Instrumentation for Methane Injection System Operation

(1) Methane temperature at entry to flow measurement nozzle: Omega type K thermocouple.

(2) Methane pressure at entry to flow measurement nozzle: Gould model PM822-50 thin film gauge differential pressure transducer and Data Tech model 73-100 digital readout meter.

2.5.3 Instrumentation for Water Injection System Operation

(1) Injected water flow rate: Brooks model 1110-08H21A rotometer.

(2) Water pressure immediately upstream of water distribution system: Weiss 0-100 psig pressure gauge.

(3) Water temperature: Omega model NX NB1-CPSS-186-12 type J thermocouple with screw type thread and readout meter.

2.6 Instrumentation and Data Acquisition for the Test Compressor

The performance of the Test Compressor was obtained as follows:

(a) During tests with air flow, the corrected mass flow, overall stagnation pressure ratio, overall static pressure ratio, overall stagnation temperature ratio, and overall static temperature ratio were established.

(b) During tests with air-methane mixture flow, the mixture ratio of methane to air was established in addition to the quantities mentioned in (a) above.

(c) During tests with water injection the corrected mass flow of air and the mass flow of water entering the compressor were established in addition to the overall ratios of static temperature, static pressure and stagnation pressure across the Test Compressor.

In all of the cases, the mass rate of air flowing into the Test Compressor was regulated by the setting of the throttle valve and measured in the nozzle located in the air supply duct (Figure 2.3) utilizing the instrumentation described under 2.5.2 items (4) - (6).

During the air flow tests and the air-methane mixture flow tests, the same instrumentation was employed to measure the total pressure, static pressure, and temperature at both compressor inlet and outlet. A United Sensor model PDC-12-G-10-KL pitot-static pressure probe along with a Gould model PL121TC-10 differential pressure transducer was employed at the Test Compressor inlet to measure static and total pressures. The total and static pressure at the Test Compressor outlet were obtained using a standard kiel probe and a wall static tap,

respectively. The pressure probes at the Test Compressor outlet were employed in conjunction with a Gould model PL131TC-50 differential pressure transducer. Connections from the pressure probes to the transducers were made using tygon tubing. Each Gould transducer was attached to a 48-port model 48J7-1/QTMMM24-30 Scanivalve. The inlet and outlet pressures were recorded on a Honeywell model 1612 oscillograph. Omega type K thermocouples were employed at Test Compressor inlet and outlet to measure the temperature of air. The temperatures were displayed on a Daytronic model 9515 digital indicator.

The probes for pressure and temperature measurement employed for gas-phase only are not suitable for tests with water injection; therefore, special probes were obtained. Details regarding the special probes for use in two-phase flow have been given in Section 2.6.2.

The mass flow rates of methane and of water were measured as follows. The mass flow rate of injected methane was measured by means of a choked flow nozzle in conjunction with an Omega type K thermocouple and a Gould model PM822-50 differential pressure transducer. (Details of the methane system have been presented in section 2.3 of this Report). The measurement of mass flow rate of water through the test compressor is achieved by employing a Brooks rotometer in the water supply system and a water collection system in the bell-mouth section. The rotometer measured the amount of water injected while the collection system determined the amount of injected water that did not flow through the Test Compressor. The difference between the two mass flow rates thus provided the mass flow rate of water into the Test Compressor. (Details of the water injection system have been given in section 2.4 of this Report).

The instrumentation and data acquisition systems utilized in conjunction with the Test Compressor were as follows:
    (1) Laboratory ambient temperature and relative humidity: Edmund Scientific model 61,151 Lufft Outdoor Window Weather Station.

(2) Ambient barometric pressure: Princo Standard Mercurial Barometer.

(3) Test Compressor inlet and outlet temperatures during air flow and air-methane mixture flow: Omega Type K model TJ96-CASS-116U-6 thermocouples.

(4) Test Compressor inlet and outlet temperatures during water injection tests: United Sensor and Control Corp. type TK-8-C/A-36-F Aspirate thermocouples.

(5) Digital readout of Test Compressor air temperatures: Daytronic model 9515 digital indicator.

(6) Thermocouple channel caller: Daytronic model 9328 thermocouple channel caller.

(7) Thermocouple signal conditioner: Daytronic model 911K thermocouple conditioner for type K thermocouples.

(8) Analog indicator of scanning valve transducer pressure and temperatures: Honeywell model 1612 Viscorder Oscillograph.

(9) Test Compressor pressures: Gould model PL131TC-10-0-10 psig differential pressure transducer and Gould model PL131TC-50-0-50 psig differential pressure transducer.

(10) Transducer bridge balance unit: Accudata model 105 bridge balance unit.

(11) Amplification of signal current before entering oscillograph: Honeywell model T6GA-500 galvanometer amplifier.

(12) Voltage gain signal amplifier: Beckman amplifier with a Beckman model P-44-A amplifier power supply.

2.6.1 Measurement of Uniformity of Flow in the Test Compressor Inlet

In order to assess the uniformity of flow in the bell-mouth and the Test Compressor inlet, two pitot-static tube rakes were employed as follows:

(1) Large rake consisting of 6 pitot-static heads spaced 1.50 in. apart: this was located in the bell-mouth section.

(2) Small rake consisting of 5 pitot-static heads spaced 0.5 in. apart: this was located in the connecting section between the bell-mouth section and the Test Compressor inlet.

Figure 2.16 shows schematically the location of the two rakes. The design of the probes has been shown in Figures 2.17(a) and 21.7(b). These probes were insensitive to the tangential (or whirl) component of velocity, if any, but it appeared unlikely that the inlet flow had any rotational component.

2.6.2 Special Probes for Use in Two-Phase Flows

The measurement of temperature and pressure of the gas phase in an air-water droplet mixture flow has not been developed adequately to date.

In the current investigation the temperatures at the entry and exit of the Test Compressor during two phase flow operation were measured utilizing standard aspirated thermocouples, namely an United Sensor and Control Corp. type TK-8-C/A-36-F. The Test Compressor outlet thermocouple was self-aspirated because of the relatively large difference between ambient pressure and the Test Compressor discharge pressure. The thermocouple at the inlet to the Test Compressor was connected to a Neptune Products Inc. model 2 Dyna vacuum pump to aspirate the probe since the inlet pressure was always slightly less than the ambient pressure.

As part of the current investigation, a probe for the measurement of static and stagnation pressures in two-phase flows was designed in association with E.G. & G. Idaho, Inc. Details regarding this probe have been given in Appendix 7 of this Report. The probe needed detailed calibration before use, and therefore, was not utilized in the current investigation.

CHAPTER III

THE TEST SERIES

The experimental investigations undertaken may be divided into the following groups.

(1) Calibration of thermocouples and transducers (Section 3.1);

(2) Tests on the Test Compressor with air flow (Section 3.2);

(3) Tests on the Test Compressor with (i) air flow and (ii) air-methane mixture flow (Section 3.3) and

(4) Tests on the Test Compressor with (i) air flow and (ii) air-water droplet mixture flow (Section 3.4).

It may be observed that other than proving tests, no tests were conducted on the Drive Engine. The proving tests were extensive and were undertaken at various times between July 1978 and October 1978, in view of various difficulties that arose in the operation of the engine and the modifications required to overcome them.

It may be recalled that an operating point of the Test Compressor is defined by (a) the mass flow and (b) the speed. The desired mass flow through the Test Compressor was set approximately by opening the Test Compressor Air Throttle Valve (details concerning which are provided in Appendix 3 of this Report) to a desired position. The speed of the Test Compressor was set by regulating the speed of the power turbine in the Drive Engine utilizing the fuel throttle valve.

The air flow through the Test Compressor was measured during each test utilizing the air flow metering nozzle in the air flow metering section located upstream of the Test Compressor. The Test Compressor

Air Throttle Valve was utilized, therefore, to set the air mass flow approximately at the desired mass flow rate.

It may also be pointed out that the performance of the Test Compressor Air Throttle Valve is a function of the local flow conditions at entry to the valve. Those conditions would be different in different tests, for example because of (a) changes in ambient and operating conditions, (b) injection of methane and (c) injection of water. It was also observed that the metal temperature of the Air Throttle Valve also varied during different tests, especially with water ingestion. The air mass flow, as measured by the air flow metering nozzle, would settle down to a steady state value within 2.0 minutes after any change. In other words, a finite, but short, time was required for the Air Throttle Valve to attain a steady state operating condition. However, the Air Throttle Valve was utilized only as a means of regulating the flow through the Test Compressor, and its setting was _not_ employed for determining the flow during a test.

The Test Compressor speed was a linear function of the power turbine speed in the Drive Engine. The power turbine speed was measured utilizing a tachometer which was graduated in 100's of revolutions per minute. The accuracy of speed setting was therefore limited by (a) the tachometer and (b) the steadiness with which the fuel throttle valve could be held at a desired setting. It was observed during all of the tests that the Test Compressor speed could be held within $\pm$ 100 R.P.M. and in most cases to a better accuracy.

In view of the fact that test results were eventually correlated with respect to the corrected speed of the Test Compressor, the speed of operation of the Test Compressor had to be adjusted corresponding to changes in the Test Compressor inlet temperature. While such corrections were generally small during tests with air flow, the correction during water injection could be of the order of several hundred RPM. During tests with air flow, the speed had to be generally increased because of changes in test cell ambient conditions. On the other hand, during water injection, the air flow temperature at the inlet to the Test Compressor

(measured by means of an aspirated thermocouple) generally became reduced, compared to the condition of no-water-injection, and therefore, the speed of the Test Compressor had to be reduced in order to obtain a constant corrected speed during a particular test series.

A discussion on the possible inaccuracies in the operational and performance parameters of the Test Compressor is presented in Section 3.5.

3.1 Calibration of Thermocouples and Transducers

The thermocouples employed in the tests were as follows:
(i)   Standard shielded thermocouples, chromel-alumel junction, with connectors; and
(ii) Standard aspirated thermocouples, chromel-alumel junction, with connectors.

The pressure transducers employed were as follows:
(i)   Differential pressure transducers; and
(ii) Thin film strain gage pressure transducers.

The specifications for the thermocouples and the transducers have been given in Appendix 8 to this Report.

The procedure adopted for the calibration of the thermocouples and the transducers, and the results obtained from the calibration tests have also been given in Appendix 8 to this Report.

3.2 Basic Tests with Air Flow

A map of the performance characteristics of a compressor that corresponded very nearly to the Test Compressor was supplied along with the Test Compressor. It was not clear how far the Test Compressor departed from the one for which performance data were supplied. The performance map presented the overall stagnation pressure ratio and

efficiency as a function of the corrected mass flow for a number of corrected speeds of operation. In view of the fact that a map of the Test Compressor map did not seem to have been generated at any time, it was decided to conduct a series of tests with air flow and obtain a performance map for reference in the current series of tests.

The so-called basic tests with air flow were performed according to the Schedule for Air Flow Tests presented in Table 3.1.

The performance parameters obtained during the tests have been listed in Table 3.2.

Further details regarding this part of the tests have been given in Appendix 9 to this Report.

3.3 Tests with Air-Methane Mixture Flow

The series of tests with air-methane mixture flow were conducted according to the schedule presented in Table 3.3.

The performance parameters obtained during the tests have been listed in Table 3.4.

It may be observed that during this series of tests, the Test Compressor performance parameters were obtained with air flow at each chosen operating condition before the performance parameters with air-methane mixture flow were obtained.

Further details regarding this part of the tests have been given in Appendix 9 to this Report.

3.4 Tests with Air-Water Droplet Mixture Flow

The series of tests with air-water droplet mixture flow were conducted according to the schedules presented in Table 3.5.

TABLE 3.1

SCHEDULE OF AIR FLOW TESTS

Variable	Value or Range
1. Speed	60, 70, 80 and 90 per cent
2. Air flow throttle setting	Five values

TABLE 3.2

PERFORMANCE PARAMETERS MEASURED
DURING AIR FLOW TESTS

		Measured Quantities
I.	Ambient Conditions	Temperature; Pressure; and Humidity.
II.	Compressor Entry Conditions	Static temperature; Stagnation temperature; Static pressure; and Stagnation pressure.
III.	Compressor Exit Conditions	Static temperature; Stagnation temperature; Static pressure; and Stagnation pressure.
IV.	Compressor Speed	Power turbine speed.
V.	Compressor Air Mass Flow at Air Flow Metering Nozzle	Stagnation temperature; Static pressure; and Differential pressure across nozzle.

TABLE 3.3

SCHEDULE OF AIR-METHANE MIXTURE
FLOW TESTS

Variable	Value or Range
1. Speed	60, 70, 80 and 90 per cent
2. Air flow throttle setting	Five values
3. Methane supply pressure	One value.

TABLE 3.4

PERFORMANCE PARAMETERS MEASURED
DURING AIR-METHANE MIXTURE FLOW TESTS

		Measured Quantities
I.	Ambient Conditions	Temperature; Pressure; and Humidity.
II.	Compressor Entry Conditions	Static temperature; Stagnation temperature; Static pressure; and Stagnation pressure.
III.	Compressor Exit Conditions	Static temperature; Stagnation temperature; Static pressure; and Stagnation pressure.
IV.	Compressor Speed	Power turbine speed.
V.	Compressor Air Mass Flow at Air Flow Metering Nozzle	Stagnation temperature; Static pressure; and Differential pressure across nozzle.
VI.	Methane Injection Conditions	Temperature; and Supply pressure at Metering Nozzle.

TABLE 3.5

SCHEDULE OF AIR-WATER DROPLET
MIXTURE FLOW TESTS

Variable	Value or Range
1. Speed	60, 80 and 90 per cent
2. Air flow throttle setting	Five values
3. Water content injected	Four values
4. Water droplet size	Two values

The performance parameters obtained during the tests have been listed in Table 3.6.

It may be observed that during this series of tests, the Test Compressor performance parameters were obtained with air flow at each chosen operating condition before the performance parameters were obtained with water injection.

Further details regarding this part of the tests have been given in Appendix 9 to this Report.

3.5   Accuracy of Test Compressor Operational and Performance Parameters

3.5.1.   Operational Parameters

Uncertainties existed during the tests in regard to the following:
(1)   ambient conditions;
(2)   power turbine speed; and
(3)   throttle setting.

Therefore, although tests were conducted with different in-flow conditions at the same nominal settings of power turbine speed (and therefore, the corrected speed of the Test Compressor) and Test Compressor flow control throttle setting, there was strictly no "one-to-one" correspondence between one operating condition and another in every case. The power turbine speed was adjusted in every case with reference to the Test Compressor inlet temperature so as to obtain the same corrected speed for the Test Compressor for a given series of tests. However, the operation of the air flow control throttle was dependent greatly upon the ambient conditions, the test fluid and the particular operating conditions. At the same time, it should be noted that the air flow control throttle setting was in no case utilized for the measurement of flow rate through the Test Compressor, but only to regulate the flow rate.

TABLE 3.6

PERFORMANCE PARAMETERS MEASURED
DURING AIR-WATER DROPLET MIXTURE
FLOW TESTS

		Measured Quantities
I.	Ambient Conditions	Temperature; Pressure; and Humidity.
II.	Compressor Entry Conditions	Static temperature; Stagnation temperature; and Static pressure.
III.	Compressor Exit Conditions	Static temperature; Stagnation temperature; and Static pressure.
IV.	Compressor Speed	Power turbine speed.
V.	Compressor Air Mass Flow at Air Flow Metering Nozzle	Stagnation temperature; Static pressure; and Differential pressure across nozzle.
VI.	Water Injection Conditions	Water flow rate; and Water collected through drain in the bell-mouth section.

3.5.1.1. Ambient Conditions

The ambient conditions of interest were the following:

(1) atmospheric temperature, pressure and humidity;

(2) temperature of the test cell and air supply ducting; and

(3) pressure and temperature of the injected fluids, namely methane and water.

The duration of a test for obtaining the performance data on the Test Compressor ranged from twenty to forty minutes depending upon whether it was a test with air flow or one with water injection; a methane-injection test took a little less than thirty minutes. During such a period of time, all of the ambient conditions varied to some extent. The atmospheric conditions and the temperature of the injected fluids varied only to a minor extent.

The major changes arose in the temperature of the test cell and therefore in the air supply ducting. Those changes occurred because of the presence of the exhaust ducting of the Drive Engine in the test cell. As a consequence, the temperature of the air supply ducting and the Test Compressor inlet temperature became altered during the duration of a test. It was observed that the Test Compressor inlet temperature varied by about 2^0C during a test with air flow and with air-methane mixture flow, and by about 1^0C during a test with air-water droplet mixture flow. However, it should be noted that (a) sufficient time was allowed for the temperature to stabilize in every test and (b) the temperature at Test Compressor inlet was recorded in each test several times at the end of the period of time allowed for stabilization of temperatures. Nevertheless, some uncertainty existed in regard to the Test Compressor inlet temperature because of continuous heating of the test cell and of the air supply ducting.

3.5.1.2. Power Turbine Speed

The power turbine speed in the Drive Engine was set by adjusting the fuel flow throttle opening which in turn was set by the fuel throttle lever in the control room. The power turbine speed was read on a tachometer graduated in 100-RPM. It was found that the power turbine speed could be held (manually, for the duration of a test) within ± 50 RPM. However, since this was based on visual observation, there was some uncertainty in the speed of the power turbine and hence in that of the Test Compressor.

CHAPTER IV

THE TEST DATA

The compressor performance data obtained during the tests are presented in three parts.

(i)   Performance with air flow;

(ii) Performance with air-methane mixture flow; and

(iii) Performance with air-water droplet mixture flow.

4.1 Performance with Air Flow

The tests were conducted according to the schedule presented in Table 3.1. The performance parameters measured during the tests have been presented in Table 3.2.

The measured values of (i) the compressor stagnation temperature ratio and (ii) the compressor stagnation pressure ratio at different throttle settings and at different speeds have been presented in Figures 4.1 through 4.8. The figures include the uncertainties in the measurements.

4.2 Performance with Air-Methane Mixture Flow

The tests were conducted according to the schedule presented in Table 3.3. The performance parameters measured during the tests have been listed in Table 3.4.

The measured values of (i) the compressor stagnation temperature ratio and (ii) the compressor stagnation pressure ratio at different compressor throttle settings and at different speeds have been presented

in Figures 4.9 through 4.14. No test data have been presented for operation at 70 per cent design speed of the Test Compressor. It was found that there occurred an unusually high amplitude of vibration in the Test Compressor at that speed for all but one throttle setting. Data were obtained for that one low vibration throttle setting, but are not included here. The figures include the uncertainties in the measurements.

4.3 Performance with Air-Water Droplet Mixture Flow

The tests were conducted according to the schedule presented in Table 3.5. The performance parameters measured have been listed in Table 3.6.

The measured values of (i) the compressor stagnation temperature ratio and (ii) the air mass flow at entry to the compressor at different compressor throttle settings and at different speeds for (a) different water injection rates and (b) the two (nominal) sizes of droplets have been presented in Figures 4.15 through 4.24. The figures include the uncertainties in the measurements.

4.4 General Observations

i) During injection of methane, the change in temperature of air at entry to the Test Compressor was about $1.0^{\circ}C$.

ii) During injection of water into the air stream, substantial changes in stagnation temperature at entry to the Test Compressor were recorded by the aspirated probe. These changes necessitated adjustment of the speed of the Test Compressor in order to obtain the same corrected speed for tests at a chosen (air flow regulating) throttle valve setting.

iii) The amount of water ingested into the Test Compressor was obtained as the difference between the amount of water injected into

the air stream and any water collected at the drain located in the bell
mouth section (Figure A.2.1). In every case, it was found that the
amount of water collected at the drain in the bell-mouth section was
very small, less than 5 c.c. per run.

iv) In all of the tests with water ingestion, the discharge air
from the Test Compressor contained water. When the amount of water in
the inlet mixture was under 4.0 per cent, the water in the discharge
air was generally in misty form. With larger amounts of water, it was
observed that there was a continuous flow of water along the wall of
the discharge duct.

v) Each series of tests was conducted at a fixed throttle setting
and a fixed value of operating speed, and then varying the amount of
water injected into the air stream starting (and ending) with the water
injection turned-off. A chosen throttle setting could be expected to
provide different amounts of regulation with different amounts of water
because of (a) change in flow area due to altered mixture temperature,
(b) change in flow area due to presence of water, especially in film
form when the water content was large and (c) change in acoustic speed
due to the presence of water compared to that for air flow only. It
may be recalled that the air flow into the Test Compressor was measured
well upstream of the water injection section. The rate of injection of
water was measured by a rotometer. In each test care was taken to allow
sufficient time for the air flow to become stabilized before test data
were recorded. In other words, the throttle valve regulating the flow
through the Test Compressor was only a means of setting a value of flow
and measurements of air and water flow were done elsewhere.

vi) It was observed in preliminary tests that, when water was
injected, there arose a differential expansion between the Test Com-
pressor and the plenum section following it. A small amount of water
had leaked out of the Test Compressor exit section. The junction was
sealed utilizing RPV-106 adhesive.

vii) During each test, when water was injected into the air stream, it was found that the Test Compressor vibration characteristics became generally worse. The change in amplitude as recorded by the vibration transducer did not seem to depend upon the amount of water, but at certain speeds the vibration reached values in the neighborhood of 1.0 in. per second, compared to about 0.40 in. per second with air flow only. The increased vibration lasted as long as water was being injected but the Test Compressor would return in each case to the original level immediately after the water was turned off.

viii) At a chosen speed of operation, several throttle settings and several water content values at each throttle setting were investi- gated. At low mixture (or gas phase) flow rates, care was taken to prevent surging of the Test Compressor by attention to both throttle setting and water injection rate. Nevertheless the Test Compressor did surge on three or four occasions. It was not possible to establish in every case whether this was due to too low a mixture flow rate setting or too high a water content. At the higher speeds, the Test Compressor generally displayed larger changes in performance with water ingestion and seemed to go into surge mode at low mixture flow rate settings with increased amounts of water. At a low speed, such as 60 per cent of design/speed, changes in performance were small, especially at low mixture flow rate settings, and tests could be carried out even with 10.0 and 12.0 per cent of water in the mixture.

ix) The data presented in Figures 4.15-4.24 were obtained util- izing the aspirated probes at entry and exit sections of the Test Com- pressor. The probes were located at the mid-span sections in the annulus. A thermocouple was also located in the vicinity of the casing wall at the Test Compressor exit section and the output from that thermocouple was recorded in all cases. It was observed that the thermocouple at the casing wall recorded approximately the same temp- erature for given entry (and ambient) conditions. The thermocouple was presumed to be flooded by the water film formed at the casing wall due to centrifuging and to be recording the water temperature.

x) During operation at the low speed of 60 per cent design speed, it was observed that the aspirated probe at the Test Compressor exit section registered nearly the same temperature (within ± 1.0°C) when the water content was about 10.0 per cent or higher. The temperature so registered was within ± 4.0°C of the temperature registered by the thermocouple at the casing wall in the same exit location (Figure 5.7). The aspirated thermocouple was yielding a temperature close to that of water.

xi) The data presented for large droplet ingestion is more extensive than the data presented for small droplet ingestion since it was observed that droplet size changes of the type investigated (90 μm as small droplets compared with 600 μm as large droplets) did not seem to cause appreciable differences in performance. Further discussion of droplet size effects is presented in Chapter V.

CHAPTER V

DISCUSSION, CONCLUSIONS AND RECOMMENDATIONS

The performance data obtained from the Test Compressor tests, as presented in Chapter IV of this Report, were compared with the predictions of performance obtained utilizing the PURDU-WICSTK program.

The Test data and the predicted results have been analyzed in Sections 5.1, 5.2 and 5.3. The conclusions from this investigation have been presented in Section 5.4. The last section, 5.5, is devoted to recommendations for future investigations in this area.

Several aspects of the investigation have been analyzed earlier in References 22 and 23. A more complete analysis of all aspects of the investigation can be found in Reference 24.

The test data consisted of overall performance parameters of the Test Compressor. In the case of tests with air-water droplet mixture flow, only the stagnation temperature ratio across the Test Compressor was measured. The stagnation pressure ratio across the Test Compressor was not measured since calibrated probes for two phase flow were not available.

In all cases the predictions were based on the entry conditions to the Test Compressor as obtained during the tests. The results have been presented utilizing the corrected gas phase mass flow at entry to the Test Compressor and the corrected operating speed. The predicted results take into account the humidity of ambient air. The entry conditions to the Test Compressor were assumed to be uniform in all cases.

In Figures 5.1 through 5.8 the predicted results have been shown at the hub, mean and tip sections.

The predicted results and the test data have been analyzed as follows:

a) Comparison of predictions with test data in the case of operation with air flow, Section 5.1.

b) Analysis of predictions, and comparison of predictions with test data in the case of operation with air-methane mixture flow, Section 5.2.

c) Analysis of predictions, and comparison of predictions with test data in the case of operation with air-water mixture flow, Section 5.3.

It may be pointed out at the outset that the PURDU-WICSTK program was designed for calculation of meanline performance on a one-dimensional basis. The performance at the hub, mean and tip sections is obtained by locating the streamline/stream tube employed for calculation at the appropriate spanwise location.

In dealing with air-methane mixture flow, the PURDU-WICSTK program takes into account the changes in the molecular weight and the ratio of specific heats of the mixture for the chosen value of methane and water vapor content (due to humidity). In addition to the predictions based upon the PURDU-WICSTK program, the changes in the performance of the Test Compressor with air-methane mixture flow were also calculated utilizing the modified UD-300 Code. The latter code and its modifications have been discussed in Reference 22.

In dealing with air-water droplet mixture flow, the PURDU-WICSTK program distinguishes between large and small droplets in respect of (a) flow-blade interactions and (b) centrifugal displacement of droplets. Details have been provided in Reference 23.

In the following (and also everywhere else in the Report) the flow coefficient always refers to the flow coefficient at entry to the Test Compressor corresponding to the gas phase flow and the local conditions of pressure and temperature. The corrected conditions are always based on the mixture stagnation temperature and the gas phase stagnation pressure.

In presenting the test data and the predictions for the case of water ingestion, the water content in the mixture is expressed as a mass fraction; thus, water content given as X_w per cent implies that the fraction of water in the mixture is X_w.

The experimental studies with water ingestion were conducted utilizing air and water at ambient conditions. When water was injected, there occurred a reduction in the stagnation temperature of the gas phase at entry to the Test Compressor. The test data and the predictions have been presented based on the local conditions at entry to the Test Compressor, but corrected with respect to standard temperature and pressure conditions.

It may be recalled that provision existed in the test set up for obtaining a desired temperature at entry to the Test Compressor by mixing, for instance, heated air with ambient or laboratory supply air so as to obtain the same value of stagnation temperature at entry to the Test Compressor whether or not water was injected. Such tests were not undertaken during the current series of tests.

5.1 Operation with Air Flow

The performance of the Test Compressor with air flow was predicted at 100 per cent design speed utilizing (i) the UD-300 program (Reference 25) and (ii) the PURDUE-WICSTK program (Reference 23). The predicted values of overall stagnation temperature ratio and overall stagnation pressure ratio have been compared in Figures 5.1 and 5.2, respectively. Each performance parameter is shown as a function of

corrected mass flow. The differences in predictions arise on account of the differences between the two codes, the PURDU-WICSTK program not incorporating the three dimensional effects that have been taken into account in the UD-300 program.

The predictions according to the two codes were compared with the predictions provided by the U.S. Air Force. The latter, shown in Figure 5.3, were not clearly identified with a spanwise location on the blade and may have represented the mean performance.

The test data obtained during the current investigation have been presented in Figures 4.1 through 4.8 for different rotating speeds. The overall stagnation temperature ratio and the overall stagnation pressure ratio were compared with the predictions obtained utilizing the PURDU-WICSTK program. Figures 5.4 and 5.5 provide a comparison between predictions and test data for stagnation temperature ratio and stagnation pressure ratio, respectively, each shown as a function of corrected mass flow and corrected speed. In view of uncertainties in the location of probes at the exit section of the Test Compressor, the predictions have been shown at three sections along the span, namely hub, mean and tip.

The PURDU-WICSTK program yields predictions generally compatible with measured performance. The differences between the mean of the predicted values and the experimentally determined values show no noticeable trends.

5.2 Operation with Air-Methane Mixture Flow

A compressor may operate with air-water vapor mixture flow under two circumstances: (i) when there is a high value of humidity in the intake air, especially at high temperature, and (ii) when there arises a phase change of water during water ingestion. In the latter case, when the phase change is complete at a particular stage within the

compressor, the remaining downstream stages operate entirely with air-water vapor mixture. Preliminary calculations showed that the Test Compressor could not be expected to operate with a total phase change of ingested water within the compressor except at unrealistically high inlet temperatures. However, it was considered of interest to establish the nature of changes that would arise in performance with high humidity values in air at entry to the Test Compressor.

Table 5.1 presents the saturation values of water vapor corresponding to various possible inlet and inter-stage stagnation temperature and stagnation pressure conditions. It may be observed from Part A of that table that the water vapor content may reach fairly high values at the inlet to a compressor. In Part B of the table, the saturation values of water vapor are shown to become indefinite beyond a value of stagnation temperature equal to $100^{\circ}C$ irrespective of the value of stagnation pressure. The amount of water vapor that may arise under those conditions depends upon the amount of water present locally and the heat and mass transfer processes. Under certain conditions, it is also possible to visualize the occurrence of supersaturation conditions locally.

Tests were proposed to be conducted with air-water vapor mixture, but could not be undertaken due to the nonavailability of a boiler, as stated earlier. An air-methane mixture flow was considered as a substitute for air-water vapor mixture flow based on similarities in the relevant physical properties such as molecular weight and specific heats (Reference 22). However, there are still differences between the two types of mixtures.

5.2.1 Predictions with Air-Methane Mixture Flow

The performance of the Test Compressor with air-methane mixture flow was predicted at 100 per cent design speed utilizing (i) the UD-300 program (Reference 25) and (ii) the PURDU-WICSTK program (Reference 23). The predicted values of overall stagnation temperature ratio and overall stagnation pressure ratio have been compared in

TABLE 5.1

SATURATION VALUES OF WATER VAPOR
UNDER TYPICAL CONDITIONS

| TEMPERATURE | PRESSURE | WATER VAPOR | |
| | | w_s | w_s^* |
$(^\circ F)$	(psi)	$\left(\dfrac{lb_m,\ vapor}{lb_m,\ dry\ air}\right)$	$\left(\dfrac{lb_m,\ vapor}{lb_m,\ mixture}\right)$
59	14.696	0.011	0.011
86	14.696	0.027	0.026
104	14.696	0.049	0.047
$125.4^{(1)}$	$22.402^{(4)}$	0.060	0.057
$155.8^{(2)}$	$22.402^{(4)}$	0.148	0.129
$176.1^{(3)}$	$22.402^{(4)}$	0.275	0.216
$65.1^{(5)}$	$12.648^{(6)}$	0.025	0.024
212	15.698	9.124	0.901
212	15.494	11.459	0.920
212	15.365	13.661	0.932

Note: Condition corresponding to

($_1$) Mach number = 0.8 when T = $59^\circ F$

($_2$) Mach number = 0.8 when T = $86^\circ F$

($_3$) Mach number = 0.8 when T = $104^\circ F$

($_4$) Mach number = 0.8 when p = 14.696 psi

($_5$) Mach number = 0.8 when T = $5.55^\circ F$ ⎤
($_6$) Mach number = 0.8 when p = 8.298 psi ⎦ 15,000 ft. altitude

Figures 5.6 and 5.7, respectively. Each performance parameter is shown as a function of corrected mass flow. The corrected mass flow, the overall stagnation temperature ratio and the overall stagnation pressure ratio decrease with air-methane mixture flow compared with air flow. It may be observed that the UD-300 program, in view of the large computer times required to operate it, was exercised only at selected values of mass flow rate for the purposes of comparison with predictions based on the PURDU-WICSTK program. The difference in the predictions according to the two codes arise because of the three dimensional effects taken into account only in the UD-300 program.

5.2.2 Comparison of Predictions with Test Data

The test data obtained during the current investigation have been presented in Figures 4.9 through 4.14. The overall stagnation temperature ratio and the overall stagnation pressure ratio were compared with the predictions obtained utilizing the PURDU-WICSTK program. Figures 5.8 and 5.9 provide a comparison between predictions and test data for overall stagnation temperature ratio and overall stagnation pressure ratio, respectively, each shown as a function of corrected mixture mass flow and corrected speed. The test data display the same trends as the predictions. The effect of adding methane to the flow was accounted for in the PURDU-WICSTK program through appropriate changes in the molecular weight and the specific heats. It may be observed that the PURDU-WICSTK program predicts the trend of changes with the presence of methane reasonably satisfactorily.

5.2.3 Comparison of Performance with Air-Methane Mixture Flow and Air-Water Vapor Mixture Flow

In order to illustrate the difference between air-methane mixture flow and air-water vapor mixture flow, calculations were undertaken for the Test Compressor, utilizing the PURDU-WICSTK program, under the following conditions:

Operating speed...90 per cent design speed;

Water vapor or Methane content 1.0 and 2.0 per cent by weight. Figures 5.10 and 5.11 present a comparison between air flow, air-methane mixture flow and air-water vapor mixture flow for overall stagnation temperature ratio and overall stagnation pressure ratio, respectively. The amount of methane and water vapor was 2.0 per cent each for the calculations illustrated in those figures. The predictions have been shown for the hub, mean and tip sections of the Test Compressor.

The comparisons have also been provided in Figures 5.12 and 5.13 where the changes in overall stagnation temperature ratio and in overall stagnation pressure ratio, respectively, have been shown as a function of methane and water vapor content in the mixture.

It may be observed that the changes in the performance with air-methane mixture flow are larger than the changes with air-water vapor mixture flow. This trend is justified by noting that the molecular weight and ratio of specific heats for water vapor are closer to those of air than they are for methane, while both gases are vastly different from air. The changes produced by 2.0 per cent by weight of methane in the air-methane mixture flow in respect of the Test Compressor performance can be shown to correspond to roughly 2.4 per cent by weight of water vapor in an air-water vapor mixture flow. No simple scaling of the effects of the presence of methane and water vapor is feasible in a multistage compressor such as the Test Compressor.

5.3 Operation with Air-Water Droplet Mixture Flow

The predictions of the performance of the Test Compressor with water ingestion have been carried out utilizing the PURDU-WICSTK program. The test data obtained with air-water droplet mixture flow have been presented in Figures 4.15 through 4.24. It may be recalled that during the tests, at each speed and throttle setting water, injection into the air stream (and therefore, water ingestion into the Test

Compressor) was varied over a wide range starting from zero per cent. Both large (600 μm nominal diameter) and small (90 μm nominal diameter) droplets were utilized using different injectors. In the case of injection of large droplets tests were conducted at 90, 80 and 60 per cent of design speed, while in the case of injection of small droplets tests were conducted only at 90 and 80 per cent of design speed. When water was injected into the air stream, there was a reduction in the compressor inlet stagnation temperature, and the compressor operating speed was adjusted to obtain the same corrected speed for each throttle setting. Measurements were made only of (i) the air mass flow upstream of the water injection section, (ii) the mass flow of water injected and actually ingested into the Test Compressor, (iii) the overall stagnation temperature ratio across the compressor and (iv) the static temperature at the casing wall in the exit section of the compressor.

A set of comparisons between the predictions and the test data has been presented in the following figures:

Figures 5.14: Overall stagnation temperature ratio as a function of corrected speed and corrected gas phase mass flow at entry utilizing as a parameter the mass fraction of water in the air-water droplet mixture for the case of injection of large droplets.

Figure 5.15: Overall stagnation temperature ratio as a function of corrected speed and corrected gas phase mass flow at entry utilizing as a parameter the mass fraction of water in the air-water droplet mixture for the case of injection of small droplets.

In both of those figures the predicted overall stagnation temperature ratio has been presented at the hub, mean and tip sections. The predictions were carried out in each case corresponding to the inlet conditions obtained during the tests taking into account the humidity of ambient air.

The test data for the changes in gas phase mass flow during water ingestion have been summarized in the following figures:

Figure 5.16: Corrected gas phase mass flow as a function of water content and corrected speed for the case of large droplet ingestion.

Figure 5.17: Corrected gas phase mass flow as a function of water content and corrected speed for the case of small droplet ingestion.

The following observations may be made from Figures 5.14 through 5.17:

(i) The predictions obtained utilizing the PURDU-WICSTK program confirm the trends in changes of overall stagnation temperature ratio and gas phase corrected mass flow as obtained during the tests.

(ii) Water ingestion decreases the gas phase mass flow into the compressor at the same speed and throttle setting.

(iii) Water ingestion decreases the overall stagnation temperature ratio across the compressor, and hence the work absorbed by the working fluid, at all speeds and throttle settings.

(iv) The changes in gas phase mass flow and overall stagnation temperature ratio are larger at higher speeds than at lower speeds.

(v) The changes in gas phase mass flow and overall stagnation temperature ratio at a given speed are greater at larger flow rates. The changes are much smaller towards the surge condition, although the occurrence of surge itself is affected.

(vi) Within the range of variation of nominal droplet size during the tests, from 90 μn to 600 μm, the effect of change in droplet size appears negligible in the Test Compressor.

Other observations made during the tests have been described in Section 4.4 of this Report.

5.3.1   Changes in Stagnation Temperature, Water Content and Water Vapor Content along the Test Compressor

During water ingestion into a compressor there arises at each opearting condition a redistribution of the content of water and vapor in the mixture along the compressor. Because of centrifugal action, the hub section of the compressor becomes depleted of water and there arises a progressive accumulation of water towards the tip region.

The local water content affects in each stage of the compressor (i) the aerodynamic performance of the stage and (ii) the heat and mass transfer processes. The manner in which the stagnation temperature of the gaseous phase varies along the compressor at the hub or the tip section becomes quite different with water ingestion from the manner in which it would vary while the compressor operates with air flow. The temperature of water also varies along the compressor. Finally, the water vapor content changes along the compressor causing changes in the total mass flow of the gaseous phase. It may be pointed out that while the centrifugal action is independent of both the water content and the mean droplet size, the aerodynamic performance and the heat and mass transfer processes are functions of those two parameters.

In order to illustrate the nature of the changes, calculations performed utilizing the PURDU-WICSTK program have been illustrated in the following figures for the case of Test Compressor operation at 90 per cent design speed and a particular throttle setting corresponding to a flow coefficient of 0.48 with the water being in the form of large droplets.

> Figure 5.18:   Change in water content along the compressor at the hub, mean and tip sections.
>
> Figure 5.19:   Change in vapor content along the compressor at the hub, mean and tip sections.
>
> Figure 5.20:   Change in the stagnation temperature along the compressor at the hub, mean and tip sections.

The following observations may be made from Figures 5.18 through 5.20:

(i) The hub section becomes depleted of water in the first few stages of the Test Compressor and then yields a performance corresponding to air-water mixture flow.

(ii) The tip section is most strongly affected on account of the accumulation of centrifuged water.

(iii) The mean section appears to remain unaffected. However, it should be noted that if the three dimensional flow effects are fully accounted for, some changes will be observed even at the mean section.

(iv) Changes in water content due to centrifugal action are independent of the initial water content. However, the heat and mass transfer processes depend upon the absolute content of water. Thus in the later stages of the compressor, the change in water content is affected by the mass transfer process.

(v) Changes in vapor content show recognizable trends.

5.3.2 Temperature Rise Ratio Factor

In order to illustrate the change in the stagnation temperature rise and thus in the work absorbed by the working fluid with different amounts of water in the mixture, a temperature rise ratio factor, TRRF, was defined as follows:

$$TRRF = \left[\left(\frac{\Delta T_0}{T_{0_1}} \right)_A - \left(\frac{\Delta T_0}{T_{0_1}} \right)_M \right] \bigg/ \left(\frac{\Delta T_0}{T_{0_1}} \right)_A \qquad (5.1)$$

where ΔT_0 refers to the stagnation temperature rise, T_{0_1} is the stagnation temperature at inlet to the Test Compressor. It may be recalled that at a given throttle setting and speed of operation of Test Compressor, injection of water into the air stream caused a reduction in T_{0_1}. The TRRF as defined in Equation 5.1 takes into account such changes.

Figures 5.21 through 5.23 provide a comparison between predictions and measured data of the TRRF at 90, 80 and 60 per cent speeds, respectively, for the case of ingestion of large droplets. In each case the

predicted results are presented for selected values of flow coefficient and at the hub, mean and tip sections.

The following observations may be made from those figures:

(i) Increasing amounts of water content caused increasing changes in the TRRF at all values of flow coefficient.

(ii) At a given value of water content, a decrease in the flow coefficient caused decreasing amount of changes in the TRRF.

(iii) The variation of TRRF with flow coefficient appears to be small at low and comparatively large values of water content ingested. At low values, the absolute amount of water is small at all values of flow coefficient, and therefore, the overall effect of the presence of water may be small and constant. At large values of water ingestion, the absolute amount of water is comparatively large at all values of flow coefficient, and therefore, the overall effect of the presence of water may be large, but again nearly constant for all values of flow coefficient. It is possible to visualize, through extrapolation, that eventually at very large values of water ingestion there may arise a single value of TRRF for a range of values of speed and flow coefficient.

(iv) When the flow coefficient was low, the TRRF seemed to become somewhat erratic indicating that several of the stages might be stalled and the Test Compressor might be tending towards a surge condition. For example at 90 per cent design speed, the magnitude of TRRF corresponding to a flow coefficient of 0.42, as shown in Figure 5.21 for large droplet ingestion, is multiple valued at both 4.0 per cent and 6.0 per cent of water content.

(v) While the aspirated probes employed for obtaining the stagnation temperature were located at the mid-span section both at the inlet and the outlet, the measured TRRF value did not always correspond to the predicted TRRF value at the mean section.

5.3.3 Interaction of Individual Processes during Water Ingestion

The predictive scheme for establishing the changes across a stage for given initial and operating conditions takes into account (a) the

aerodynamic performance of the stage with two phase flow, (b) the centrifugal action, (c) the heat and mass transfer processes and (d) the droplet size change processes. A series of limiting cases were generated as follows in order to establish the relative impact of those processes on the overall performance change in the Test Compressor in terms of changes in the TRRF:

i)   Case 1: including all of the processes
ii)   Case 2: neglecting only the heat and mass transfer processes
iii) Case 3: neglecting only centrifugal action
iv)   Case 4: neglecting both heat and mass transfer processes and centrifugal action, thus accounting only for aerodynamic changes

Those limiting cases were calculated under the following conditions: 90 per cent and 60 per cent of design corrected speed with various values of flow coefficient and water content, all of them for the case of large droplet ingestion.

The predictions have been presented in the following figures:

Figure 5.24: TRRF versus water content at the hub, mean and tip sections for operation at 90 per cent design speed and flow coefficients of 0.44, 0.46, and 0.48.

Figure 5.25: TRRF versus water content at the hub, mean and tip sections for operation at 60 per cent design speed and flow coefficients of 0.36, 0.40, and 0.44.

In addition, for the case of operation at 90 per cent design speed, the test data for TRRF have been compared with predictions for the four theoretical cases in Figure 5.26.

The following observations may then be made from Figures 5.24 through 5.26.

(i) The predicted TRRF values at the tip section are the largest at both of the speeds for all values of flow coefficient considered and in all of the four limiting cases. This is due to the largest values of water content occurring in that section because of the centrifugal

action on droplets. The influence of individual processes, as illus-
trated by the TRRF values for the four limiting cases, is clearly
identifiable in the tip region.

(ii) The predicted TRRF values at the mean section are inter-
mediate between the values at the tip and the hub sections. The model
for centrifugal action in the one-dimensional analysis is such that
the content of water is unaffected at the mean section. It appears
that Cases (1) and (3) are generally distinguishable from Cases (2) and
(4) in all of the predictions at the mean section. The predicted values
for Cases (1) and (3) are nearly identical because the centrifugal
action does not influence the mean section. That the predicted values
for Cases (2) and (4) are nearly identical is easily understood since
they both account only for the aerodynamic changes at the mean section.

(iii) The predicted TRRF values at the hub section are the least
different from zero compared to the other sections. The centrifugal
action depletes the hub section of water within the first one or two
stages (as can be seen in Figure 5.18), thus leaving the balance of the
compressor to operate with the gas phase only at the hub section. It
appears that Cases (1) and (2) are generally distinguishable from Cases
(3) and (4). This can be readily unde stood by noting (a) the manner
in which centrifugal action depletes water from the hub section and
(b) the significance of interphase heat and mass transfer processes
only when water is present. It is also noteworthy that the TRRF values
differ very little from zero at the hub section for Cases (1) and (2),
and may in fact attain slightly negative values at large values of water
content at compressor inlet, thus indicating a gain in work input to
the compressor fluid. This is due to the temperature and gas phase mass
flow change in the first stage and therefore may be design-specific for
the Test Compressor.

(iv) The experimental data presented in Figure 26 are overall
values of the TRRF at different values of water content ingested into
the Test Compressor and at different flow coeffic:ents. It may be
pointed out that Figure 25 applies to a fixed value of speed, namely 90
per cent design speed, and therefore the centrifugal action itself is

constant whatever the water content or the flow coefficient. (However, the effect of centrifugal action, through a change in the flow coefficient, on the work input is not constant at different values of water content.) The experimental data could not be analyzed in terms of the individual processes since the necessary measurements were not made in that detail. However, the predictions appear to underpredict the TRRF at all values of water content ingested. Considering the experimental data with the predictions shown in Figure 5.26, it can be concluded that at the larger values of water content, the heat transfer is under-predicted and at the lower values of water content, the centrifugal action and therefore the aerodynamic losses are underpredicted.

5.3.4 Surging of the Test Compressor

In the course of the experiments, the Test Compressor accidentally went into a surge condition three or four times, but no specific investigations were conducted in the surging condition. At each speed of operation, the water content was increased at low flow coefficient values until it was felt that a surging condition was imminent. The value of content of water at which the compressor surged at a chosen value of flow coefficient and operating speed was not established.

In the predictive scheme, no specific criterion was introduced for the occurrence of surge. The various processes occurring during water ingestion are nonlinearly coupled. The entry conditions to any following stages cannot be scaled with respect to changes in the entry conditions to the first stage in a multistage compressor. Considering, for example, operation of the Test Compressor at a chosen value of flow coefficient, namely 0.44, and speed, namely 90 per cent design speed, if the water content is changed from 4.0 per cent to 6.0 per cent, the change in the entry conditions to the third stage, for instance, cannot be obtained by any method of scaling. A detailed stage-to-stage calculation under the new entry conditions is required. The initial design of various stages of the compressor play a significant role in the outcome of such a stage-to-stage calculation.

In order to illustrate roughly the effect of water ingestion when the Test Compressor tends towards a surge condition at different speeds, Figure 5.27 was constructed based on the predictions obtained for the TRRF utilizing the PURDU-WICSTK program. In that figure, the corrected gas phase mass flow at entry to the Test Compressor has been normalized by the corrected mass flow corresponding to the peak-pressure value at each speed. The TRRF values have been presented for various values of water content in the mixture at each operating speed. It must be emphasized that the TRRF values were obtained with the change in gas phase temperature resulting from the injection of water.

5.3.5 Water Ingestion into Jet Engines

When water is ingested into a jet engine, the performance of each component of the engine may become affected and hence there may arise (a) a mismatch in the equilibrium running of the engine and (b) a change in the surge margin. Considering the compressor of the engine, three types of changes may be recognized depending upon whether and how much of the water undergoes a change of phase. When the conversion of water into vapor is due only to the attainment of thermodynamic equilibrium, without large changes in gas phase enthalpy, the diffuser and the combustor following the compressor may have to operate with water in the flow. The turbine and the nozzle may also have to operate with water when the initial water content has been large and there does not arise a total change of phase of water in the combustor. On the other hand, when substantial quantities of water undergo evaporation, there will arise (a) a change in the gas phase stagnation temperation and (b) an increase in the vapor content of the mixture and hence in the gas phase mass flow at the exit of the compressor. Two regimes of operation may be considered in that case: (i) when there is evaporation of a part of the water and there remains some water at the exit of the compressor and (ii) when there is total conversion of water into vapor in the compressor, either at the exit or at an intermediate stage.

The presence of water in the flow through a combustor may lead to flame extinction in the burner. The operation of the diffuser, the combustor, the turbine and the nozzle are also affected by the presence of water vapor in various ways.

In all of the cases, the equilibrium running of the engine and the available surge margin may be affected due to the following changes in the engine compressor:

(i) Changes at the inlet to the compressor in (a) mass flow, (b) temperature, (c) pressure and (d) uniformity of flow conditions.

(ii) Changes at the compressor exit in (a) mass flow, (b) temperature, (c) pressure and (d) variation of flow properties spanwise and circumferentially.

The current compressor test program with water ingestion was conducted with the Test Compressor driven mechanically by a Drive Engine with an independent power shaft. Accordingly, the Test Compressor data may only be utilized indirectly to determine the behavior of an engine suffering water ingestion into its compressor.

The test data and the predictions show that the effects of water ingestion on jet engines may be scaled even qualitatively only among individual classes of engines. The engines may be classified, from the point of view of effects of water ingestion, based upon the following design values:

(i)   speed,

(ii)   compressor pressure ratio,

(iii) engine pressure ratio, and

(iv)   bypass ratio.

In general, the effects of water ingestion have to be determined in each case although some universal trends can be foreseen; for example, with respect to the mismatch between the components, the changes in surge margin and the response to fluid state and flow distortion in various components.

5.4 Conclusions

The conclusions may be divided broadly into the following categories:

1) Phenomenological considerations, Section 5.5.1;

ii) Experimental findings, Section 5.5.2; and

iii) Predictive capability, Section 5.5.3.

5.4.1 Phenomenological Considerations

1) The processes occurring in a compressor stage with water ingestion may be analyzed with respect to (a) the state of the fluid, (b) the initial design of the blading and (c) the operational parameter. The state of the fluid is determined by (i) the composition, air, water vapor and water, (ii) the state of water, principally the mean droplet size and (iii) the inlet temperature and pressure. In regard to the initial design of blading, the parameters of interest are (i) the geometry of the blading and its variation along the span, (ii) the aspect ratio and (iii) the hub radius. The operational parameters are the flow coefficient and the speed.

2) The interaction between blading and the air-water mixture requires consideration of (i) droplet ingestion trajectory, (ii) droplet impact and rebound from the blades, (iii) film formation on the blades, (iv) reingestion of water into the wakes and (v) droplet size adjustment.

3) In view of the presence of rotating blades and the whirl component of velocity of the mixture, the redistribution of water and vapor due to centrifugal action is an extremely important factor. Centrifugal action diverts water towards the tip region and water vapor towards the hub region. Gravitational action is negligibly small in comparison with centrifugal action.

4) The difference between the gas and the liquid phases causes heat and mass transfer processes. The magnitude of those processes depend upon (i) the difference in temperatures between the gas and the liquid phases, (ii) the water temperature, (iii) the vapor content, (iv) the gas pressure, (v) the absolute content of water and (vi) the mean droplet size.

5) The droplets can be expected to follow the gas phase trajectory only in the final stages of decay in size. Until they attain such a size, the various processes associated with the discreteness of droplets can be assumed to be independent of their size.

6) A compressor stage tends towards a surge condition at low flow coefficients, especially in the tip region, as the amount of water is increased. At large flow coefficients, a choking condition sets in as the amount of water is increased. The influence of the change in acoustic speed of the mixture has also to be taken into account in estimating the choking condition.

7) The phenomenology of compressor processes with water ingestion can be analyzed in three regimes: (i) prior to setting in of boiling of water, (ii) following the commencement of boiling of water and (iii) completion of phase change of liquid to vapor everywhere. In regime (ii), there arises a large change in gas phase and liquid phase (a) mass flow and (b) temperature and also a change in gas phase composition. In regime (iii) one is dealing with a mixture of air and water vapor.

8) The performance of a compressor stage is adversely affected by the presence of water as well as by the presence of water vapor, although for entirely different reasons. In regime (ii) of item (7) above, the adverse effects are compounded in various ways.

9) In a multistage compressor, the changes in the performance parameters of any stage and in the intensity of the various processes

depend upon the entry conditions to that stage. The change over from regime (i) to regimes (ii) and (iii) (as described in item (7) above) depends upon the extent of changes and the length of residence time of the mixture along the compressor.

10) It is in general not possible to derive simple scaling laws for the performance of (a) a given compressor under vastly differing operating conditions or (b) largely dissimilar compressors.

5.4.2 Experimental Findings

1) The experimental studies have been limited by (a) the physical size of the Test Compressor, (b) the low pressure ratio across the compressor at design condition and (c) the nonavailability of sufficiently small, calibrated probes for use in two phase flows. In the measurement of overall changes across the Test Compressor, there was always some ambiguity about a precise definition of the spanwise station at which the measurement applied, especially at the exit plane and during air-water mixture flow. The pressure ratio across the Test Compressor was too low to permit operation of the Test Compressor in other than the regime where no boiling of water occurred - (Regime (i) as described under item 7 of Section 5.5.1).

2) The overall performance parameters are adversely affected by the ingestion of water both by a reduction in the gas phase mass flow and also in the work input absorbed by the mixture.

3) The effects of water ingestion were more severe at higher speeds and larger mass flow at any speed.

4) The influence of flow coefficient on the amount of work input absorbed by the fluid could be illustrated in terms of a temperature rise ratio factor (TRRF). In particular the tendency towards (a) surging at low flow coefficients and (b) choking at high flow coefficients

with large amounts of water ingestion was clearly brought out by the use of the TRRF.

5)   The differences in performance parameters due to change in droplet size of water injected into the air stream (90 µm and 600 µm mean diameter) were negligibly small.

6)   The amount of water collected in the bell mouth section located between the Test Compressor and the water injection ring was negligibly small in all cases, indicating that nearly all of the water injected into the air stream was ingested into the Test Compressor. Thus the bell mouth entry section was found to be suitable.

7)   A film of water formed in all cases at the exit section of the Test Compressor casing wall as indicated by the nearly constant temperature recorded by a thermocouple at the casing wall.

8)   The overall performance parameters (mass flow, overall stagnation temperature ratio and overall stagnation pressure ratio) are adversely affected by the injection of methane at all speeds and flow coefficients compared to the values obtained with air flow.

5.4.3 Predictive Capability

The PURDU-WICSTK program which has been developed and utilized for the prediction of compressors performance is a (one-dimensional) meanline code. By shifting the meanline to the desired spanwise section, at the hub, mean or tip section of the compressor, the performance of the compressor at that section can be determined for given initial and operating conditions. The most important drawback of this scheme is that the radial spread of stream tubes is not accounted for, thus introducing errors especially in the calculation of redistribution of water due to centrifugal action and the resulting changes in other parameters.

1) The predicted results obtained by utilizing the PURDU-WICSTK program show the same general trends as the experimental results obtained during (a) air-methane mixture flow and (b) air-water mixture flow.

2) In terms of the three principal processes associated with two phase fluid flow that have been incorporated into the model, namely aerodynamic performance changes, redistribution of water due to centrifugal action and heat and mass transfer processes, centrifugal action and the resulting redistribution of water content have the major influence on compressor performance changes.

3) The aerodynamic performance changes due to blade-two phase flow interactions can be separated from the other processes.

4) Unless the water content is small and the pressure ratio is large in a compressor, the heat and mass transfer processes are not as dominant as centrifugal action.

5) When the water content is very small, there is a similarity between the effects produced by the presence of water and that of water vapor.

6) The general trend of performance changes with air-steam mixture flow compared with air flow is the same as that of changes with air-methane mixture flow, although the latter changes are larger in magnitude.

5.5 Recommendations

1. The development of measurement techniques is of the greatest urgency in droplet-laden flows. The four major quantities that require measurement in a compressor environment are the following:

    (i)   temperatures of the two components of the flow;

    (ii)   pressure of the gas phase;

(iii)   vapor concentration;

(iv)   water content distribution; and

(v)   water droplet size and velocity distributions.

Both imbedded and non-intrusive instrumentation need further development.

Regarding temperature and pressure of the gaseous phase, both stagnation and static values are required.

The vapor and water content distributions can be determined utilizing concentration probes.

In droplet-laden flows the distributions of droplet size and velocity are generally important parameters. In the problem of water ingestion into a compressor, the droplet size distribution is of especial significance (a) at entry to each stage of a compressor and (b) during the final stages of vaporization of droplets when such inter-phase heat and mass transfer processes arise. The droplet velocity distribution needs to be related to the size distribution. The size and velocity distributions affect the flow-blade interactions. It appears extremely complicated to undertake the measurement of size and velocity distributions except at the inlet and outlet sections of a compressor and possibly, of a compressor stage.

An important aspect of the development of probes is the need for extensive calibration in well-defined flows.

2. Diagnostic studies pertaining to overall performance changes are required in multistage and single-stage compressors utilizing the probes developed under item (1) above.

A small multistage compressor, while not permitting adequate interstage and spanwise resolution, has the advantage of being operated with controlled inlet conditions, especially the inlet temperature and humidity values.

The effects of (a) increased physical size and (b) stage characteristics can be studied with single stage machines.

3. The analysis of a compressor flow field needs extension taking account of the three-dimensional flow field.

The analysis based on the identification of the following processes has proved useful:
    (i)   aerodynamic performance changes with two phase flow, including effects of fluid composition and blade-flow interactions;
    (ii)   centrifugal action on droplets and water vapor;
    (iii) inter-phase heat and mass transfer processes; and
    (iv)   droplet-size readjustment.
Those processes are significant both in small, high rotating speed, low pressure-ratio compressors as well as in large, comparatively low rotating speed, high pressure ratio compressors, although the influence of the various processes may be different in magnitude. Thus, inter-phase heat and mass transfer may become dominant in high pressure ratio compressors and affect the droplet size distribution, the vapor content and the aerodynamic performance of the blades. A small compressor, on the other hand, may be affected most directly by the centrifugal action on droplets and the local water content.

In all cases, the radial displacement of streamlines and the spanwise redistribution of the fluid mixture are of crucial importance. They may be taken into account adequately only through a three-dimensional flow analysis.

4. The PURDU-WICSTK program which takes into account each of the governing processes at a fundamental level is suitable (a) for the calculation of overall performance of a compressor and (b) for establishing the relative influence of different processes within a compressor. The program is a mean-line stage-stacking code and therefore may be utilized

at any desired spanwise location. It does not, of course, account for three-dimensional effects.

The program is also adaptable for a compressor incorporating a fan with a second stream of air.

The program, furthermore, permits taking into account bleeds where they are used.

An extensive use of the PURDU-WICSTK program in estimating the performance of different (small and large) compressors will aid in the evolution of a standard code for the estimation of the performance of a compressor with water-ingestion, that is adequate for other studies on overall engine performance. In particular, the predictions will be useful in the design of control systems.

5. An important aspect of the development of an analysis and a numerical code for the estimation of performance of a compressor with water ingestion is the unavoidable empiricism in regard to (i) two phase flow-blade interactions, (ii) the fluid state in the vicinity of casing walls and (iii) compressibility effects arising on account of the presence of droplets. A hybrid-analytical approach is necessary in regard to those.

An investigation on a single-stage machine of sufficiently large size with adequate flexibility in (i) blade setting, (ii) inter-stage spacing, (iii) rotating speed and (iv) inlet conditions is required.

6. A compressor, whatever the working fluid or the number of stages, suffers two critical conditions at each speed of operation, namely (i) surging and (ii) choking. Detailed experimental and analytical studies are required to understand and to quantify the physical processes underlying the phenomena occurring under those conditions.

7. Two mechanical effects of water ingestion into a compressor are (i) the differential thermal expansions at the joints and (ii) the aero-elastic vibrations. The latter requires further study, especially under the critical conditions referred to in item (6), with particular attention to (a) flow-blade interactions including impact and reingestion of droplets and (b) fluid compressibility changes.

FIGURES
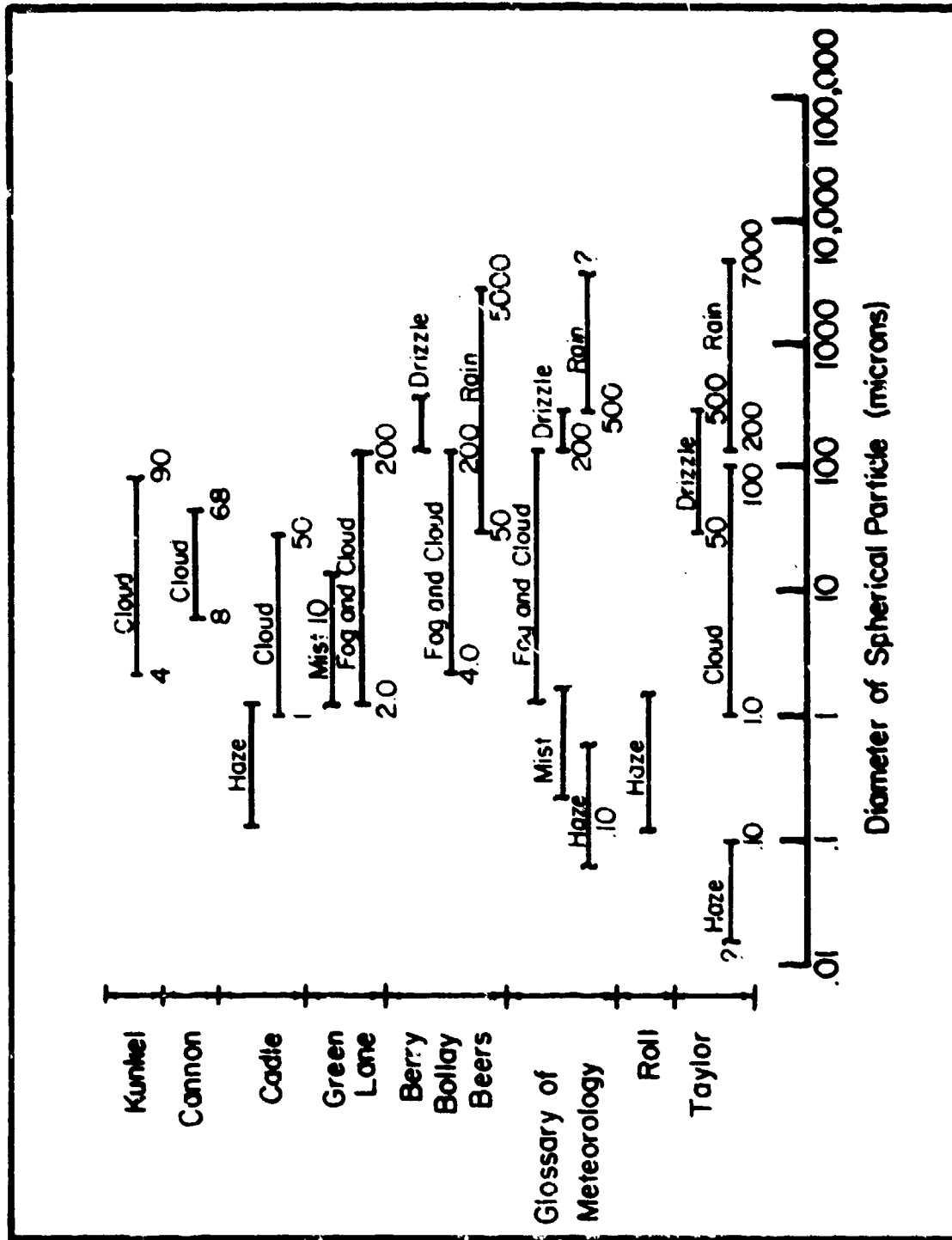
Figure 1.1   Droplet Size Range in Mist and Rain

Figure 2.1   Photograph of Drive Engine and Test Compressor
            Assembly
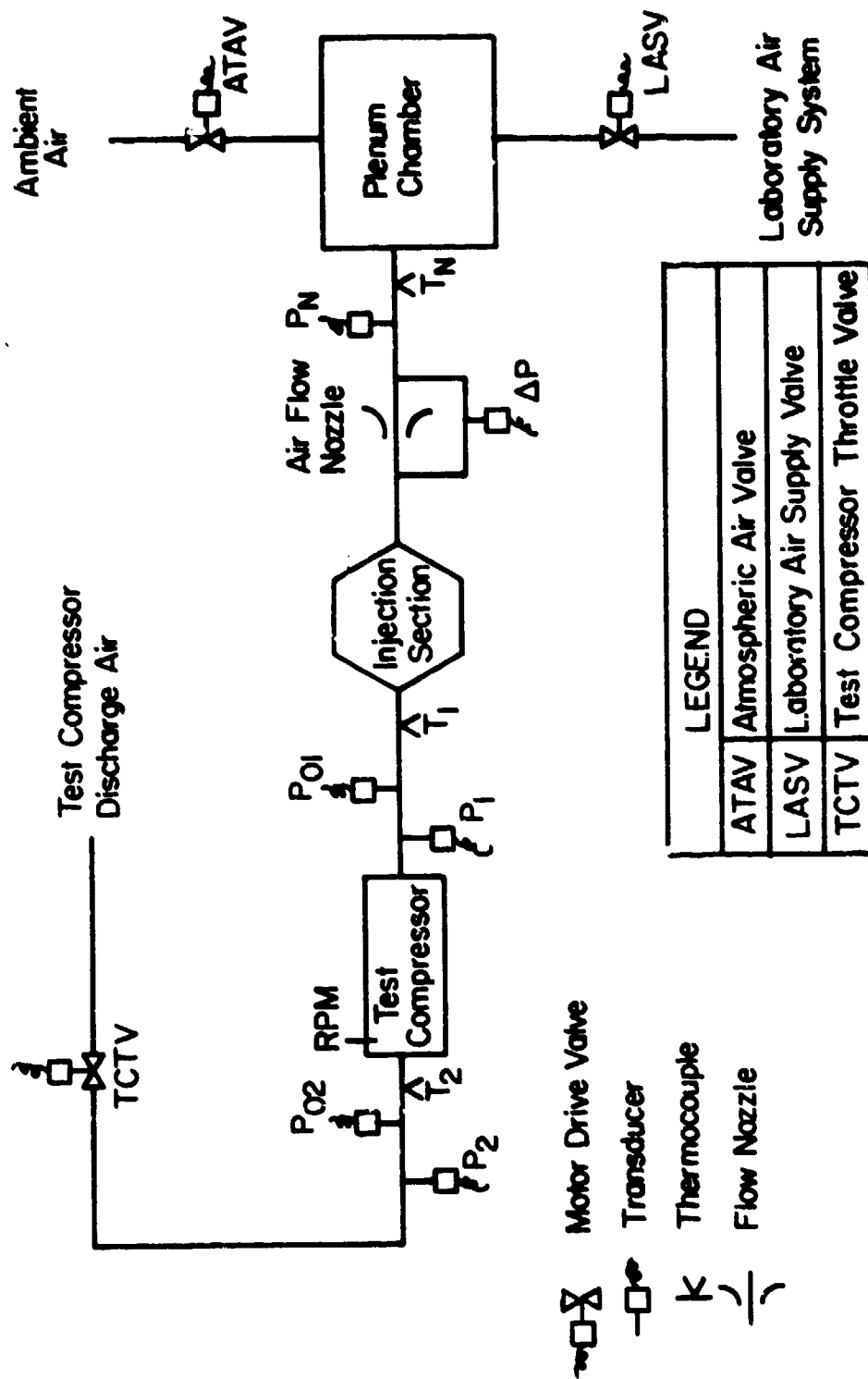
Figure 2.2   Test Comoressor Air Supply System
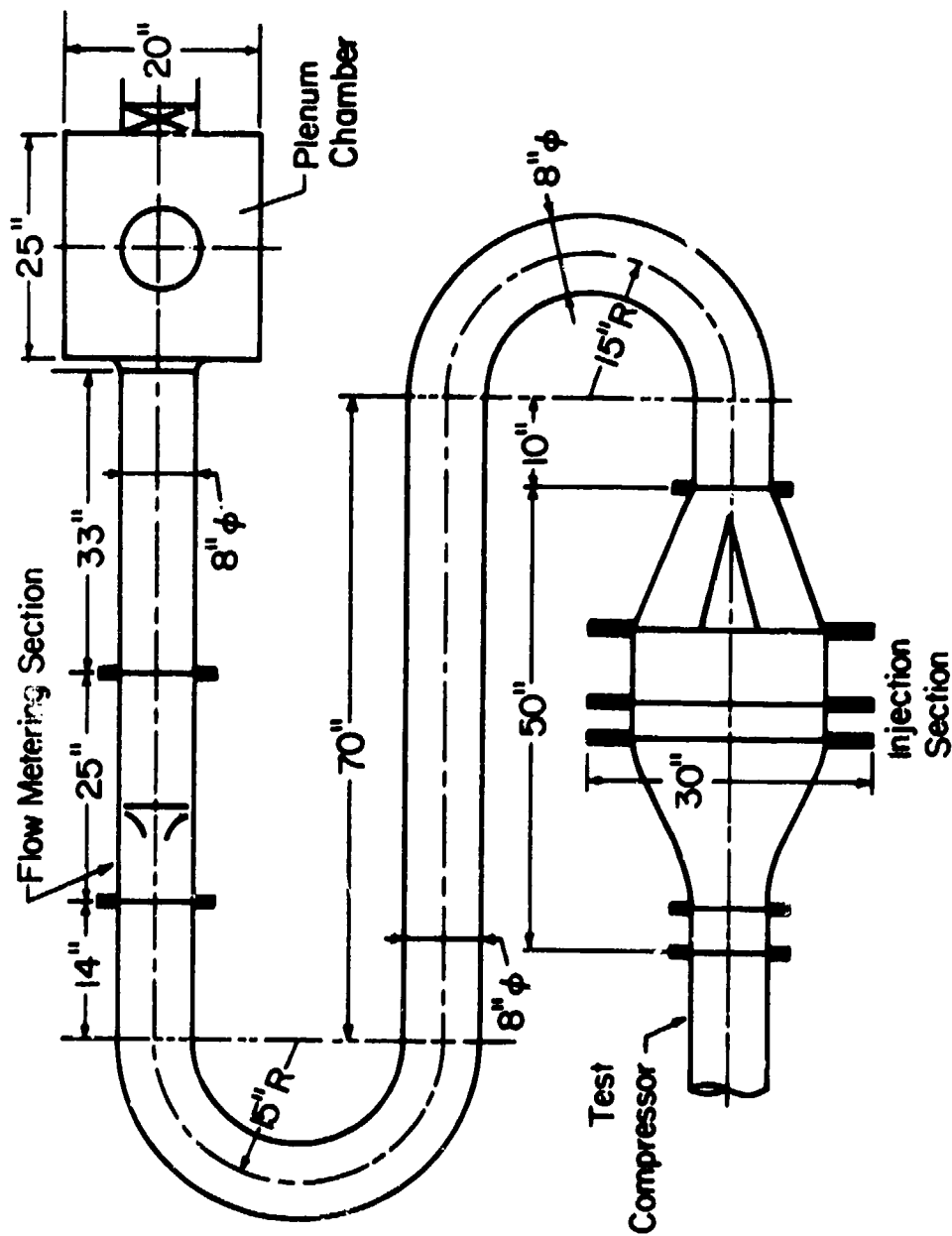
Figure 2.3 Air Supply Ducting from Plenum Chamber to Test Compressor
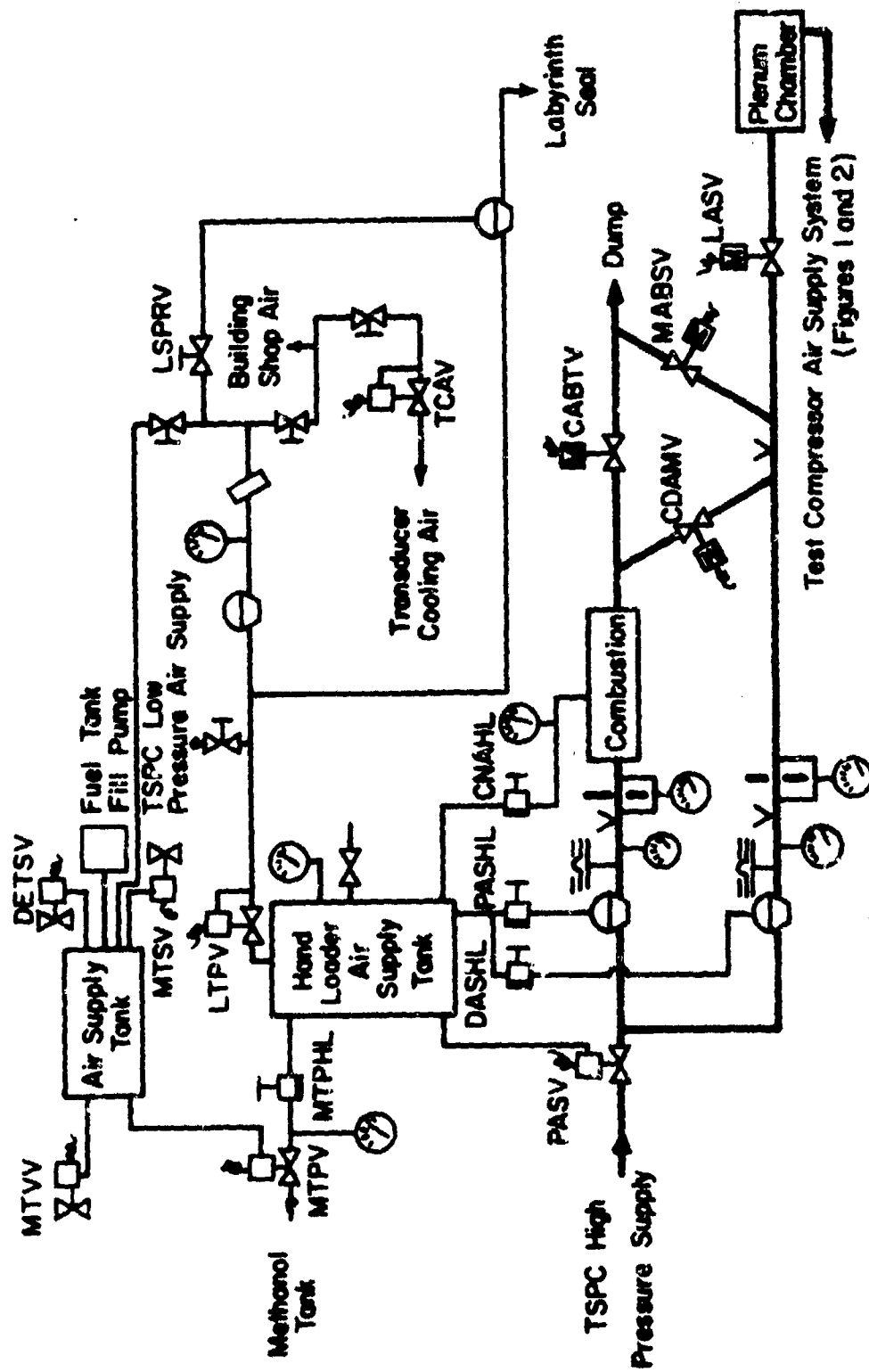
Figure 2.4 Laboratory Air Supply System

⋈ Pressure Relief Valve

⋈ Manual Valve

⊘ Pressure Gauge

⊓ Grove Hand Loader

⧓ Burst Diaphragm

◇ Filter

K Thermocouple

⊖ Dome Regulator

⋈ Air Operated Valve

⋈ Motor Driven Valve

| Orifice Plate

CABTV	Combustor Air Bypass Throttle Valve
CDAMV	Combustion and Diluent Air Mixing Valve
CNAHL	Combustor Nozzle Air Hand Loader
DASHL	Diluent Air Supply Hard Loader
DETSV	Drive Engine Tank Supply Valve
HPASV	High Pressure Air Supply Valve
LASV	Laboratory Air Supply Valve
LSPRV	Labyrinth Seal Pressure Regulating Valve
LTPV	Loader Tank Pressurization Valve
MABSV	Mixed Air Bypass Shutoff Valve
MTPHL	Methanol Tank Pressurization Hand Loader
MTPV	Methanol Tank Pressurization Valve
MTSV	Methanol Tank Supply Valve
MTVV	Methanol Tank Vent Valve
PASHL	Primary Air Supply Hand Loader
TCAV	Transducer Cooling Air Valve

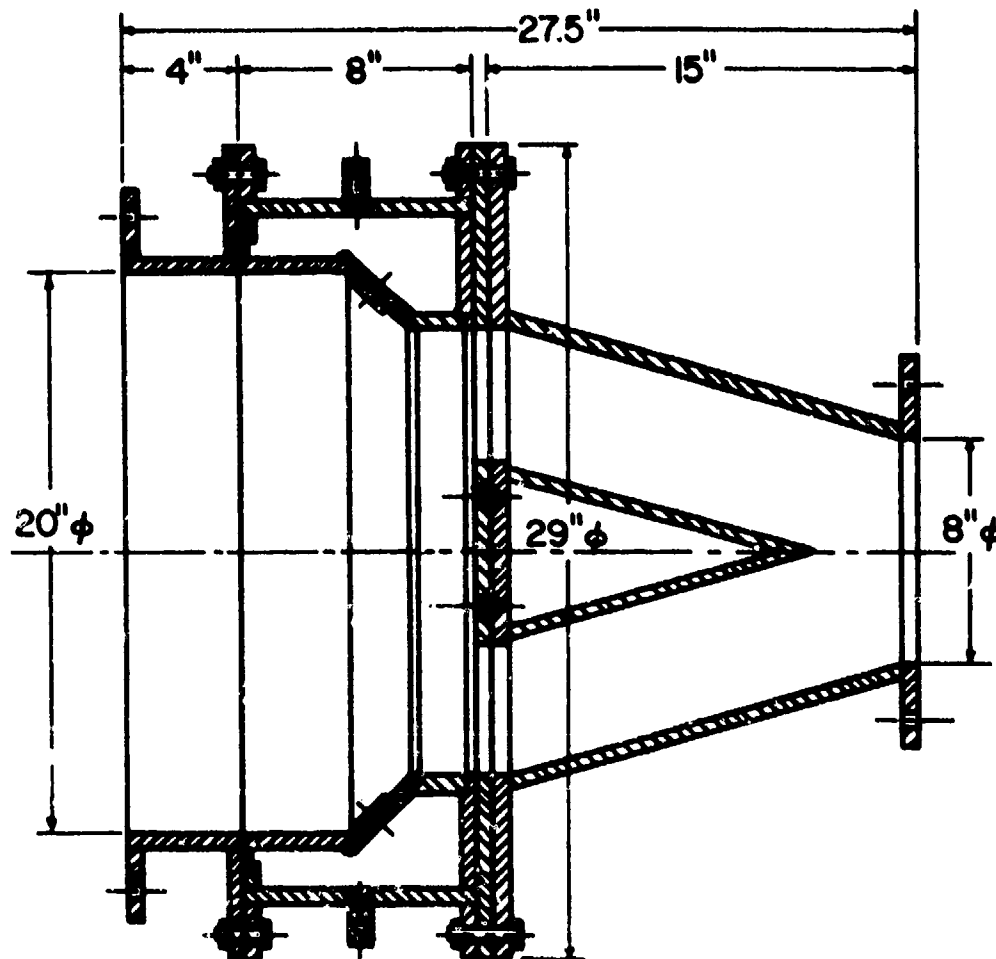Figure 2.4 Laboratory Air Supply System (continued)

Figure 2.5 Gas Injection Ring

d=1/16", 100 Holes

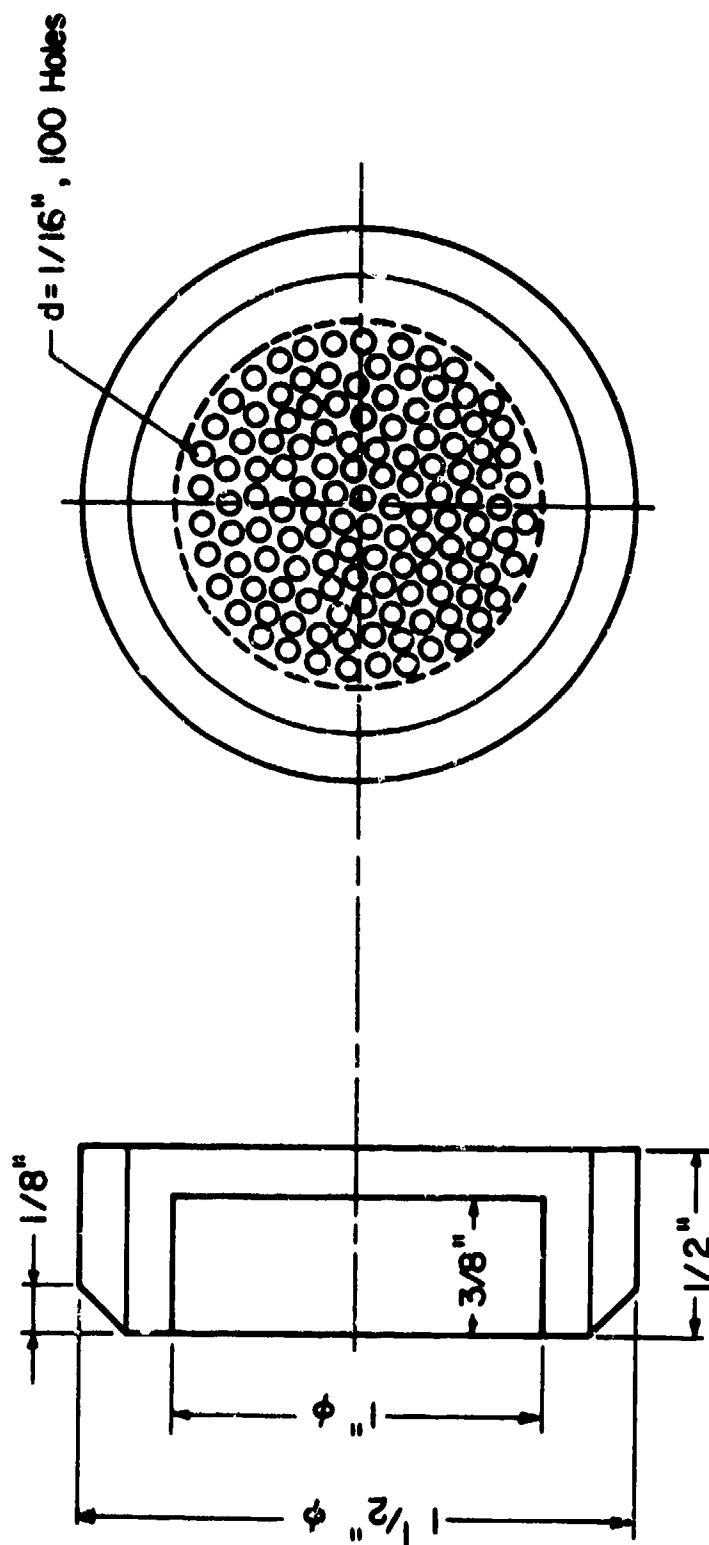1" φ

1 1/2" φ

1/8"

3/8"

1/2"

Figure 2.6 Methane Injector

Figure 2.7 Photograph of Methane Injector and Ring
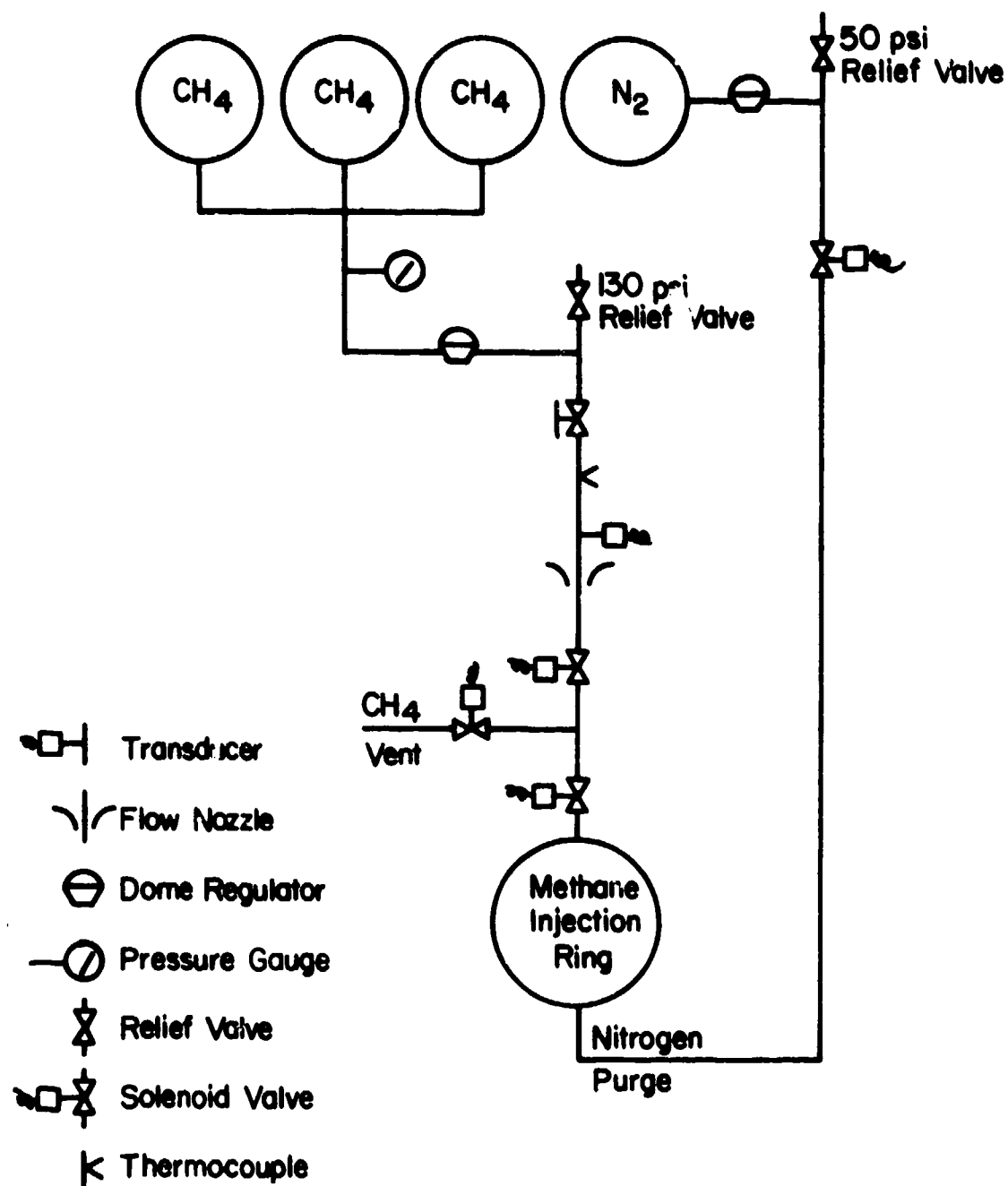
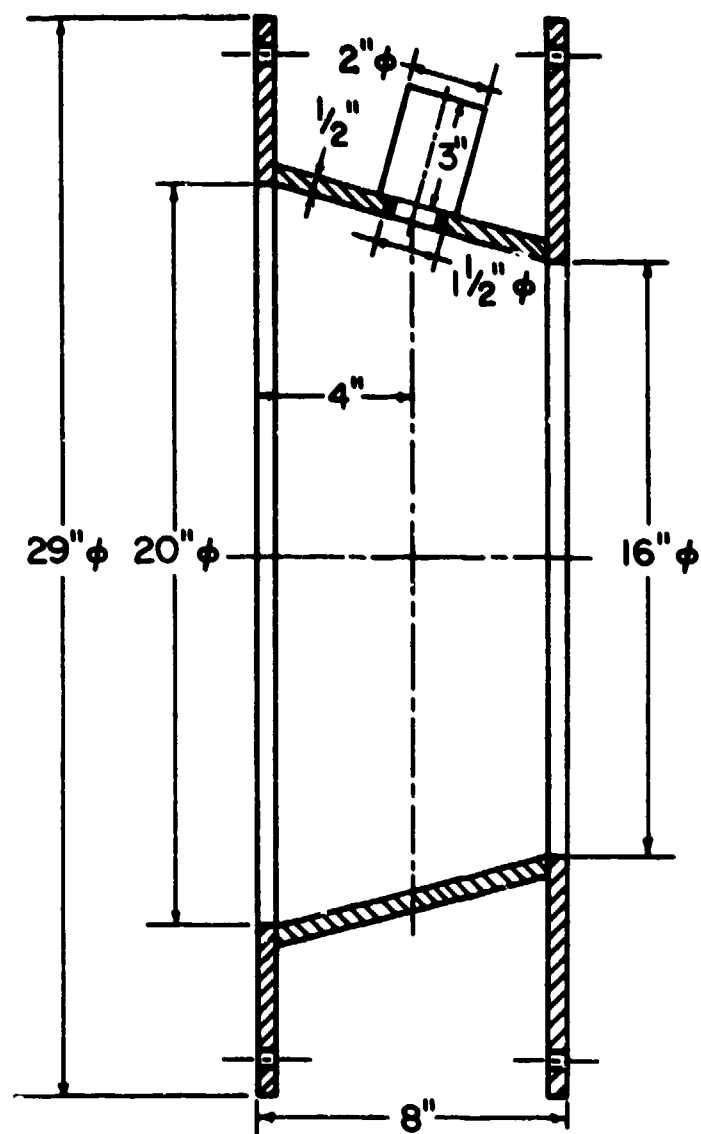Figure 2.8   Methane Gas Supply System
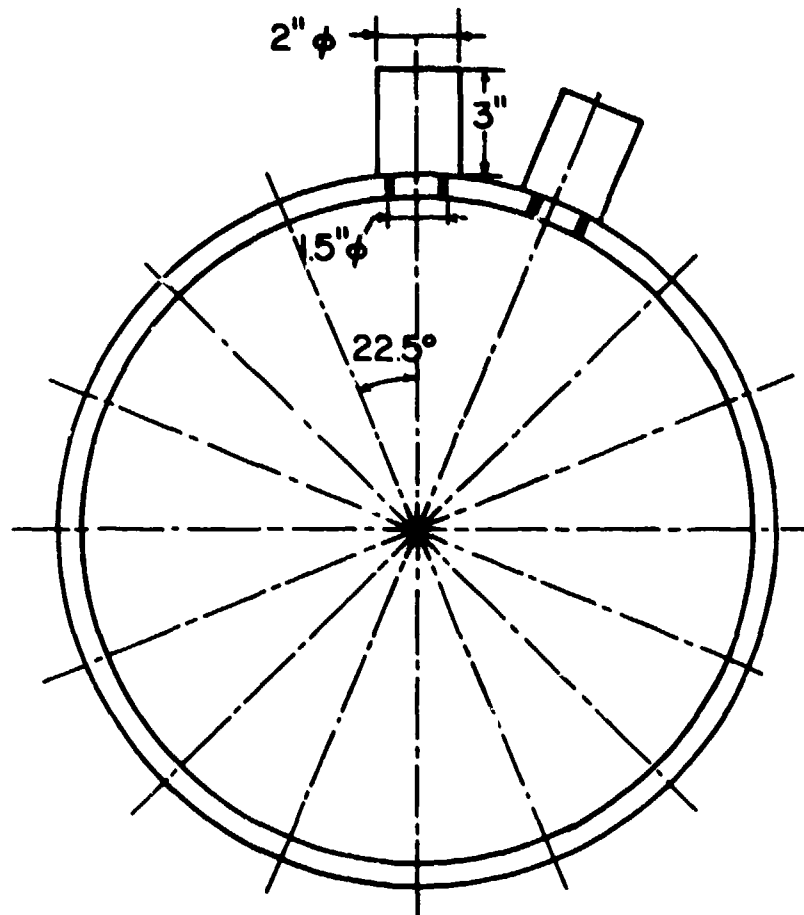
Figure 2.9 Water Injection Ring

Figure 2.9 Water Injection Ring (continued)

Figure 2.10 Water Injector Locator
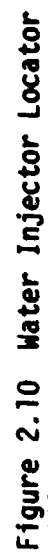
Figure 2.11   Photograph of Water Injector Locator and Ring
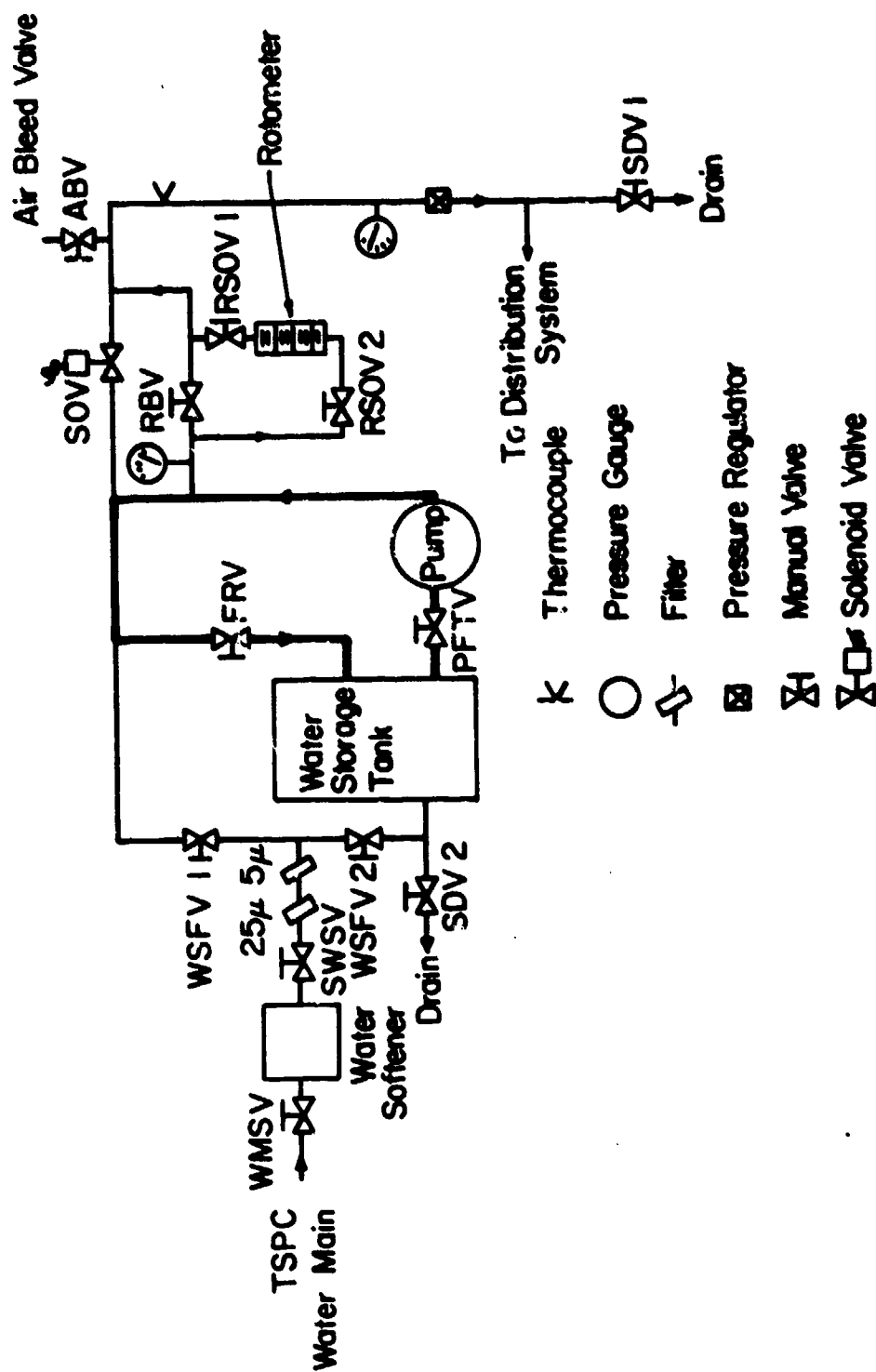
Figure 2.12 Water Supply System
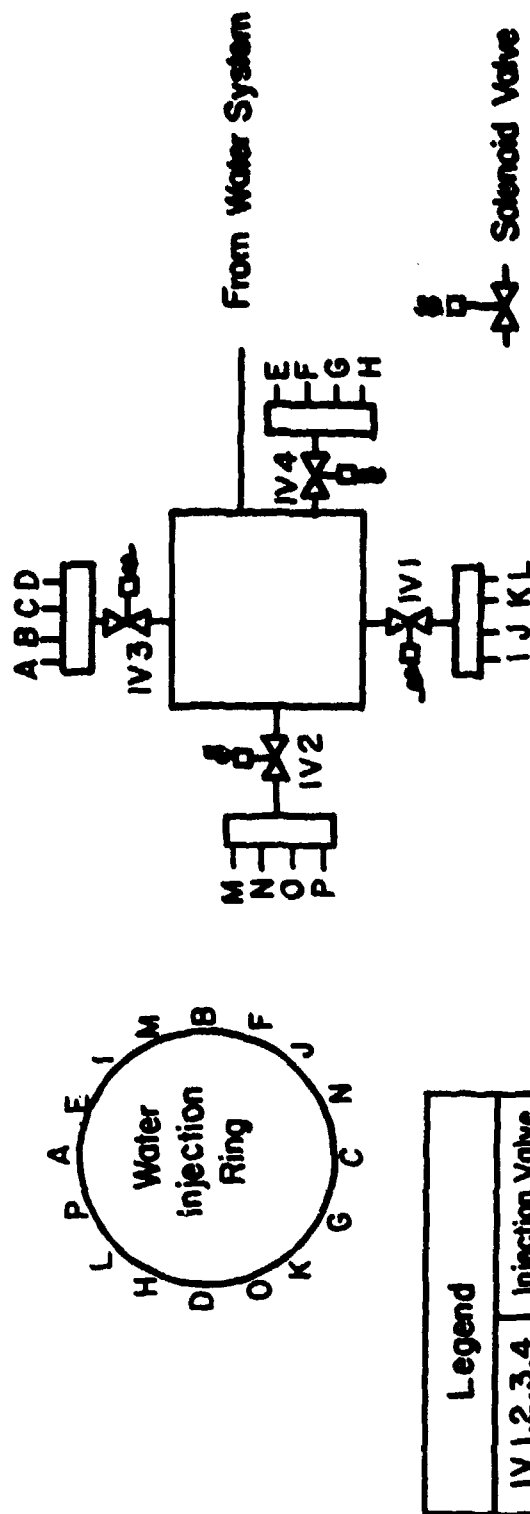
Figure 2.13 Water Distribution System
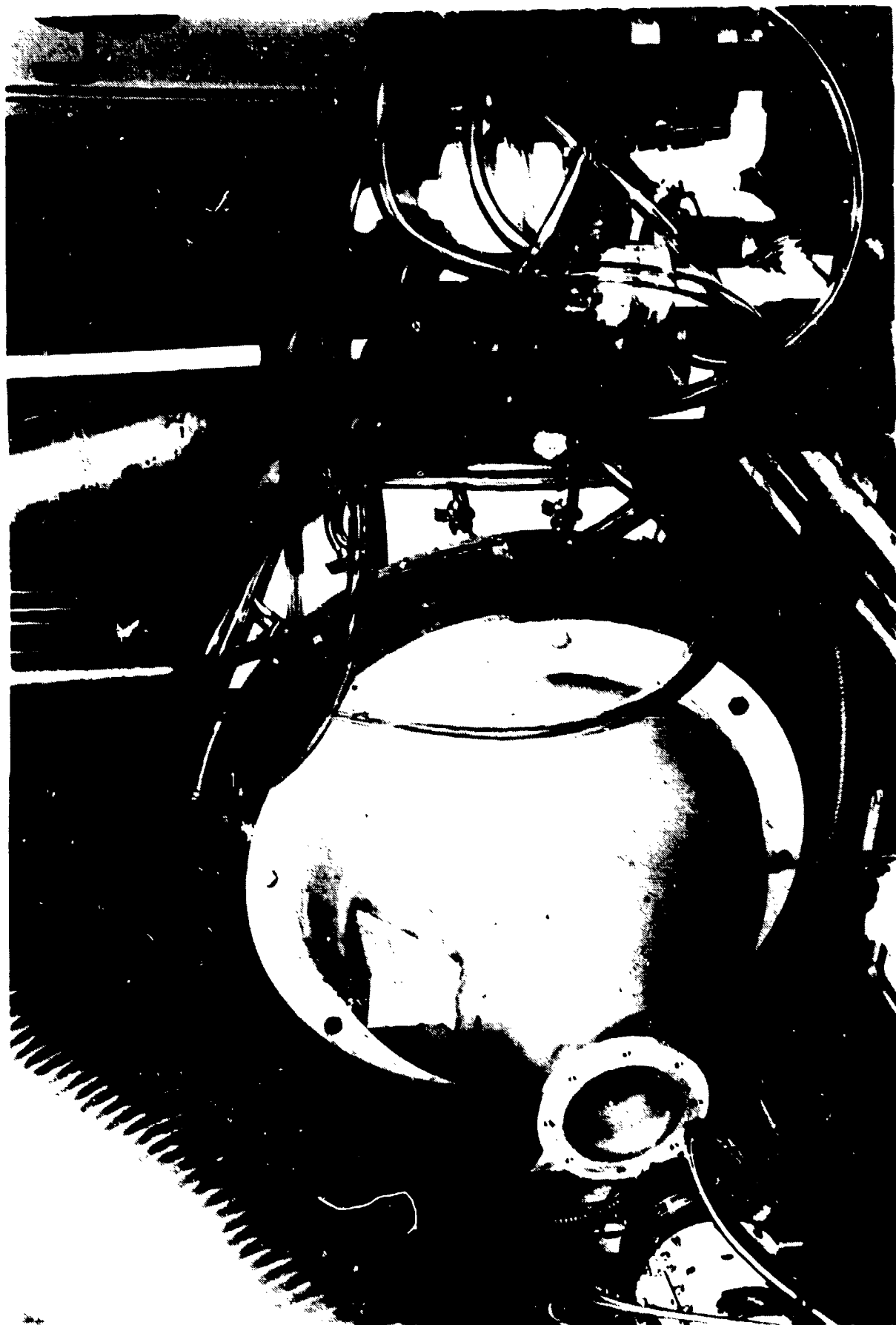
Figure 2.14 Photograph of Water Distribution System
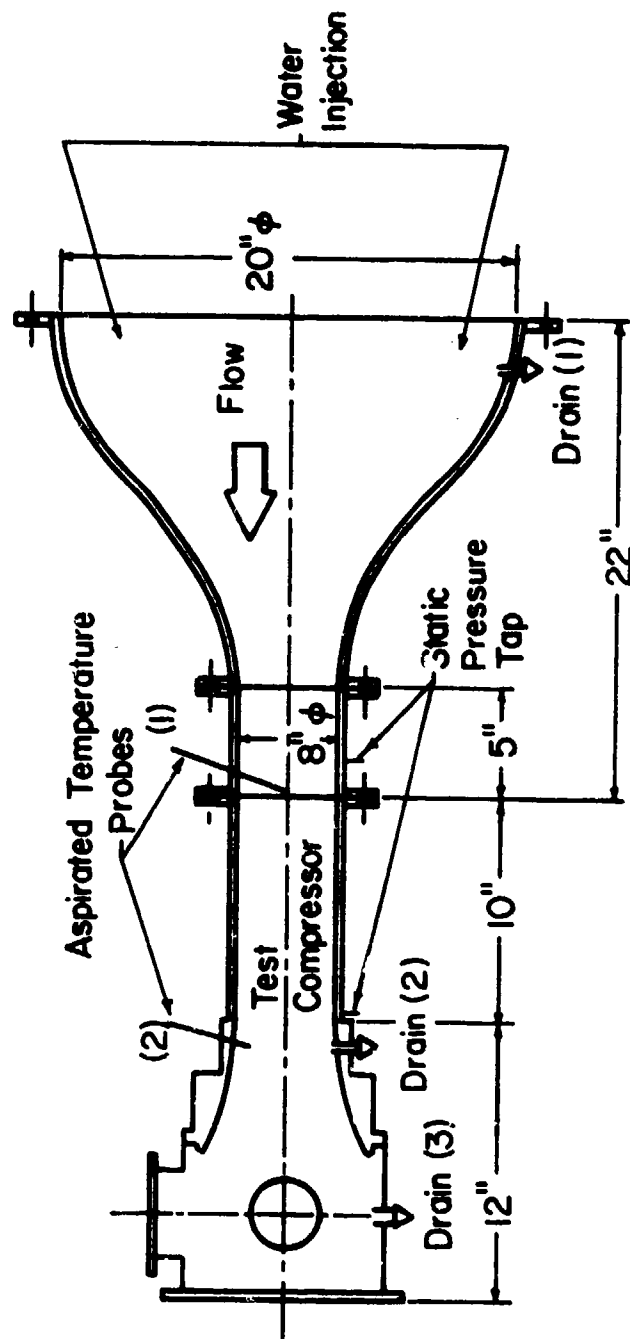
Figure 2.15 Location of Drainage of Water
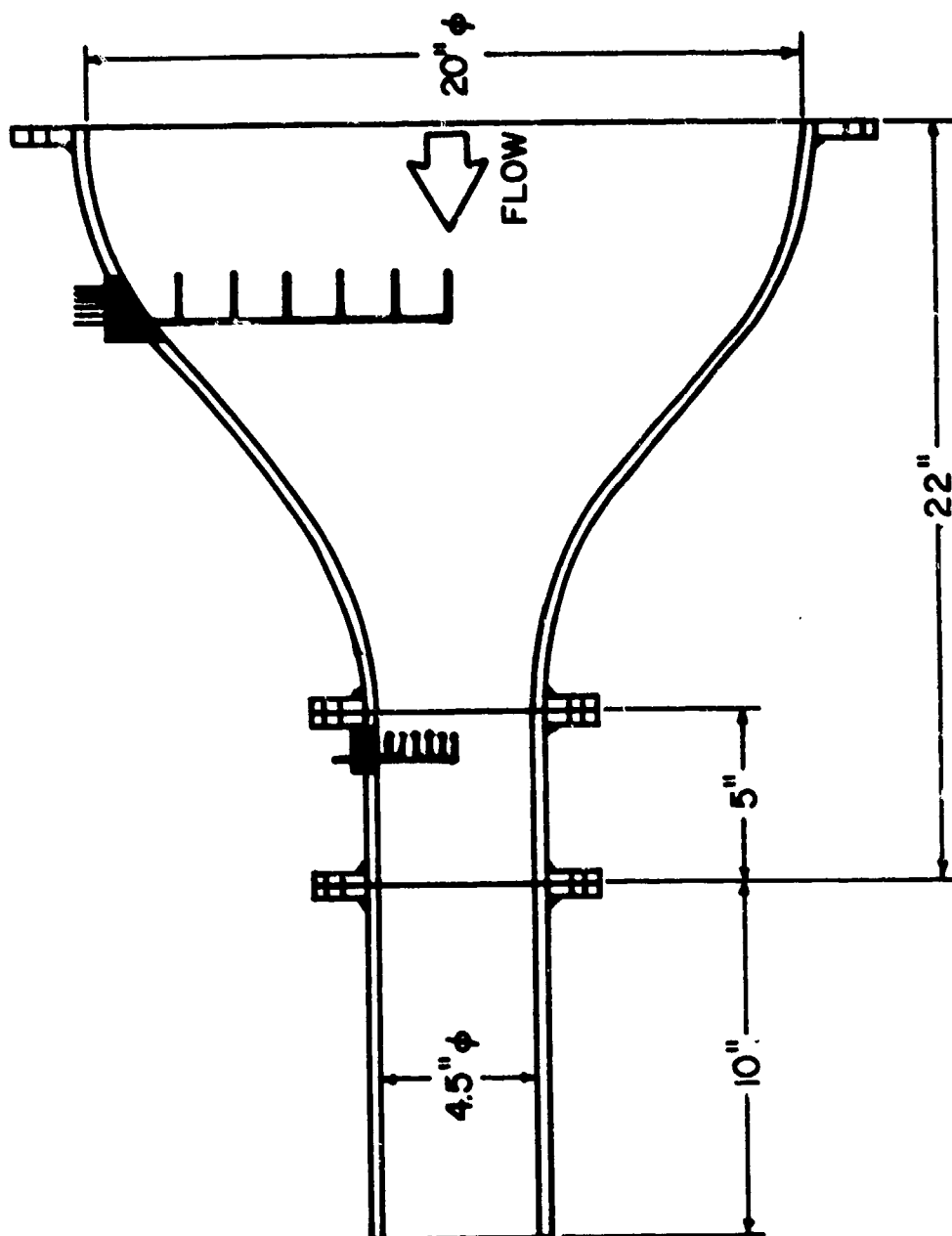
Figure 2.16 Location of Pitot Tube Rakes
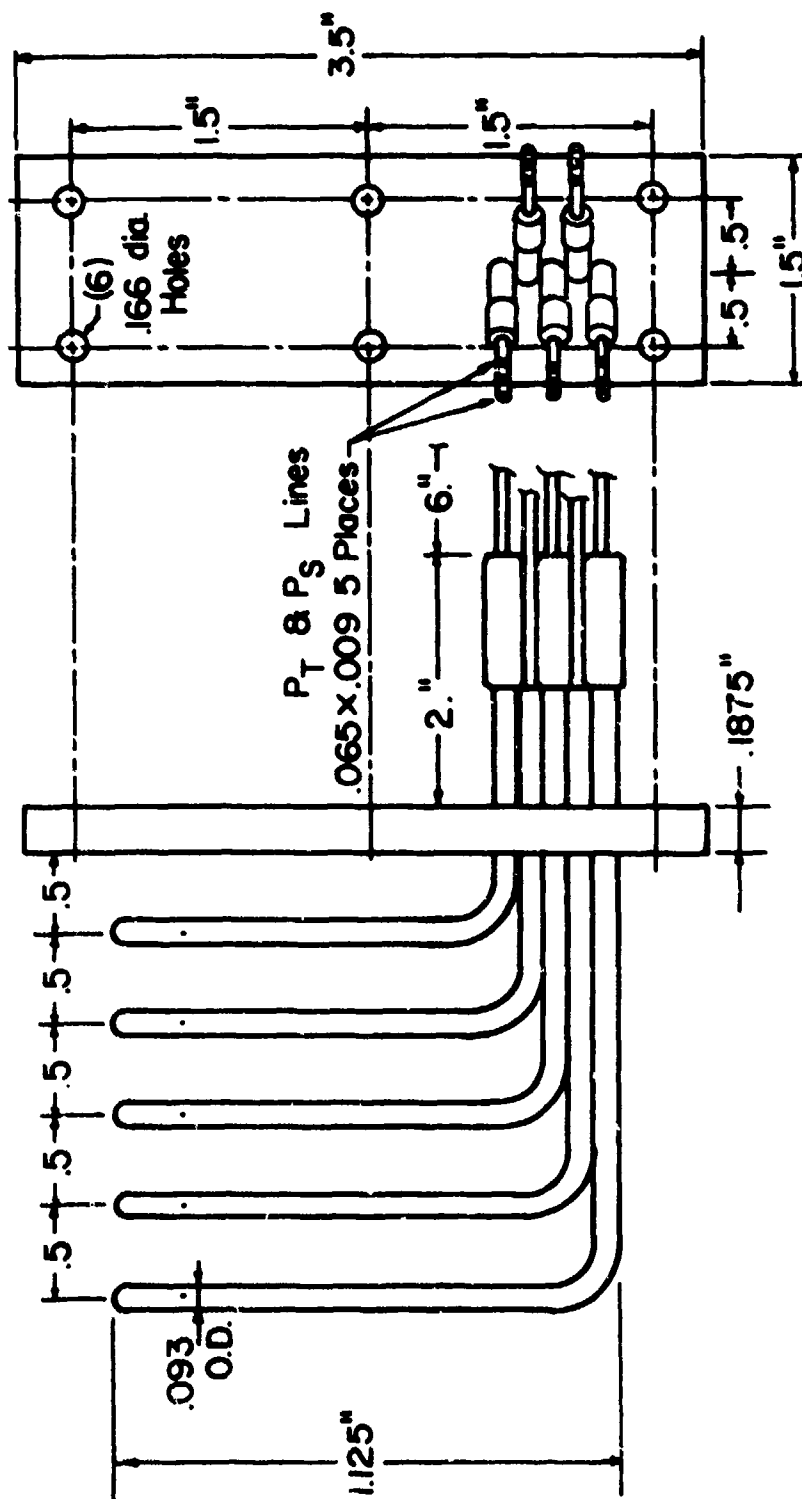
Figure 2.17(a) Design of Pitot Tube Rake (Larger Size)

Figure 2.17(b) Design of Pitot Tube Rake (Smaller Size)

Figure 4.1

Performance of the Test Compressor Obtained From Tests with Air Flow (Overall Total Temperature Ratio vs. Corrected Mass Flow Rate: $N/\sqrt{\theta}=90\%$)

Figure 4.2

Performance of the Test Compressor Obtained From
Tests with Air Flow (Overall Total Pressure Ratio
vs. Corrected Mass Flow Rate: $N/\sqrt{\theta}=90\%$)

Figure 4.3

Performance of the Test Compressor Obtained From
Tests with Air Flow (Overall Total Temperature Ratio
vs. Corrected Mass Flow Rate: $N/\sqrt{\theta}=80\%$)

Figure 4.4

Performance of the Test Compressor Obtained From
Tests with Air Flow (Overall Total Pressure Ratio
vs. Corrected Mass Flow Rate: $N/\sqrt{\theta}$=80%)

Figure 4.5

Performance of the Test Compressor Obtained From
Tests with Air Flow (Overall Total Temperature Ratio
vs. Corrected Mass Flow Rate: N/√θ=70%)
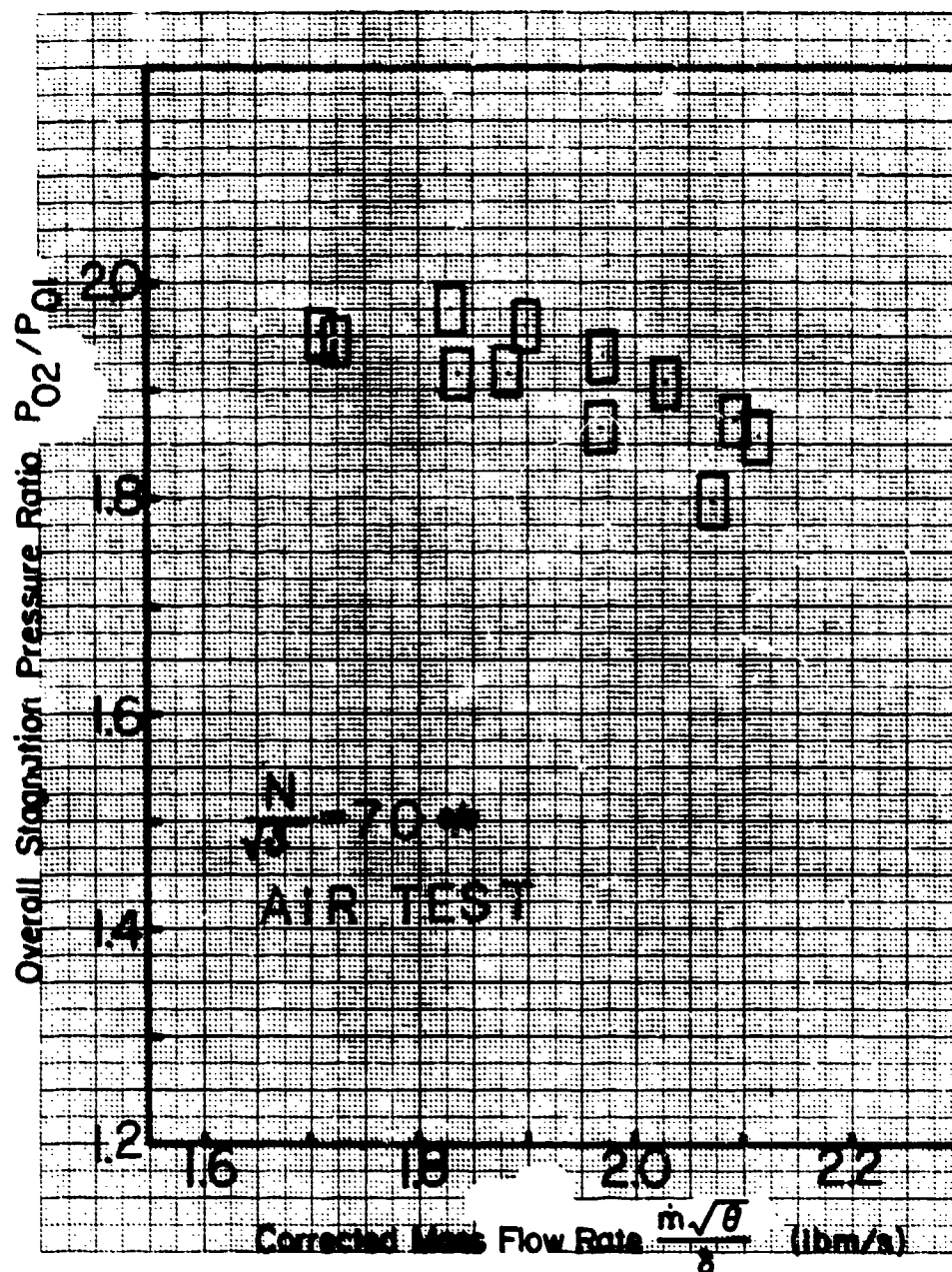
Figure 4.6

Performance of the Test Compressor Obtained From
Tests with Air Flow (Overall Total Pressure Ratio
vs. Corrected Mass Flow Rate: $N/\sqrt{\theta}=70\%$)

113
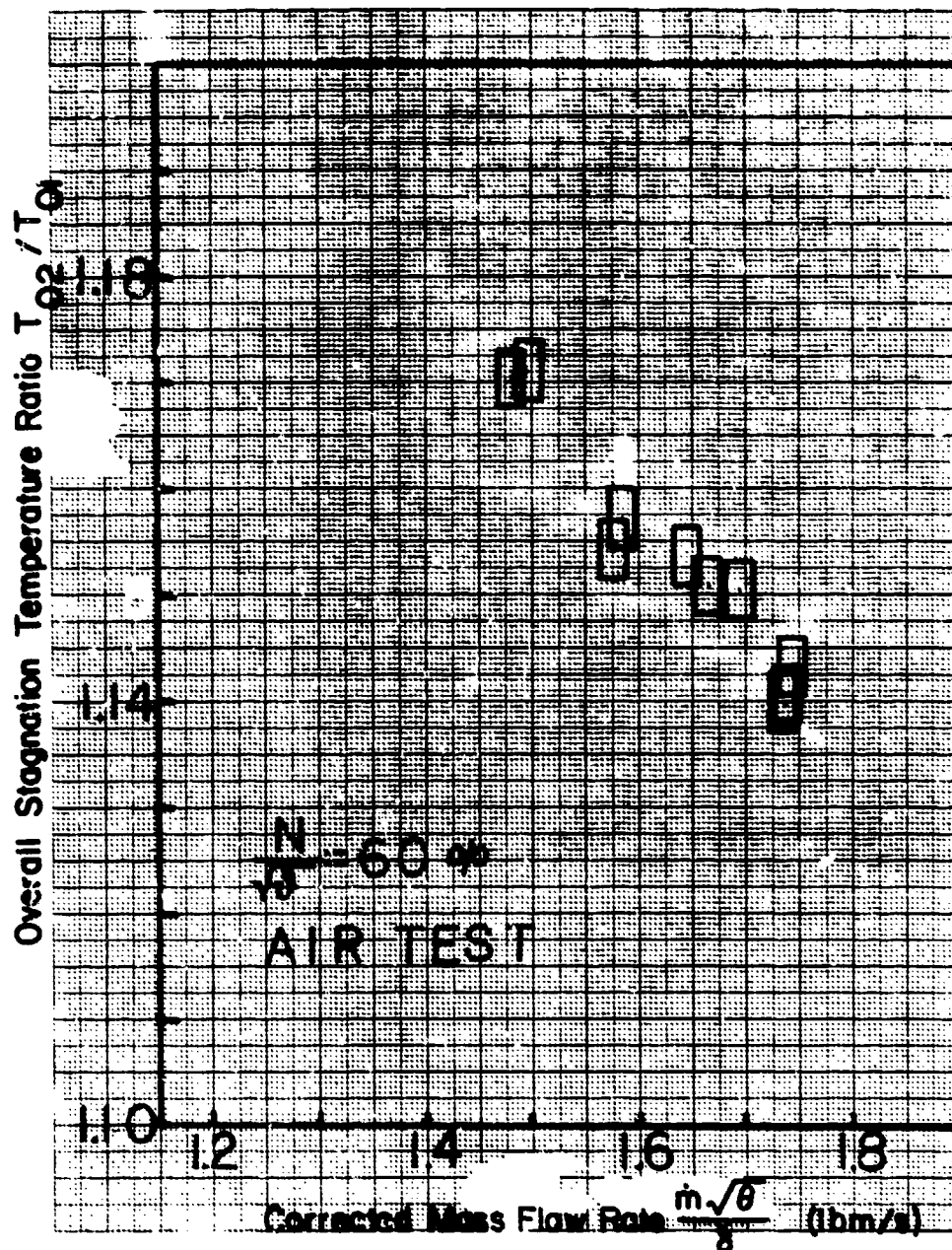
Figure 4.7

Performance of the Test Compressor Obtained From
Tests with Air Flow (Overall Total Temperature Ratio
vs. Corrected Mass Flow Rate: N/√θ=60%)
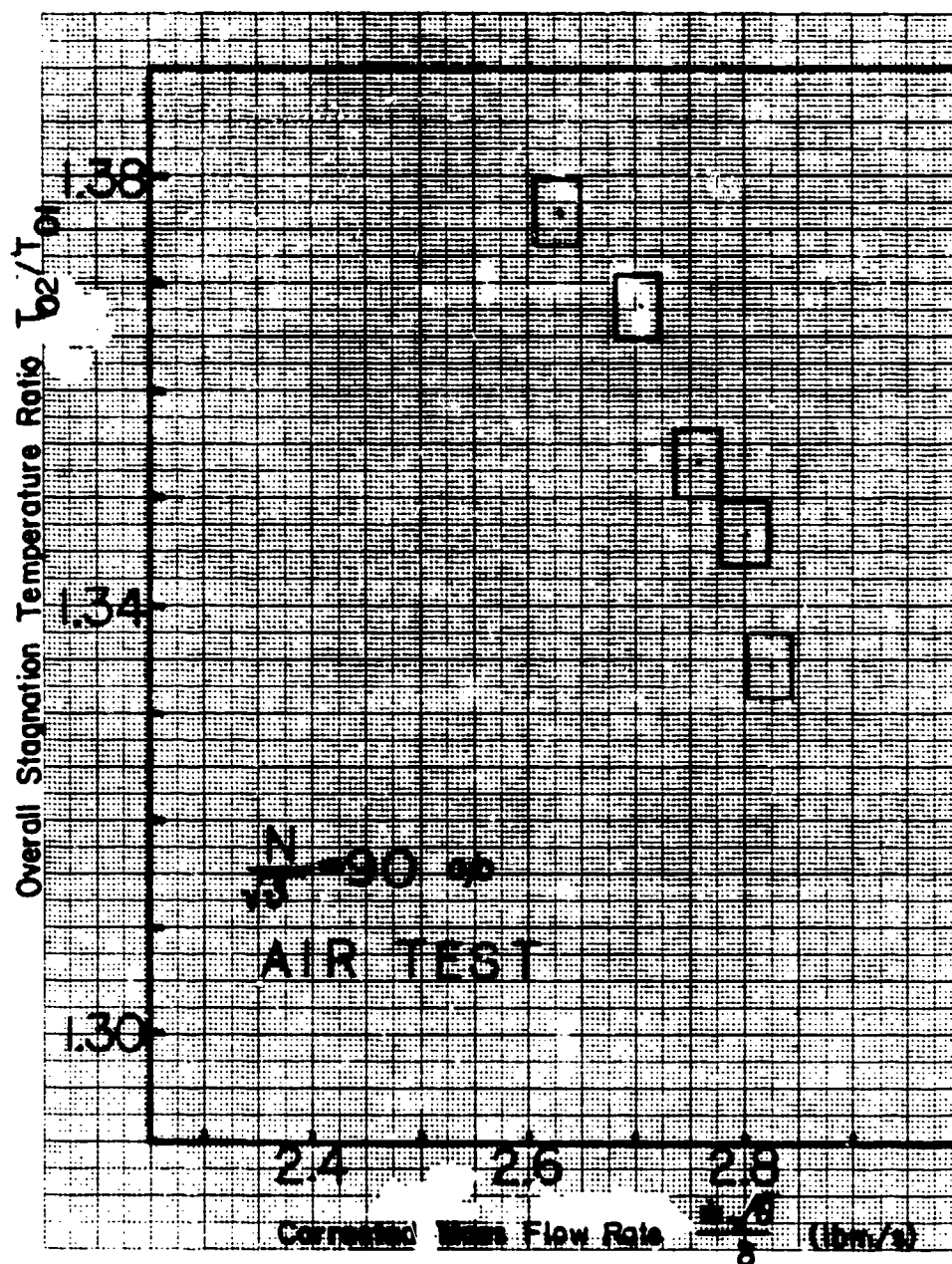
Figure 4.8

Performance of the Test Compressor Obtained From
Tests with Air Flow (Overall Total Pressure Ratio
vs. Corrected Mass Flow Rate: $N/\sqrt{\theta}=60\%$)

Figure 4.9

Performance of the Test Compressor Obtained From
Tests with Air-Methane Mixture Flow (Overall Total
Temperature Ratio Vs. Corrected Mass Flow Rate: $N/\sqrt{\theta}$=90%)
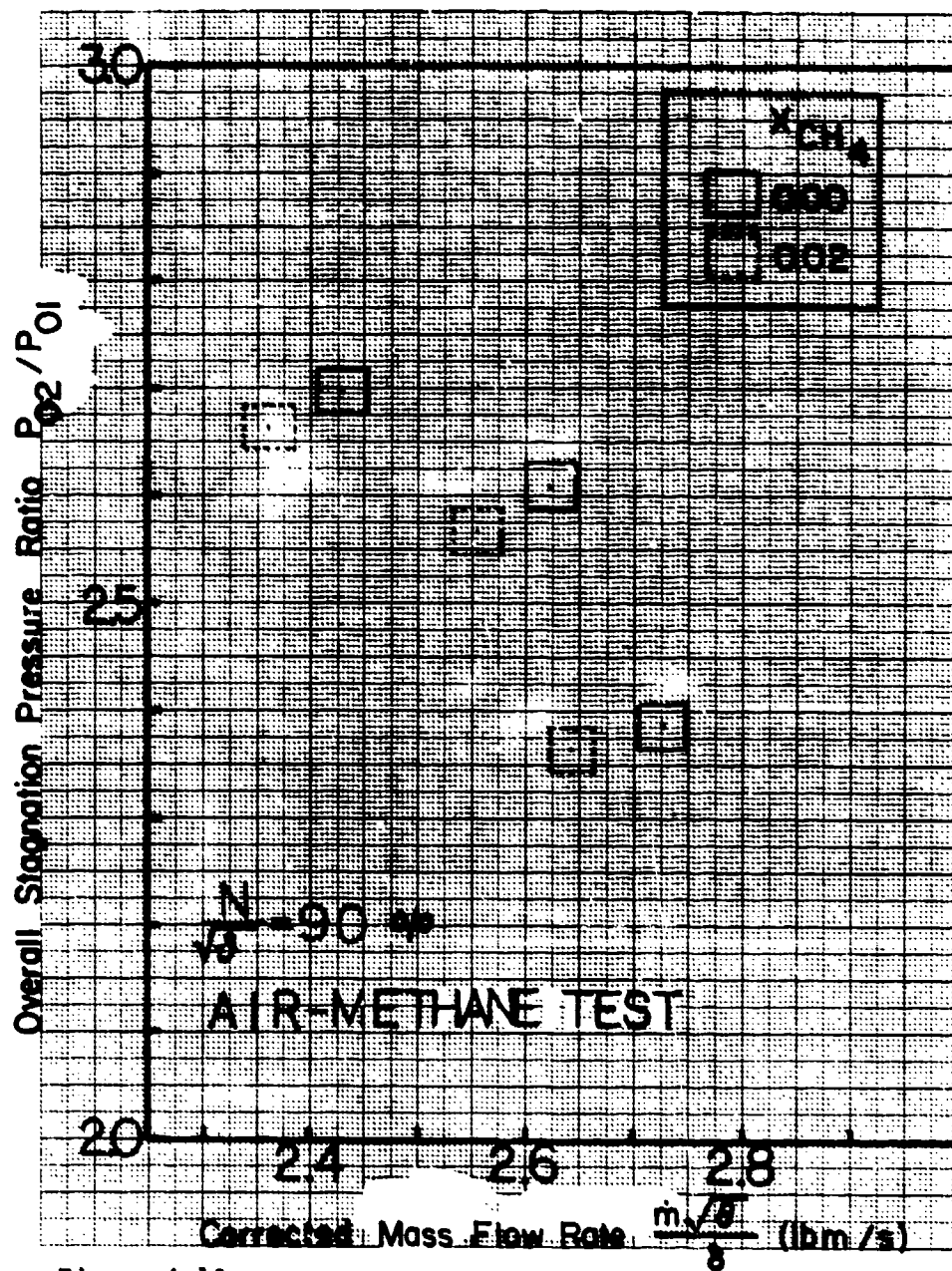
Figure 4.10

Performance of the Test Compressor Obtained From
Tests with Air-Methane Mixture Flow (Overall Total
Pressure Ratio vs. Corrected Mass Flow Rate: N/√θ=90%)

Figure 4.11

Performance of the Test Compressor Obtained From
Tests with Air-Methane Mixture Flow (Overall Total
Temperature Ratio vs. Corrected Mass Flow Rate: $N/\sqrt{\theta}=80\%$)
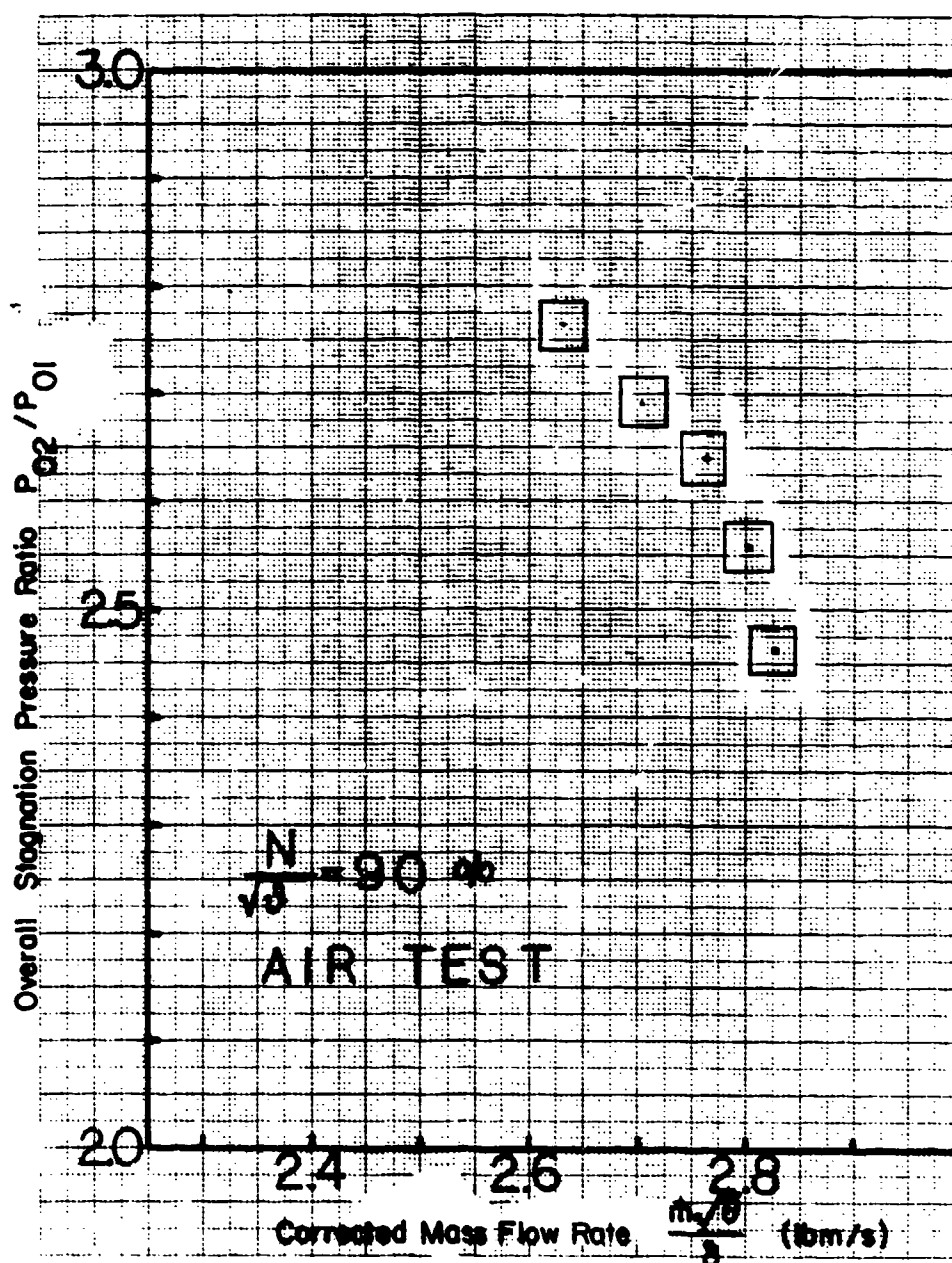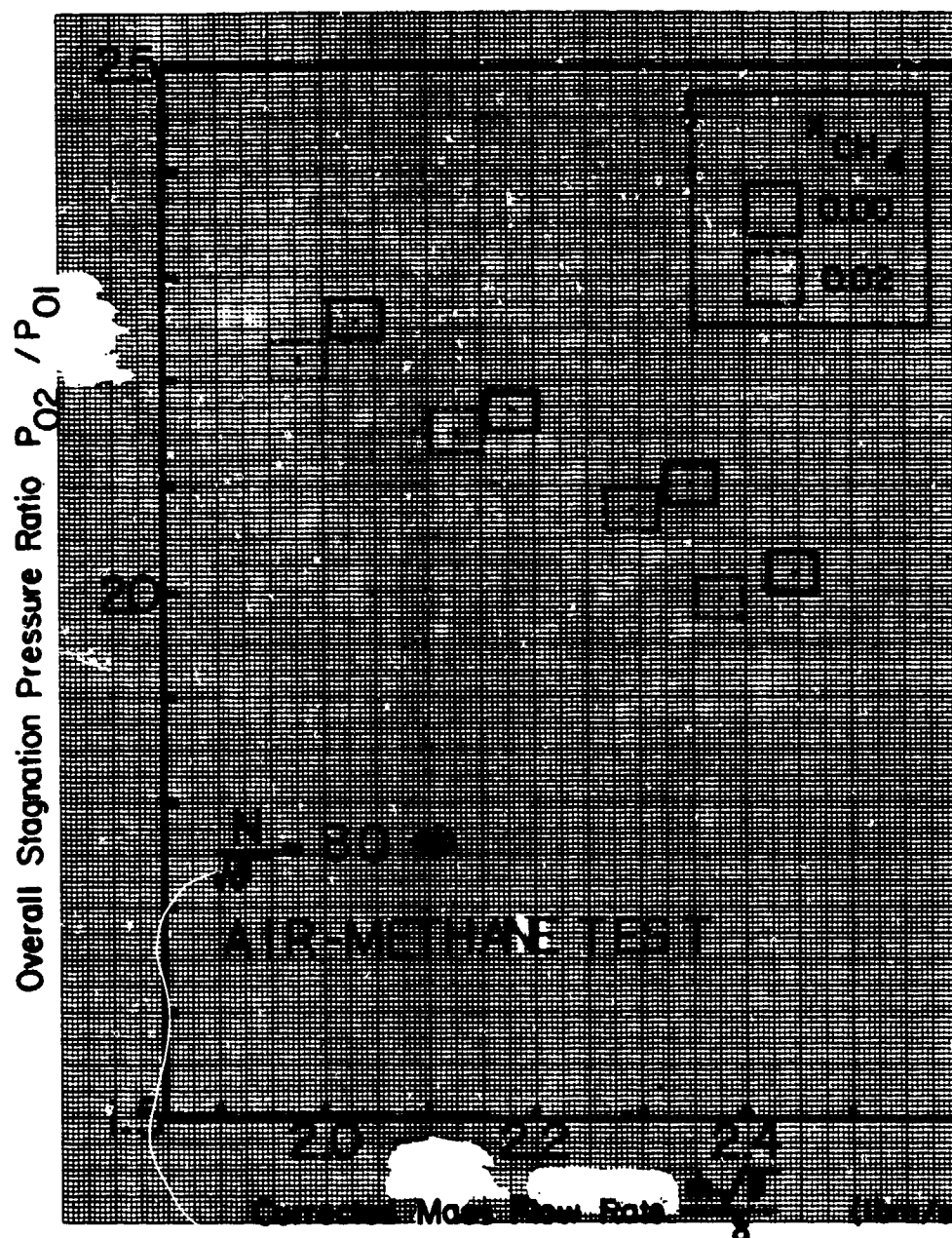
Figure 4.12

Performance of the Test Compressor Obtained From
Tests with Air-Methane Mixture Flow (Overall Total
Pressure Ratio vs. Corrected Mass Flow Rate: $N/\sqrt{\theta} \approx 80\%$)

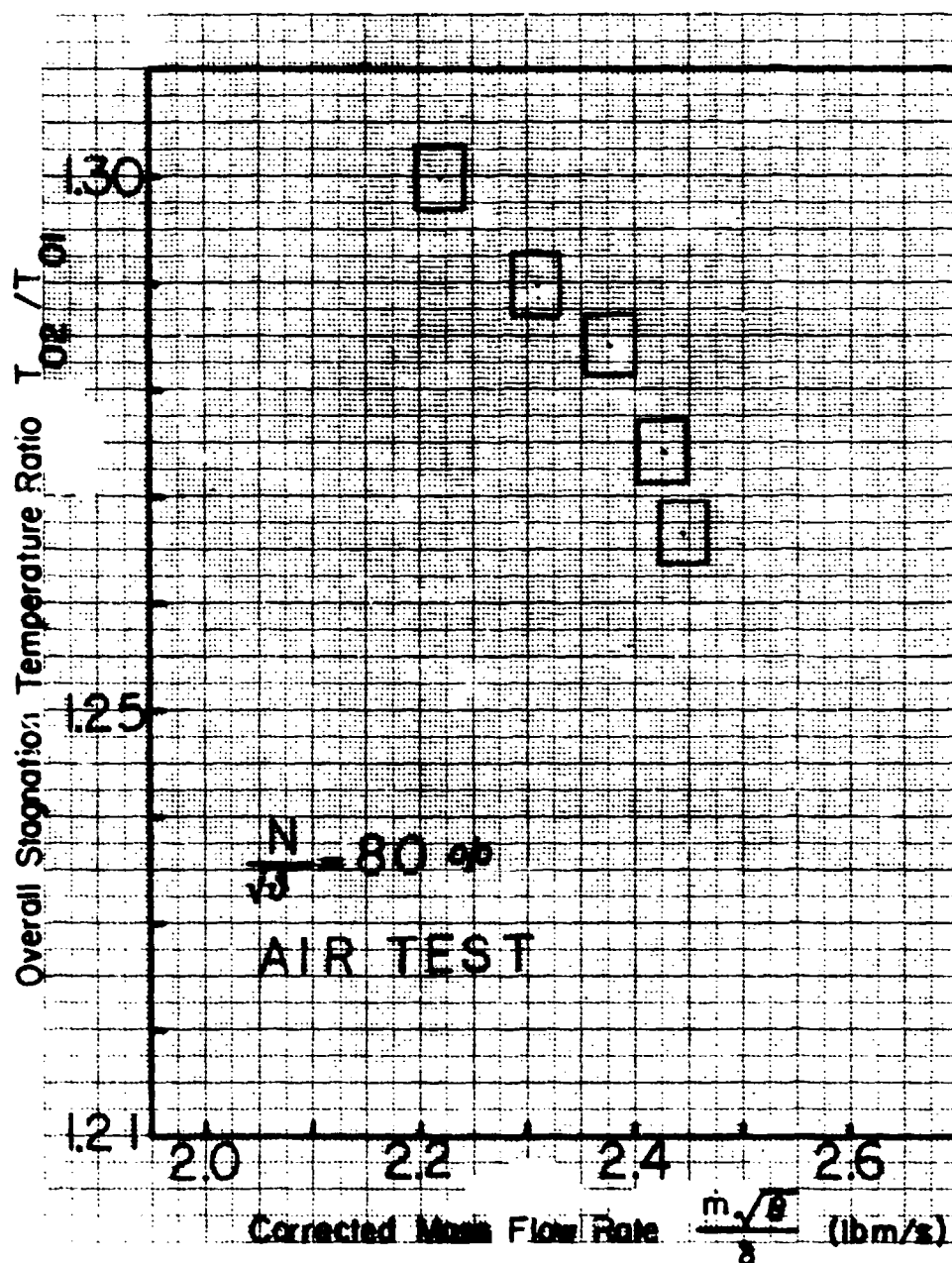
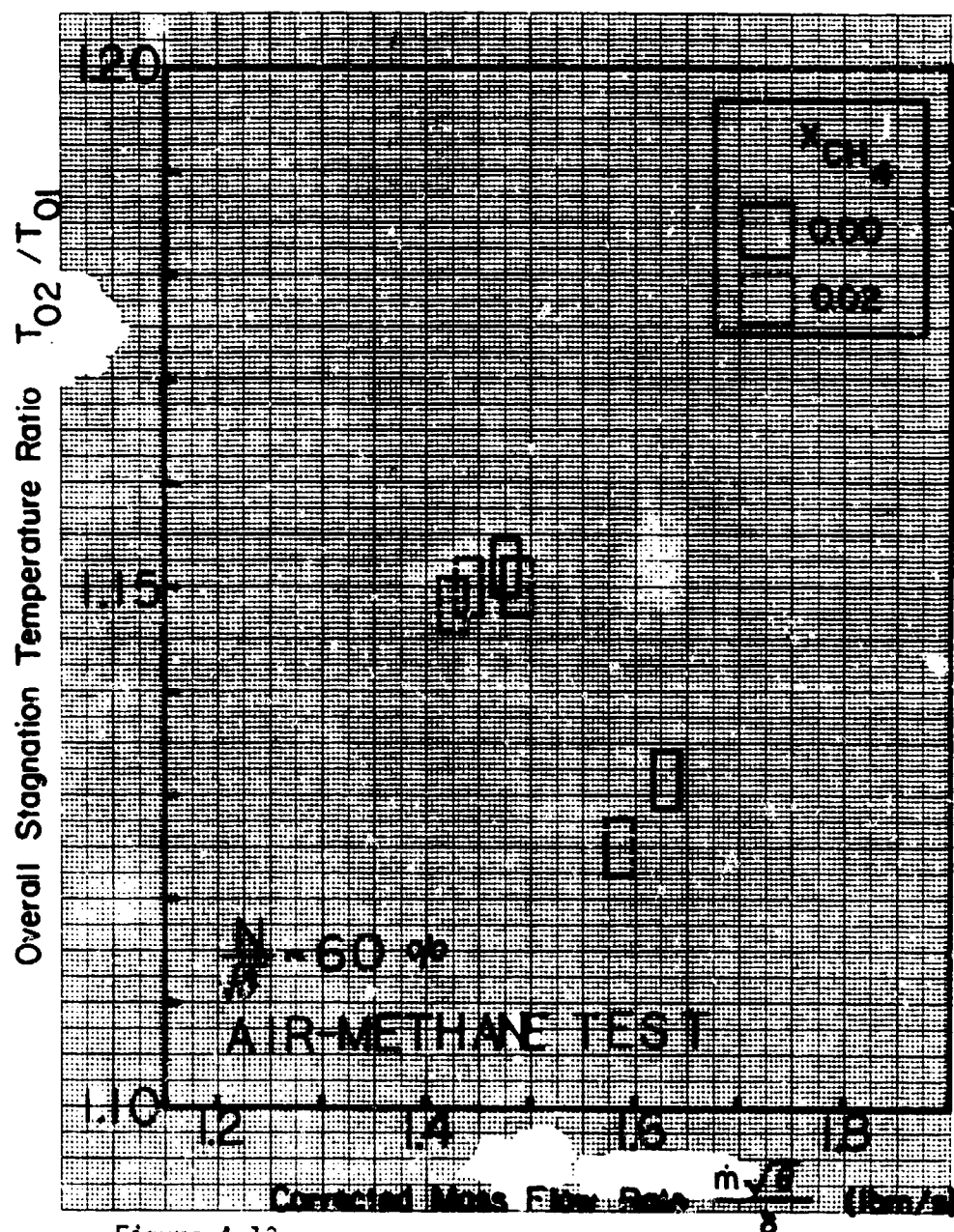
Figure 4.13

Performance of the Test Compressor Obtained From
Tests with Air-Methane Mixture Flow (Overall Total
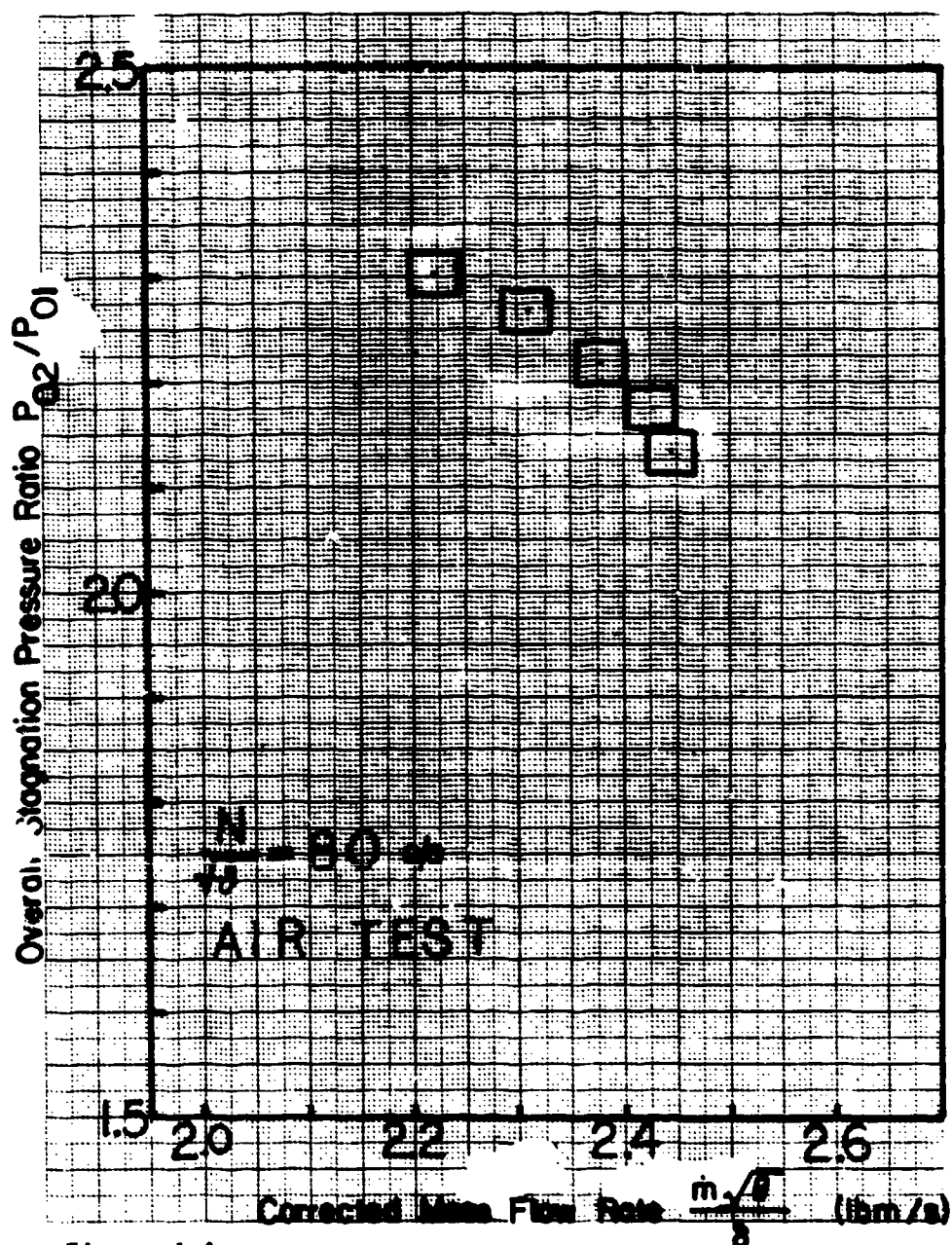Temperature Ratio vs. Corrected Mass Flow Rate: $N/\sqrt{\theta}=60\%$)
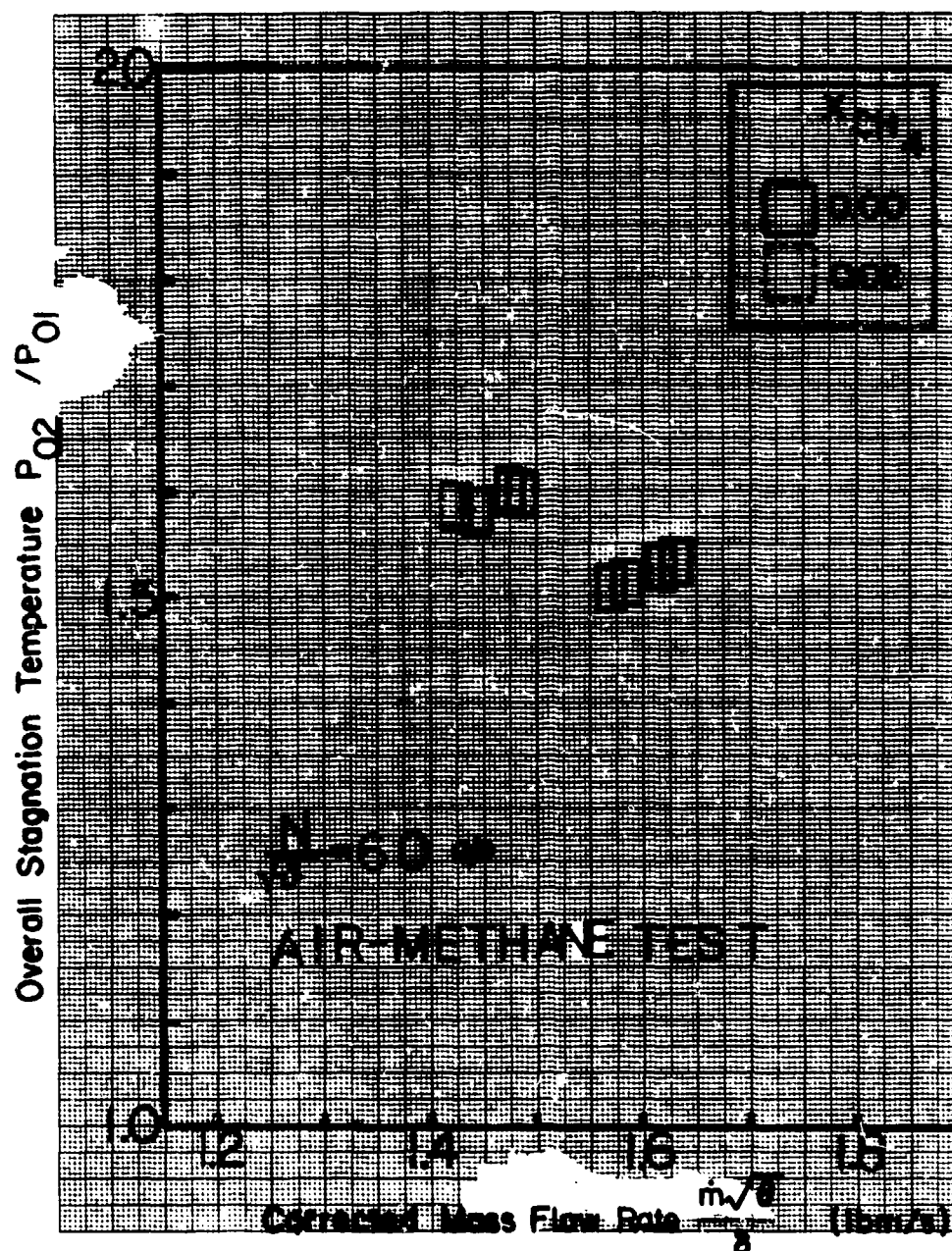
Figure 4.14

Performance of the Test Compressor Obtained From
Tests with Air-Methane Mixture Flow (Overall Total
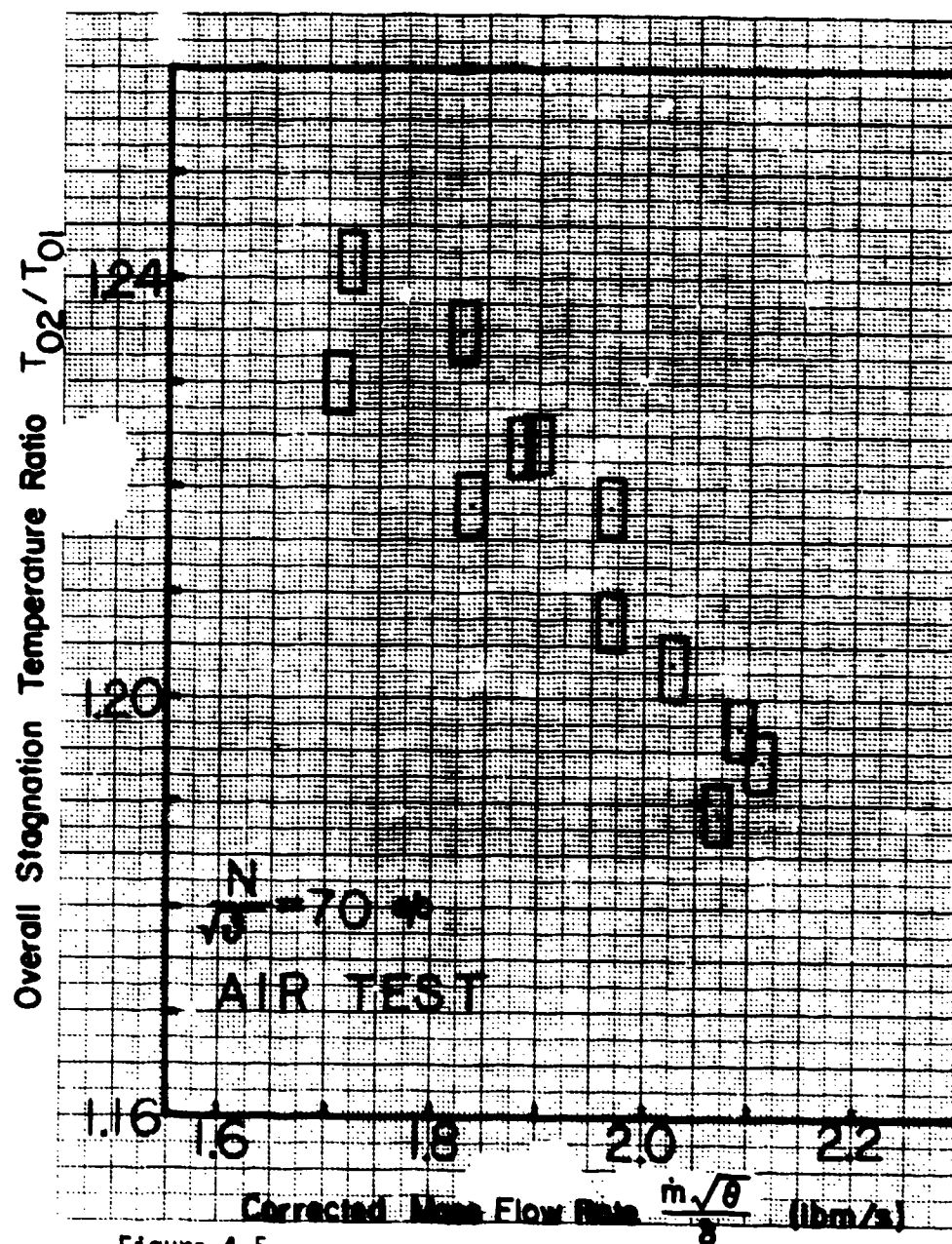Pressure Ratio vs. Corrected Mass Flow Rate: N/√θ=60%)
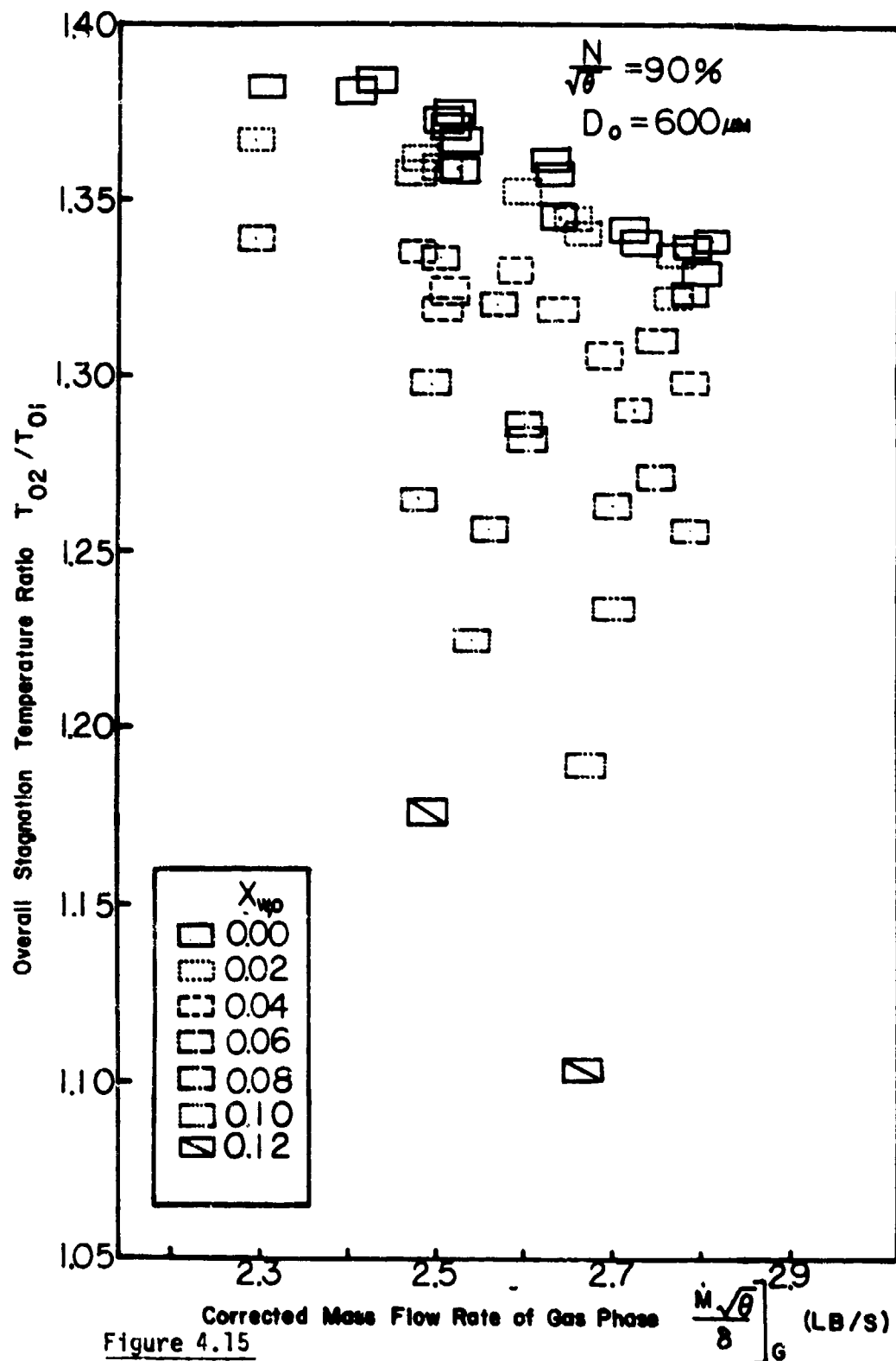
Figure 4.15

Performance of the Test Compressor Obtained From
Tests with Air-Water Droplet Mixture Flow (Overall
Total Temperature Ratio vs. Gas Phase Corrected
Mass Flow Rate: N/√θ=90%, D_o=600μm)
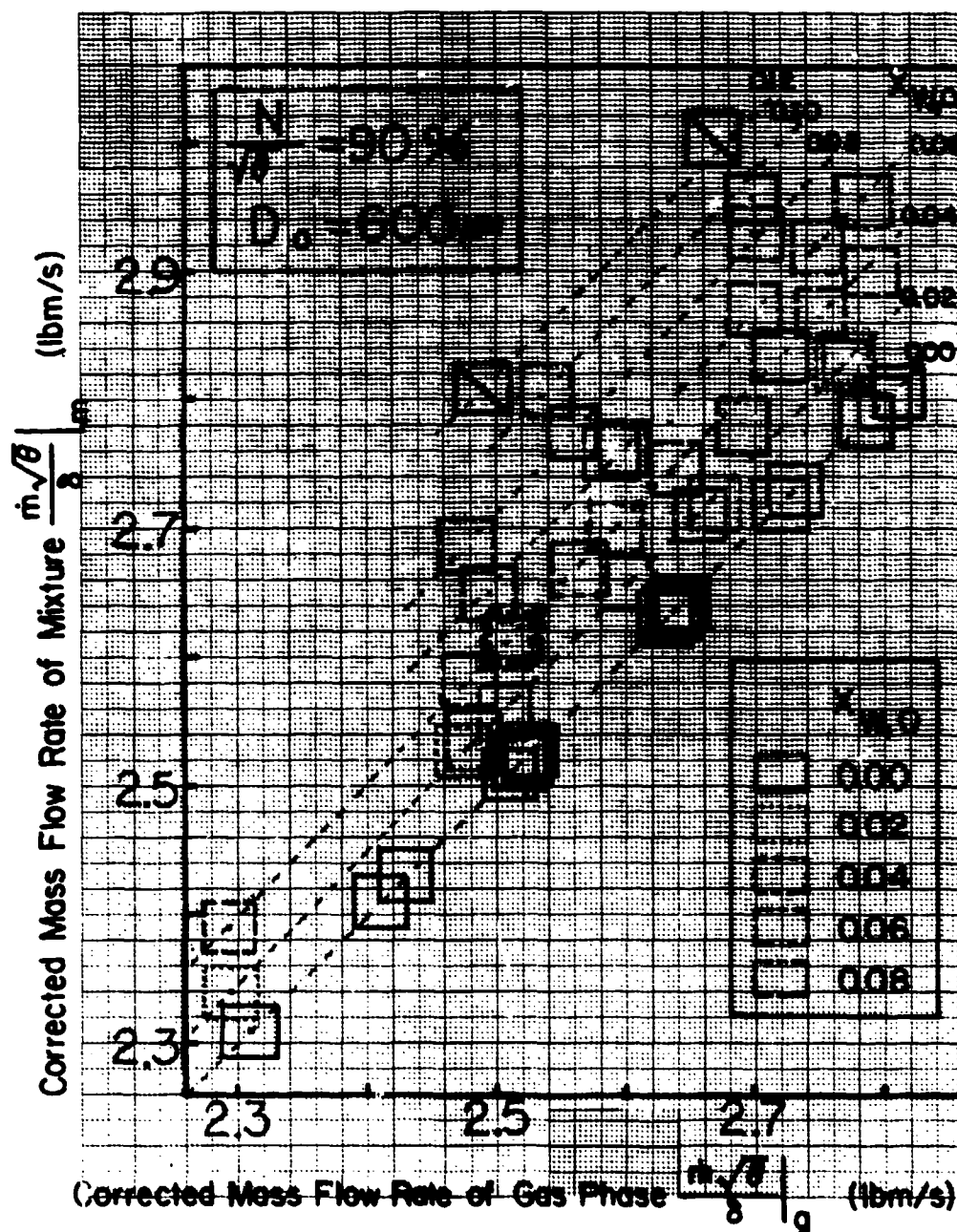
Figure 4.16

Corrected Mass Flow Rate of Gas Phase vs. Corrected Mass Flow
Rate of Air-Water Droplet Mixture: $N/\sqrt{\theta} = 90\%$, $D_o = 600\mu m$)

123

Corrected Mass Flow Rate of Gas Phase $\dfrac{m\sqrt{\theta}}{\delta}\bigg|_g$ (lbm/s)
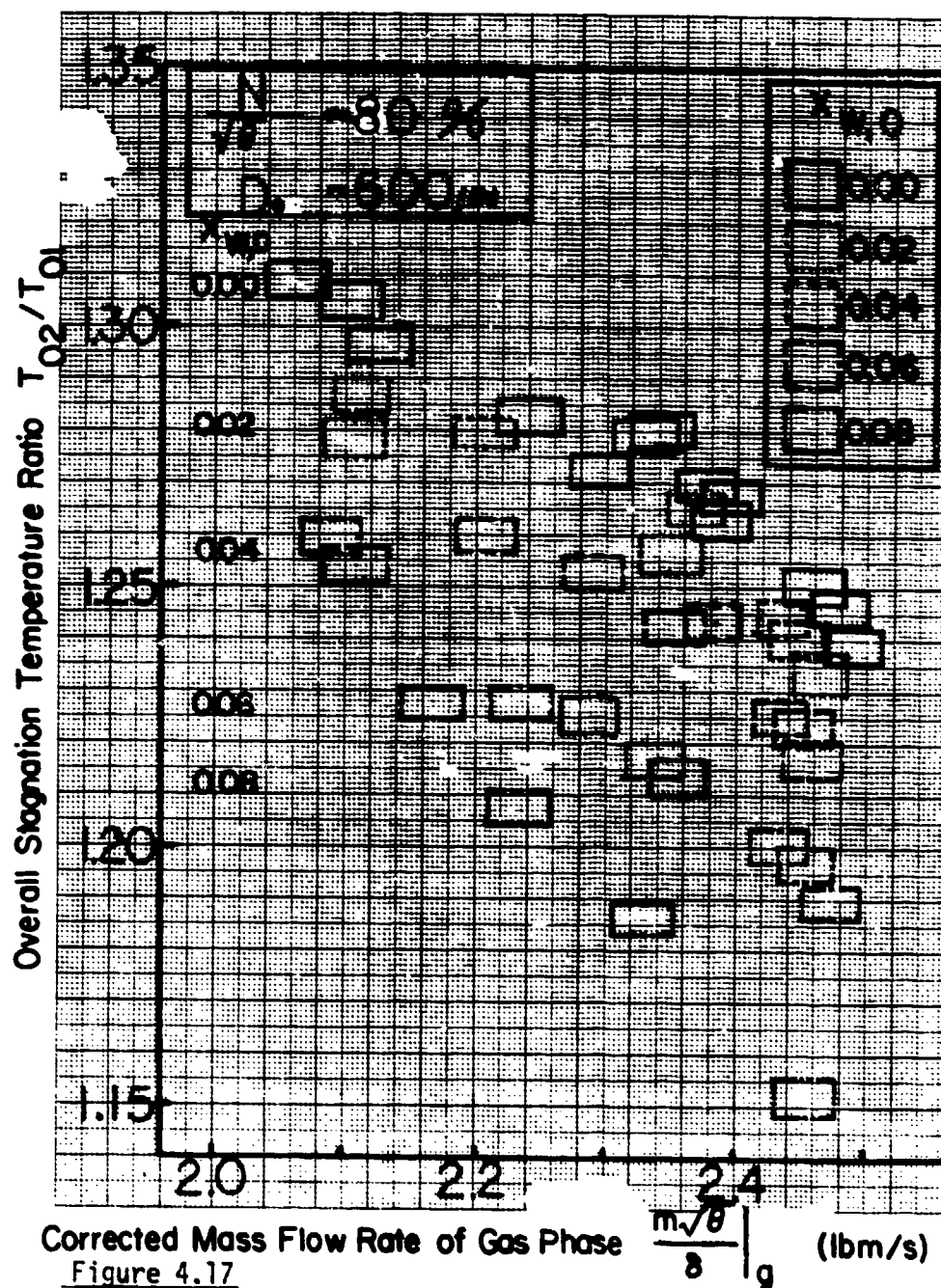
Figure 4.17

Performance of the Test Compressor Obtained From
Tests with Air-Water Droplet Mixture Flow (Overall
Total Temperature Ratio vs. Gas Phase Corrected
Mass Flow Rate: $N/\sqrt{\theta}$=80%, D_o=600μm)
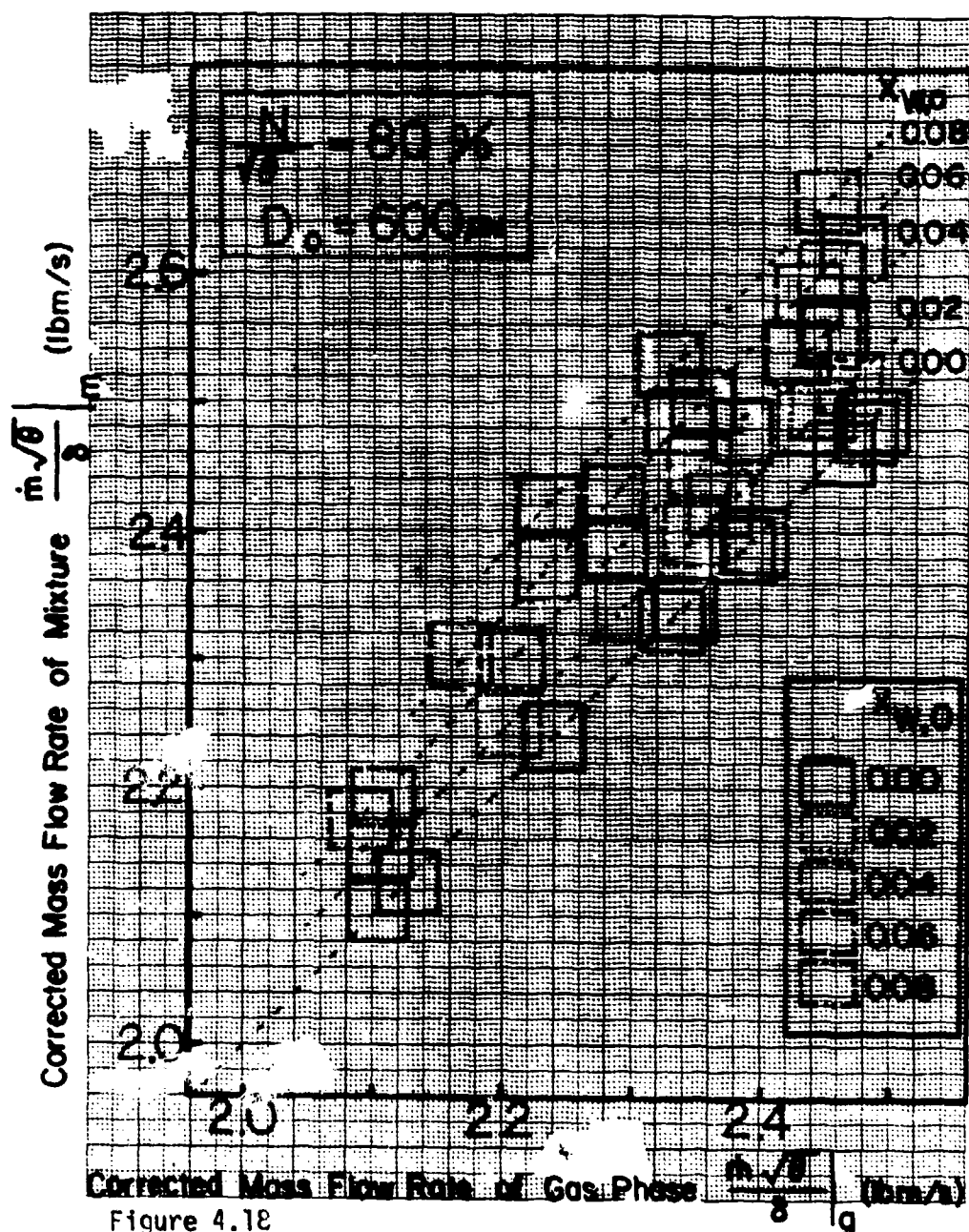
Figure 4.18

Corrected Mass Flow Rate of Gas Phase vs. Corrected
Mass Flow Rate of Air-Water Droplet Mixture: $N/\sqrt{\theta}$=80%, D_o=600μm)
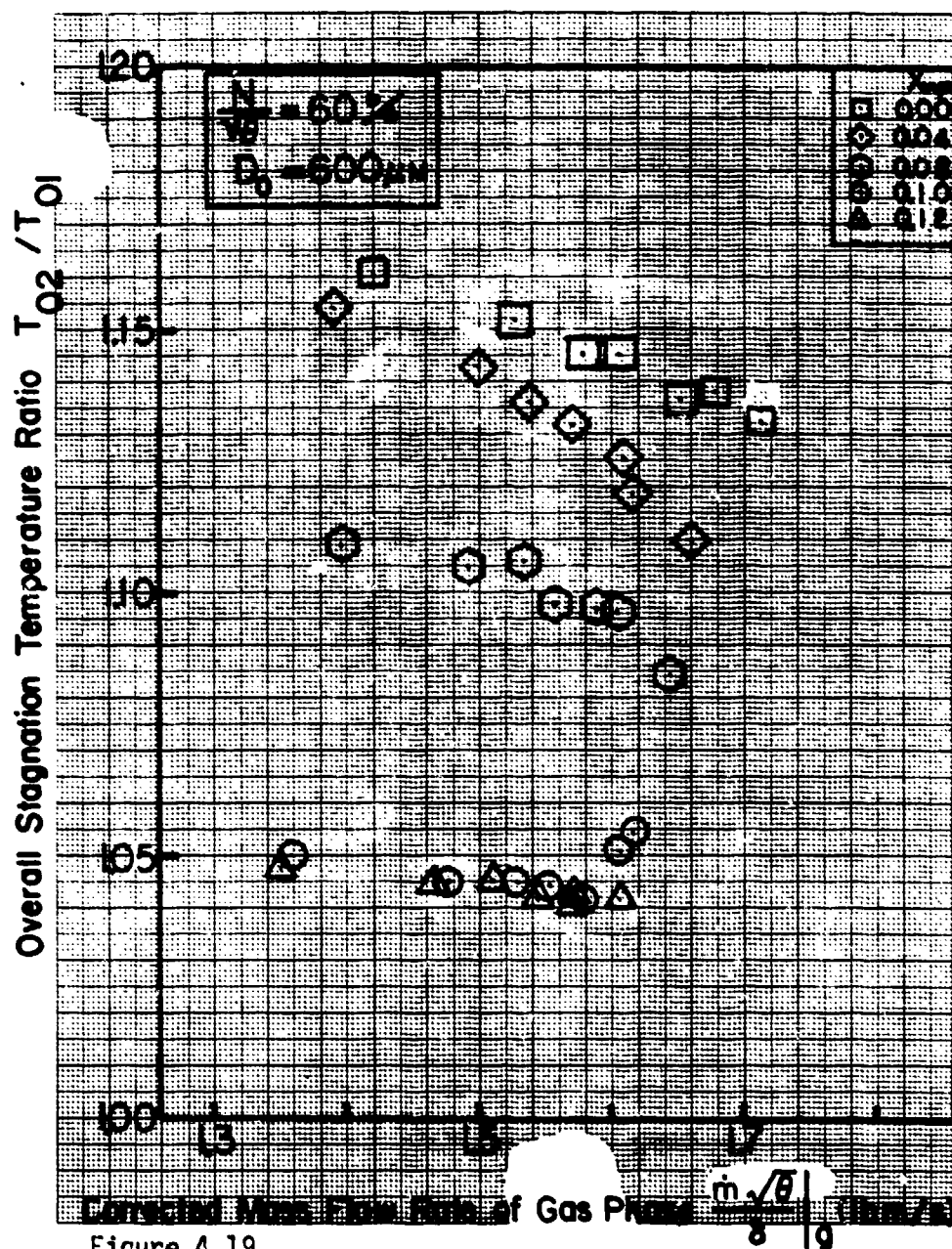
Figure 4.19
Performance of the Test Compressor Obtained From
Tests with Air-Water Droplet Mixture Flow (Overall
Total Temperature Ratio vs. Gas Phase Corrected
Mass Flow Rate: $N/\sqrt{\theta}=60\%$, $D_0=600\mu m$)
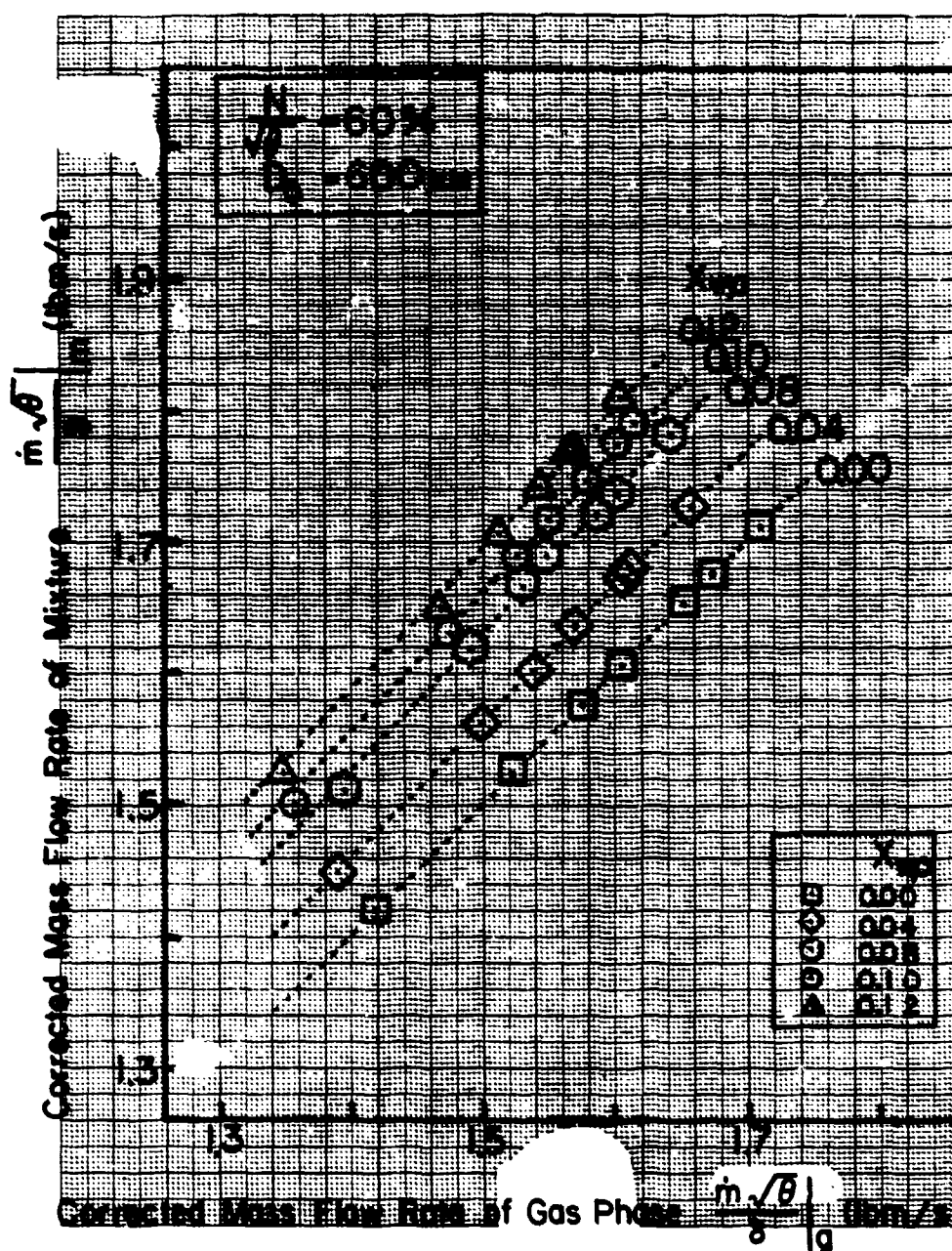
Figure 4.20
Corrected Mass Flow Rate of Gas Phase vs. Corrected
Mass Flow Rate of Air-Water Droplet Mixture: $N/\sqrt{\theta}$=60%, D_O=600μm)
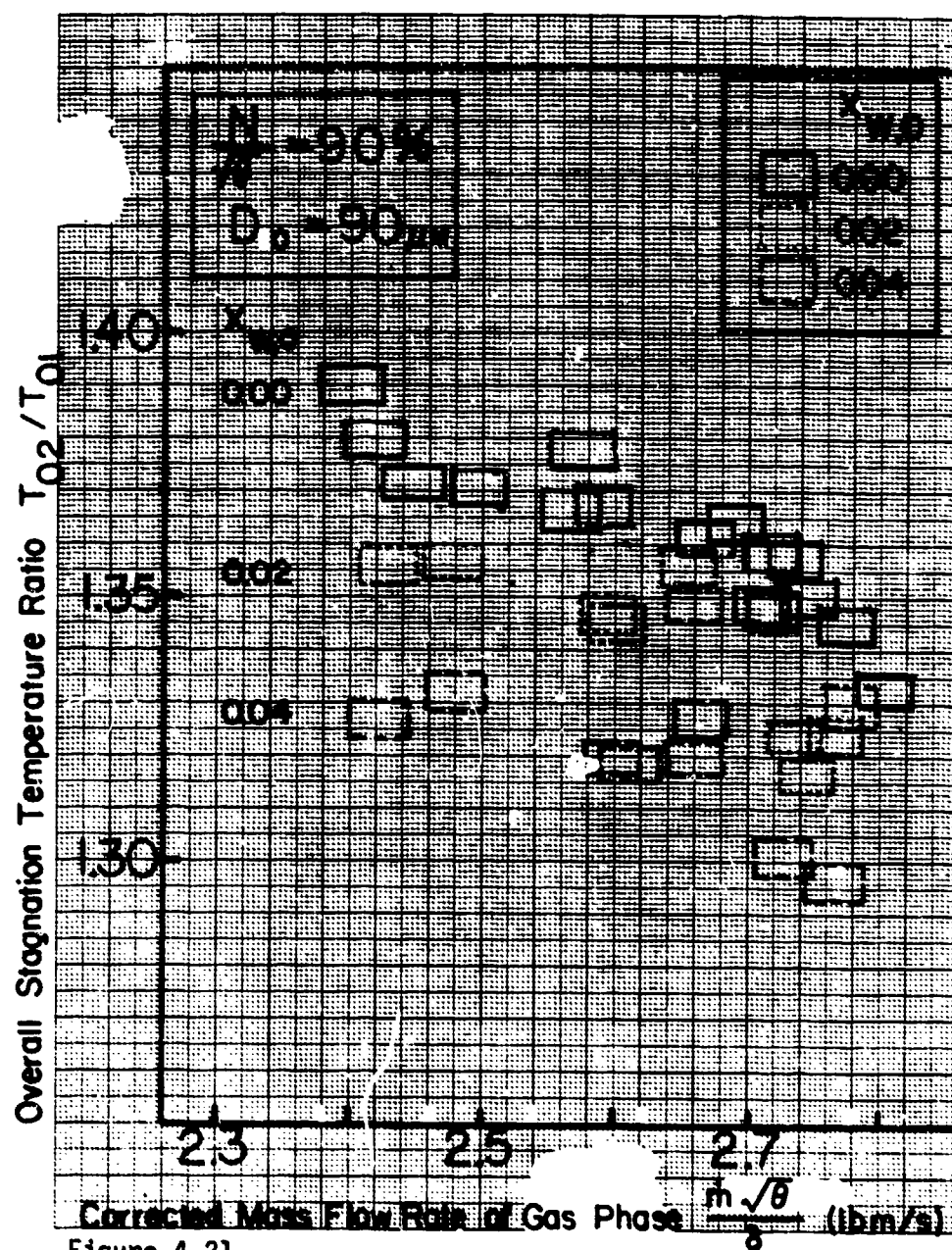
Figure 4.21

Performance of the Test Compressor Obtained From
Tests with Air-Water Droplet Mixture Flow (Overall
Total Temperature Ratio vs. Gas Phase Corrected
Mass Flow Rate: $N/\sqrt{\theta}=90\%$, $D_o=90\mu m$)
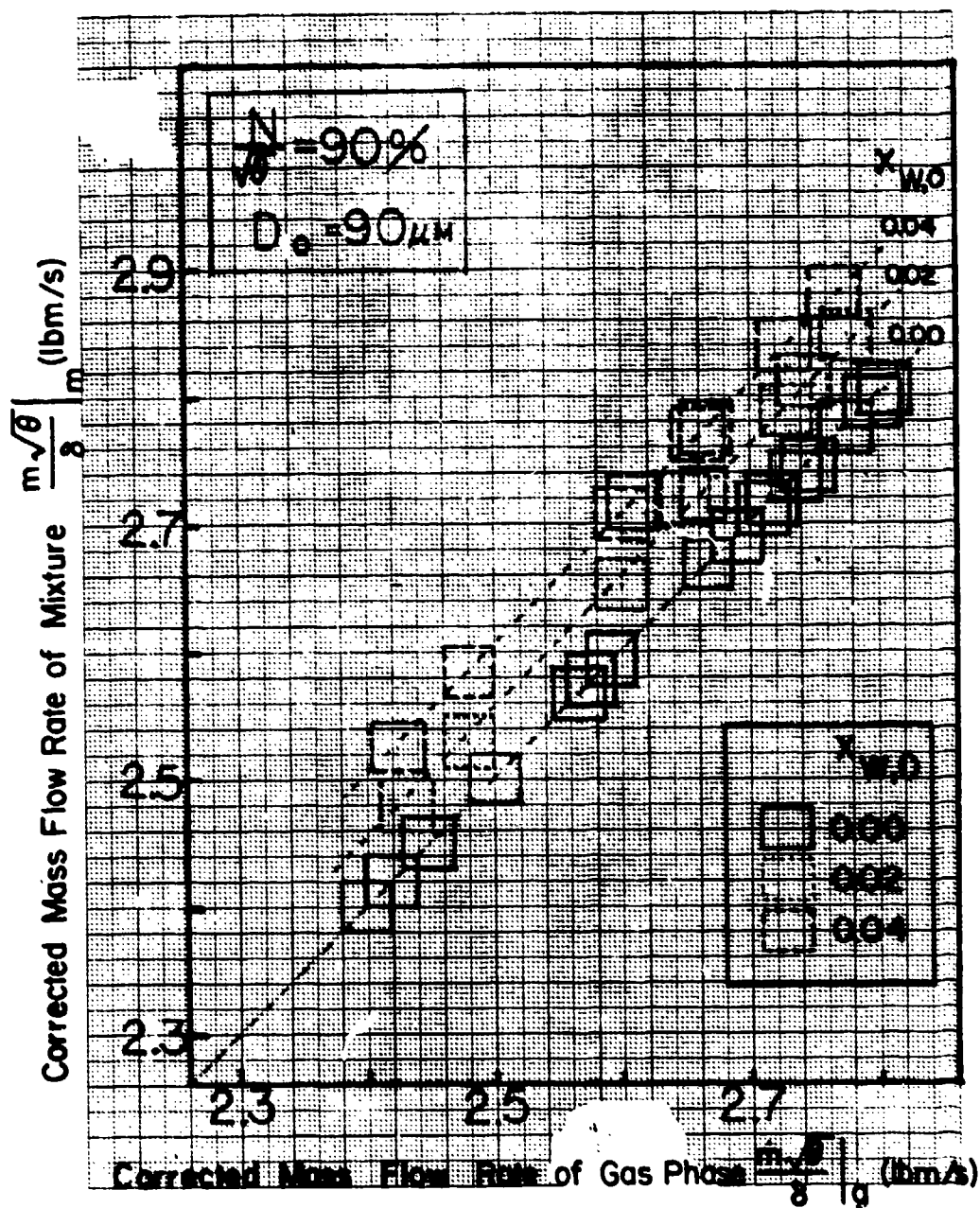
Figure 4.22
Corrected Mass Flow Rate of Gas Phase vs. Corrected
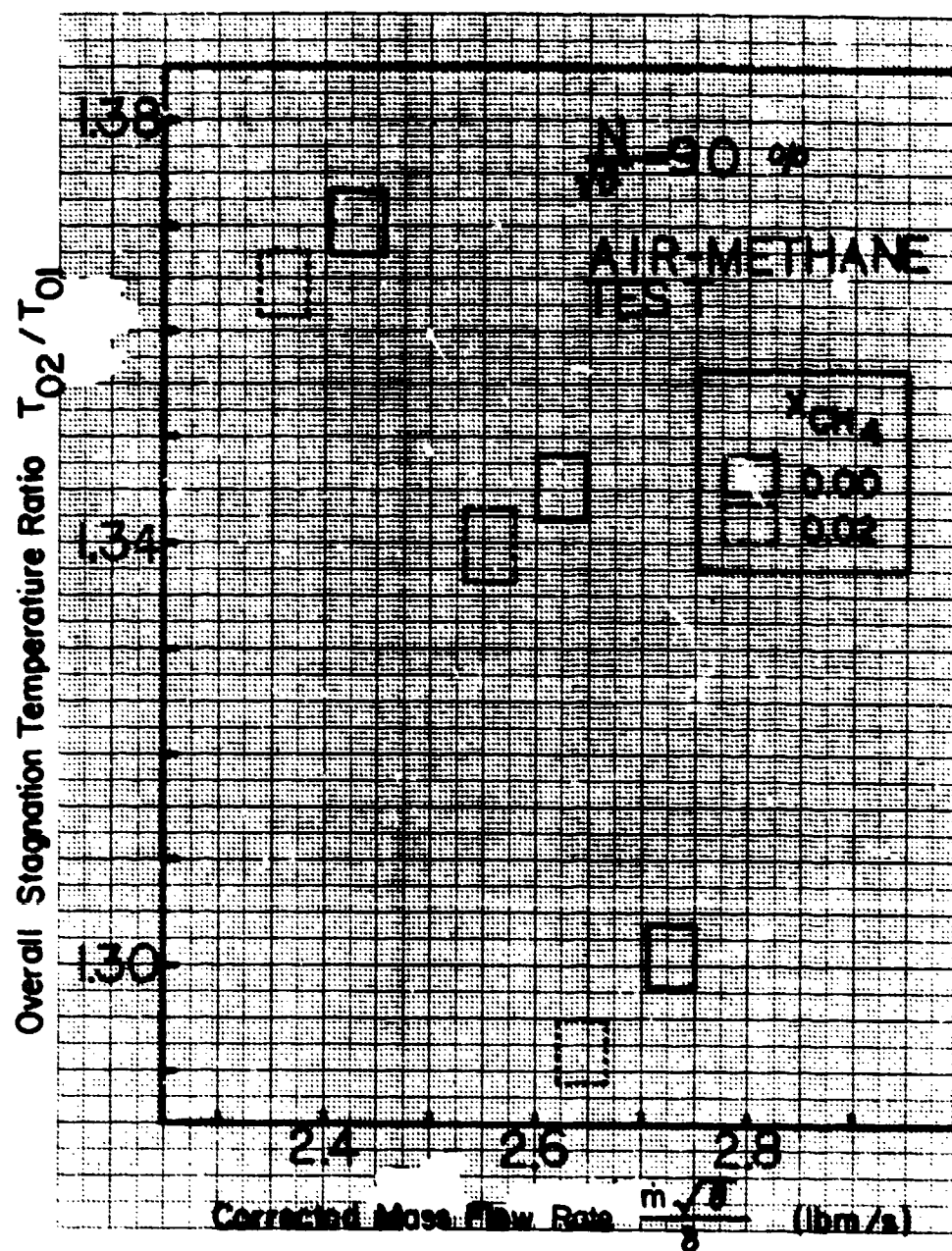Mass Flow Rate of Air-Water Droplet Mixture: N/√θ=90%, D_o=90μm)
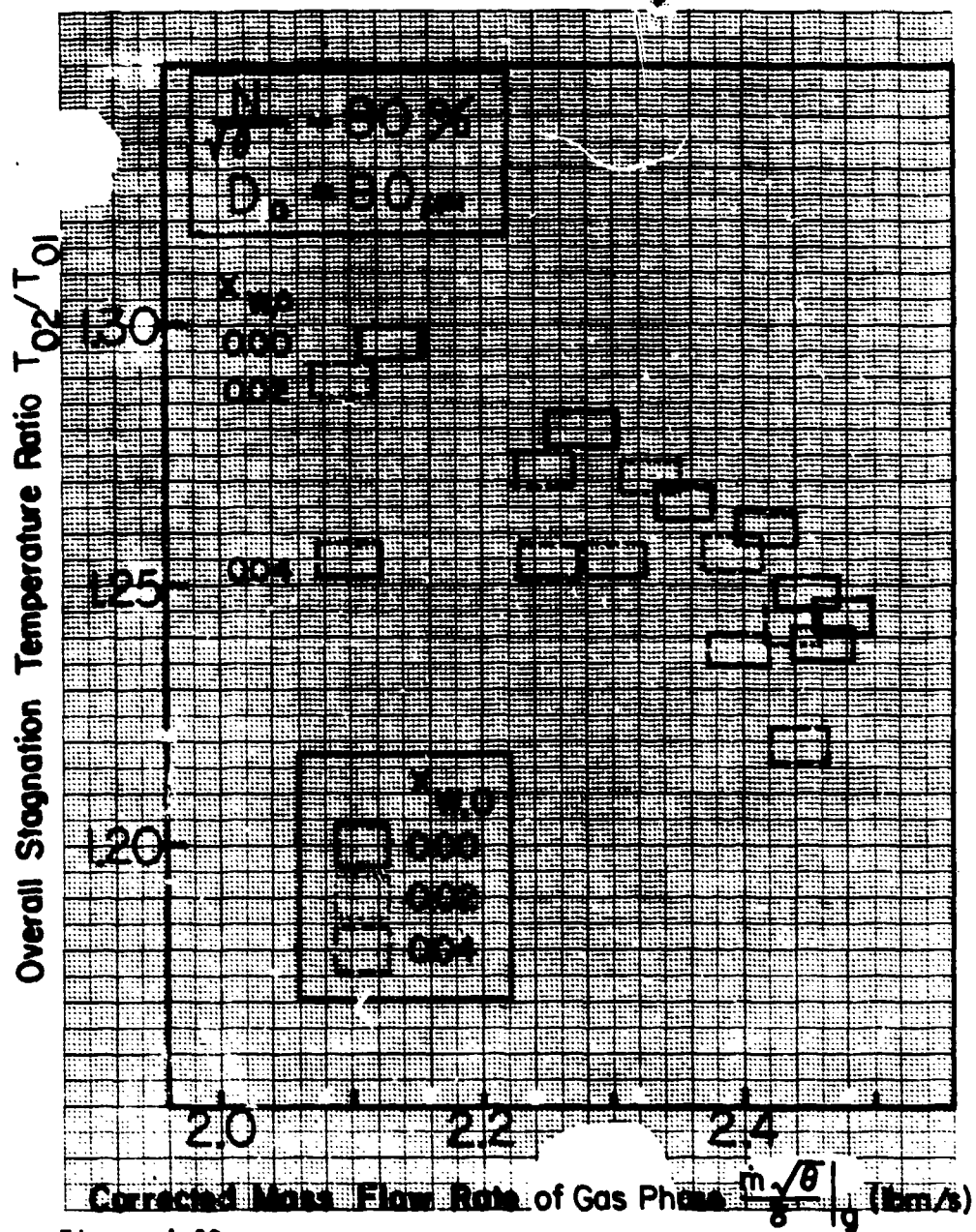
Figure 4.23

Performance of the Test Compressor Obtained From
Tests with Air-Water Droplet Mixture Flow (Overall
Total Temperature Ratio vs. Gas Phase Corrected
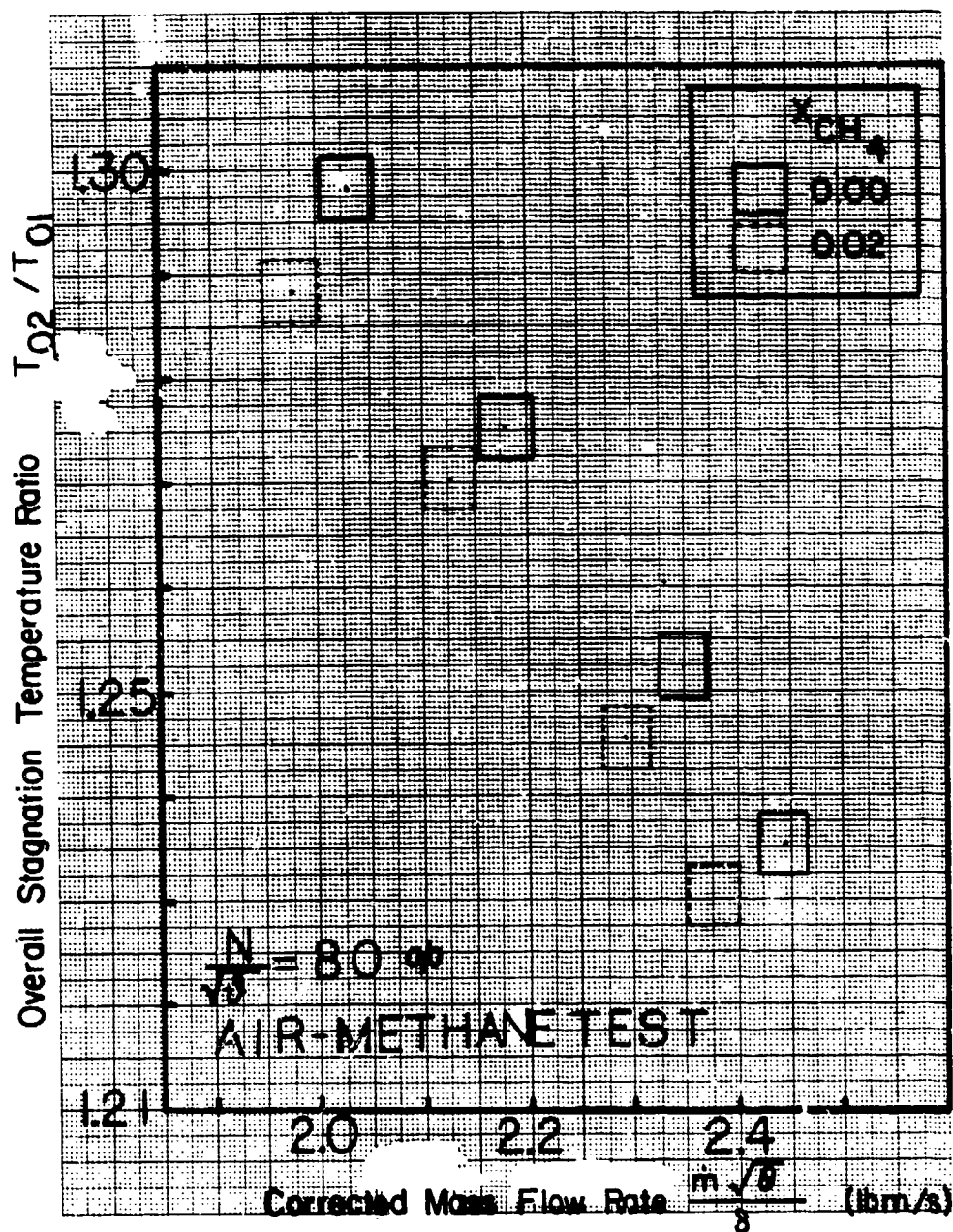Mass Flow Rate: $N/\sqrt{\theta}=80\%$, $D_o=600\mu m$)
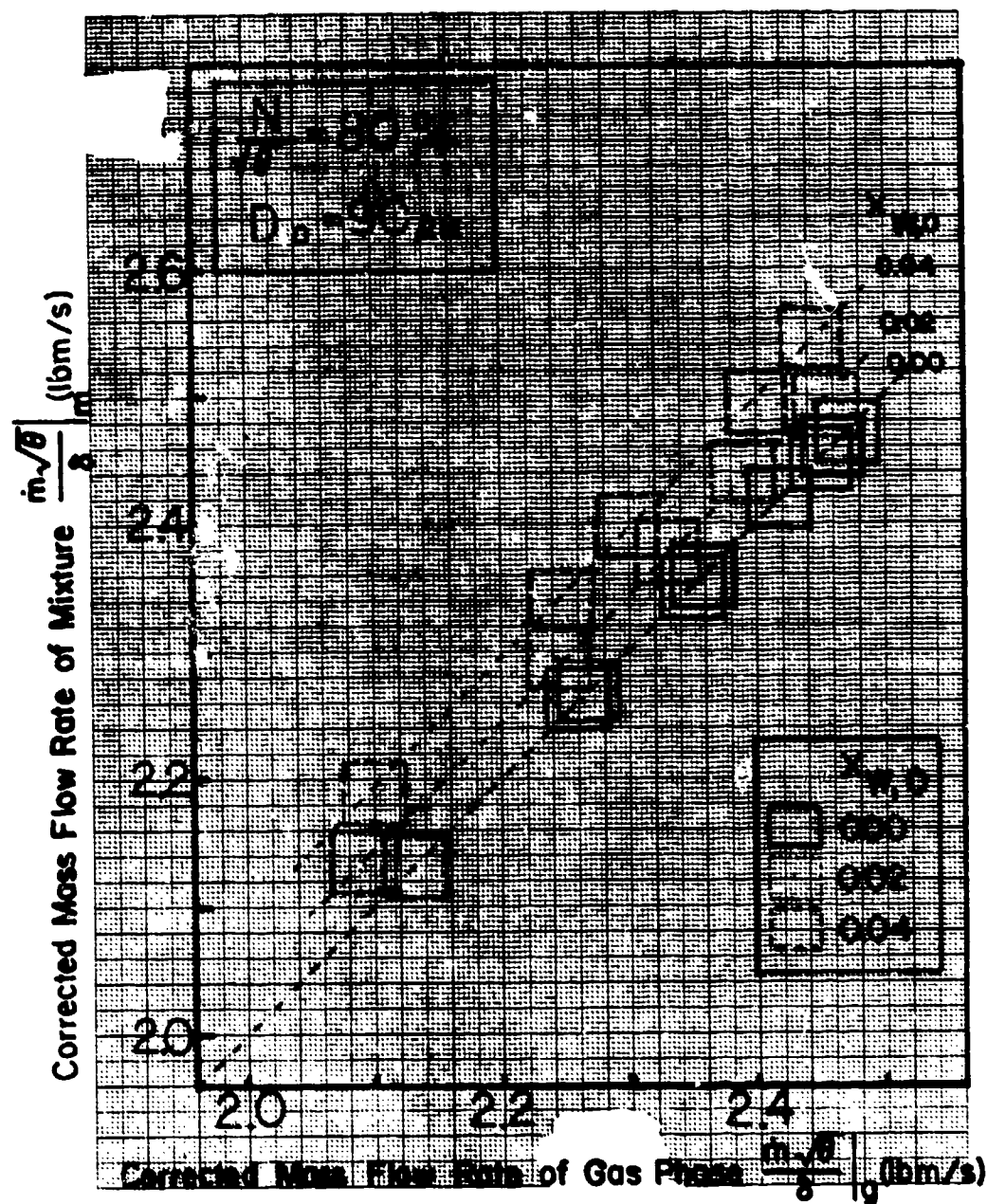
Figure 4.24

Corrected Mass Flow Rate of Gas Phase vs. Corrected
Mass Flow Rate of Air-Water Droplet Mixture: $N/\sqrt{\theta}=80\%$, $D_o=90\mu m$)
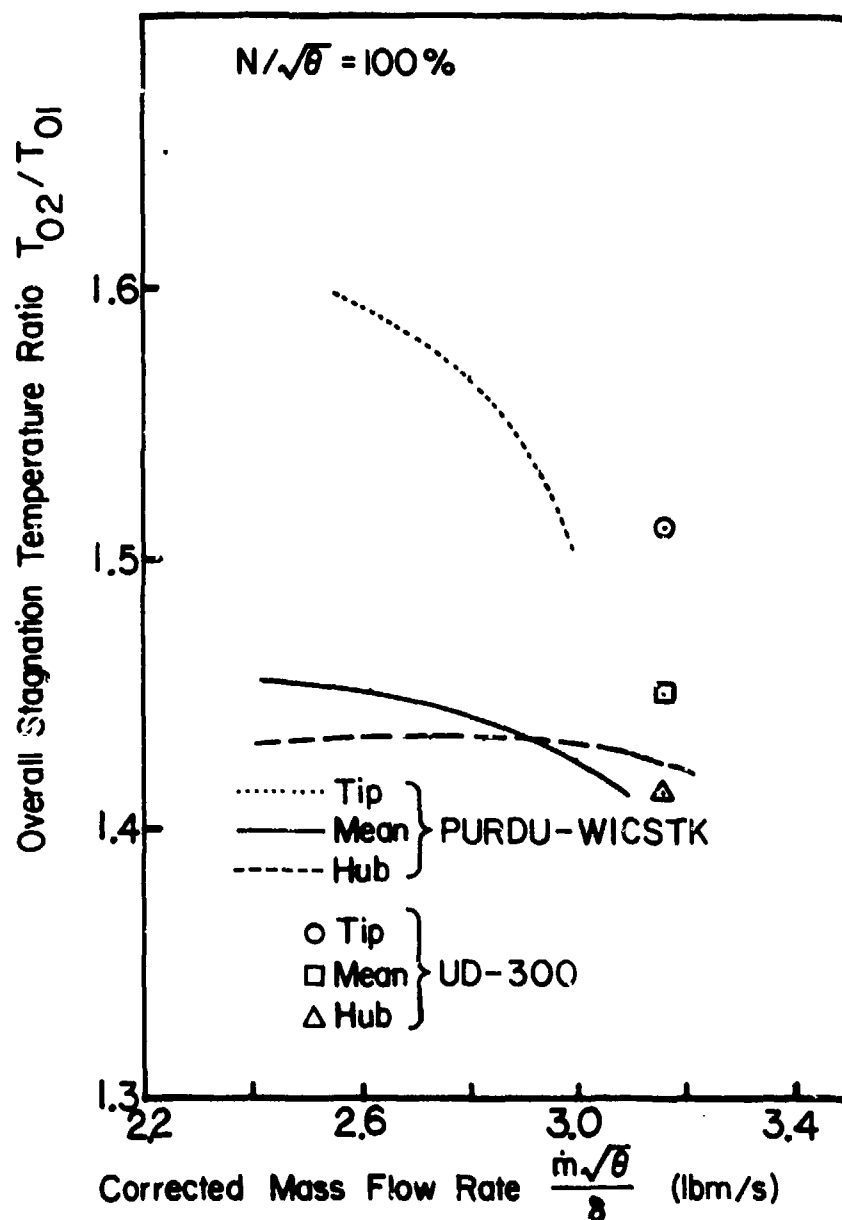
Figure 5.1

Comparison of Overall Stagnation Temperature Ratio
with Air Flow Predicted According to the UD-300 and
the PURDU-WICSTK Programs
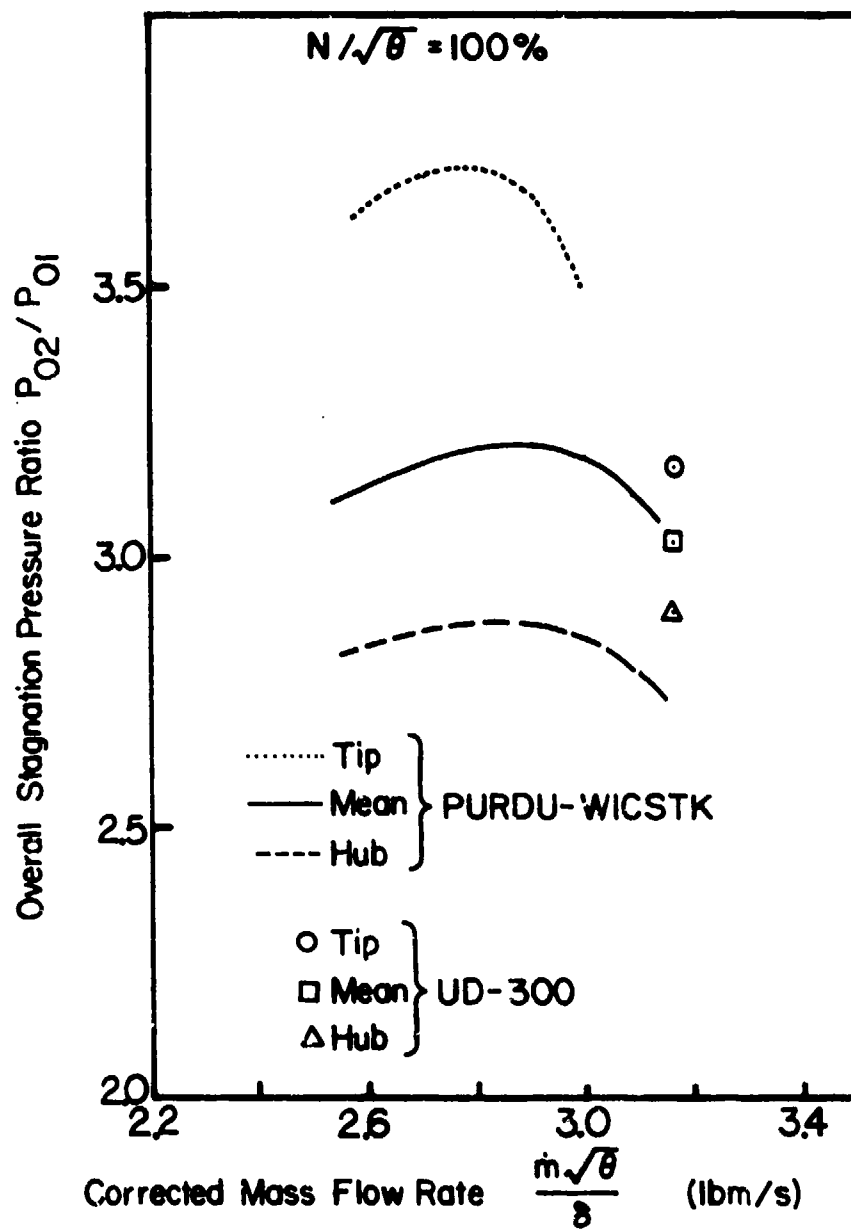
Figure 5.2
Comparison of Overall Stagnation Pressure Ratio
with Air Flow Predicted According to the UD-300 and
the PURDU-WICSTK Programs
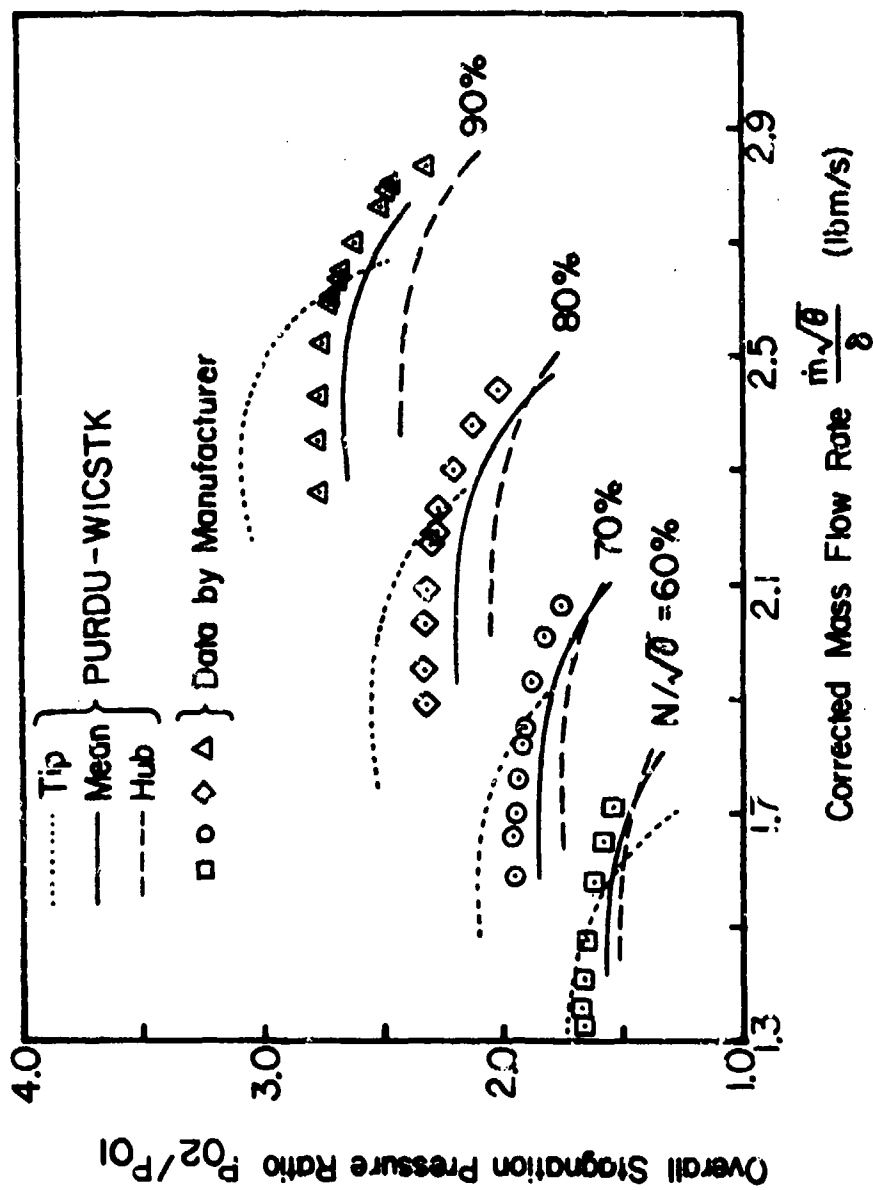
Figure 5.3

Comparison Between Compressor Performance Provided
by Manufacturer and Predictions According to the
UD-300 and the PURDU-WICSTK Programs
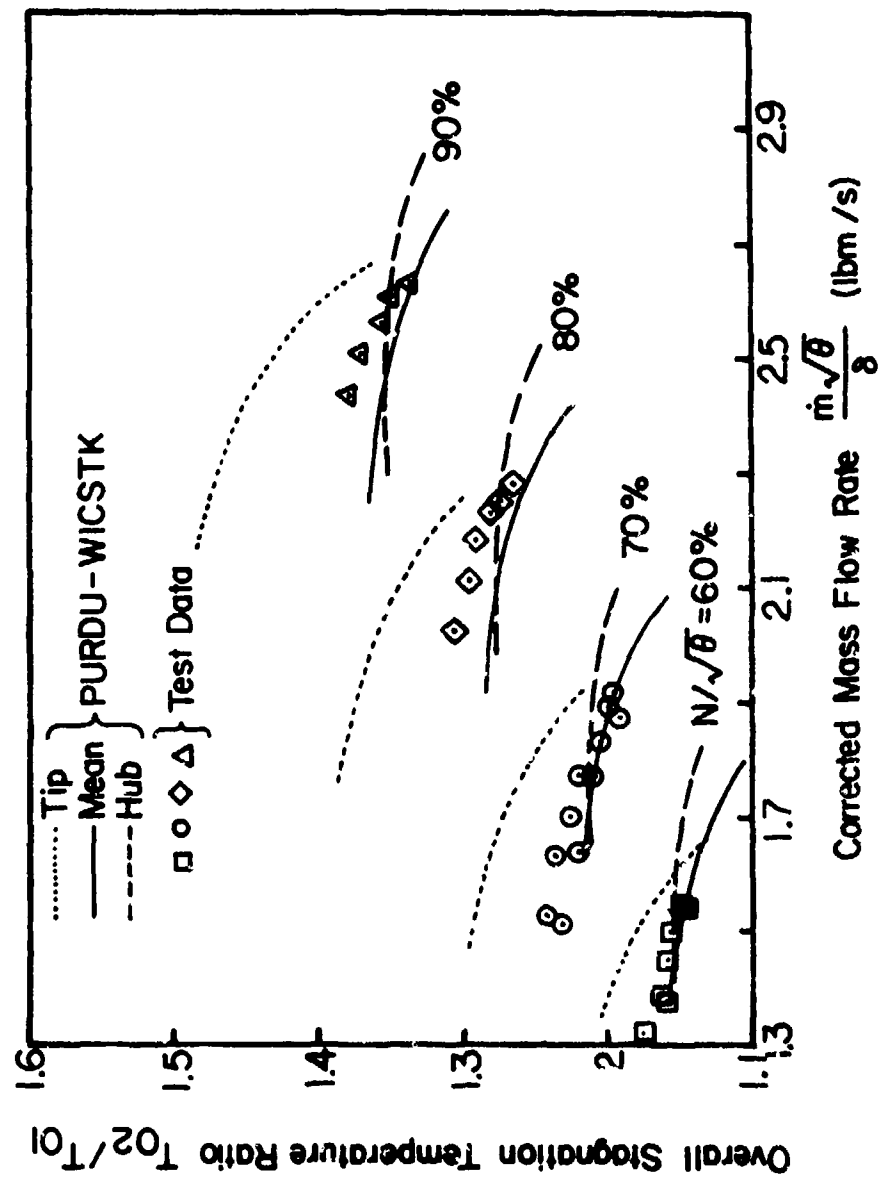
Figure 5.4

Comparison Between Predictions According to PURDU-WICSTK
Program and Test Data for Overall Stagnation Temperature
Ratio with Air Flow
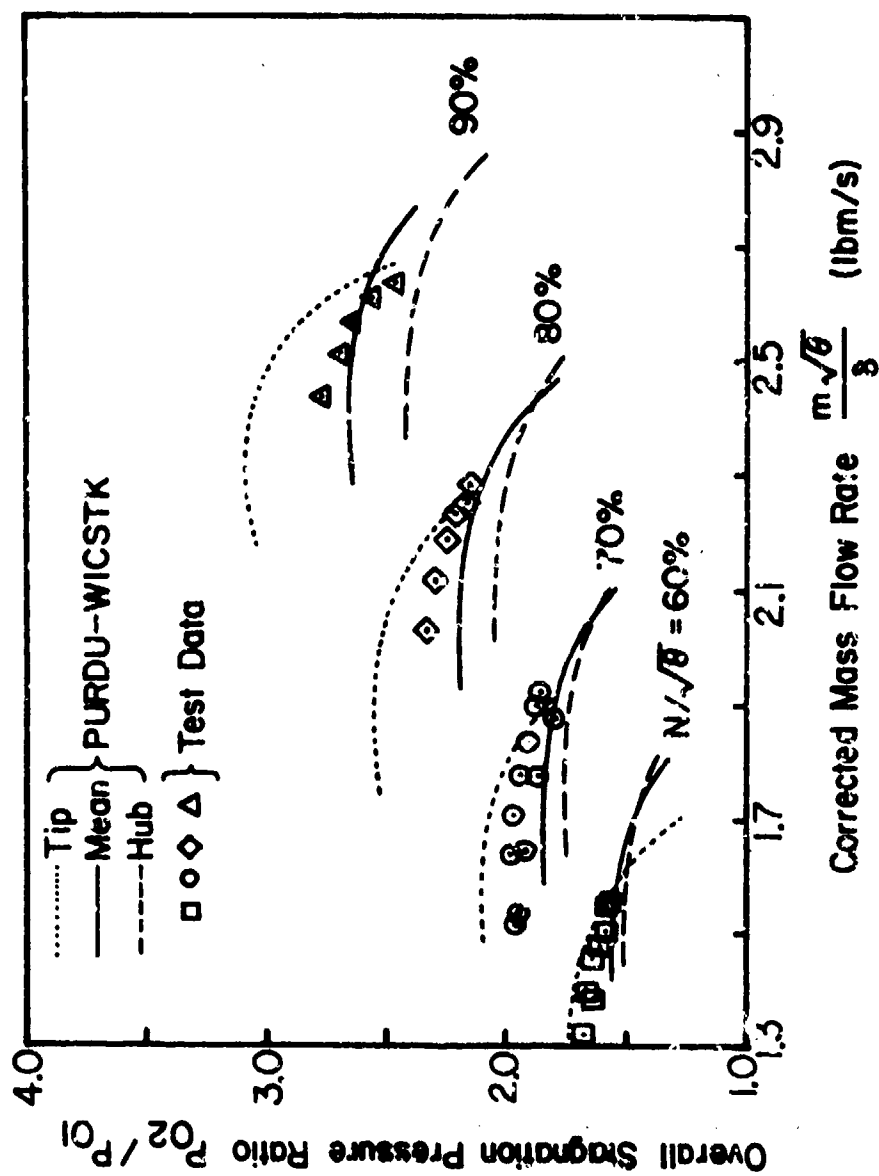
Figure 5.5

Comparison Between Predictions According to PURDU-WICSTK Program and Test Data for Overall Stagnation Pressure Ratio with Air Flow
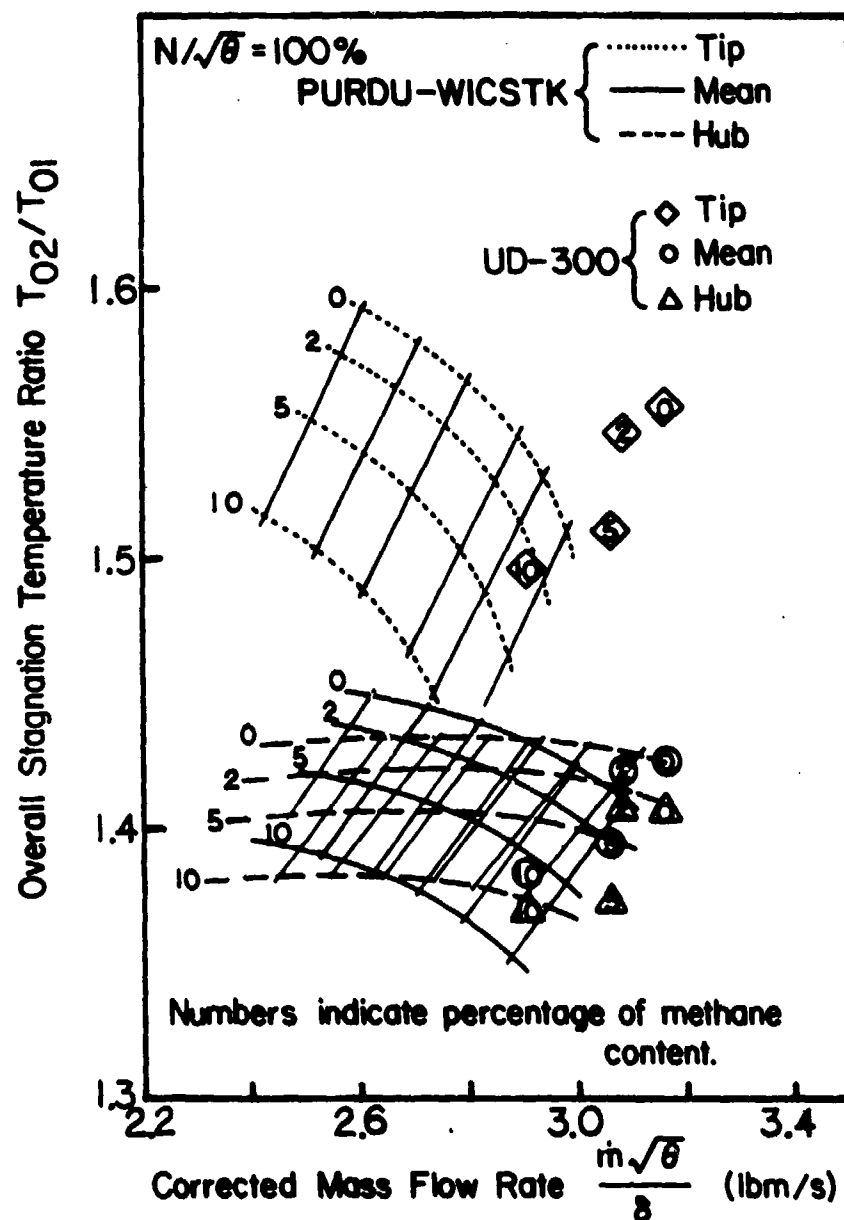
Figure 5.6

Comparison of Overall Stagnation Temperature Ratio
with Air-Methane Mixture Flow Predicted According
to the UD-300 and the PURDU-WICSTK Programs
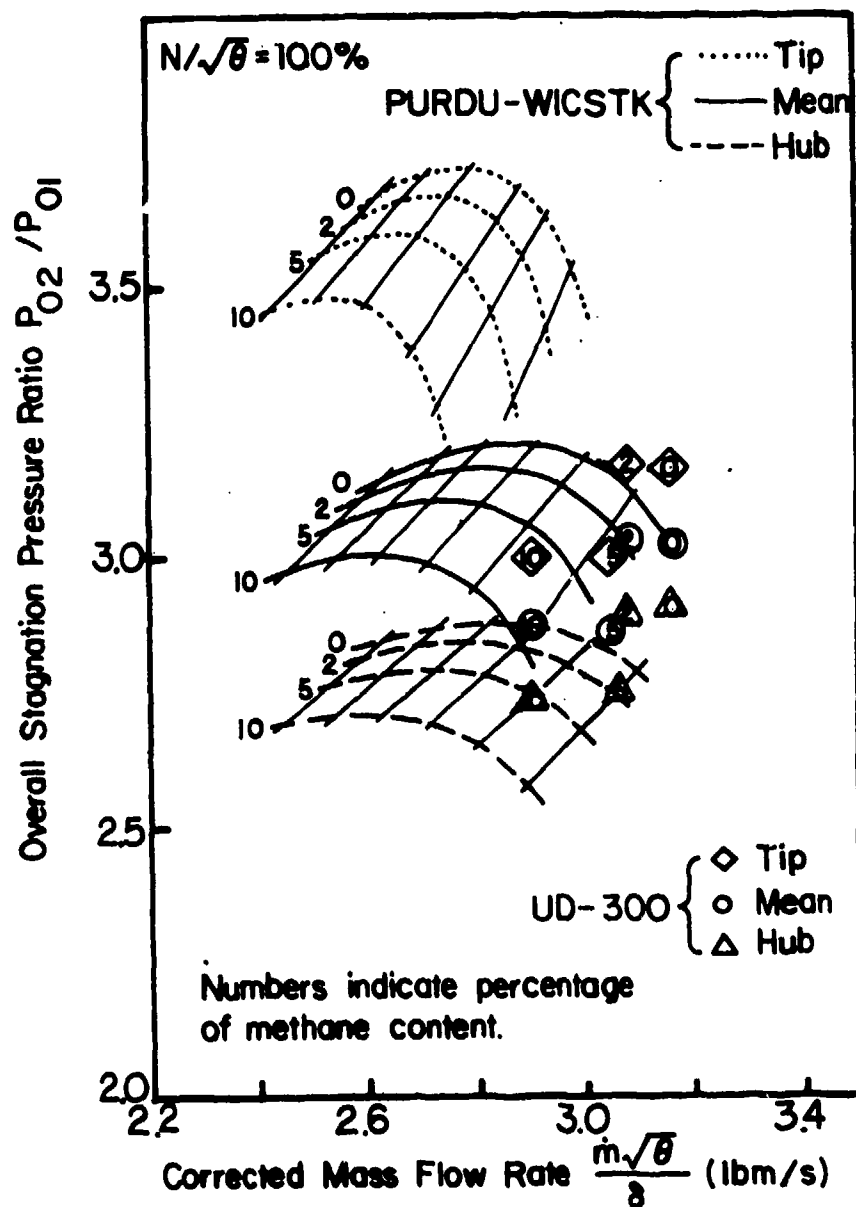
Figure 5.7

Comparison of Overall Stagnation Pressure Ratio
with Air-Methane Mixture Flow Predicted According
to the UD-300 and the PURDU-WICSTK Programs
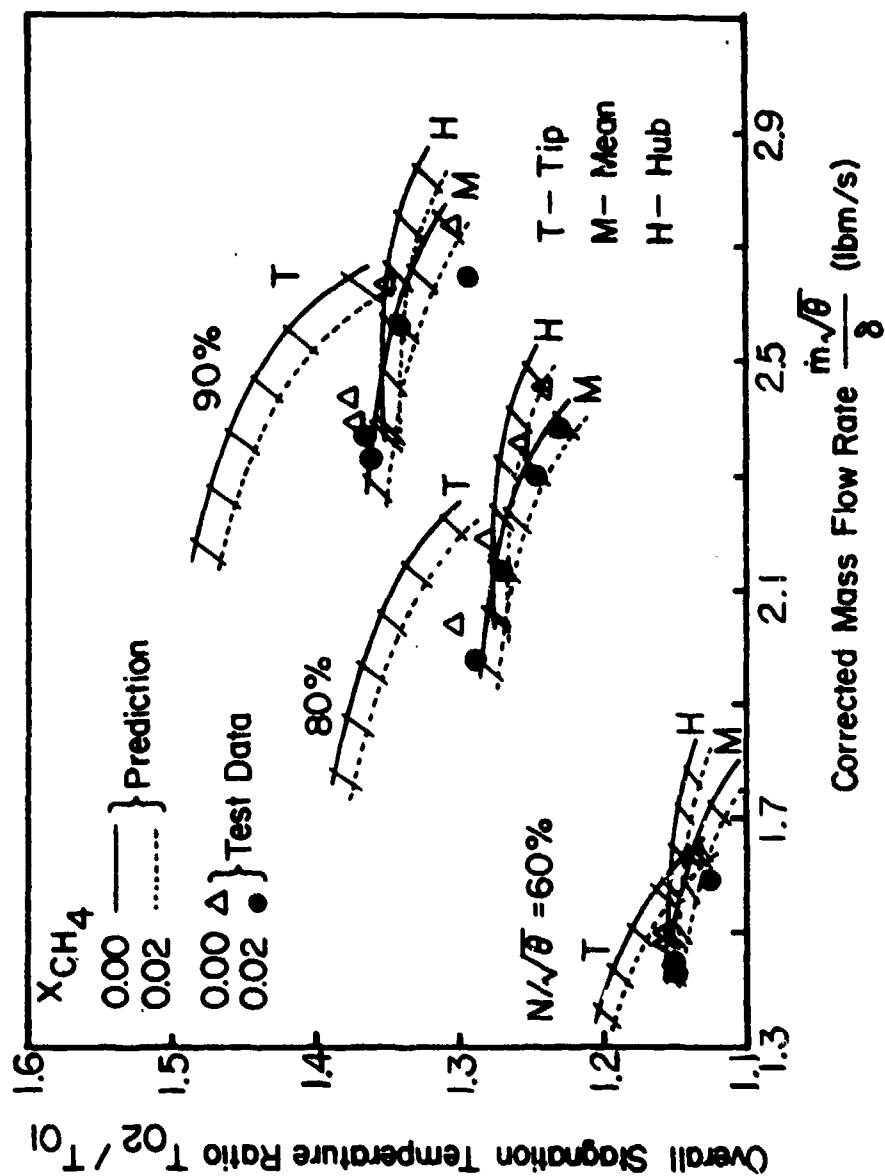
Figure 5.8

Comparison Between Predictions According to PURDU-WICSTK
Program and Test Data for Overall Stagnation Temperature
Ratio with Air-Methane Mixture Flow
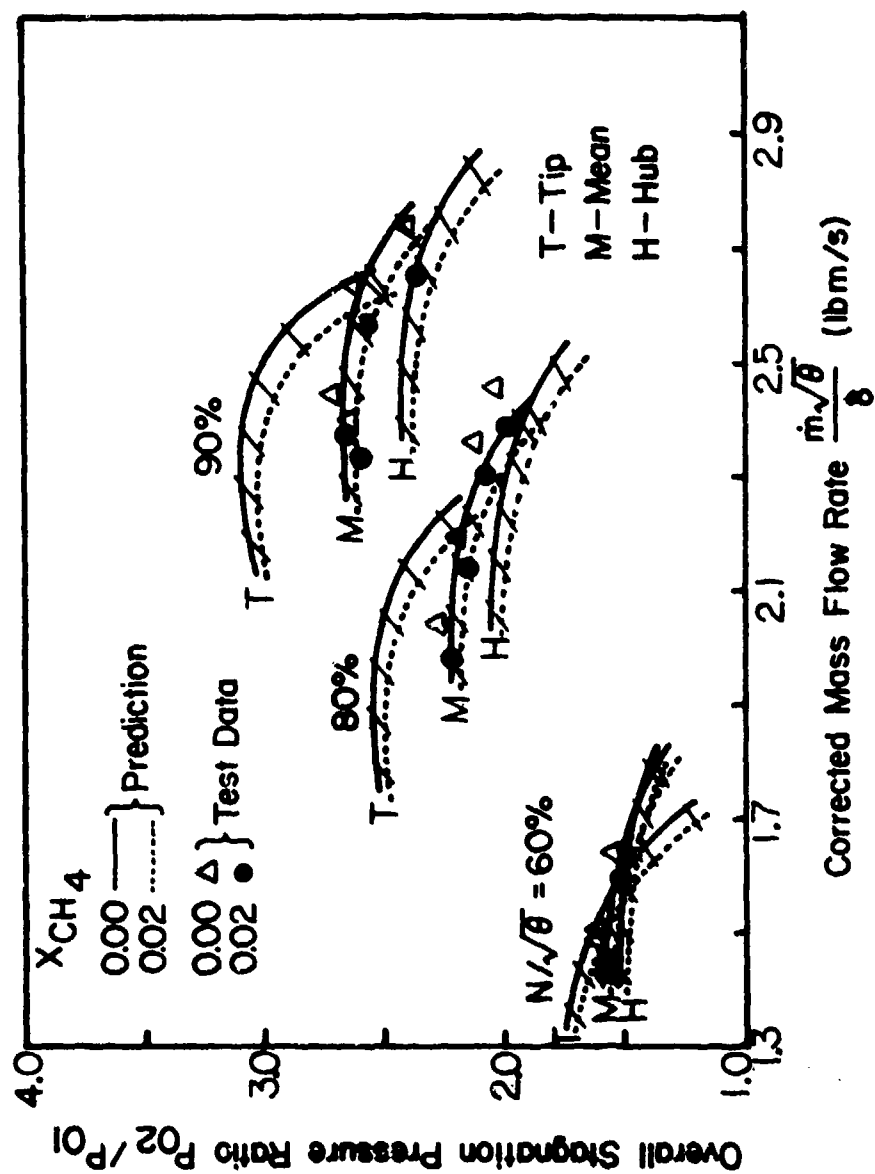
Figure 5.9

Comparison Between Predictions According to PURDU-WICSTK
Program and Test Data for Overall Stagnation Pressure
Ratio with Air-Methane Mixture Flow
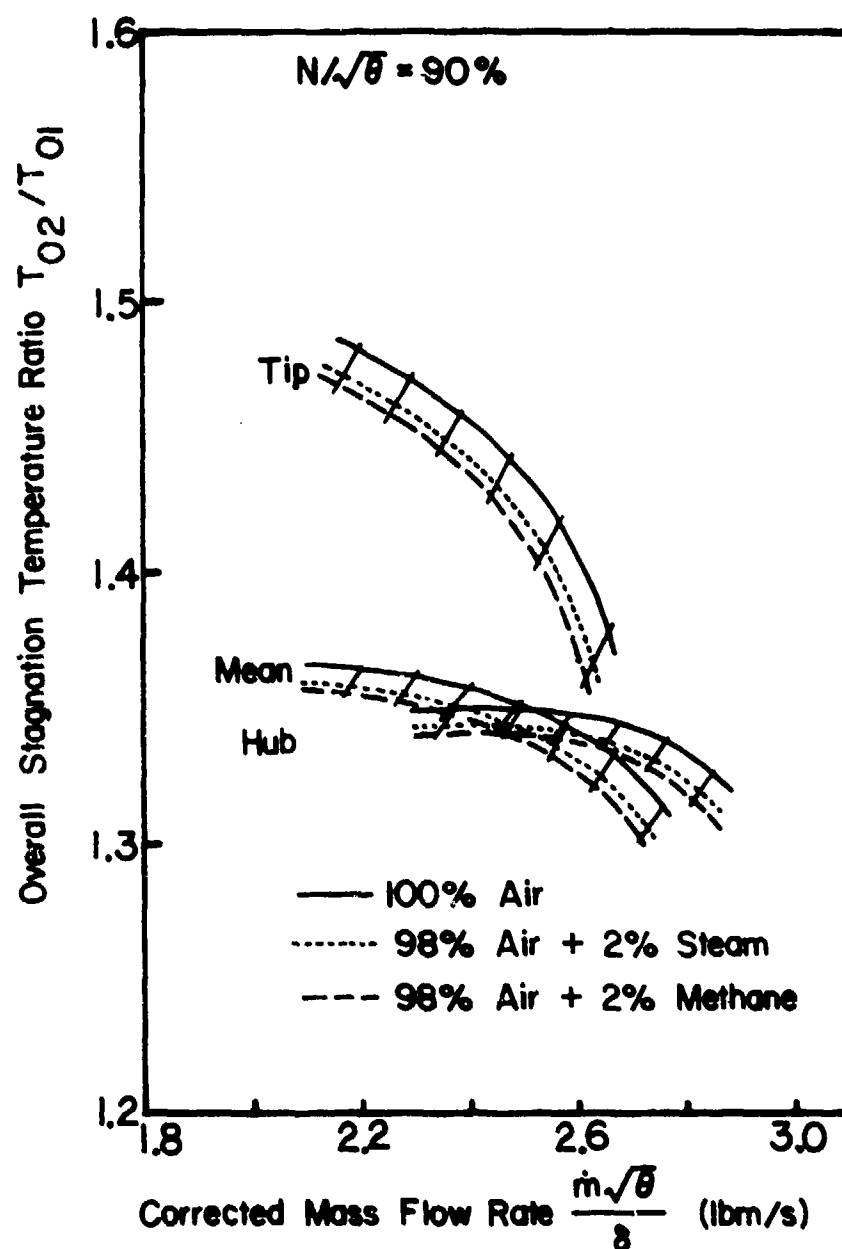
Figure 5.10

Comparison Between Predicted Performance with Air Flow,
Air-Methane Mixture Flow, and Air-Water Vapor Mixture
Flow for Overall Stagnation Temperature Ratio as a
Function of Corrected Mass Flow Rate
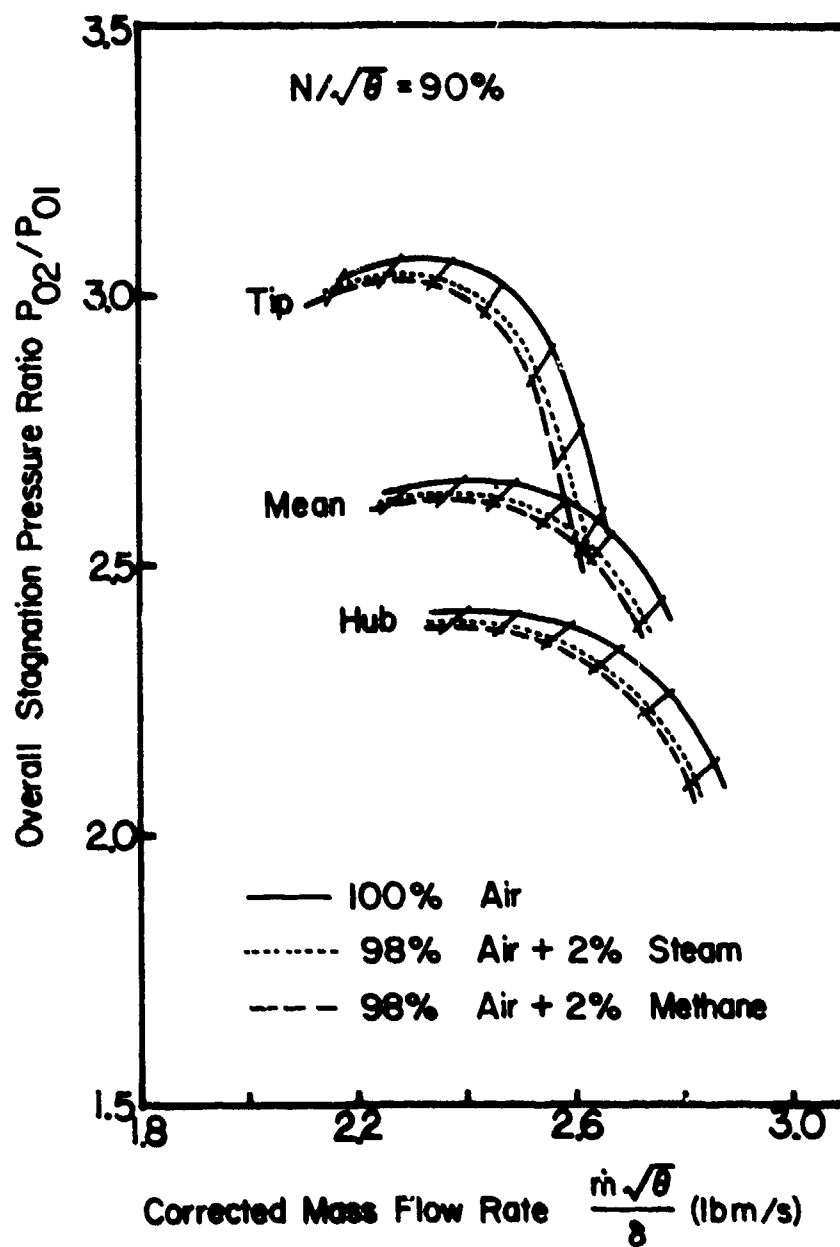
Figure 5.11

Comparison Between Predicted Performance with Air Flow,
Air-Methane Mixture Flow, and Air-Water Vapor Mixture
Flow for Overall Stagnation Pressure Ratio as a Function
of Corrected Mass Flow Rate
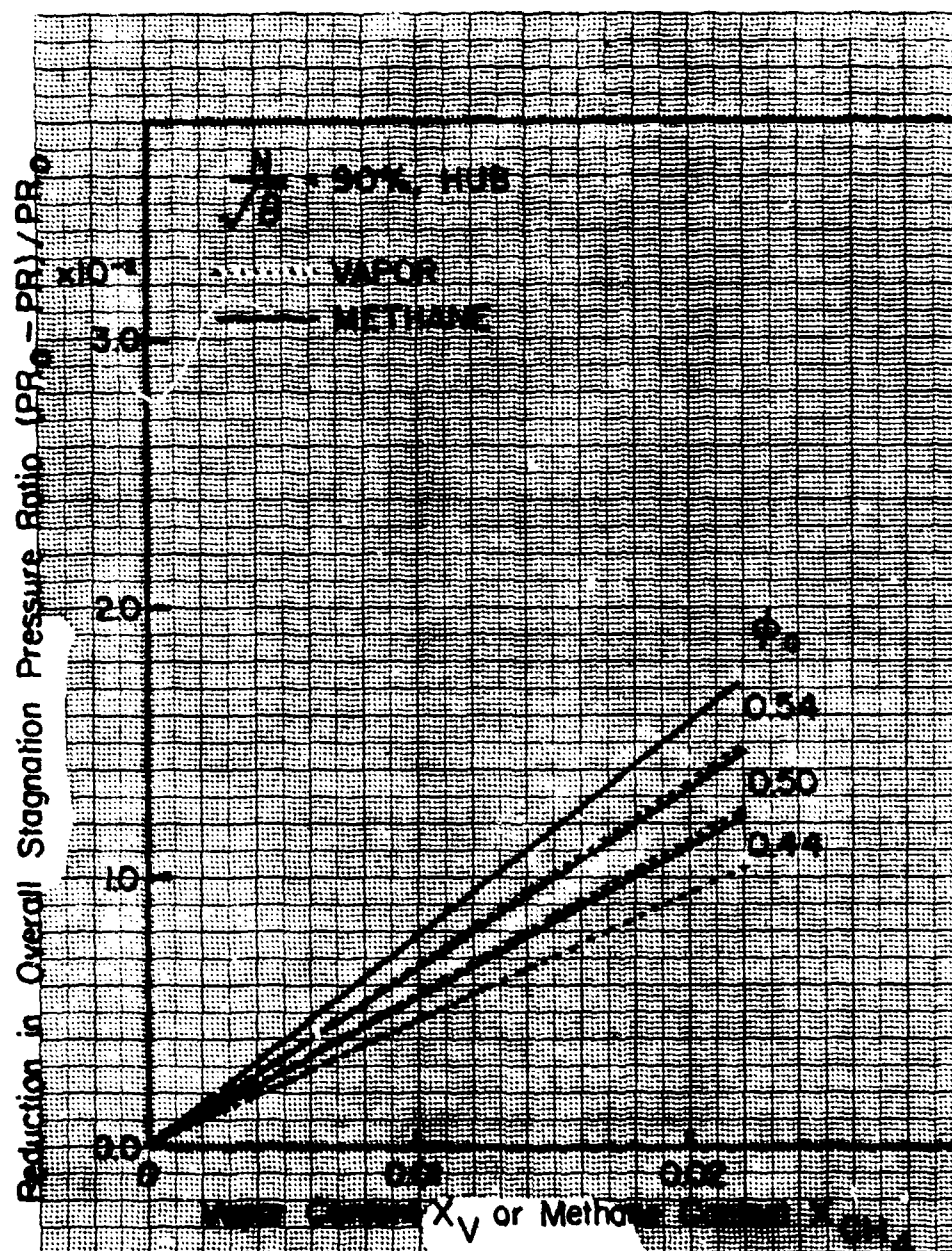
Figure 5.12(a)

Comparison Between Predicted Performance with Air Flow,
Air-Methane Mixture Flow, and Air-Water Vapor Mixture
Flow for Change in Stagnation Temperature Ratio as a
Function of Methane and Water Vapor Content at Hub
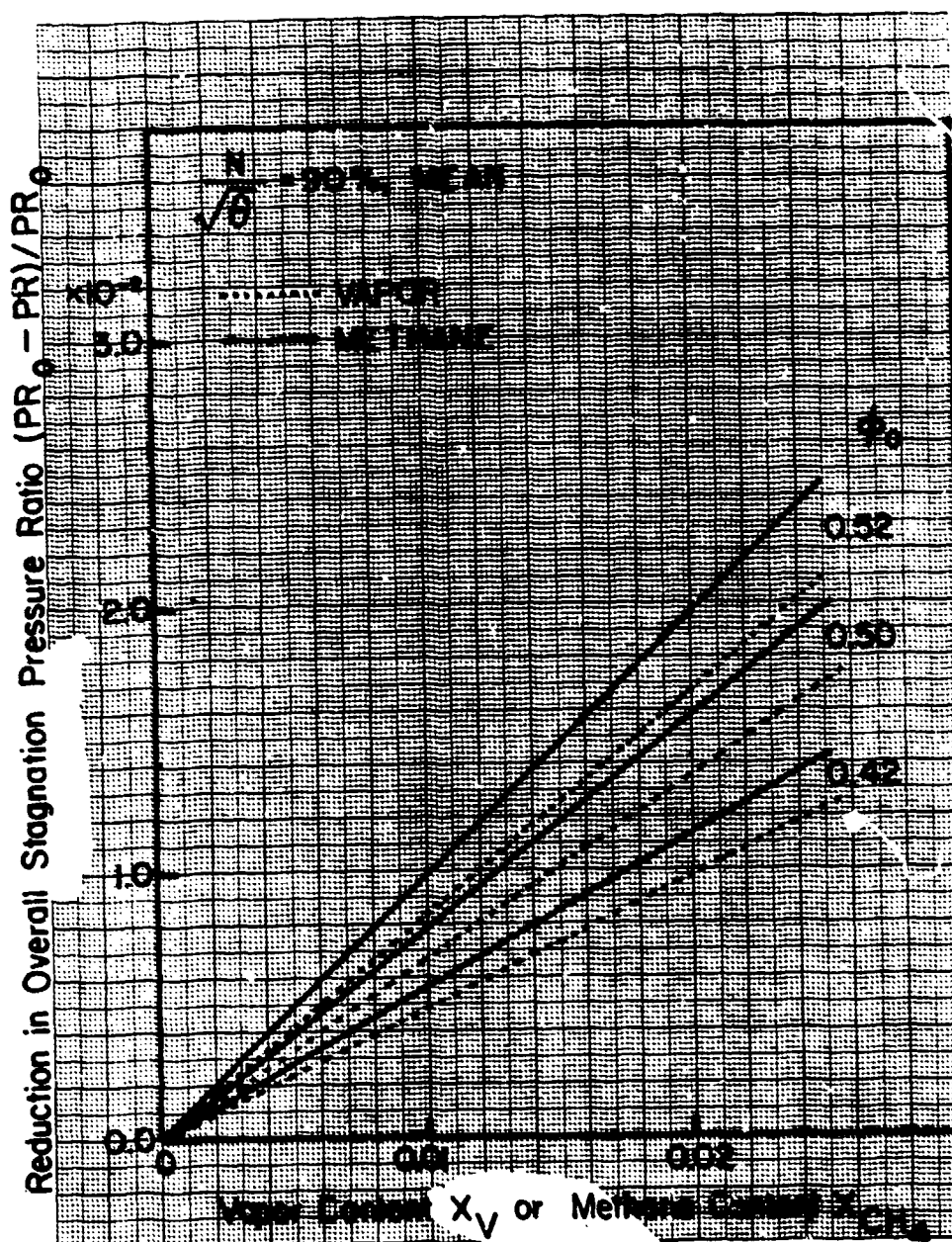
Figure 5.12(b)

Comparison Between Predicted Performance with Air Flow,
Air-Methane Mixture Flow, and Air-Water Vapor Mixture
Flow for Change in Stagnation Temperature Ratio as a
Function of Methane and Water Vapor Content at Mean
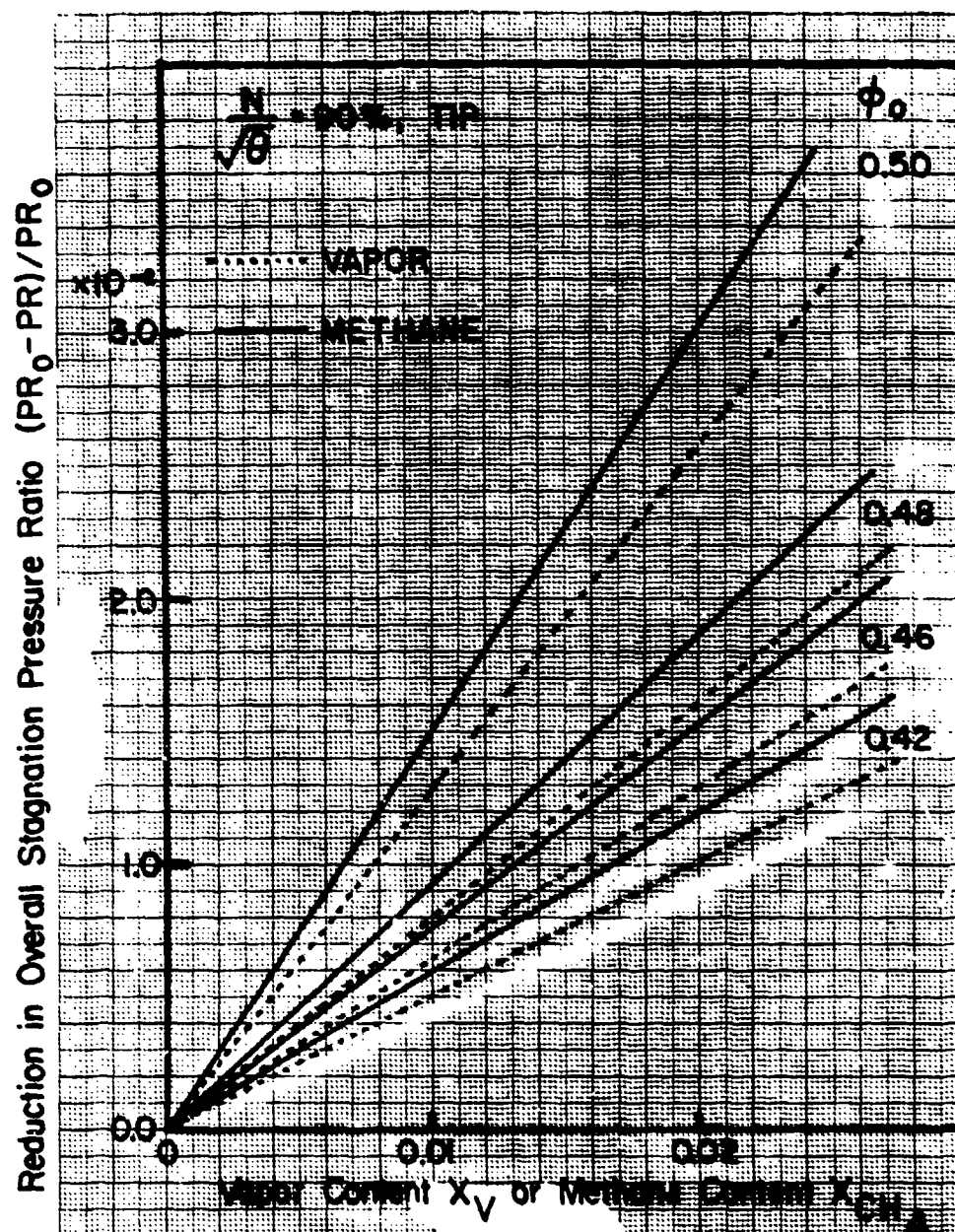
Figure 5.12(c)

Comparison Between Predicted Performance with Air Flow,
Air-Methane Mixture Flow, and Air-Water Vapor Mixture
Flow for Change in Stagnation Temperature Ratio as a
Function of Methane and Water Vapor Content at Tip
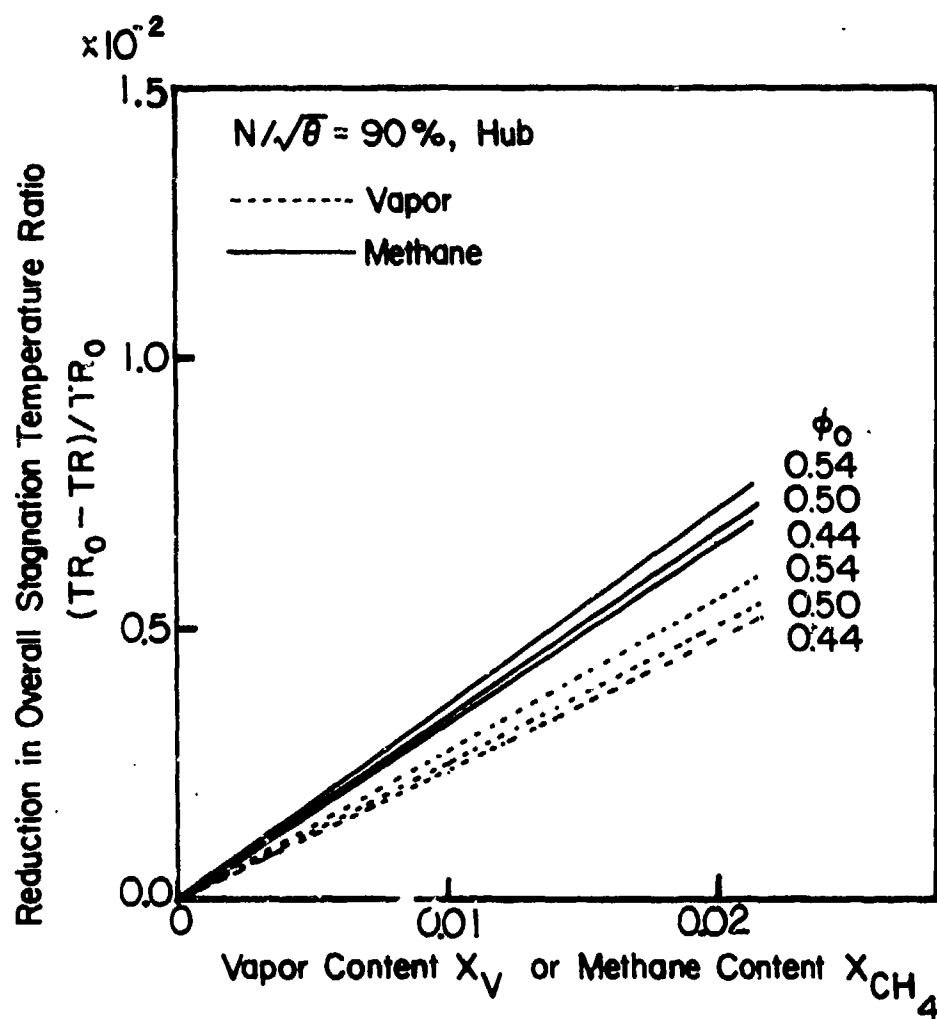
Figure 5.13(a)

Comparison Between Predicted Performance with Air
Flow, Air-Methane Mixture Flow, and Air-Water Vapor
Mixture Flow for Change in Stagnation Pressure
Ratio as a Function of Methane and Water Vapor
Content at Hub
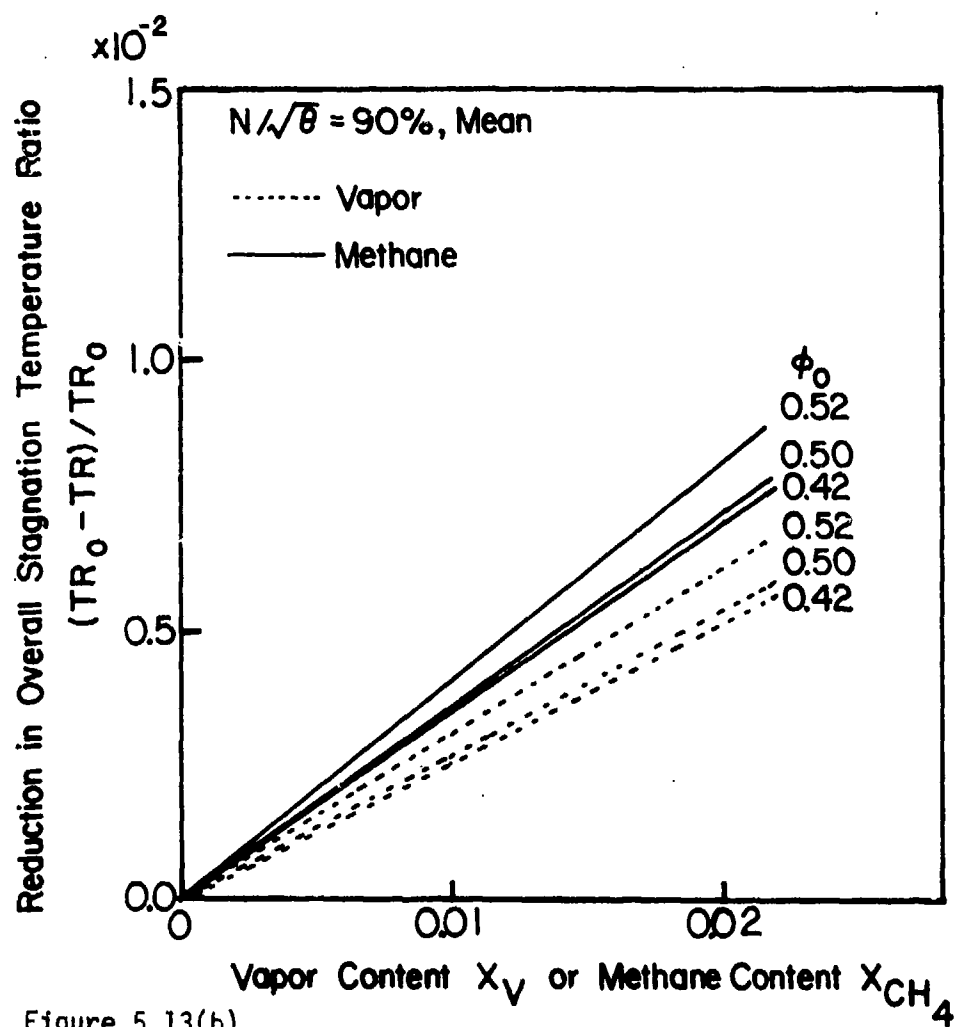
Figure 5.13(b)

Comparison Between Predicted Performance with Air
Flow, Air-Methane Mixture Flow, and Air-Water Vapor
Mixture Flow for Change in Stagnation Pressure
Ratio as a Function of Methane and Water Vapor
Content at Mean
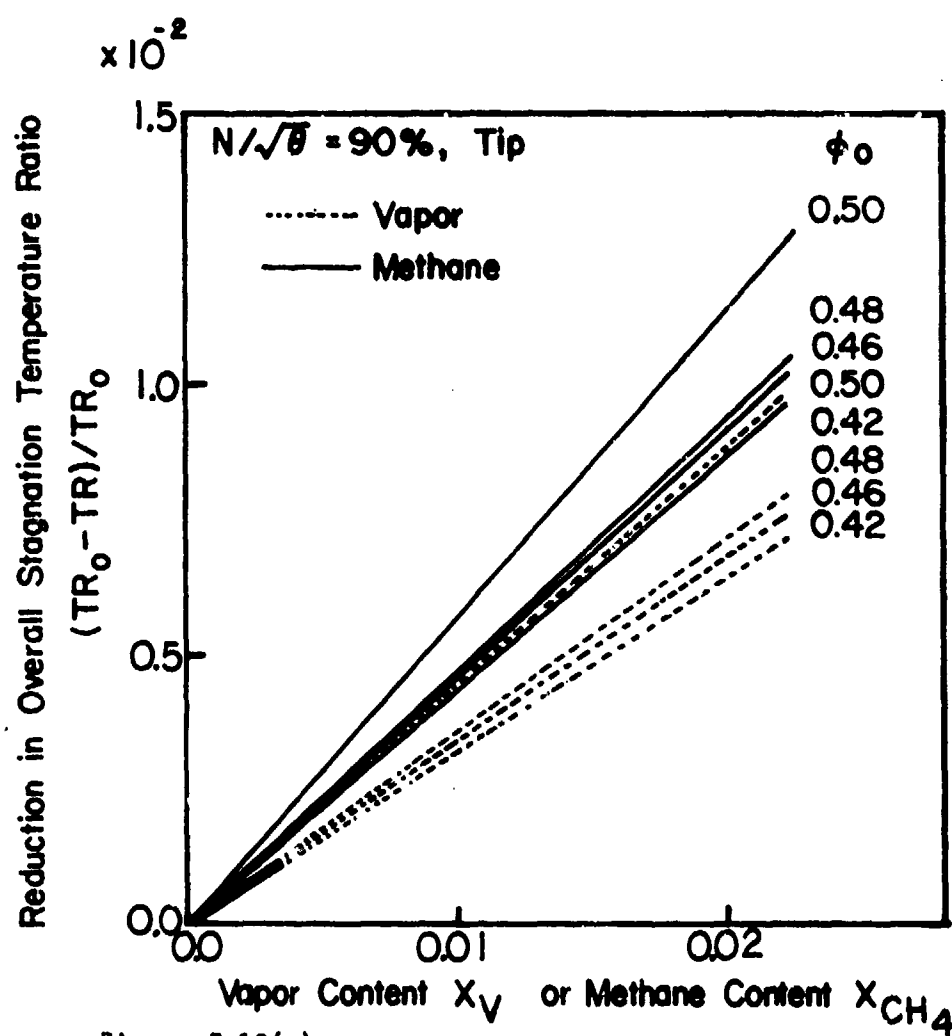
Figure 5.13(c)

Comparison Between Predicted Performance with Air
Flow, Air-Methane Mixture Flow, and Air-Water Vapor
Mixture Flow for Change in Stagnation Pressure
Ratio as a Function of Methane and Water Vapor
Content at Tip
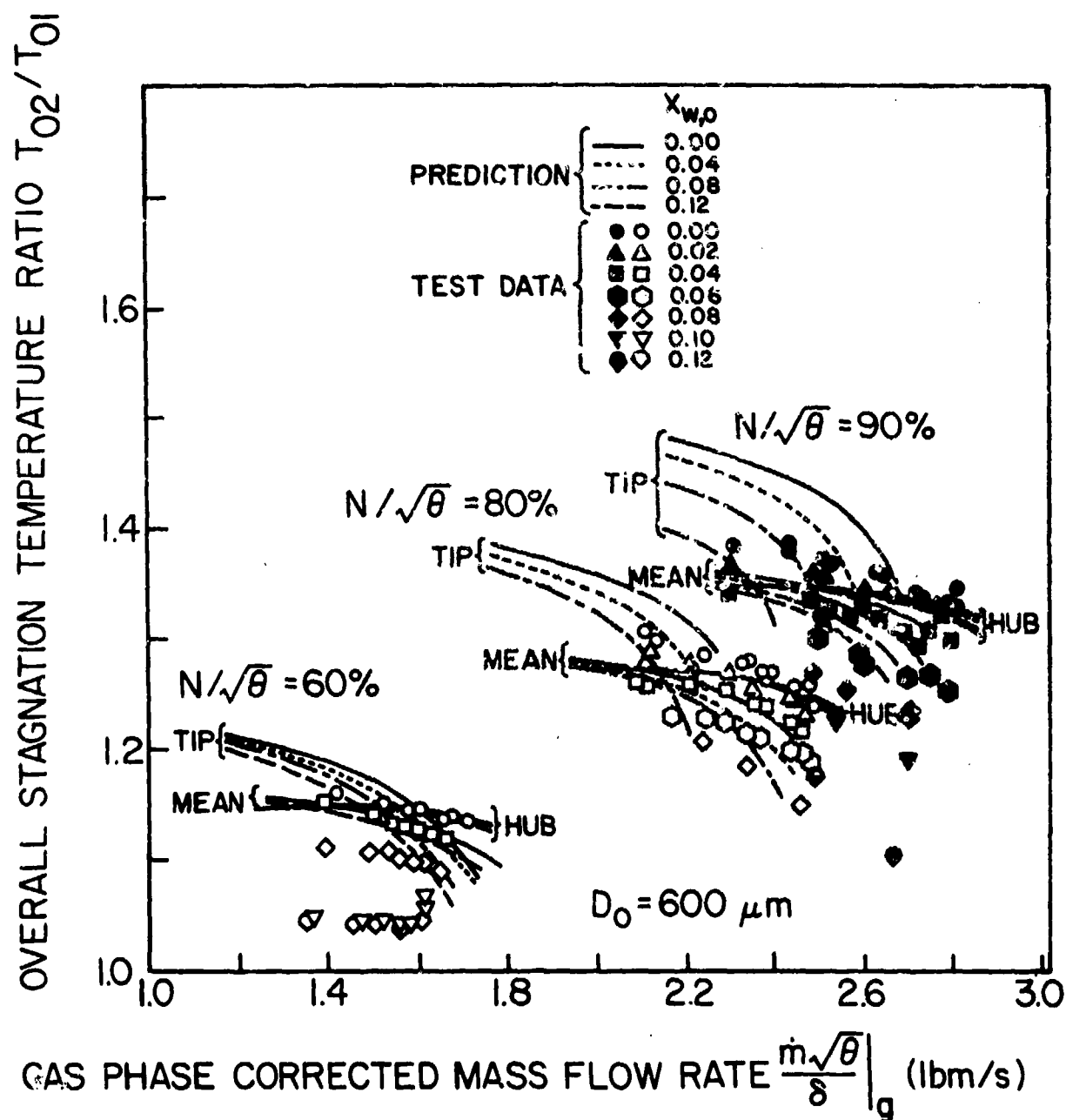
Figure 5.14

Comparison between Predictions and Test Data for Overall Stagnation
Temperature Ratio as a Function of Gas Phase Corrected Mass Flow Rate
$(D_0 = 600\mu m)$
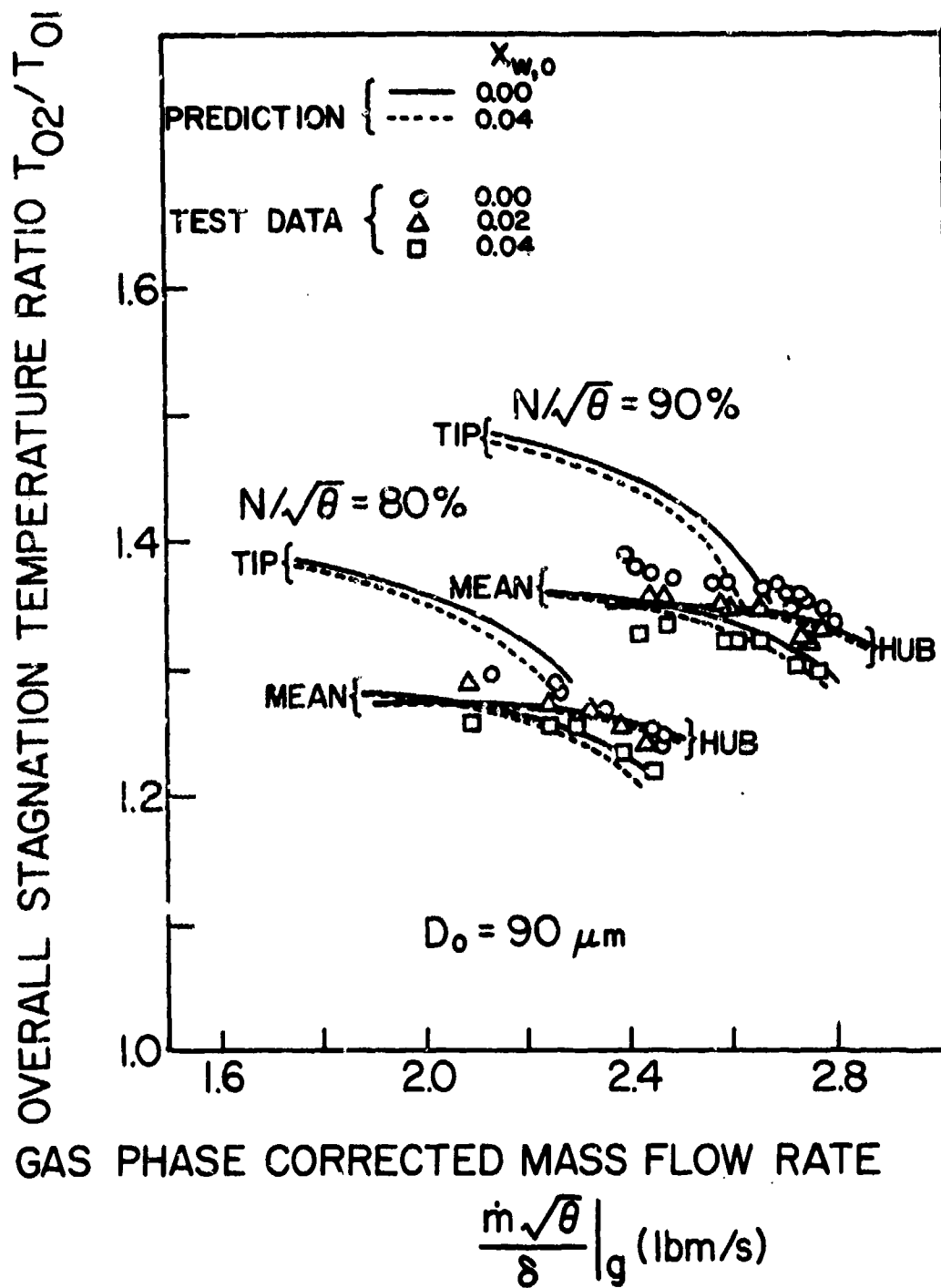
Figure 5.15

Comparison between Predictions and Test Data for Overall
Stagnation Temperature Ratio as a Function of Gas Phase
Corrected Mass Flow Rate (D_o = 600μm)
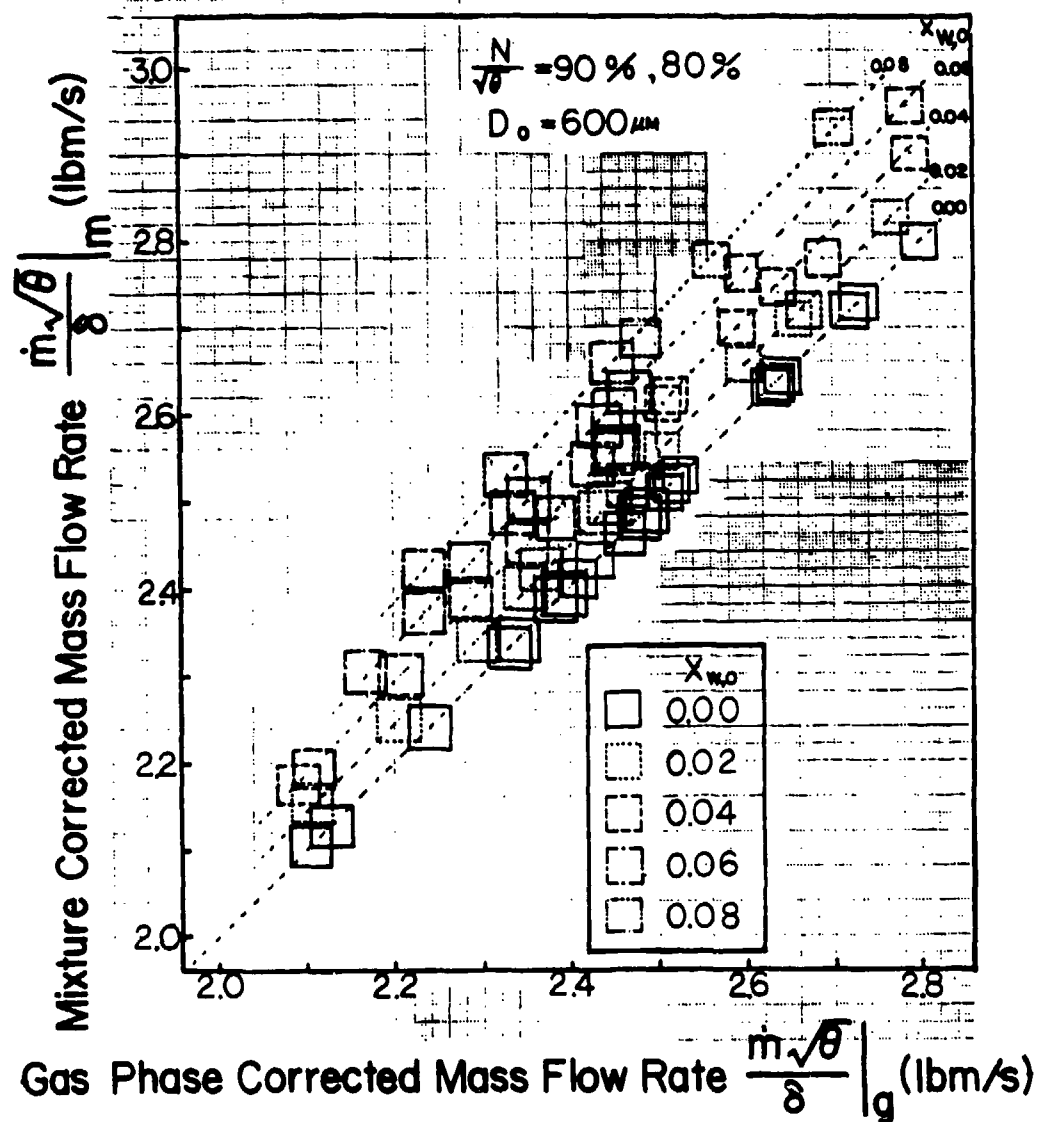
Figure 5.16

Gas Phase Corrected Mass Flow Rate as a Function of
Mixture Corrected Mass Flow Rate ($D_o = 600\mu m$)
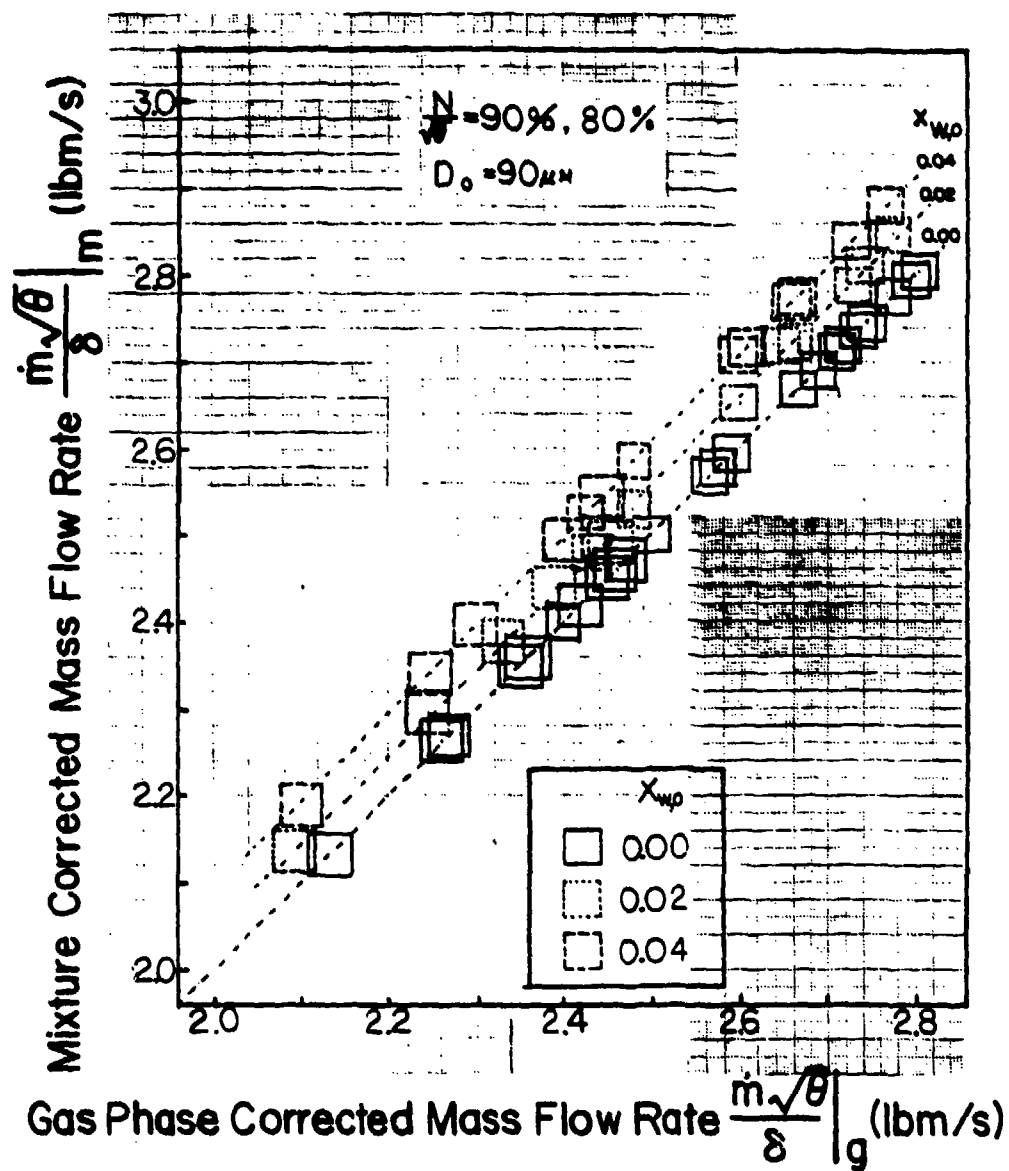
Figure 5.17

Gas Phase Corrected Mass Flow Rate as a Function of
Mixture Corrected Mass Flow Rate (D_0 = 90μm)
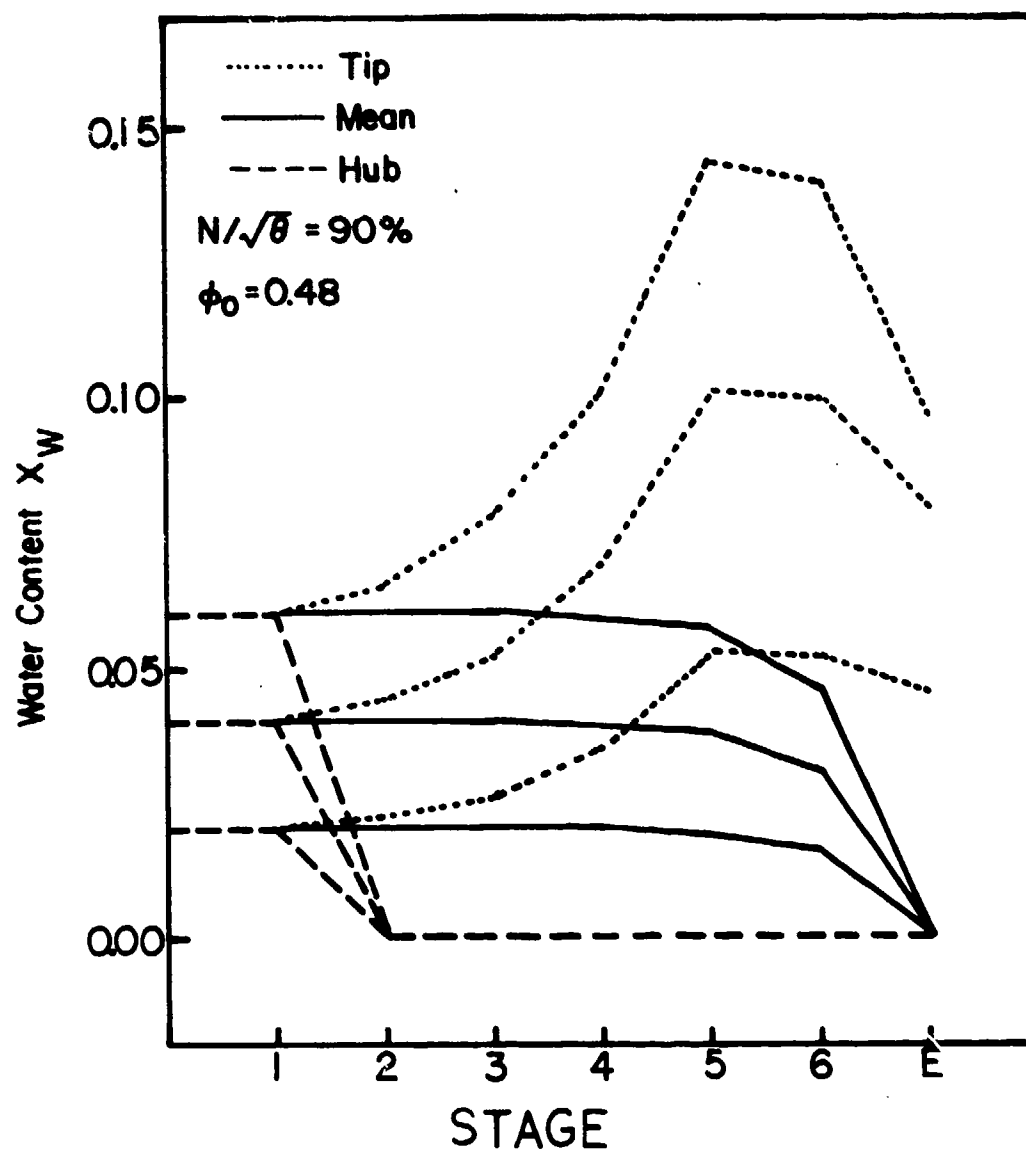
Figure 5.18

Change in Water Content Along the Compressor
at the Hub, Mean, and Tip Sections
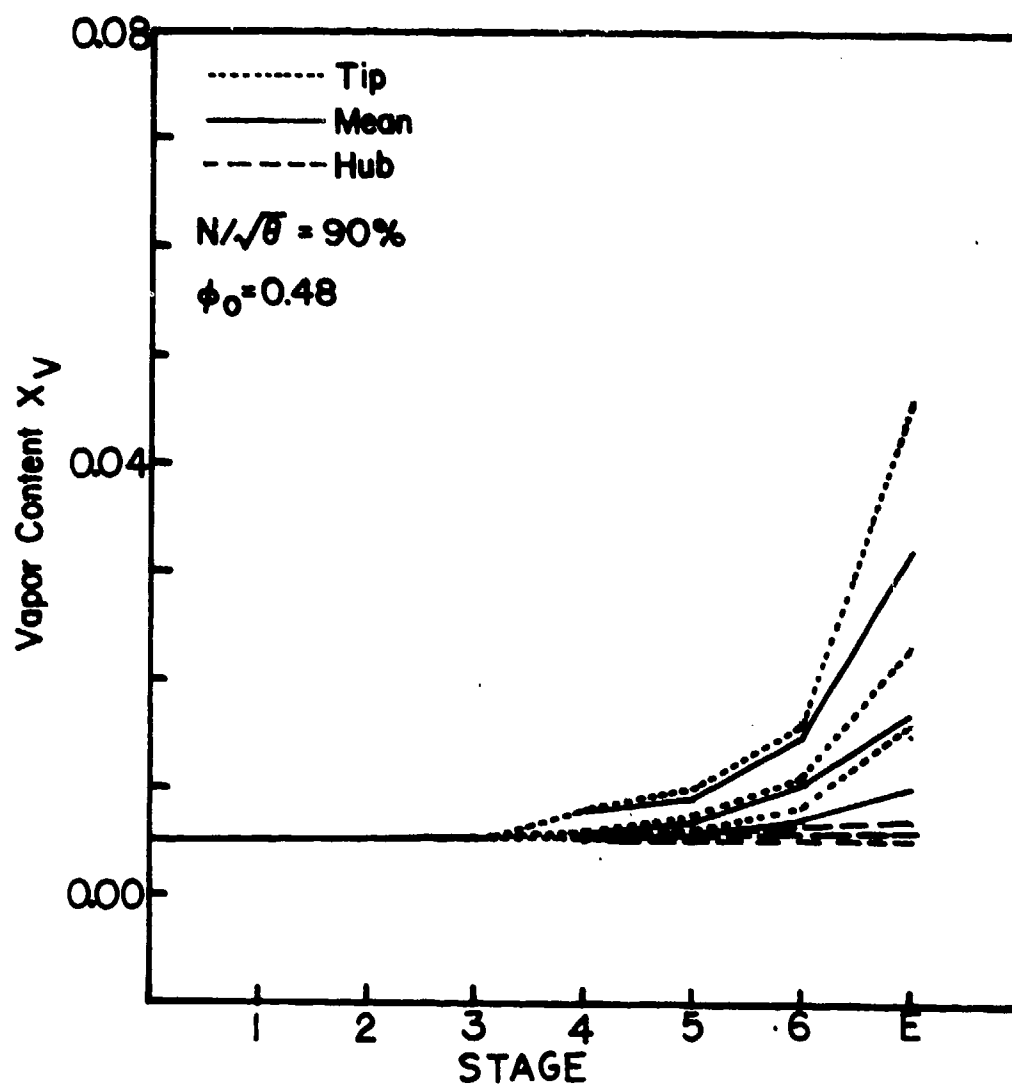
Figure 5.19

Change in Vapor Content Along the Compressor at the
Hub, Mean, and Tip Sections
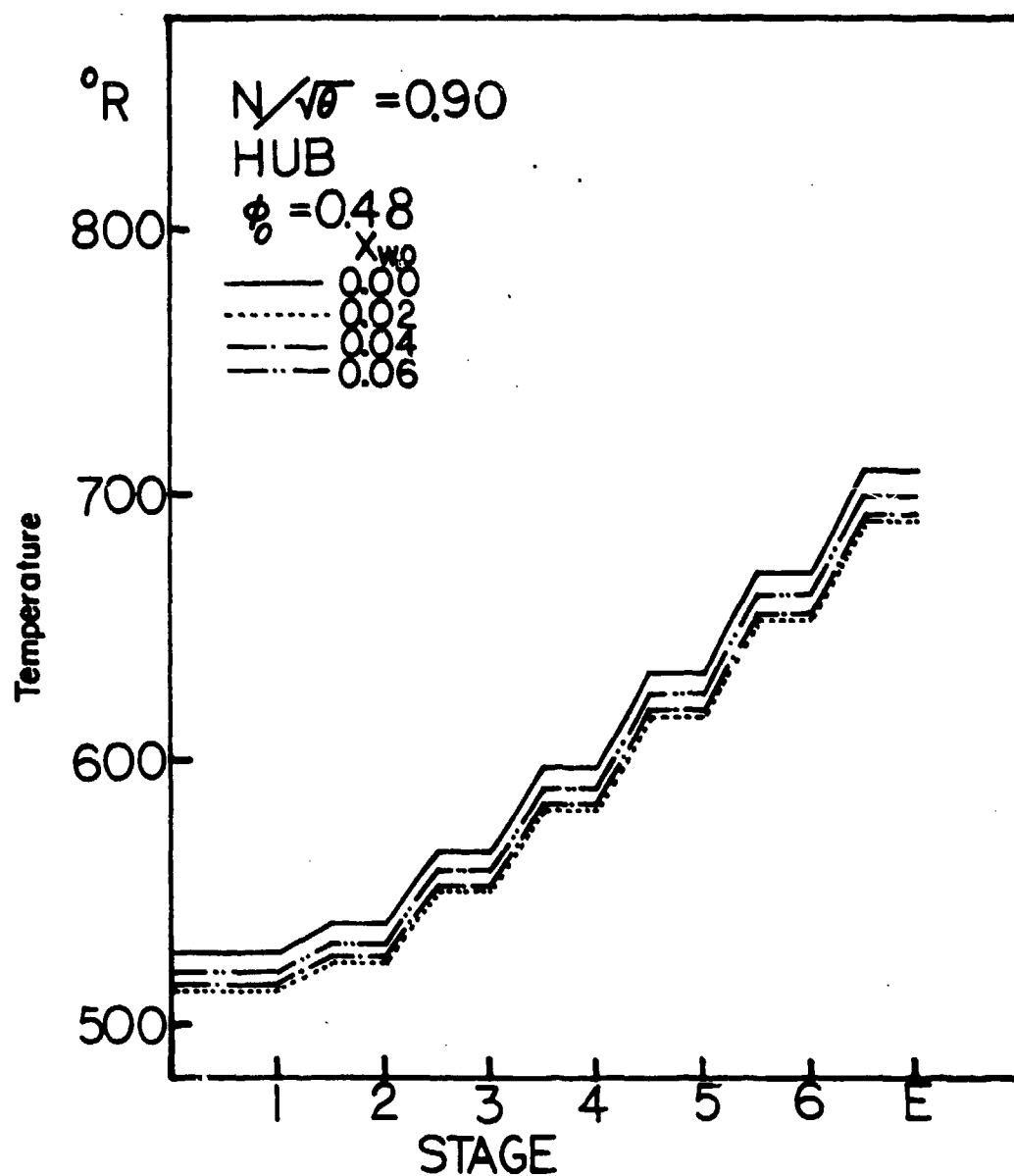
Figure 5.20(a)

Change in the Stagnation Temperature
Along the Compressor at Hub
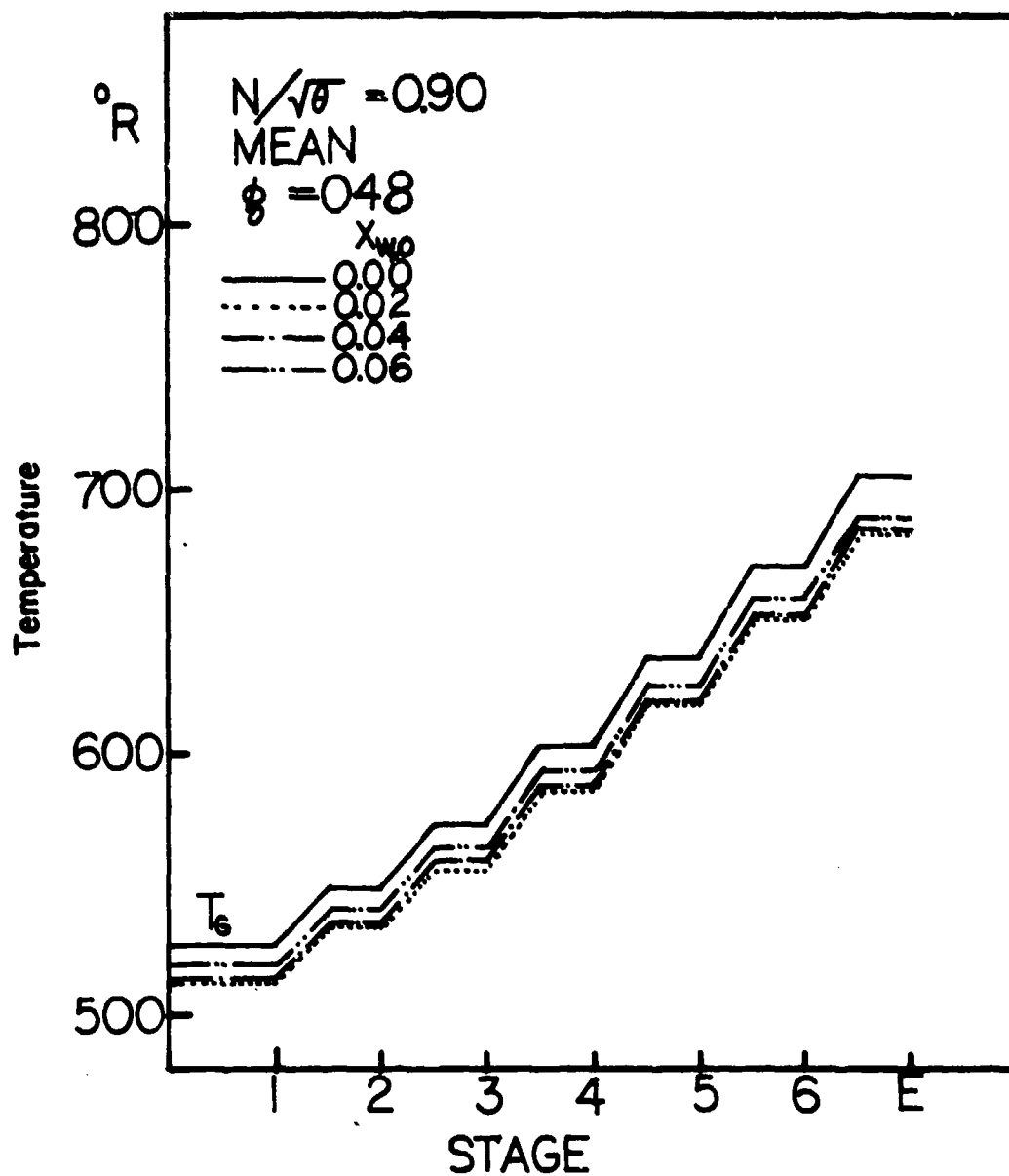
Figure 5.20(b)

Change in the Stagnation Temperature Along the
Compressor at Mean
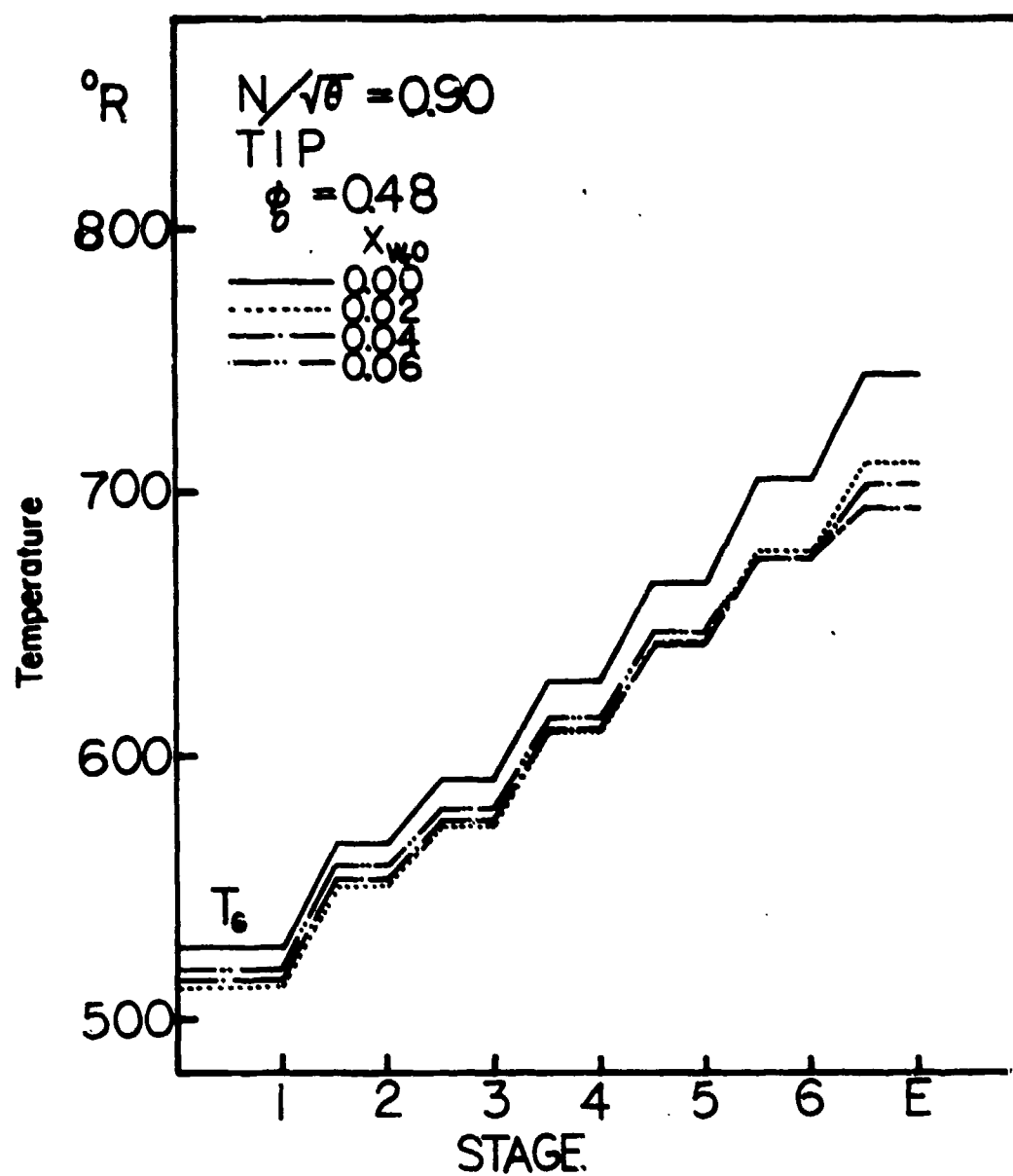
Figure 5.20(c)

Change in the Stagnation Temperature
Along the Compressor at Tip
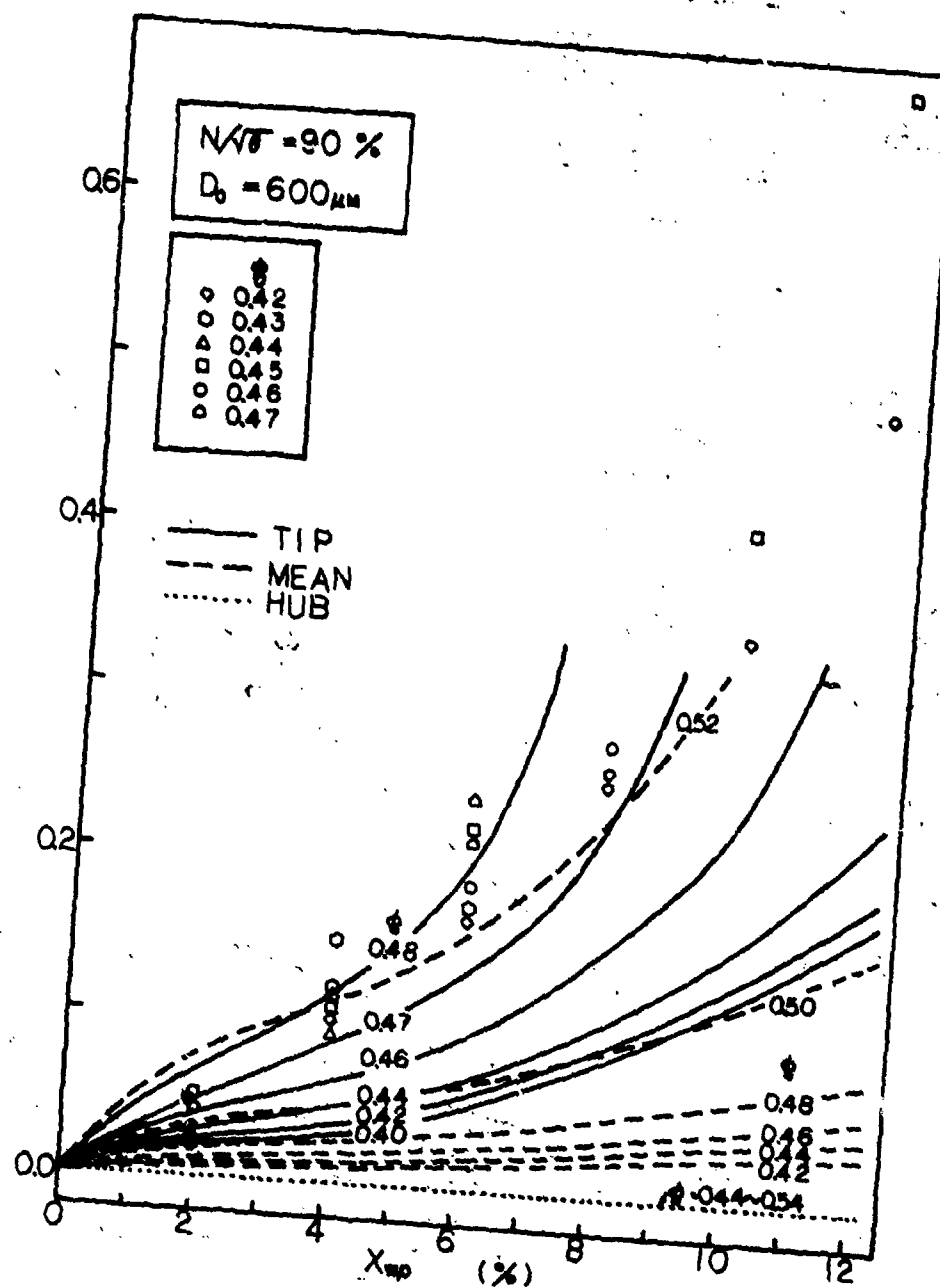
Figure 5.21

Comparison between Predictions and Test Data for Temperature Rise Ratio Factor ($N/\sqrt{\theta}$ = 90%, D_o = 600μm)
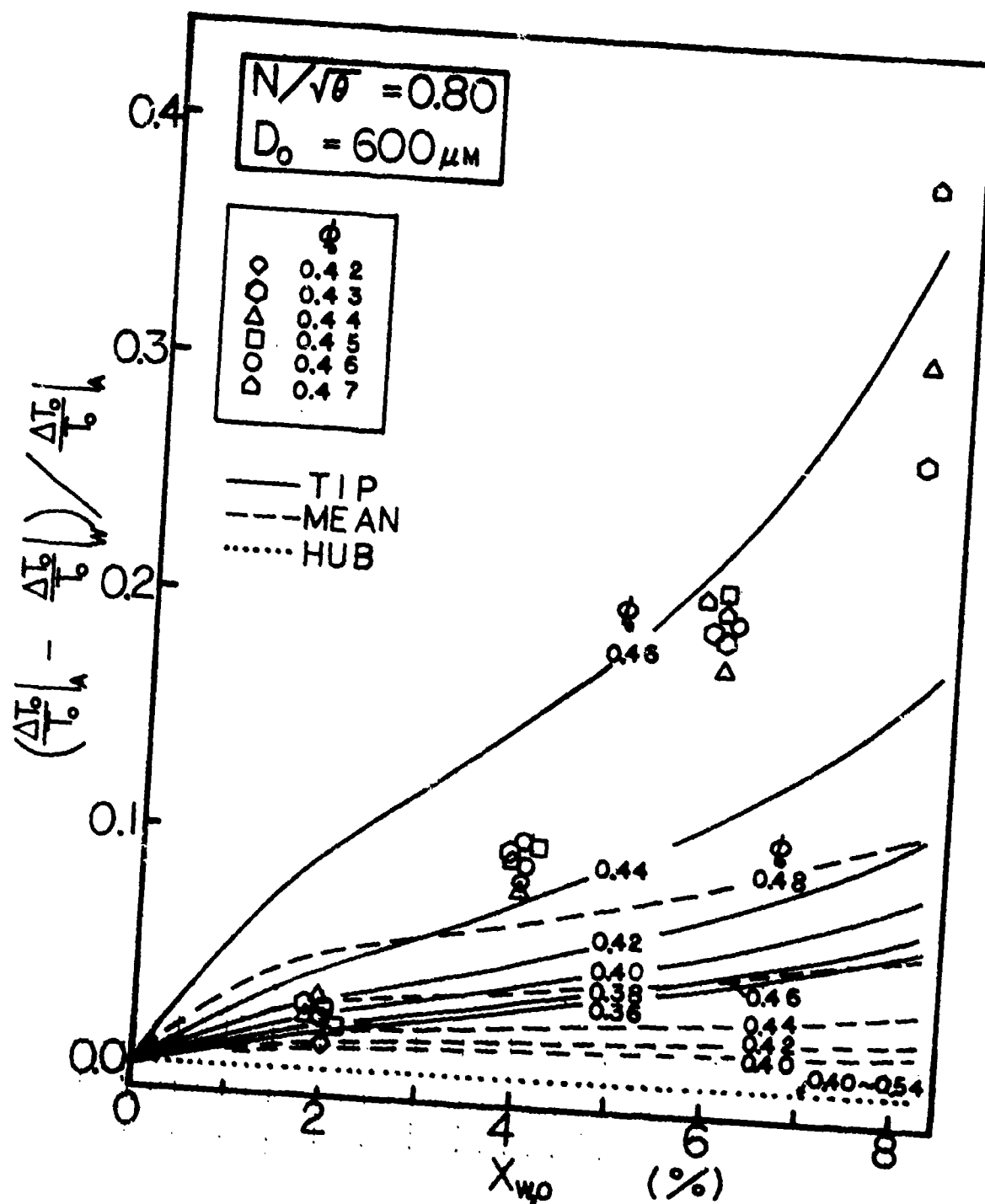
Figure 5.22

Comparison between Predictions and Test Data for Temperature Rise Ratio Factor ($N/\sqrt{\theta} = 80\%$, $D_0 = 600\mu m$)
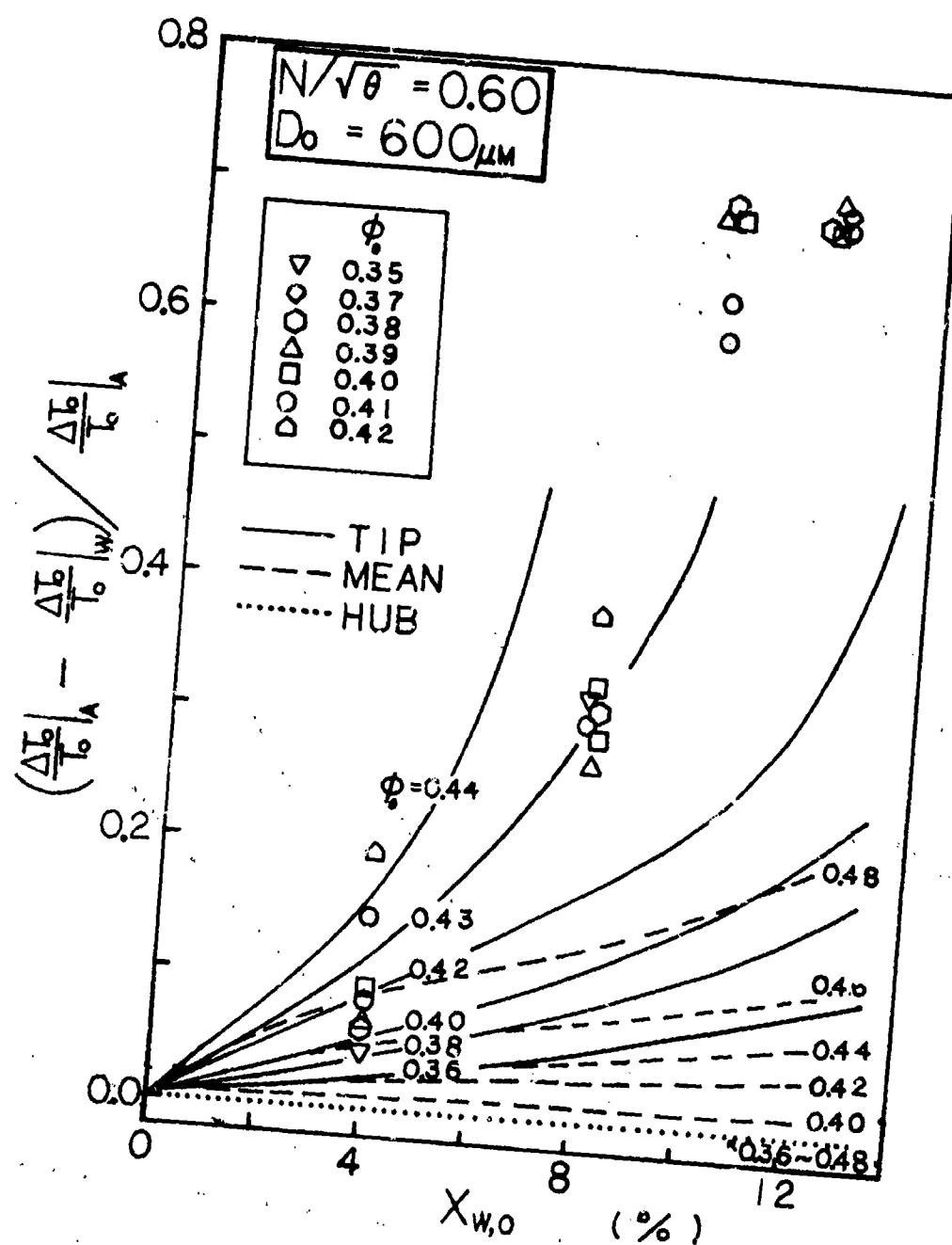
Figure 5.23

Comparison between Predictions and Test Data for Temperature
Rise Ratio Factor ($N/\sqrt{\theta}$ = 60%, D_0 = 600μm)
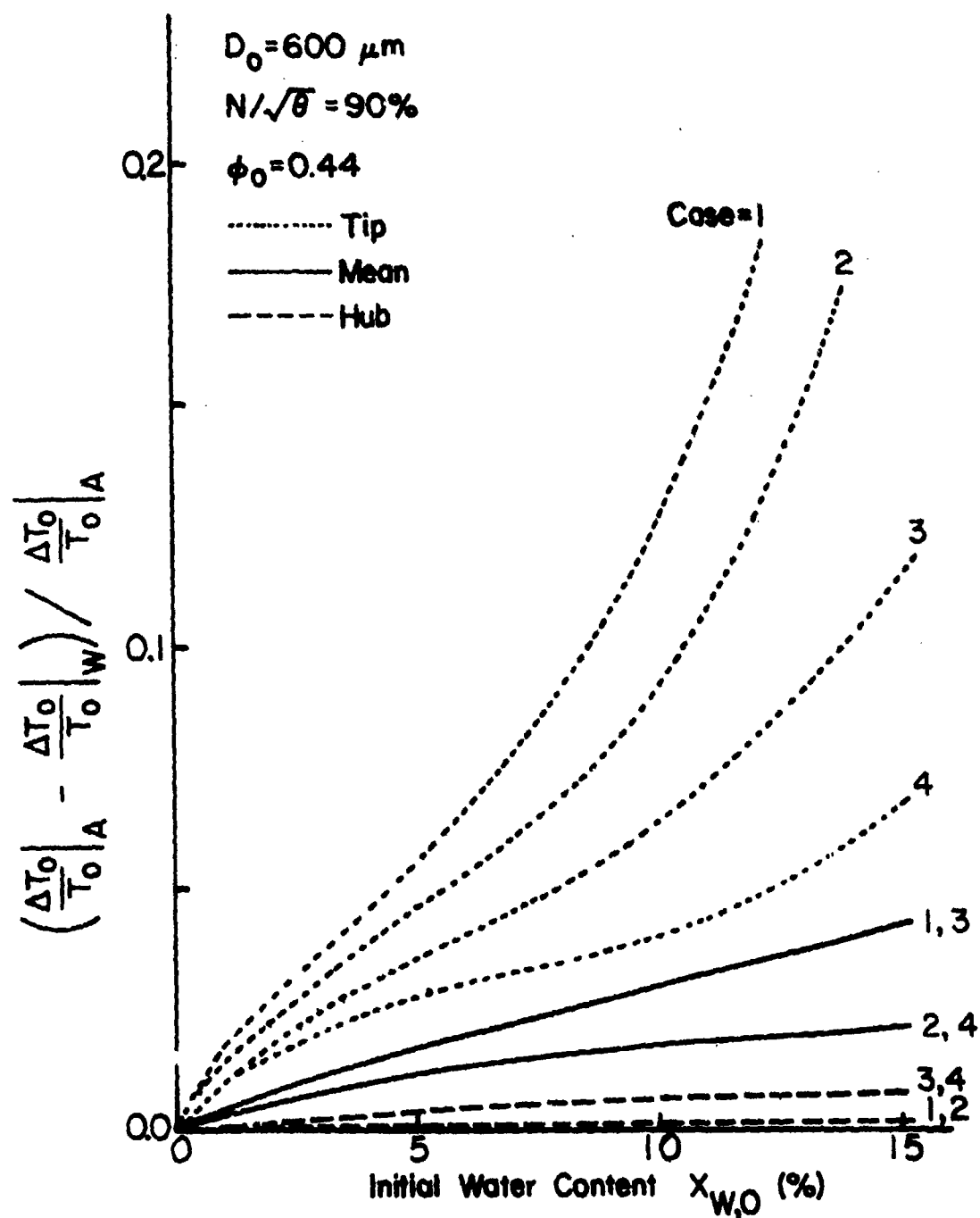
Figure 5.24(a)

Temperature Rise Ratio Factor vs. Water Content at the Hub, Mean, and Tip Sections ($N/\sqrt{\theta}$=90%, D_0=600μm, ϕ_0=0.44)

$$\left(\frac{\Delta T_o}{T_o}\Big|_A - \frac{\Delta T_o}{T_o}\Big|_W \right) \Big/ \frac{\Delta T_o}{T_o}\Big|_A$$

$D_o = 600 \ \mu m$

$N/\sqrt{\theta} = 90\%$

$\phi_o = 0.46$

.... Tip
——— Mean
– – – Hub

Case = 1   2   3   4

1, 3

2, 4

3, 4

0.0

1, 2

Initial Water Content $X_{W,O}$ (%)
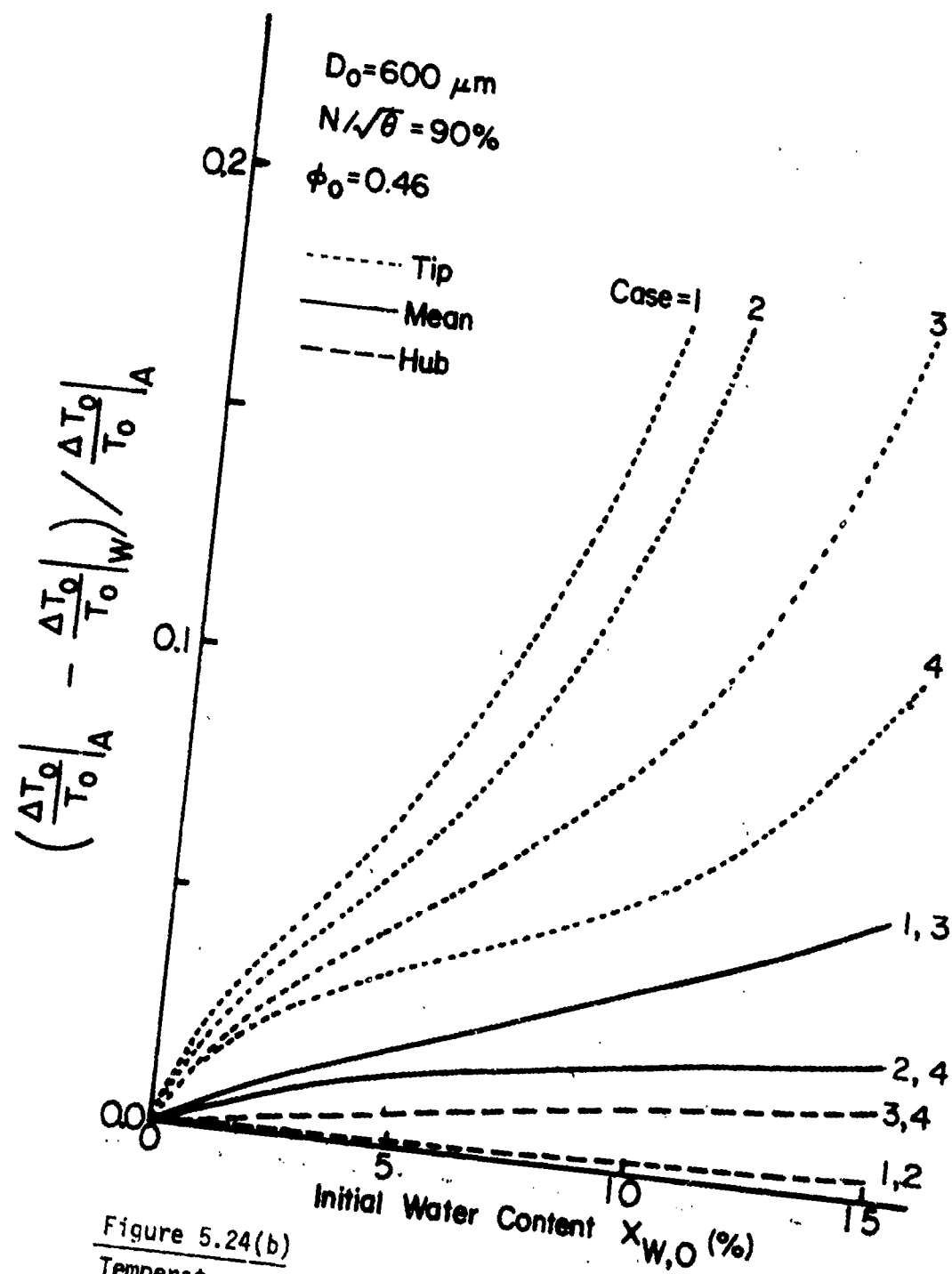
Figure 5.24(b)

Temperature Rise Ratio Factor vs. Water Content
at the Hub, Mean, and Tip Sections ($N/\sqrt{\theta}$=90%,
D_o=60μm, ϕ_o=0.46)
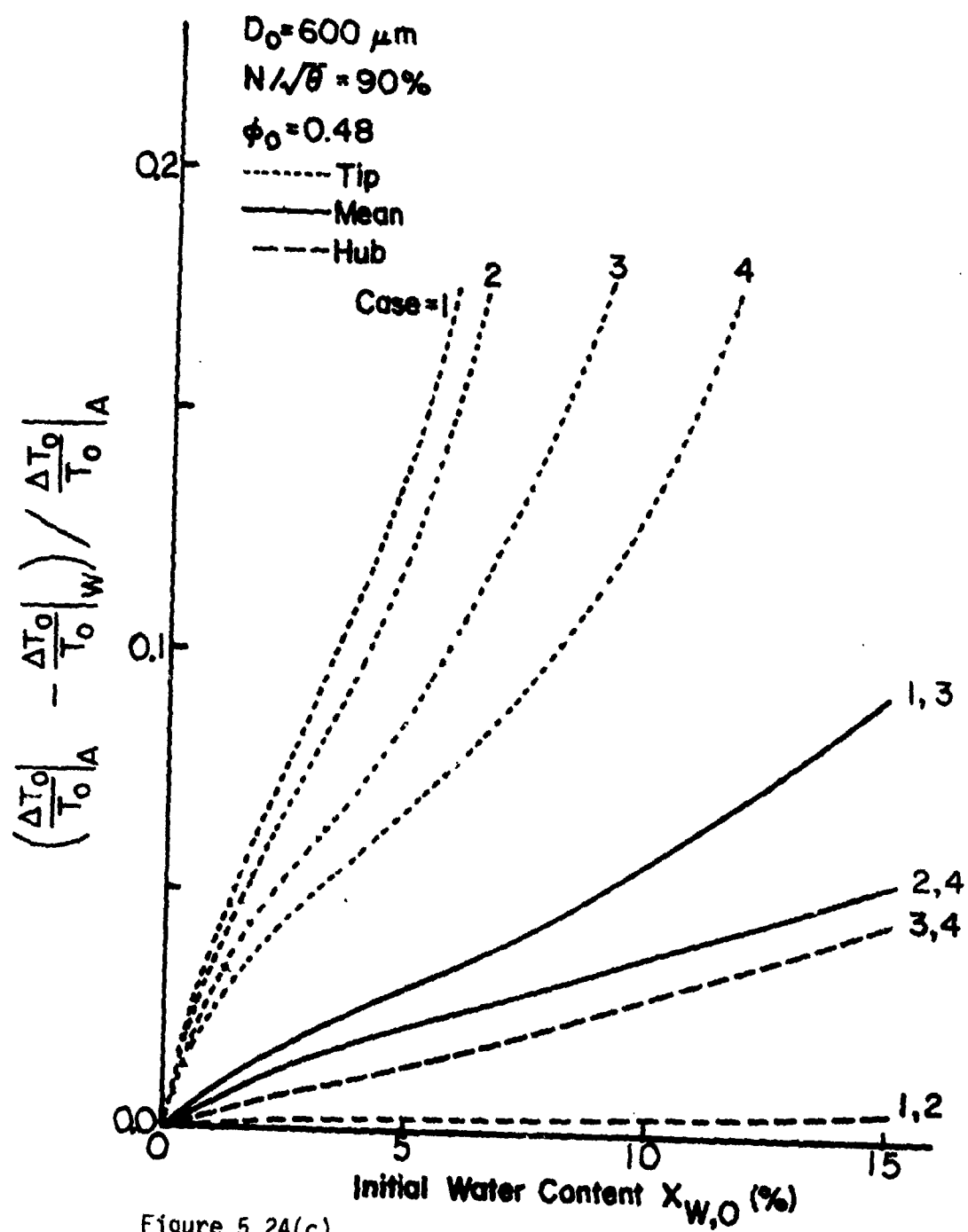
Figure 5.24(c)

Temperature Rise Ratio Factor vs. Water Content
at the Hub, Mean, and Tip Sections ($N/\sqrt{\theta}$=90%,
D_0=600μm, ϕ_0=0.50)
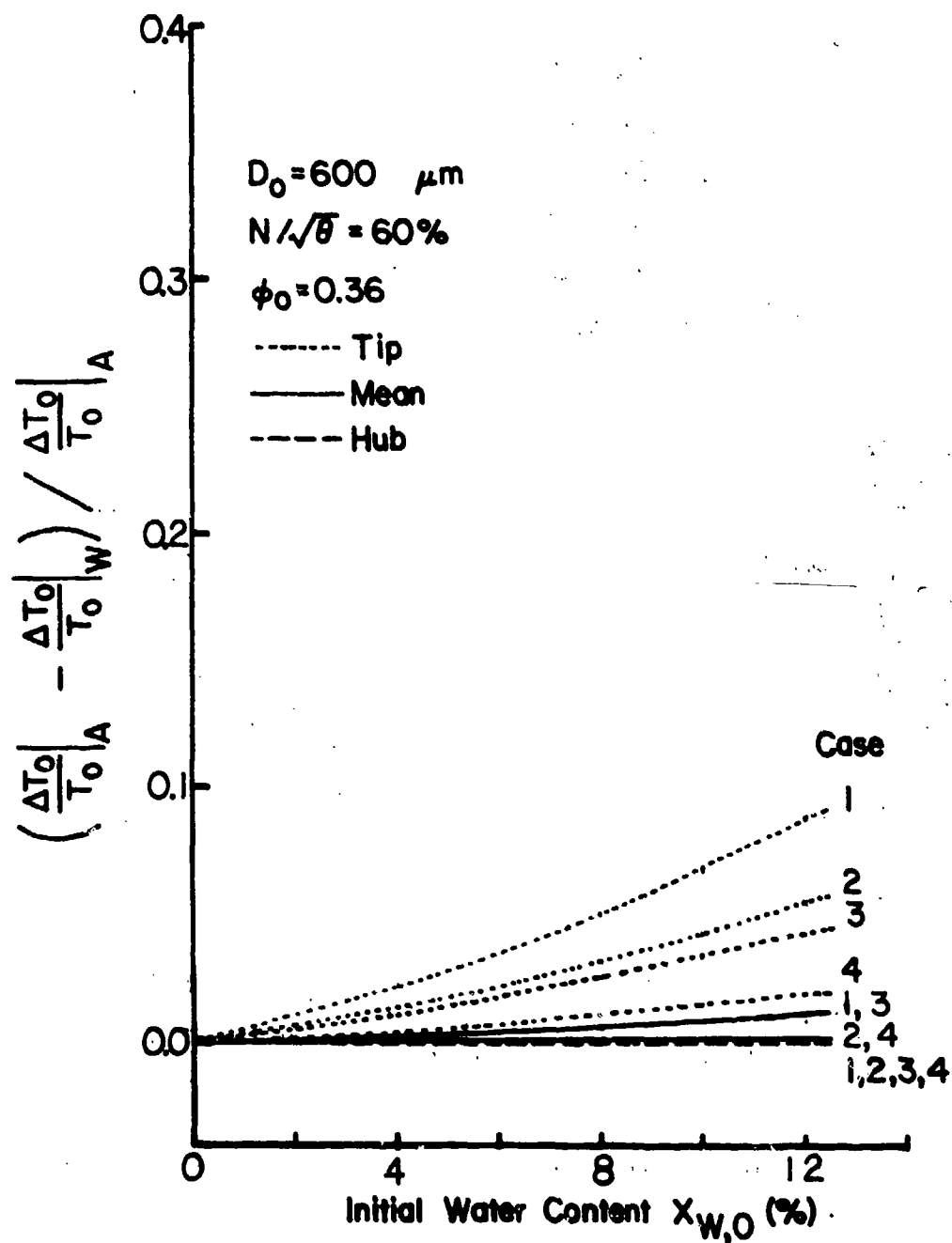
Figure 5.25(a)

Temperature Rise Ratio Factor vs. Water Content
at the Hub, Mean, and Tip Sections (N/√θ=G0%,
D_0=600μm,ϕ_0=0.36)
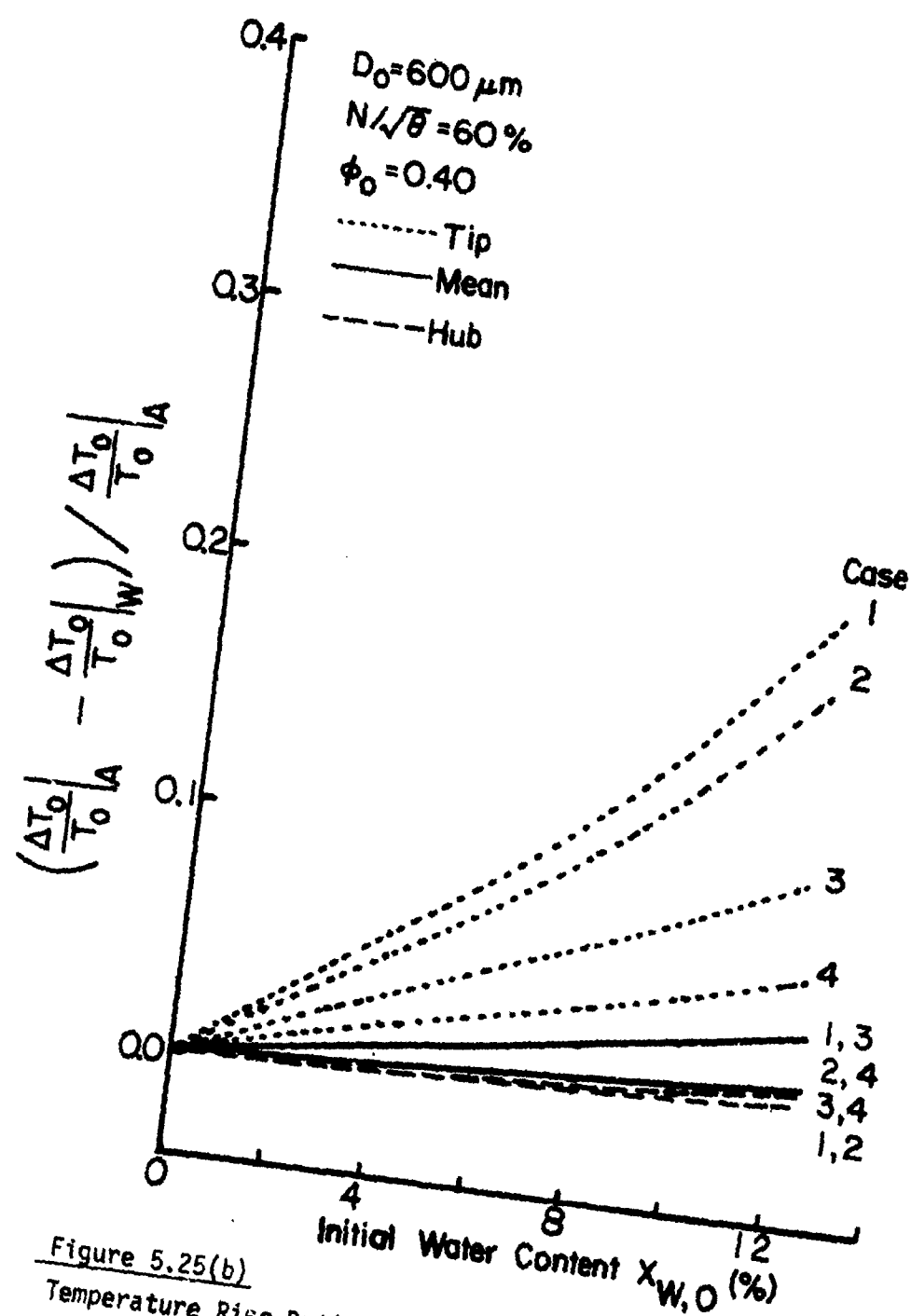
Figure 5.25(b)

Temperature Rise Ratio FActor vs. Water Content at the Hub, Mean and Tip Sections ($N/\sqrt{\theta}$=60%, D_0=600μm, ϕ_0=0.40)
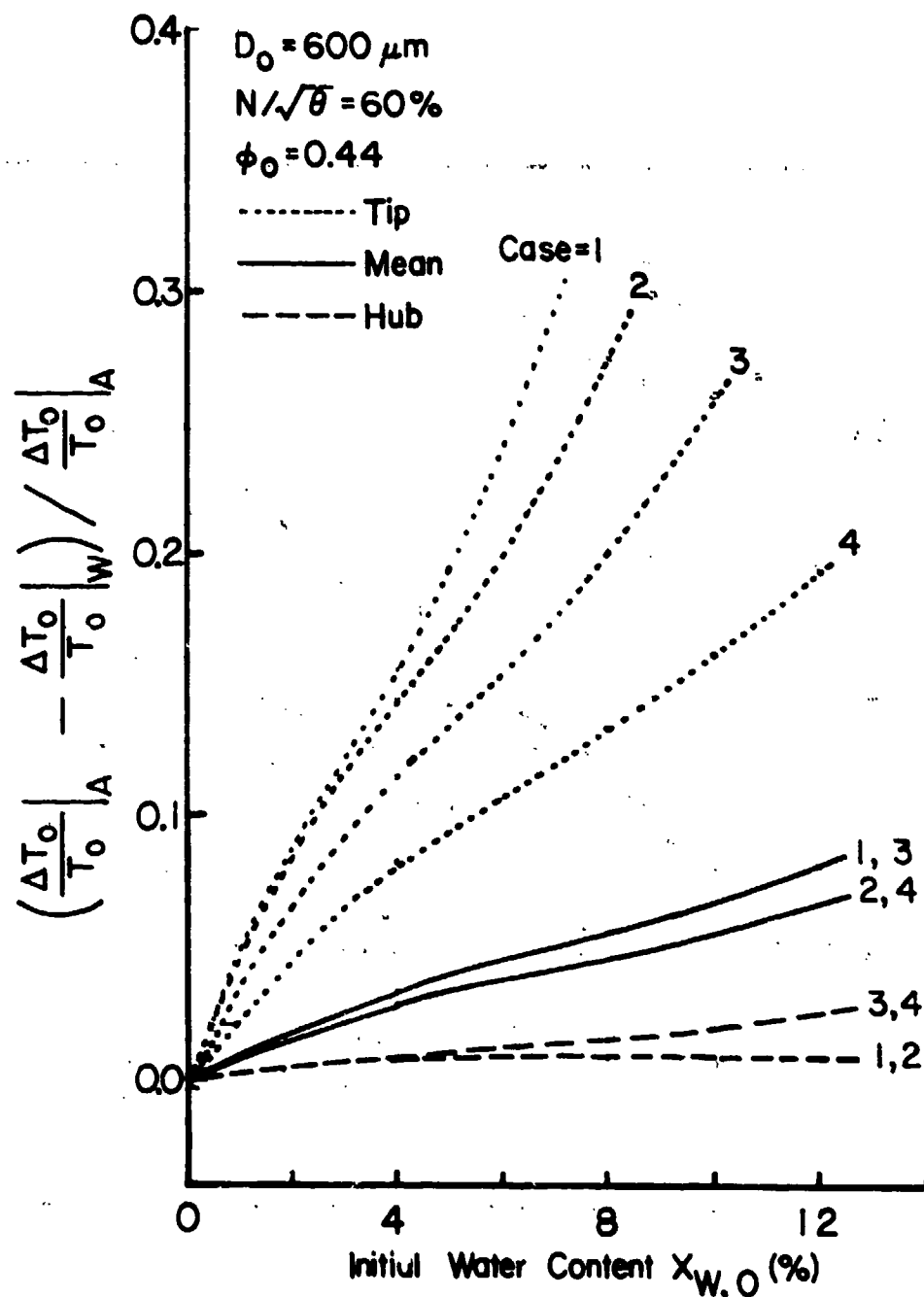
Figure 5.25(c)

Temperature Rise Ratio Factor vs. Water Content
at the Hub, Mean, and Tip Sections ($N/\sqrt{\theta}$=60%,
D_0=600μm, ϕ_0=0.44)
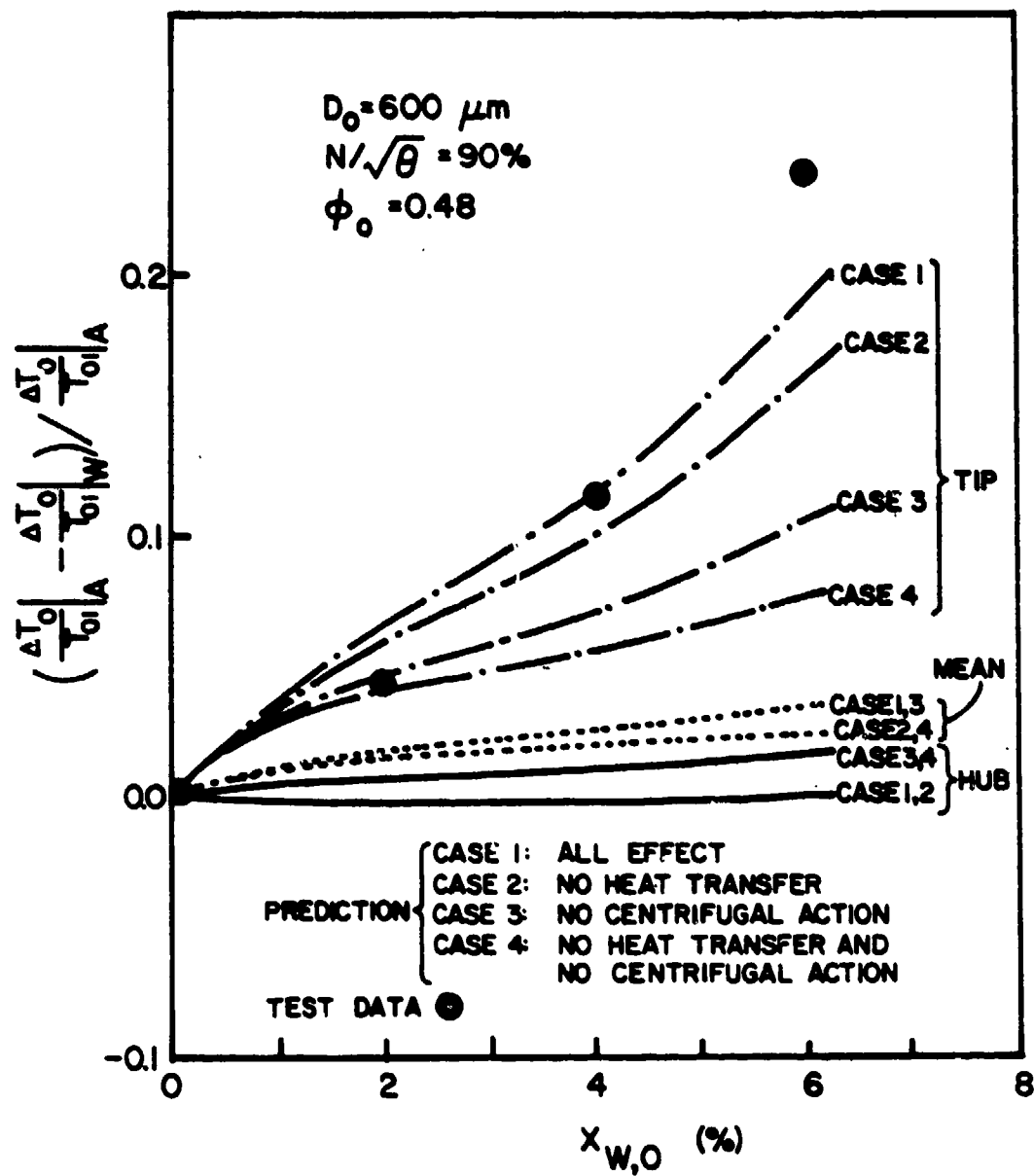
Figure 5.26
Summary of Performance with Water Ingestion ($N/\sqrt{\theta}$ = 90%)
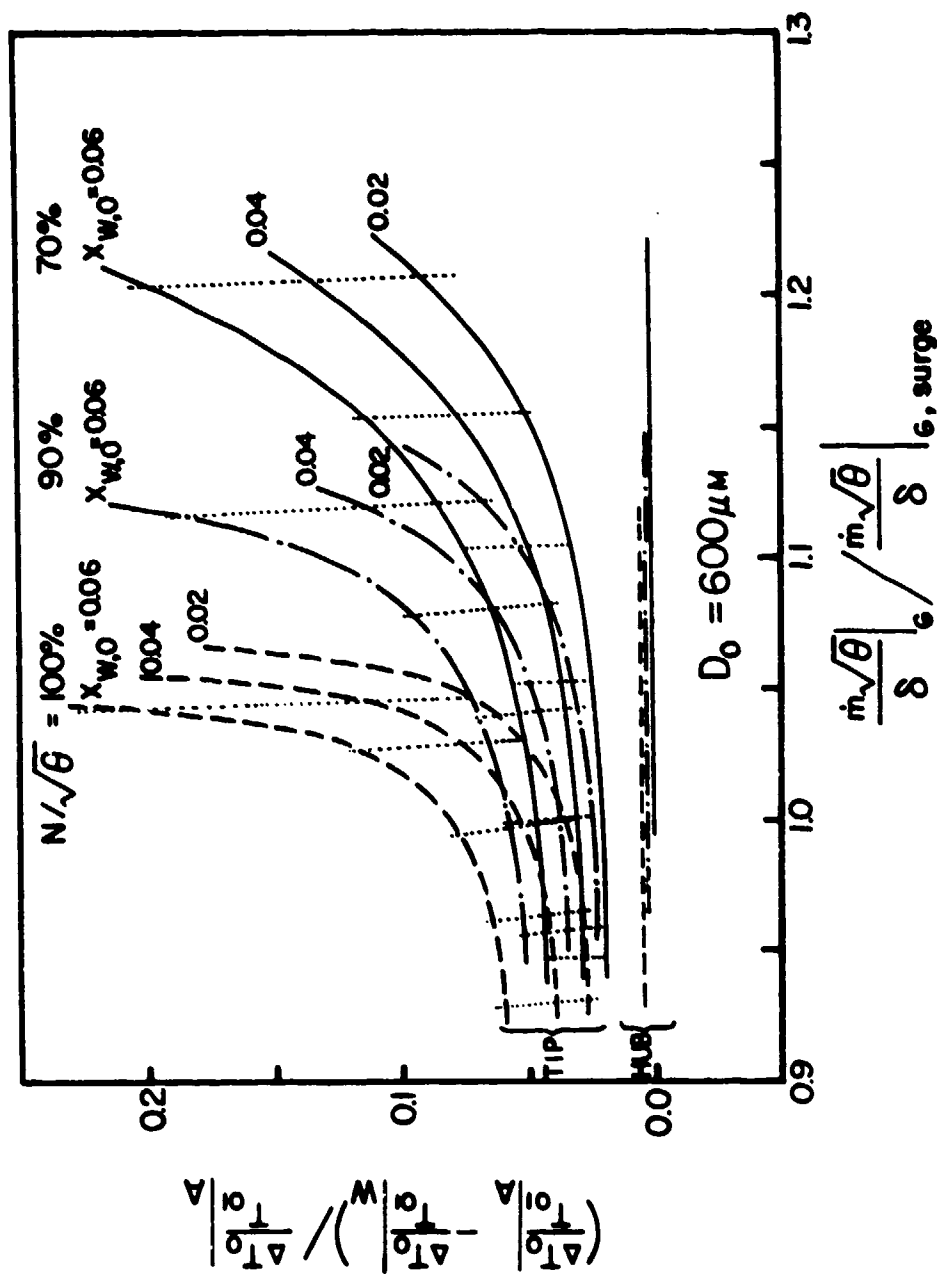
Figure 5.27

Change of Temperature Rise Ratio Factor vs. Mass Flow Parameter at Different Speed (D_0 = 600μm; $N/\sqrt{\theta}$ = 70, 90, 100%)

APPENDIX 1

DETAIL OF TEST COMPRESSOR AND DRIVE ENGINE

1. **Drive Engine**

A T63-A-5 engine is used to drive the Test Compressor. The specifications, limits, and performance ratings for the Drive Engine are as follows:

Design power output:	250 shp
Ram power rating:	275 shp

Design speeds:

Gas producer	51120 rpm (100%)
Power turbine	35000 rpm (100%)
Power output shaft	6000 rpm

Fuel Specification: MIL-J-5624E(JP-4)

The Drive Engine power turbine drives the Test Compressor through mechanical gearing. The output shaft speed has been increased to an output of 9,643 rpm at 100 per cent speed from the normal rating of 6,000 rpm. The Test Compressor is operated 110 per cent (56,251.7 rpm) while the engine operates at 100 per cent or 51,120 rpm. One power turbine tachometer is used to monitor the Test Compressor speed. The ratio of the tachometer speed to the Test Compressor speed is 0.119676.

2. **Test Compressor**

The Test Compressor consists of the six axial stages of the ALLISON T63-A-5 engine compressor. The Test Compressor has been designed and built such that various stages of the compressor can be

assembled and tested. Thus the first two, the intermediate two or the last two stages can be tested if desired, as well as the unit with all of the six stages. Only the 6-stage unit has been used in the current tests.

The first stage of the Test Compressor is preceded by an inlet guide vane row which imparts swirl to the inlet air. The relative Mach number of the incoming air at the rotor inlet is thereby reduced as far as permissible without causing inlet blockage. The axial component features unshrouded rotors, cantilever stators, and double circular arc blading in all stages. The values of T-63 compressor design velocity diagram are presented in Table A.1.1. Table A.1.3 and A.1.4 present the hardware geometry and aerodynamic design data for rotor and stator, respectively.

Figure A.1.1. to Figure A.1.6 show the stage performance character- istics of Test Compressor supplied by the manufacturer. In each of the figures, the equivalent pressure ratio, ψ, equivalent temperature ratio, τ, and stage adiabatic efficiency, η, are presented in terms of flow coefficient, ϕ. The definitions of these parameters are as follows:

(i) flow coefficient: ϕ

$$\phi = V_z/U_{tip}$$

(ii) equivalent pressure ratio: ψ

$$\psi = \left\{ (\frac{U^2_{tip}}{T_{01}})_D \, (\frac{T_{01}}{U^2_{tip}}) \left[(\frac{P_{02}}{P_{01}})^{\frac{\gamma-1}{\gamma}} - 1 \right] + 1 \right\}^{\frac{\gamma}{\gamma-1}}$$

(iii) equivalent temperature ratio:

$$\tau = (\frac{U_{tip}}{T_{01}})^2_D \cdot (\frac{\Delta T_0}{U^2_{tip}})$$

TABLE A.1.1

TEST COMPRESSOR DESIGN VELOCITY DIAGRAM VALUES

Stage	1	2	3	4	5	6	
R	2.161	2.161	2.161	2.161	2.161	2.161	
U	963.5	963.5	963.5	963.5	963.5	963.5	
V_{z1}	508.4	544.1	547.0	554.9	554.1	543.7	↑
$V_{\theta 1}$	236.5	310.0	365.1	349.3	338.8	333.8	
$W_{\theta 1}$	727.0	653.5	598.4	614.2	624.7	629.9	Rotor Inlet
α_1	25.0	29.7	33.7	32.2	31.6	31.5	
β_1	54.9	50.3	47.6	47.9	48.5	49.3	
M_{1abs}	0.513	0.563	0.578	0.560	0.538	0.512	
M_{1rel}	0.812	0.765	0.713	0.707	0.692	0.658	↓
V_{z2}	507.0	554.9	551.0	554.5	548.9	544.6	↑
$V_{\theta 2}$	405.2	501.3	598.8	614.6	625.1	630.3	
$W_{\theta 2}$	558.3	462.2	364.7	348.9	338.4	333.2	Rotor Outlet
α_2	38.6	42.1	47.4	47.9	48.7	49.2	
β_2	47.8	39.8	33.6	32.2	31.7	31.5	
M_{2abs}	0.588	0.565	0.706	0.698	0.680	0.660	
M_{2rel}	0.683	0.643	0.574	0.552	0.528	0.506	↓

Note: Symbols for Table A.1.1 are provided in Table A.1.2.

TABLE A.1.2

SYMBOLS FOR TEST COMPRESSOR DESIGN VELOCITY DIAGRAM VALUES

R	Radius, inches
U	Rotor speed at R, ft/sec.
V_z	Air axial velocity, ft/sec.
V_θ	Air absolute tangential velocity, ft/sec.
W_θ	Air relative tangential velocity, ft/sec.
α	Air absolute flow angle, degrees
β	Air relative flow angle, degrees
M	Mach number

Subscript

1	rotor inlet
2	rotor outlet
abs	absolute
rel	relative

TABLE A.1.3

TEST COMPRESSOR DESIGN DATA (ROTOR)

Stage		1	2	3	4	5	6
Radius	R	2.161	2.161	2.161	2.161	2.161	2.161
Camber Angle	θ	22.6	15.9	18.0	19.7	20.9	22.0
Stagger	γ	46.1	42.3	36.5	36.1	36.0	36.3
Incidence	i	0.0	2.0	2.0	2.0	2.0	2.0
Deviation	δ	7.3	5.4	6.0	6.0	6.1	6.2
Chord	c	0.605	0.554	0.534	0.510	0.483	0.456
Solidity	σ	0.713	0.815	0.787	0.941	0.997	1.075
Max. Thickness	t	0.036	0.039	0.037	0.036	0.034	0.032
Thickness-Chord Ratio	t/c	0.060	0.070	0.070	0.070	0.070	0.070
No. of Blades	n	16	20	20	25	28	32

Note: R, c, t in [inches] and θ, γ, δ, i in [degrees]

TABLE A.1.4

TEST COMPRESSOR DESIGN DATA (STATOR)

Stage		IGV	1	2	3	4	5	6
Radius	R	2.161	2.161	2.161	2.161	2.161	2.161	2.161
Camber Angle	θ	31.7	22.4	25.6	26.2	24.4	24.7	17.3
Stagger	γ	-15.9	31.3	36.3	36.6	36.8	37.4	42.6
Incidence	i	0.0	-2.0	-2.0	-2.0	-2.0	-2.0	-2.0
Deviation	δ	6.7	9.6	5.2	8.0	7.9	7.5	5.6
Chord	c	1.395	0.442	0.412	0.412	0.412	0.412	0.412
Solidity	σ	0.719	0.456	0.789	0.850	0.972	1.093	0.910
Max. Thickness	t	0.170	0.040	0.025	0.025	0.025	0.025	0.025
Thickness-Chord Ratio	t/c	0.122	0.09	0.06	0.06	0.06	0.06	0.06
No. of Blades	n	7	14	26	28	32	36	30

Note: R, c, t in [inches] and θ, γ, δ, i in [degrees]
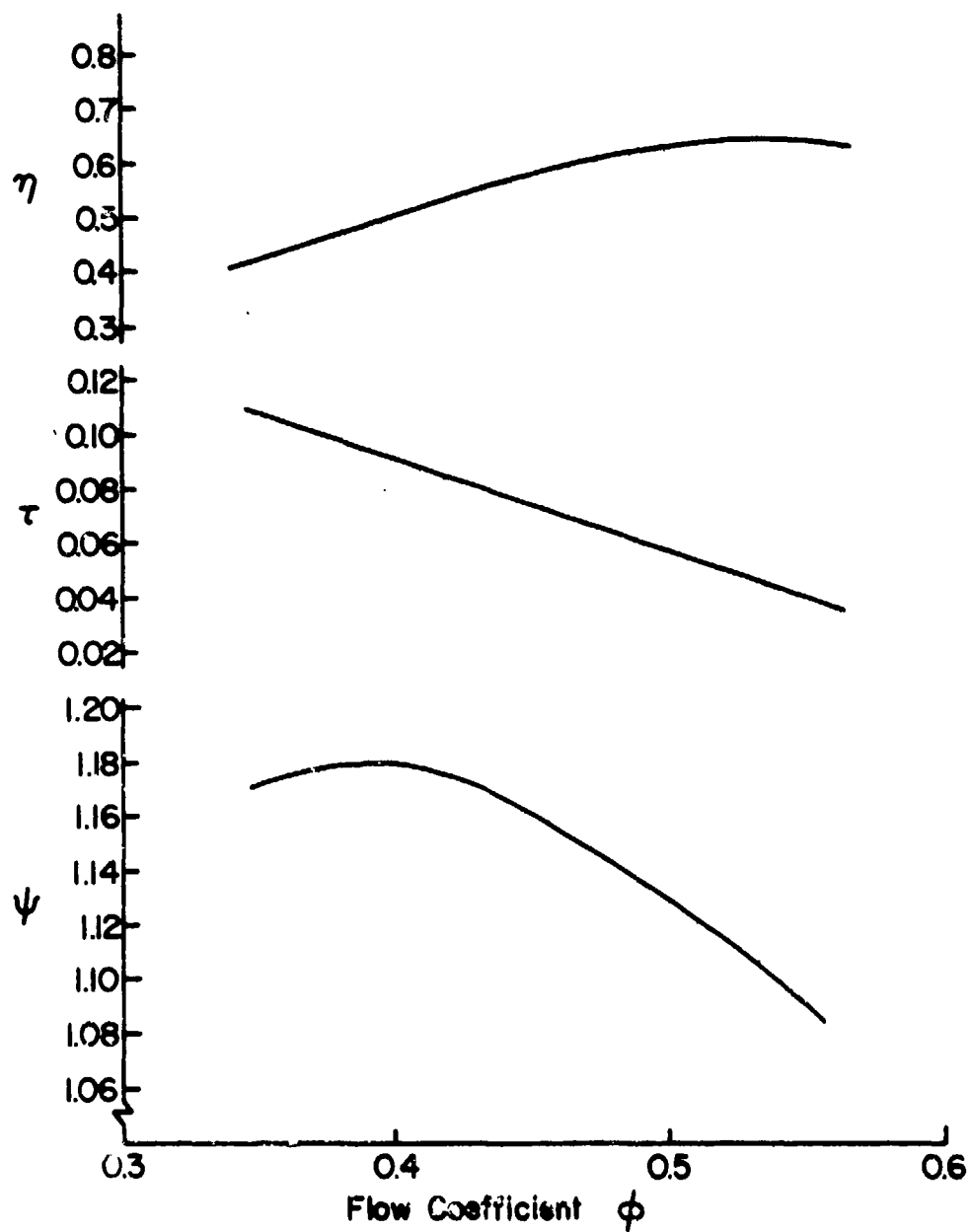
Figure A.1.1
Stage Performance Characteristics of Test Compressor
Supplied by Manufacturer (1st Stage)
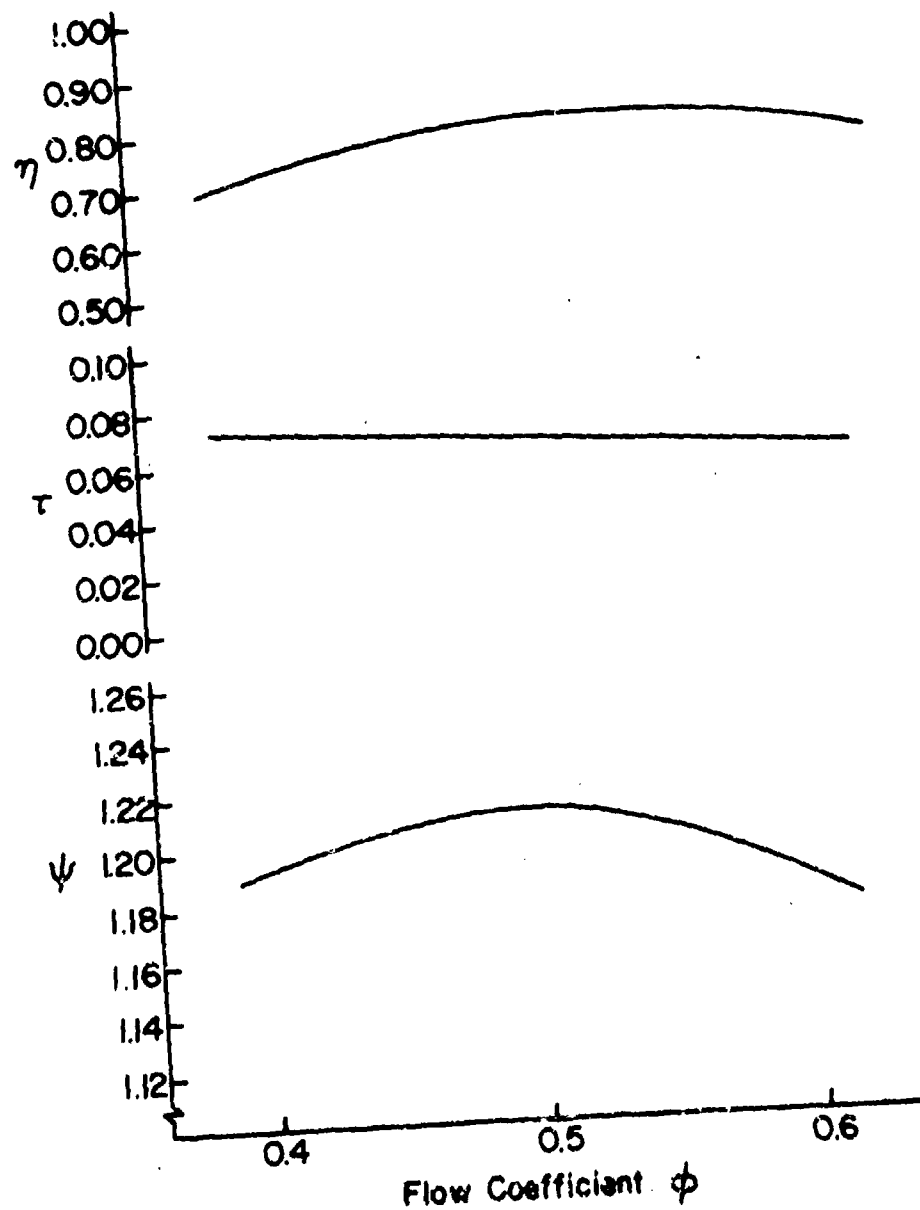
Figure A.1.2
Stage Performance Characteristics of Test Compressor
Supplied by Manufacturer (2nd Stage)
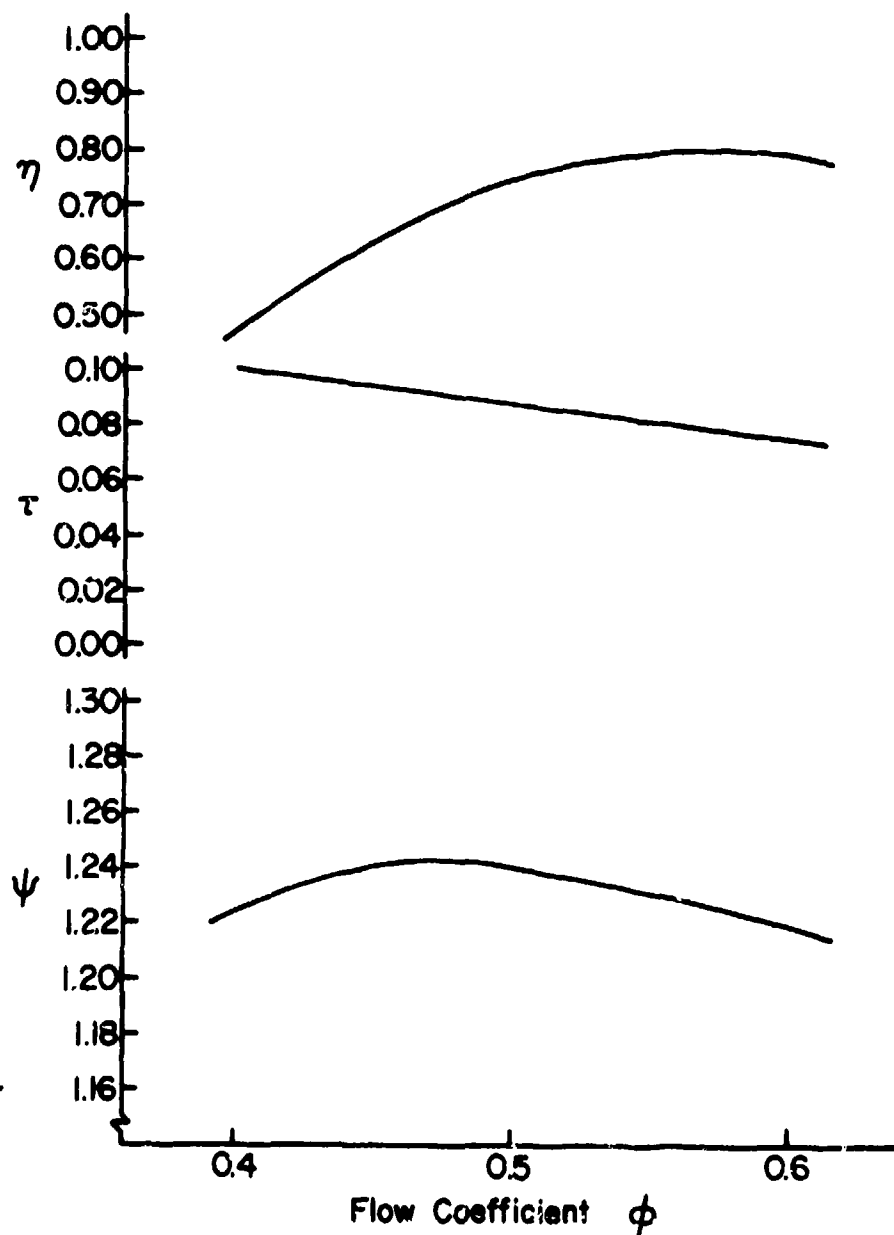
Figure A.1.3

Stage Performance Characteristics of Test Compressor
Supplied by Manufacturer (3rd Stage)
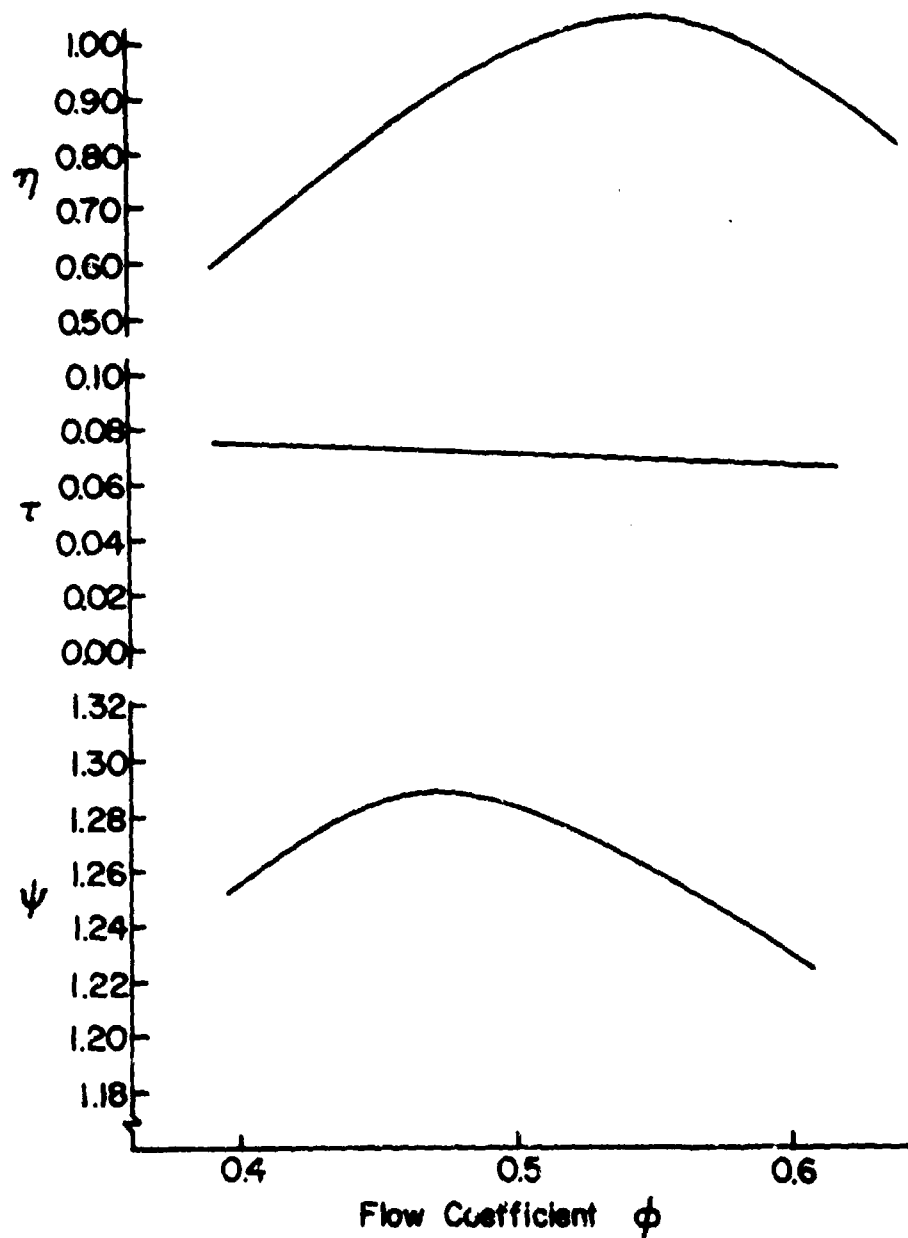
Figure A.1.4

Stage Performance Characteristics of Test Compressor
Supplied by Manufacturer (4th Stage)
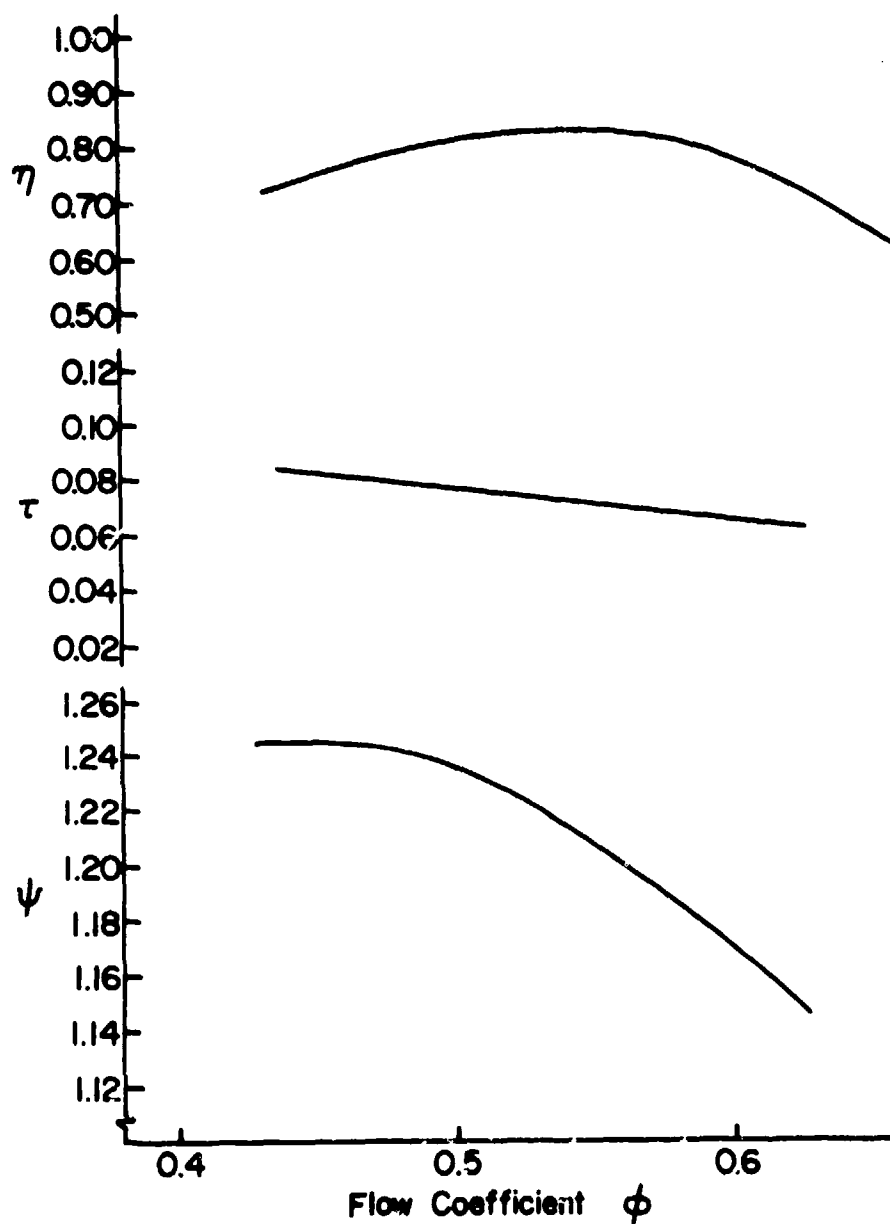
Figure A.1.5

Stage Performance Characteristics of Test Compressor
Supplied by Manufacturer (5th Stage)
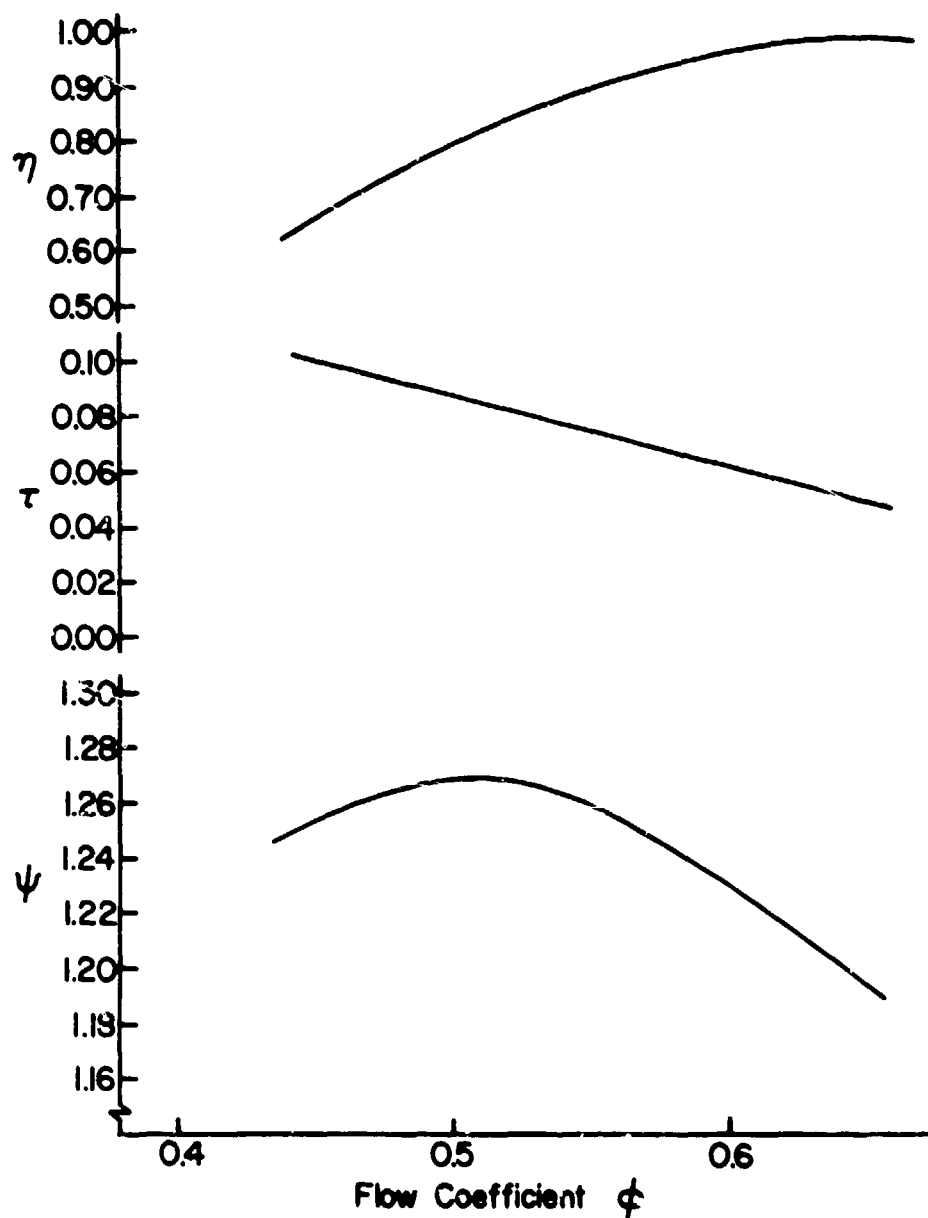
Figure A.1.6

Stage Performance Characteristics of Test Compressor
Supplied by Manufacturer (6th Stage)

(iv) stage adiabatic efficiency:

$$\eta = T_{01}\left[(\frac{P_{02}}{P_{01}})^{\frac{\gamma-1}{\gamma}} - 1\right]\frac{1}{\Delta T_0} = (\psi^{\frac{\gamma-1}{\gamma}} - 1)/\tau$$

where ΔT_0 is stage total temperature rise, P_0 total pressure, T_0 total temperatures, V_z axial velocity, U_{tip} blade tip wheel speed, γ specific heat ratio. The subscripts 1 and 2 meant inlet and outlet, respectively, and D design value.

Figure A.1.7 shows overall performance characteristics of Test Compressor supplied by the manufacturer. The performance parameters are the following:

(1) Corrected mass flow rate $= \dfrac{\dot{m}\sqrt{\theta}}{\delta}$

where $\dot{m}$ = mass flow rate

T_{01} = compressor inlet pressure

P_{01} = compressor inlet temperature

θ = T_{01}/T_{ref}

δ = P_{01}/P_{ref}

T_{ref} = 58.7°F (15.2°C)

P_{ref} = 14.7 psi (1.0132 x $10^5 N/m^2$)

(2) Corrected speed $= \dfrac{N}{\sqrt{\theta}}$

where N = rotor speed (RPM)

(3) Overall total pressure ratio = P_{02}/P_{01}

where P_{01} = compressor inlet total pressure

P_{02} = compressor outlet total pressure

(4) Overall adibatic efficiency $= \eta = \dfrac{T_{01}}{\Delta T_0}\left[(\frac{P_{02}}{P_{01}})^{\frac{\gamma-1}{\gamma}} - 1\right]$

where T_{01} = compressor inlet total temperature

ΔT_0 = compressor total temperature rise
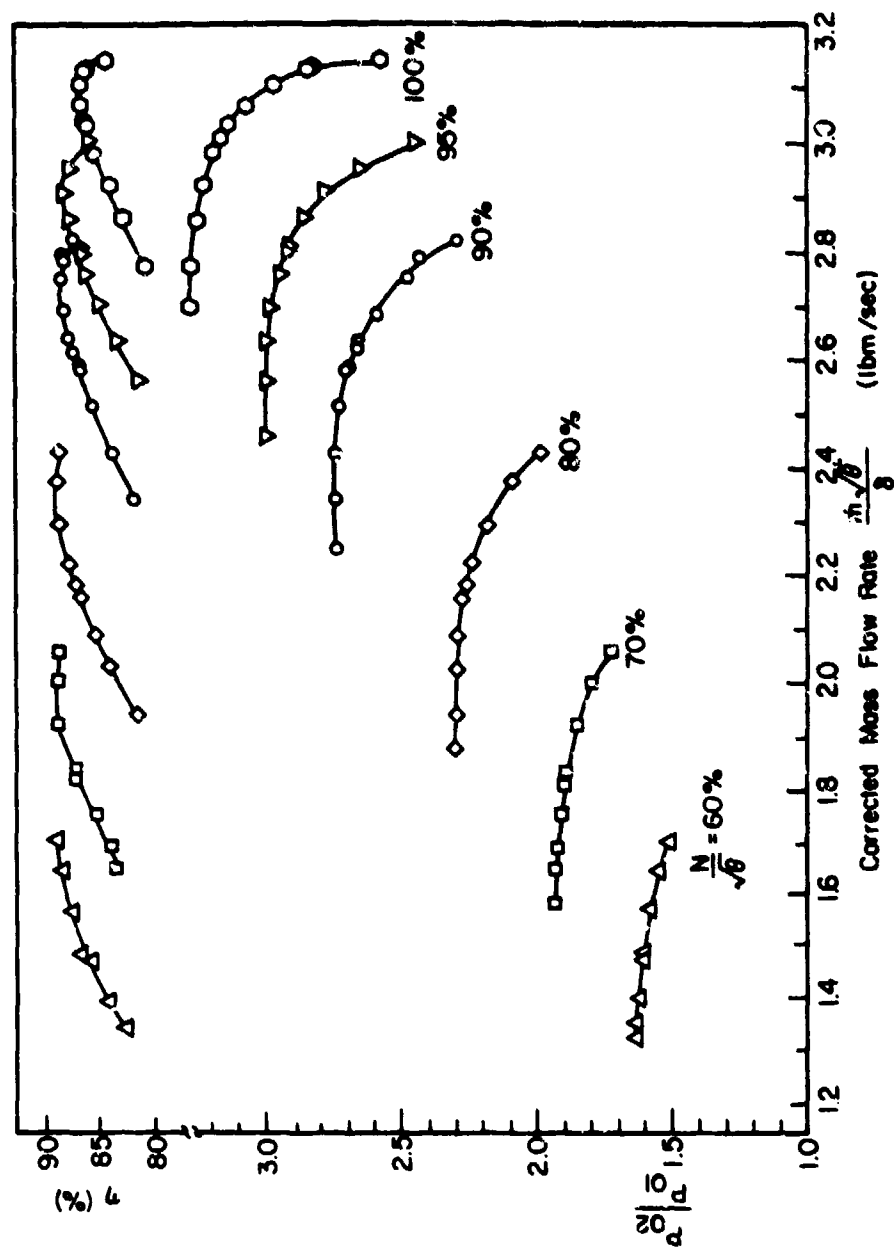
Figure A.1.7
Overall Performance Characteristics of Test
Compressor Supplied by Manufacturer

P_{02}/P_{01} = overall total pressure ratio

γ = ratio of specific heats

3. Fuel and Oil Supply Systems

3.1 The Fuel Supply System

The fuel supply system is shown schematically in Figure A.1.8. The purpose of the fuel supply system is to store and to provide fuel in the proper amounts to the Drive Engine and the laboratory air heater combustor. The drive engine fuel, Jet A, and the combustor fuel, methanol, are stored in identical tanks located next to each other in a corridor directly north of the test cell. Each tank is equipped with a sight glass for determining the volume of fuel remaining in the tank. A Gast model 4AM-FRV-13A air-operated transfer pump is used to fill the tanks from fuel storage drums. The pump is operated with air from the laboratory air supply system.

The Jet A fuel, after leaving the supply tank first passes through the manual fuel shut off valve, and then through a Jamesbury model ST 20C valve (that is remotely actuated), and finally enters the test cell in a $\frac{1}{2}$-inch stainless steel tubing. The Jet A fuel is fed to the Drive Engine fuel pump by gravity. A governor, operating in relation to the power turbine speed, determines the correct amount of fuel supplied to the fuel nozzle. Immediately upstream of the fuel nozzle is a remotely-operated fuel cut-off valve that can be shut down in an emergency.

The methanol supply tank is pressurized to 8.0 psig by the laboratory air supply system so that the methanol can be fed under pressure to the fuel nozzle in the combustor. The methanol enters the test cell and is filtered before passing through the flow regulating needle valve. The extent to which the needle valve is opened and the magnitude of the tank supply pressure, control the flow of fuel to the combustor. Between the needle valve and the combustor fuel nozzle is a Fischer & Porter model 10A1336 rotor meter for the measurement of methanol flow rate.

3.2 The Oil Supply System

The oil supply system is shown schematically in Figure A.1.9. The
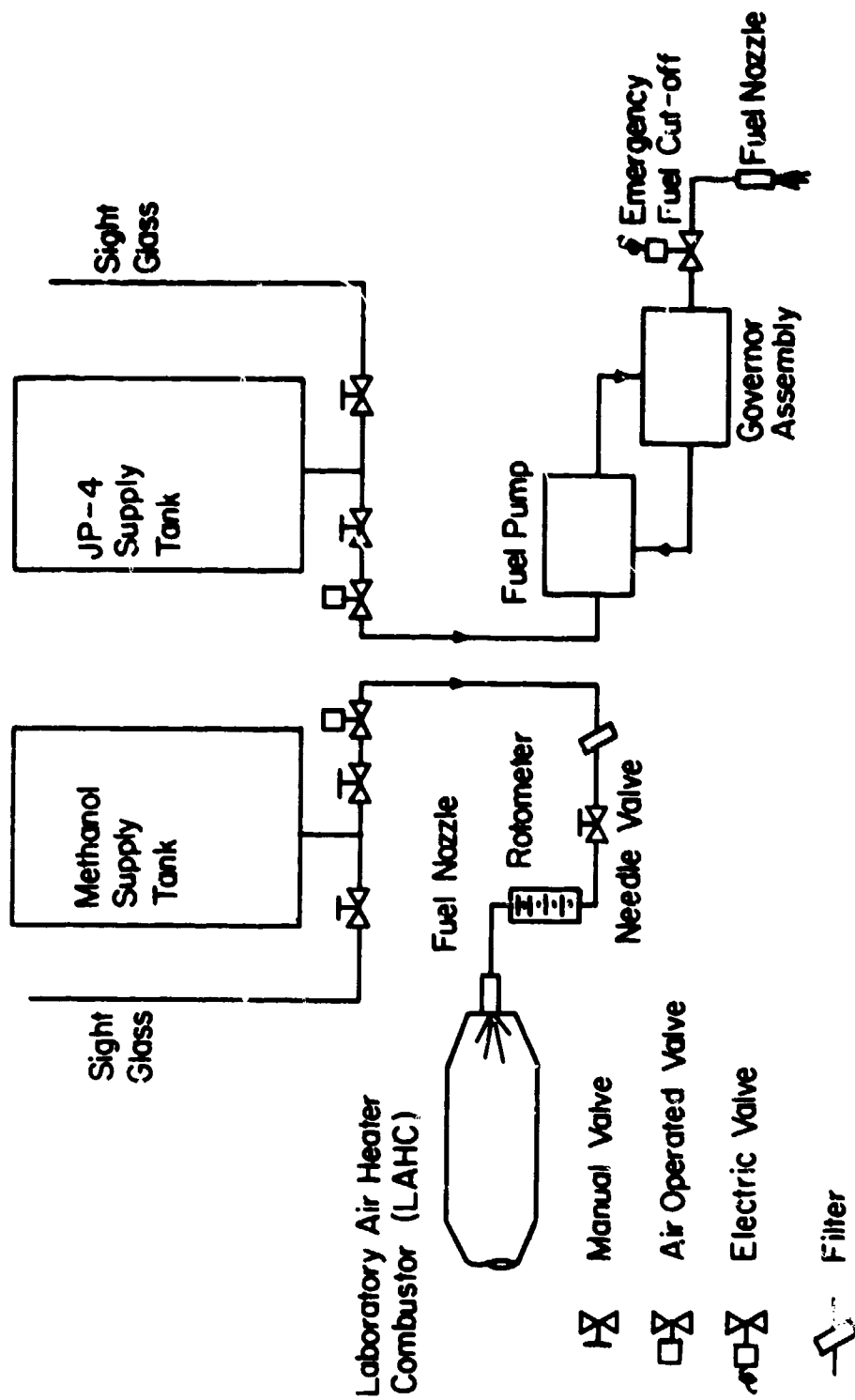
Figure A.1.8   Schematic View of Fuel Supply System
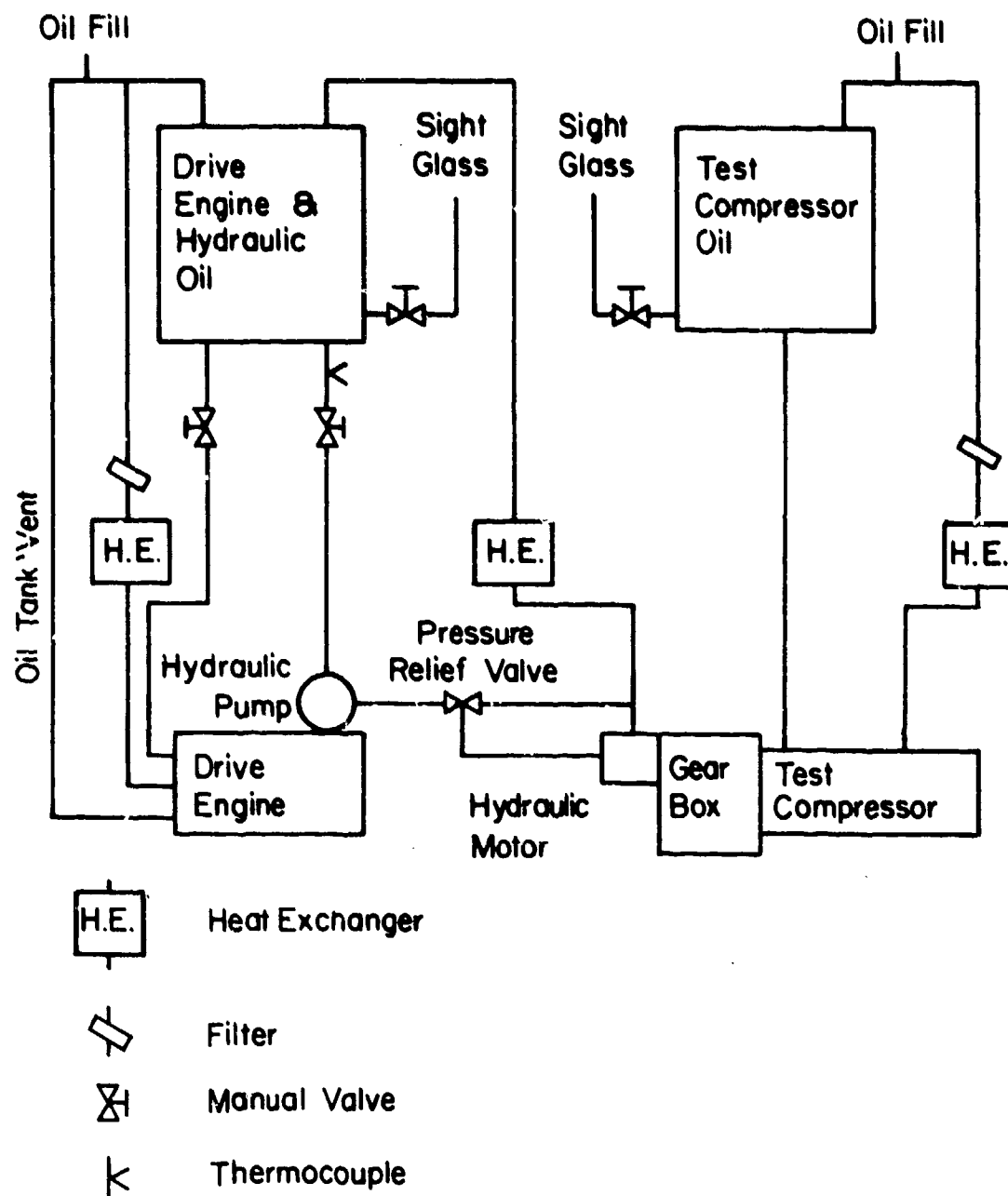
Figure A.1.9   Schematic View of Oil Supply System

oil supply system which uses Mobil II Jet Engine Oil cools and lubricates
vital Test Compressor and Drive Engine components. It also serves to
drive a hydraulic motor, which is part of the hydraulic system, to pump
oil in the Test Compressor gear box. The oil supply system consists of
two independent systems. One system (referred to as the TCO system) is
solely for the Test Compressor while the other system (referred to as the
DEHO system) supplies oil to the Drive Engine and the hydraulic system. The
oil supply tanks, heat exhangers, and oil filters are located in the corridor
directly north of the test cell near the fuel supply tanks. Each oil supply
tank is equipped with a sight glass for determining the oil level and an
Omega type K thermo-couple to monitor the oil temperature. The temperature
is read on an Omega model 402A-K-F digital readout meter.

Oil flows from the TCO system tank to the Test Compressor when a
manual shut-off valve is opened. Oil returning from the Test Compressor
passes first through a Hytech model S-702-A4-T heat exchanger and then
through a Cross 10 micron filter before it is returned to the supply tank.

The DEHO system for the Drive Engine and the hydraulic system is
more complex than the TCO system. Two separate lines supply oil to the test
cell from the DEHO tank. One of the lines supplies oil to the Drive Engine.
The oil returning from the Drive Engine is cooled by a Young model
SSF-302-HR heat exchanger and then filtered by a Cross 10 micron filter
before it is returned to the supply tank. The other line is for the
hydraulic system. The hydraulic oil is pumped to 2,200 psi by a Vickers
hydraulic pump which is driven by the Drive Engine. The high pressure oil
then passes through a relief valve. If the pressure is greater than 2,200 psi
the pressure is reduced to 2,200 psi and the excess oil returned to the
supply tank. The 2,200 psi pressure oil operates a Vickers hydraulic motor
pump which pumps oil within the Test Compressor gear box. The oil then
passes through a Ross model 47M300-8A19 heat exchanger before being returned
to the supply tank. In addition to the four oil lines just described there
is an oil tank vent line which vents the DEHO system tank to an overboard
breather mounted on the Drive Engine.

At the discharge end of the Test Compressor, there is a labyrinth seal
which is pressurized with air (from the laboratory air supply system) up

to about 5.0 psig in order to prevent leakage of oil. During a test with water injection it may be necessary to increase the air pressure slightly to prevent the oil becoming contaminated with water.

4.   Drive Engine and Test Compressor Surge Protection

The Drive Engine and the Test Compressor were protected against surging by means of an emergency fuel shut-off valve that would turn-off the Drive Engine. The fuel shut-off valve was operated by a thermocouple sensor placed at the inlet of each compressor. The Drive Engine circuit incorporated R7354A1228 Honeywell Dilatrol Indicating On-Off Controller with a range of 0-200°F, and a K-type chromel-alumel thermocouple. The Test Compressor circuit incorporated a R7350A1024 Honeywell Dilatrol Indicating On-Off Controller, operating in the range of 0-400°F, and a J-type iron-constantum thermocouple.

The Controllers were set at a desired temperature in each test. If the inlet air temperature exceeded the value that was set, the emergency fuel shut-off valve came into operation and the Drive Engine was turned-off.

5.   Drive Engine-Test Compressor System Operational Procedure

The procedure for operating the Test Compressor at a desired speed and rate of mass flow is as follows.

5.1   Initial Checks and Operations

1)   The Drive Engine starter batteries are placed on charge several hours prior to an engine run to insure adequate speed before start up.

2)   The manual low pressure air supply valve (located on the roof of the test cell) is opened.

3)   The shop air supply valve is opened.

4)   The fuel level in the Jet A fuel tank is checked to determine if sufficient fuel is available for the engine run.

5)   The manual fuel shut-off valve is opened.

6)   The levels in the DEHO, and TCO system storage tanks are checked using the sight glass on each tank (75 percent full nominal). The manually operated valve supply cooling water to the oil heat exchangers is opened.

7)   All oil supply valves are opened leading to

(a)   the Test Compressor

(b) the Drive Engine and

(c) the hydraulic system

8) The cooling (for transducers) and the Labyrinth seal air supply valves are opened. Labyrinth seal pressure is verified to be in the range of 5-7 psig by reading the seal pressure gauge. If the seal pressure is not within the prescribed limits, use the seal pressure regulating valve to make the proper change.

9) Area around both Test Compressor and Drive Engine are cleared of foreign objects.

10) The Test Compressor drive shaft is turned by hand to ascertain if the Test Compressor rotor assembley is rotating freely.

11) All switches on the Drive Engine control panel are placed in the OFF position.

12) The air intake window of the test cell is opened.

13) The protective lid covering the Drive Engine exhaust ports is removed. The lid is located on the roof.

14) The electrically operated atmospheric air valve is opened by activating a switch in the control room.

15) The emergency fuel cut-off valve is checked to be operating properly.

16) The Drive Engine throttle lever is run through its full range of operation (fuel cut-off to full open) to determine if it is operating properly. The Drive Engine throttle is visually checked to make certain that it is in the fuel cut-off position. This will aid in the prevention of hot starts.

17) The air activated fuel supply valve is opened by throwing the proper switch on the Drive Engine control panel. Once the switch is moved into the open position the valve is visually checked to determine that the valve is in the open position, If the valve is found to be operating normally the valve is then closed.

18) The Test Compressor throttle valve is placed in a predetermined position. The throttle valve center piece is moved by operating a switch on the Drive Engine control panel. The amount by which the valve is open can be read by the digital indicator above the switch. The actual amount by which the throttle valve is opened is measured and recorded.

19) The Test Compressor surge control is activated to become operational at a predetermined value of temperature at the inlet to the compressor.

20) The air-operated valve supplying cooling air to the turbine vibration transducer is opened.

5.2   Starting Procedure

21) Depending upon the corrected speed value at which the Test Compressor is desired to be operated and the temperature at the compressor inlet during the particular test, the speed at which the Test Compressor should be operated is calculated and noted.

22) The fuel supply valve is opened.

23) The emergency fuel cut-off switch on the Drive Engine control panel is energized.

24) The starter switch is depressed and held.

25) When the gas producer speed reaches a maximum and the measure turbine entry temperature reaches a minimum, the ignition switch is energized and the throttle is advanced until the engine lights off.

26) The ignition switich is de-energized.

27) The Drive Engine fuel throttle is slowly advanced until the power turbine speed begins to rise. At this point the measured gas temperature should begin to decrease. If this happens the starter switch is released.

28) The Drive Engine throttle is advanced until the power turbine speed becomes equal to the predetermined value.

29) If the turbine entry temperature increases beyond the precribed maximum value, the emergency fuel shut-off valve and the fuel supply valve are shut down.

6.   Limitations, Preliminary Trials and Refurbishment

The Test Compressor is driven, through a mechanical gear train, by the power turbine of the Drive Engine. The 6-stage Test Compressor has been utilized in the past for up to 30 hours. The available lifetime for further use of that Test Compressor has been uncertain.

The Test Compressor has a plastic coating on the casing that supports the stator blade rings. The mechanical and thermal strength of

the coating has been uncertain since the casing was built over ten years ago and may have aged. At design point, the Test Compressor temperature rise is about 192°F, (106°C) when the inlet-air temperature is 58.7°F, (15.2°C). A casing has been replaced by a second casing during preliminary testing.

The throttle regulating the Test Compressor mass flow at any given speed of operation consists of a conical center piece that can be set at any desired location concentrically in a diverging section which is then opened to atmospheric conditions following a straight duct. The center piece can be moved utilizing an electric motor. The throttle (annulus) area that is available during center piece motion is shown in Figure A.3.2. It is possible to set the throttle to within a tenth of an inch (about 2.0 mms) during horizontal traverse of the throttle centerpiece. At a given Test Compressor speed, a chosen throttle setting may yield one of two types of performance: (i) when it is unchoked, the pressure ratio across the throttle (the downstream pressure being related to the atmospheric pressure) determines the mass flow throughout the Test Compressor and (ii) when the throttle area is too large for passing the mass flow through the Test Compressor with a particular set of inlet conditions, the Compressor will operate under free-wheeling conditions.

The Test Compressor assembly with the gear box connecting it to the Drive Engine is such that there is no simple access to its outlet section for locating adequate instrumentation or adjusting probes to establish compressor outlet conditions. The gear box disassembly and removal of the compressor outlet ducting are required each time any access is desired to the compressor outlet section.

A number of preliminary tests were conducted on the Drive Engine and the Test Compressor. During these tests, the following were observed.

(1) Unusually high amplitudes of vibration of Test Compressor at frequencies not wholly related to shaft critical speeds: The Test Compressor was re-balanced.

(2) Deterioration of Test Compressor casing coating at certain locations: The casing was replaced with the casing from another Test

Compr sor configuration.

(3) Malfunction of fuel supply pump: the pump was disassembled and the sealing-ring was replaced.

(4) Malfunction of hydraulic pump: the pump was disassembled and a sealing-ring was replaced. The pump failed more than once on account of the failure of the sealing ring.

(5) Excessive heating of engine oil: separate oil coolers were installed for the Drive Engine and the Test Compressor.

The Drive Engine and the Test Compressor were refurbished in the following respects by the Detroit Diesel Allison of Indianapolis, who were the original manufacturers of both the units.

(1) Engine fuel flow control
(2) Drive shaft interconnecting the Drive Engine and the Test Compressor,
(3) Test Compressor gear box,
(4) Test Compressor bearings, and
(5) The 6-stage assembly of Test Compressor, including balancing.

Following this refurbishment and additional work undertaken at Purdue University, proof-runs undertaken on the Drive Engine - Test Compressor installation showed feasibility of satisfactory operation of the test unit.

APPENDIX 2

DESIGN OF THE BELL-MOUTH ENTRY SECTION

In order to obtain a smooth and uniform air flow into the Test Compressor a bell-mouth section was introduced ahead of the compressor inlet, as shown in Figure 2.3.

The bell-mouth section was designed based on the same design principles as adopted in the design of wind tunnel contraction sections. One of the main requirements in such axisymmetric ducts is the use of minimum length consistent with a positive velocity gradient on the wall surface that is small enough to prevent separation of the flow. Thus, a velocity distribution was chosen and specified along the wall and the bell-mouth contour was determined so as to yield the desired velocity distribution.

A method of obtaining a solution to three-dimensional, axisymmetric, incompressible, inviscid, irrotational flow equations for the flow occuring between two equipotential planar surfaces, normal to the axis of flow, is presented in Reference 26. The solution is based on expressing the axial velocity distribution in terms of a Fourier cosine series.

The bell-mouth section was designed based on the foregoing (so called Thwaite's) method. The resulting geometry is presented in Figure A.2.1.

Nozzle Dimensions

X (inch)	R_{in} (inch)	R_{out} (inch)
0.0	2.25	2.50
1.0	2.30	2.55
2.0	2.40	2.65
3.0	2.65	2.90
4.0	3.00	3.25
5.0	3.45	3.70
6.0	4.05	4.30
7.0	4.80	5.05
8.0	5.60	5.85
9.0	6.35	6.60
10.0	7.20	7.45
11.0	8.10	8.35
12.0	8.80	9.05
13.0	9.20	9.45
14.0	9.60	9.85
15.0	9.80	10.05
16.0	9.95	10.20
17.0	10.00	10.25
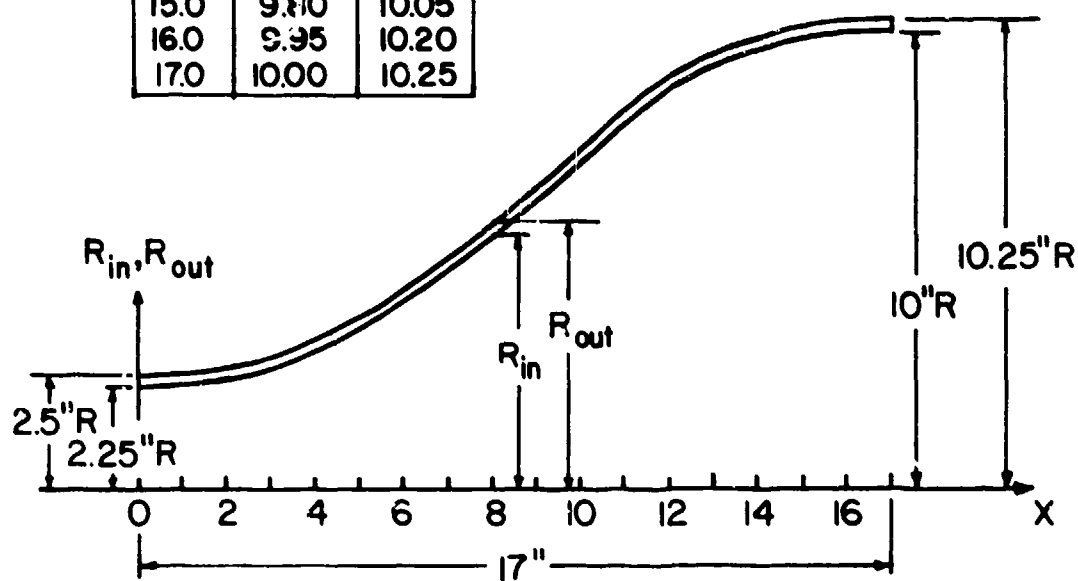
Figure A.2.1   Geometry of Bell-Mouth Inlet Section

APPENDIX 3

TEST COMPRESSOR THROTTLE VALVE

The Test Compressor throttle valve (TCTV), located in the discharge section of the Test Compressor, was employed to set the mass flow through the compressor approximately at a desired value. The air mass flow through the compressor was measured by means of the air flow measurement nozzle in every test.

The TCTV consisted of a converging-diverging nozzle with a 5.00 in. diameter throat and a cone attached to a rod that could be moved axially along the the center line of the nozzle and the following duct. Figure A.3.1. presents a schematic drawing of the TCTV. The rod and cone were moved horizontally along the axis by means of a worm-gear and 28 volt electric motor, thus changing the equivalent nozzle throat area.

The annular nozzle area available for air flow was thus a function of the position of the cone in relation to the throat of the nozzle. A servionic linear potentiometer was utilized to measure the position of the rod, the length of the rod protruding out of the nozzle being displayed in inches on a digital indicator in the control room. The digital indicator was set to indicate zero when the annular nozzle area was zero, that is when the nozzle throat was blocked fully by the cone.

From the point of view of the Test Compressor, when the rod was withdrawn by a large amount, one would obtain a large mass flow of air through the compressor, and when the rod was moved in such that the cone was blocking the nozzle opening by a large amount, one would tend towards surging flow through the Test Compressor.

By means of preliminary investigations, it was established that the discharge coefficient of the annular nozzle was 0.93 over an appreciable range of flow Reynolds numbers.

The flow area available through the annular nozzle for different
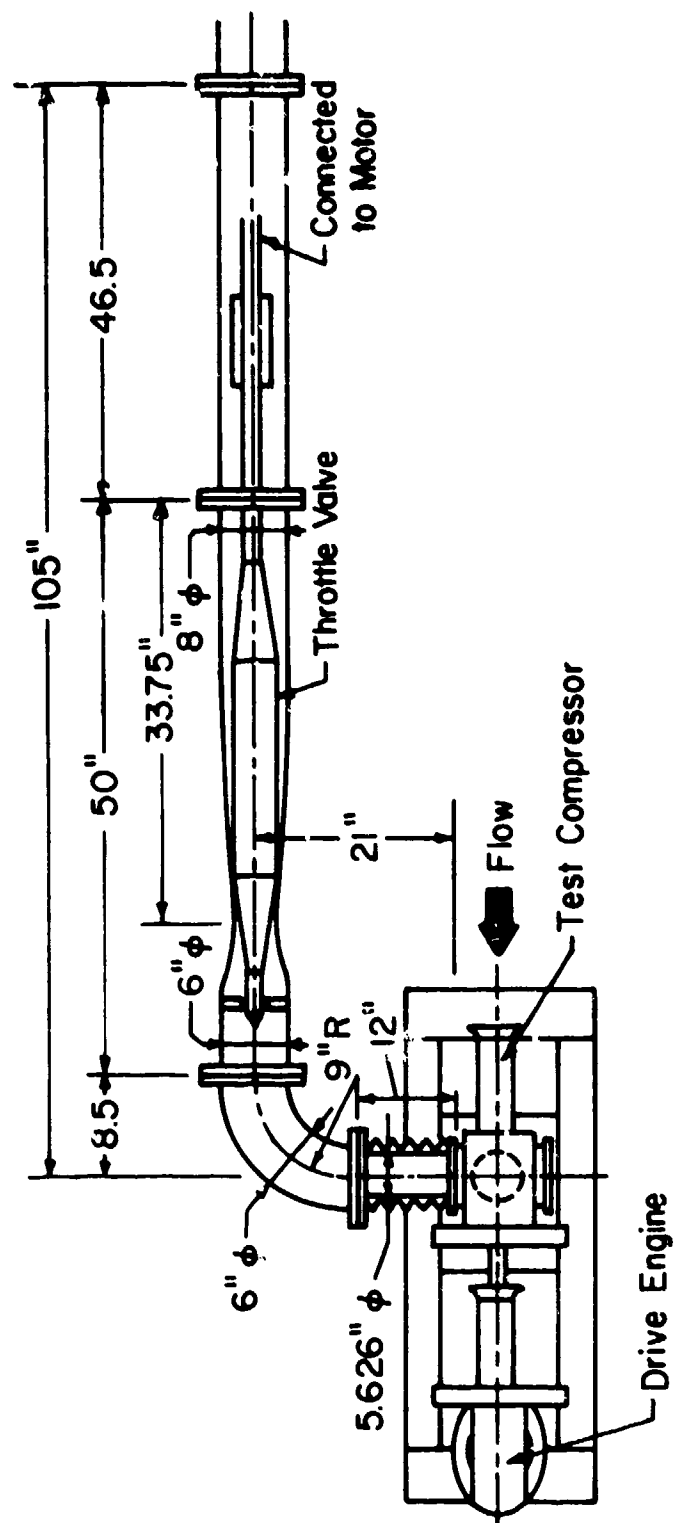
Figure A.3.1   Schematic Drawing of Test Compressor Throttle Valve

throttle valve settings has been shown in Figure A.3.2.

Utilizing the nozzle discharge coefficient value of 0.93 and the Test Compressor operating characteristics given in Figure A.1.7, the corrected mass flow rate that was obtainable at different corrected speeds of the compressor for different throttle valve settings was calculated. The resulting performance of the throttle valve in conjunction with the Test Compressor has been shown in Figure A.3.3.

It may be pointed out that the throttle valve may operate either in the choked or in the unchoked mode, depending upon the Test Compressor discharge pressure and the ambient conditions. The difference in the two modes is reflected in Figure A.3.3.

Figure A.3.3. was utilized in setting the throttle valve in order to obtain, of course approximately, a desired operating condition in a particular test.
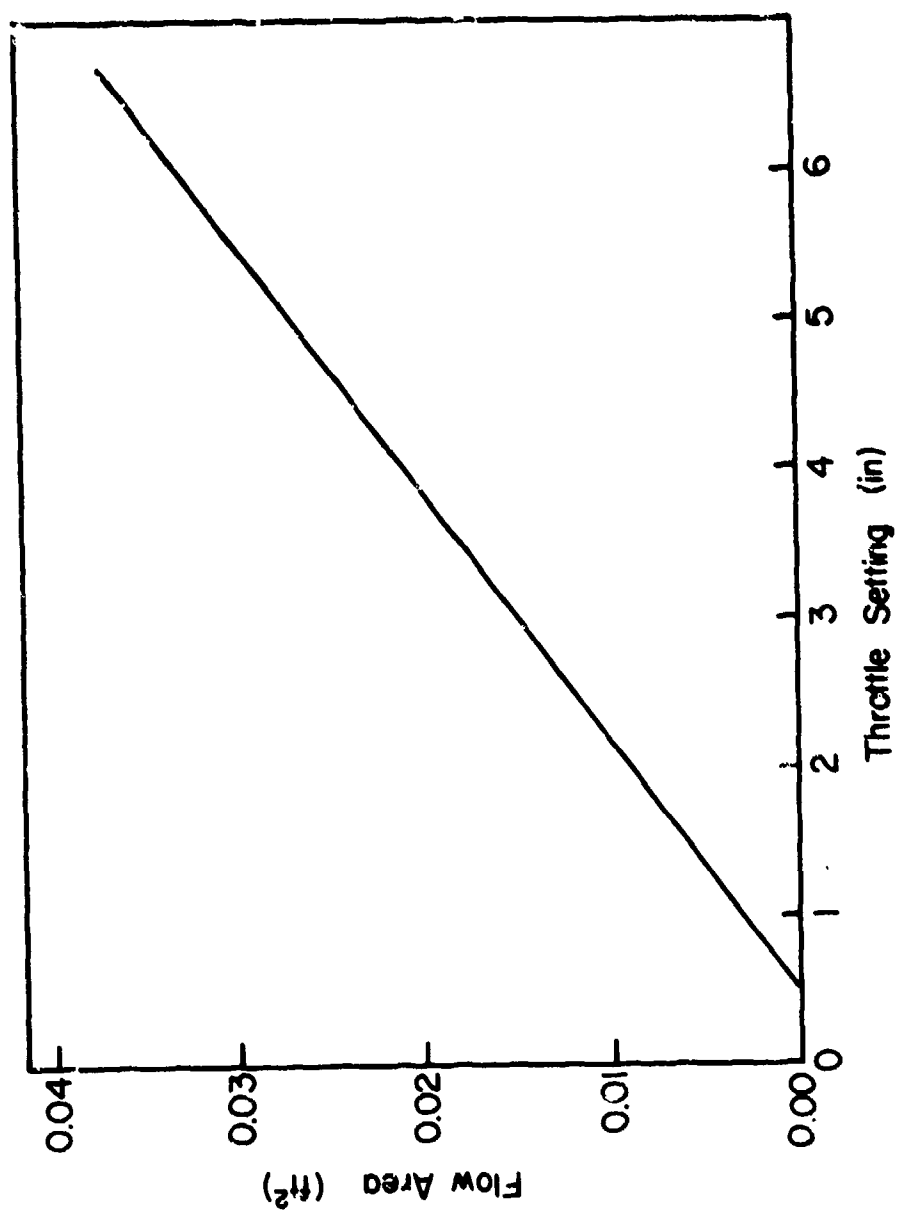
Figure A.3.2 Flow Area vs. Test Compressor Throttle Setting
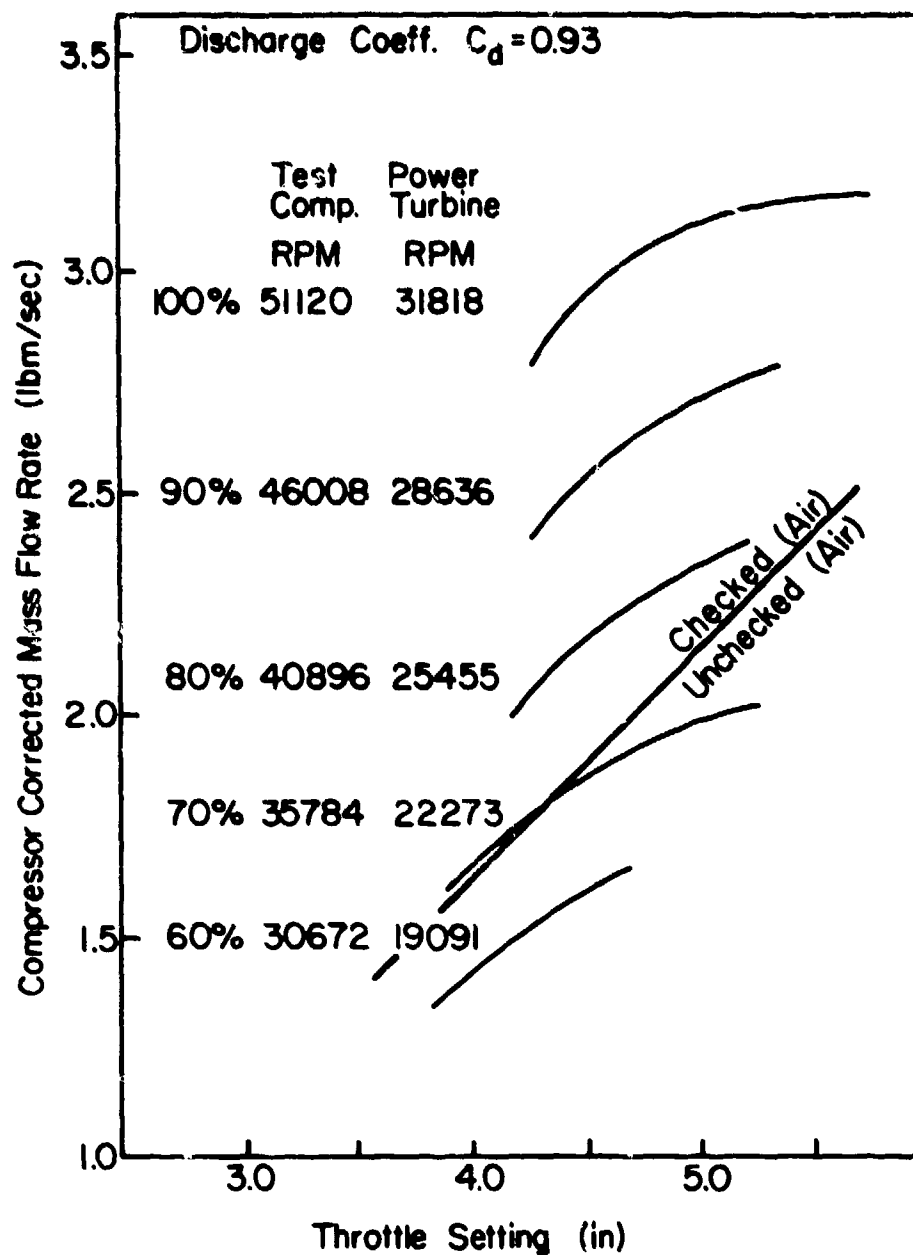
Figure A.3.3 Performance of Test Compressor Throttle Valve

APPENDIX 4

LABORATORY AIR SUPPLY SYSTEM

The Thermal Sciences and Propulsion Center (TSPC) at Purdue University has two independent stored air supplies: one referred to as the high pressure system and the other referred to as the low pressure system.

The TSPC high pressure system has a stored air supply of 2028 cubic feet at a maximum pressure of 2200 psig. Two Ingersoll-Rand compressors are employed in a two-stage process to pump air at 3,000 psig to the high pressure stored air supply at a rate of 740 scfm. In the first stage of pumping, an Ingersoll-Rand model TVH-3, 15 & 8 & 4½ x 8 stage compressor compresses the air to 500 psig. During the second stage of pumping the 500 psig, air is raised to a final pressure of 3,000 psig by an Ingersoll-Rand model ESH-2 4 & 2-3/4 x 11 booster compressor. The stored air supply is normally utilized until the storage tank pressure drops to a value of about 1,000 psig. yeilding a flow rate of 10 lbs/sec at standard atmospheric pressure over a period of 1250 seconds.

In the other system, two Ingersoll-Rand model ESH-2 12 & 6 x 11 compressors deliver 300 psiq air to the low pressure stored air supply at a rate of 808 scfm. The air supply pressure in the storage system (750 cubic feet capacity) is increased to 500 psig by a valve connected to the high pressure stored air supply.

Both the high and low pressure air lines are available in the Propulsion Laboratory building in which the test cell, used in the current investigation, is located.

The laboratory air supply system has been shown schematically in Figure 2.4. It may be observed that the laboratory air supply system utilized both the low pressure and the high pressure air supplies.

The low pressure air supply was utilized for the following purposes in the test cell.

(1) Operate the many air actuated valves in the test installation.

(2) In conjunction with Grove hand loaders to control the opening of dome regulators.

(3) Maintain test compressor labyrinth seal pressure.

(4) Cool the turbine vibration transducer during and after a drive engine run.

(5) Drive the pump to fill the drive engine and combustor fuel tanks from fuel storage drums.

(6) Pressurize methanol fuel tank.

(7) Atomize combustor fuel.

The high pressure air supply was utilized to provide "conditioned" air to the Test Compressor at the desired temperature and pressure. The air supply line, which runs along the roof of the Propulsion Laboratory from the high pressure storage tanks, was tapped to provide air to the test cell. The test cell supply line had a Jamesbury model 6800-3600 G. FOK00 AA (remotely) air-operated valve, know as the High Pressure Air Supply Valve (HPASV). Downstream of the HPASV, the test cell supply line branched into two supply lines. One branch supplied air to the laboratory air heater combustor (LAHC), while the other branch supplied the primary (diluent) air for mixing with the heated LAHC exhaust air. The primary and the LAHC air flows were controlled by Grove Power reactor regulators, model 21 2B and model 31 1B respectively, in conjunction with Grove hand loaders. Downstream of the Grove regulators two B.S. & B burst diaphragms were located in order to prevent damage to the test installation should the regulators fail.

The primary and the LAHC air flows were then brought from the roof into the test cell. In order to measure the flow rates, each branch was equipped with a standard orifice, orifice upstream pressure gauge, differential pressure gauge for measuring pressure drop across the orifice plate, and an Omega type K thermocouple. The temperature was read on a Omega model 402A-K-F digital readout meter located on the laboratory air supply control panel.

The LAHC air supply was utilized to burn methanol in the combustor and thus heat the air. The heated air then mixed with the cold diluent air in order to obtain air at the desired temperature and pressure. The ducting and the four Posi Seal butterfly valves employed for this purpose have been shown in Figure 2.4.

The "conditioned" air then entered the Test Compressor supply system at the plenum chamber.

It may be pointed out here that the LAHC exhaust air was slightly vitiated in view of the products obtained during the combustion of methanol. However, the fuel-air ratio was very low, since the desired LAHC exhaust temperature was only about 150°C. When this heated air was mixed with cold air, the resulting mixture was contaminated very little.

1. Operation of the Laboratory Air Supply System

In order to obtain a desired pressure and temperature at the outlet from the plenum chamber (Supplying air to the Test Compressor), the following procedure was adopted.

1.1 Initial Checks and Operations

1) The manual low pressure air supply valve located on the roof was opened.

2) The shop air supply valve was opened.

3) The fuel level in the methanol tank was checked to determine if sufficient fuel was available for the combustor run.

4) The manual combustor fuel supply tank pressurization valve was opened.

5) The Grove hand loaders on the laboratory air supply control panel were fully closed.

6) The valve which allowed the regulator air supply tank to be pressurized was opened.

7) The manual combustor fuel shut-off valve was opened.

8) The methanol tank manual vent valve was opened.

9) The LAHC air and the diluent air mixing valve was closed.

10) The mixed air bypass shut off valve was closed.

11) The combustion air bypass throttle valve was fully opened.

12) The laboratory air supply valve was opened.

13) The atmospheric air valve was opened.

14) The remotely operated methanol tank pressurization valve was opened.

15) The methanol fuel tank was pressurized to 8 psig by using the hand loader in conjunction with the fuel pressure gauge.

16) The fuel nozzle zir pressure hand loade· was opened until the fuel nozzle air gauge read 20 psig.

1.2 Operating Procedure

17) The high pressure supply valve was opened.

18) The Grove hand loader controlling the primary air supply was opened until the combustor air orifice inlet pressure gauge read the desired value, as obtained from calibration data.

19) The combustor fuel ignition switch was turned on.

20) The remotely operated combustor fuel shut-off valve was opened.

21) The combustor fuel ignition switch was turned off when steady state combustion was established.

22) The Grove hand loader controlling the diluent air supply was opened until the diluent air orifice inlet pressure gauge read the desired value, as obtained from the calibration data of desired pressure and temperature with diluent air orifice inlet pressure.

23) The combustion air and diluent air mixing valve was opened.

24) The combustion air throttle valve was closed.

25) The atmospheric air valve was closed.

2. Air Flow Metering Nozzles

Two nozzles were designed for the measurement of air flow to the Test Compressor, one suitable for low flow rates and another for high flow rates. The nozzles were designed according to standard practice recommended in Reference 27. The nozzles have been illustrated in Figures A.4.1 and A.4.2
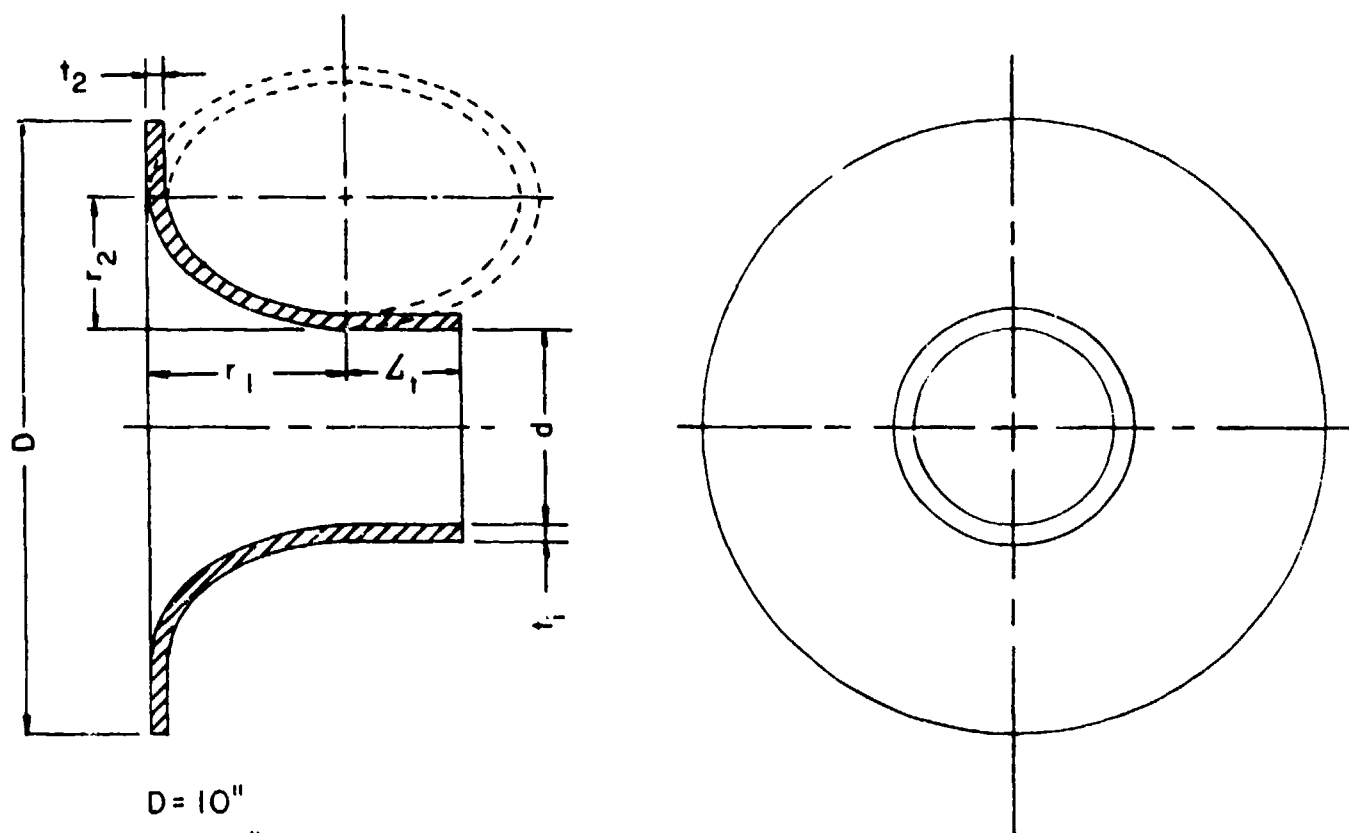
$D = 10''$

$d = 3.2''$

$r_1 = d = 3.2''$

$r_2 = (2/3)\ d = 2.13''$

$\angle_t = 0.6\ d = 1.92''$

$t_1 = 1/4''$

$t_2 = 1/4''$

Throat taper $\pm\ 0.0015$

Throat ovality $\pm\ 0.003$

Figure A.4.1   Flow Metering Nozzle for Air ($\beta = 0.4$)
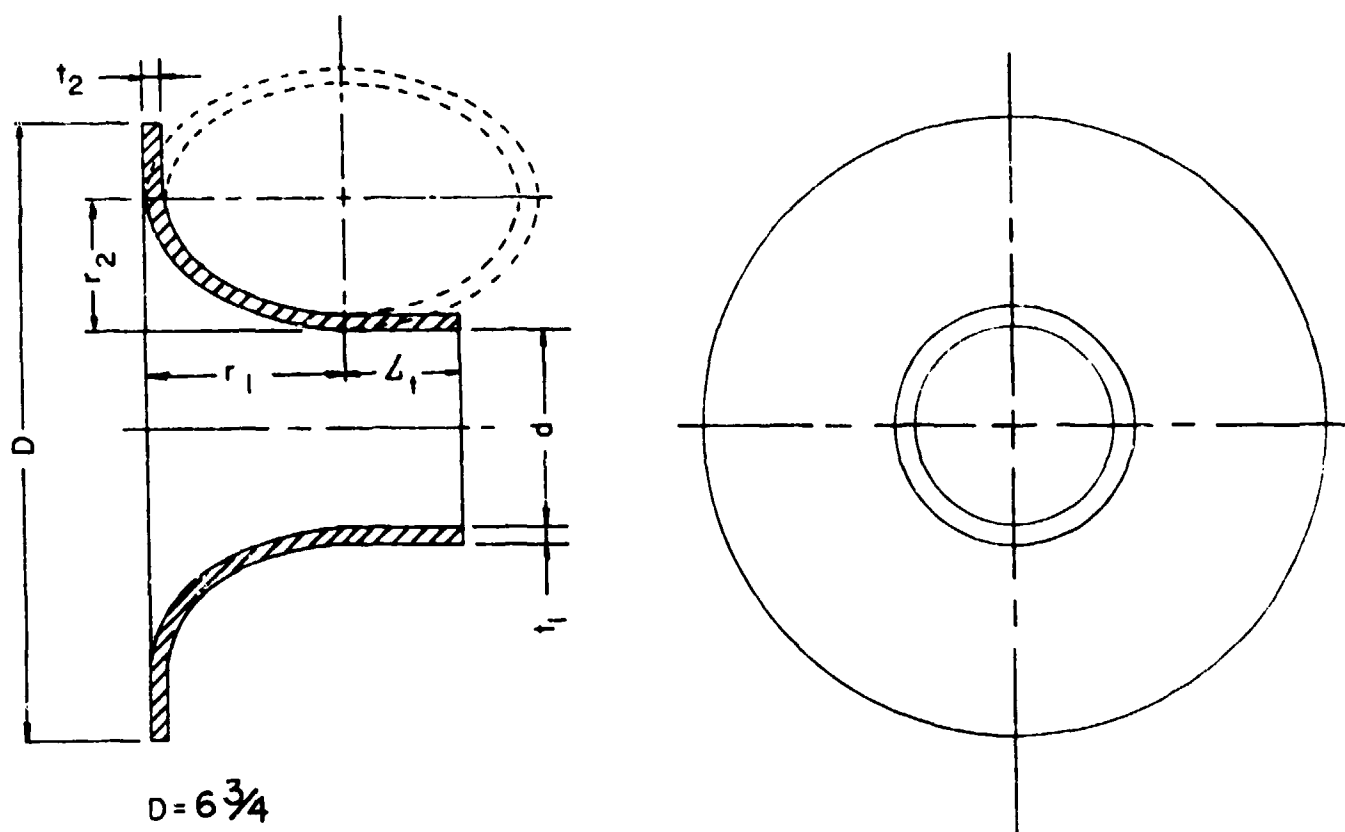
$$D = 6\frac{3}{4}$$

$$d = 2.40$$

$$r_1 = d = 2.40$$

$$r_2 = (2/3)\ d = 1.66$$

$$\mathcal{L}_t = 0.6\ d = 1.44$$

$$t_1 = 1/4''$$

$$t_2 = 1/4''$$

Throat   taper   ± 0.0015

Throat   ovality   ± 0.003

Figure A.4.2   Flow Metering Nozzle for Air (β=0.3)

APPENDIX 5

METHANE INJECTION SYSTEM

1. Description

The methane injection system was designed to inject a desir... value of mass flow of methane into the air supplied to the Test Compressor. For purposes of ensuring safety in operation, the methane injection system incorporated an injection system for nitrogen that was used to purge the methane supply line and the methane injection ring.

The methane injection ring, the injector and the injection system have been shown in Figures 2.5 - 2.8.

Commercial grade methane was stored in three Type T bottles outside the Propulsion Laboratory building. The three bottles were manifolded together into a 1/4-inch methane supply line. This line was connected to a Grove model WBX-204-K15 dome regulator. The dome regulator was remotely operated with a Grove hand loader which was part of the laboratory air supply system. The dome regulator controlled the mass flow of methane to the injection ring. Immediately downstream of the dome regulator was located a Kunkle model 600F-1 pressure relief valve which prevented an overpressure in the methane piping should the dome regulator fail. The methane flow passed through a manual valve before entering the test cell.

The measurement of methane mass flow rate was accomplished by employing a choked flow nozzle in conjunction with an Omega type K thermocouple and a Gould model PM822-50 differential pressure transducer. The temperature and pressure was read on a Daytronic model 9515 digital indicator and a Data Tech model 73-100 digital read out meter, respectively. Downstream of the flow nozzle, three Atkomatic model 15440 solenoid valves were used to regulate the flow. One of the valves, the

methane supply cut-off valve, was located immediately downstream of the flow nozzle. This valve was operated independently of the other two valves which were operated by a single 3-position switch. In the center position of the latter switch both valves were closed. If the vent position was selected the methane flowed to the outside dump. With the switch in the inject position, methane was injected into the air stream.

The nitrogen purge system was employed both during methane injection and for a period of time after the methane injection was terminated, especially when the Drive Engine was running. The nitrogen was supplied from a 240 cubic feet gas bottle, initially pressurized to 2,250 psi. The bottle pressure was reduced to 45 psi by a two stage Union Carbide model TSA-200-350 bottle regulator. A Kunkle model 00GD1 relief valve set at 50 psi was located just downstream of the bottle regulator and was set to open if the regulator failed. Nitrogen was supplied to the injection ring through a port at the bottom of the ring. The flow of nitrogen was controlled by a remotely operated Skinner model V53ADA1150 electric valve.

2.   Operation of Methane Injection System

2.1   Initial Checks and Operations

1) The manual low pressure air supply valve located on the roof of the propulsion building is opened.

2) The valve which allows the regulator air supply tank to be pressurized is opened.

3) The outside methane vent line is connected.

4) The manual valves located on the nitrogen and methane supply bottles are rotated into the full open position.

5) The nitrogen and methane supply pressure gauges are checked to determine if sufficient amount is available for the test run.

2 2   Operational Procedure

6) All other necessary check lists for operating the Drive Engine, the Test Compressor and instrumentation are completed.

7) The Drive Engine is started and the Test Compressor speed is set at the desired value.

8) The methane inject switch is placed in the vent position.

9) The methane supply switch is placed in the open position.

10) The Grove hand loader is opened until the desired pressure is set upstream of the flow measurement nozzle.

11) The nitrogen purge switch is moved into the purge position.

12) The methane inject switch is thrown into the inject position.

13) The Grove hand loader, is adjusted if necessary, so that the desired flow nozzle pressure is obtained.

3.   Flow Metering Nozzle for Methane

A flow metering nozzle for methane was designed according to standard practice recommended in Reference 27. The nozzle design has been illustrated in Figure A.5.1.
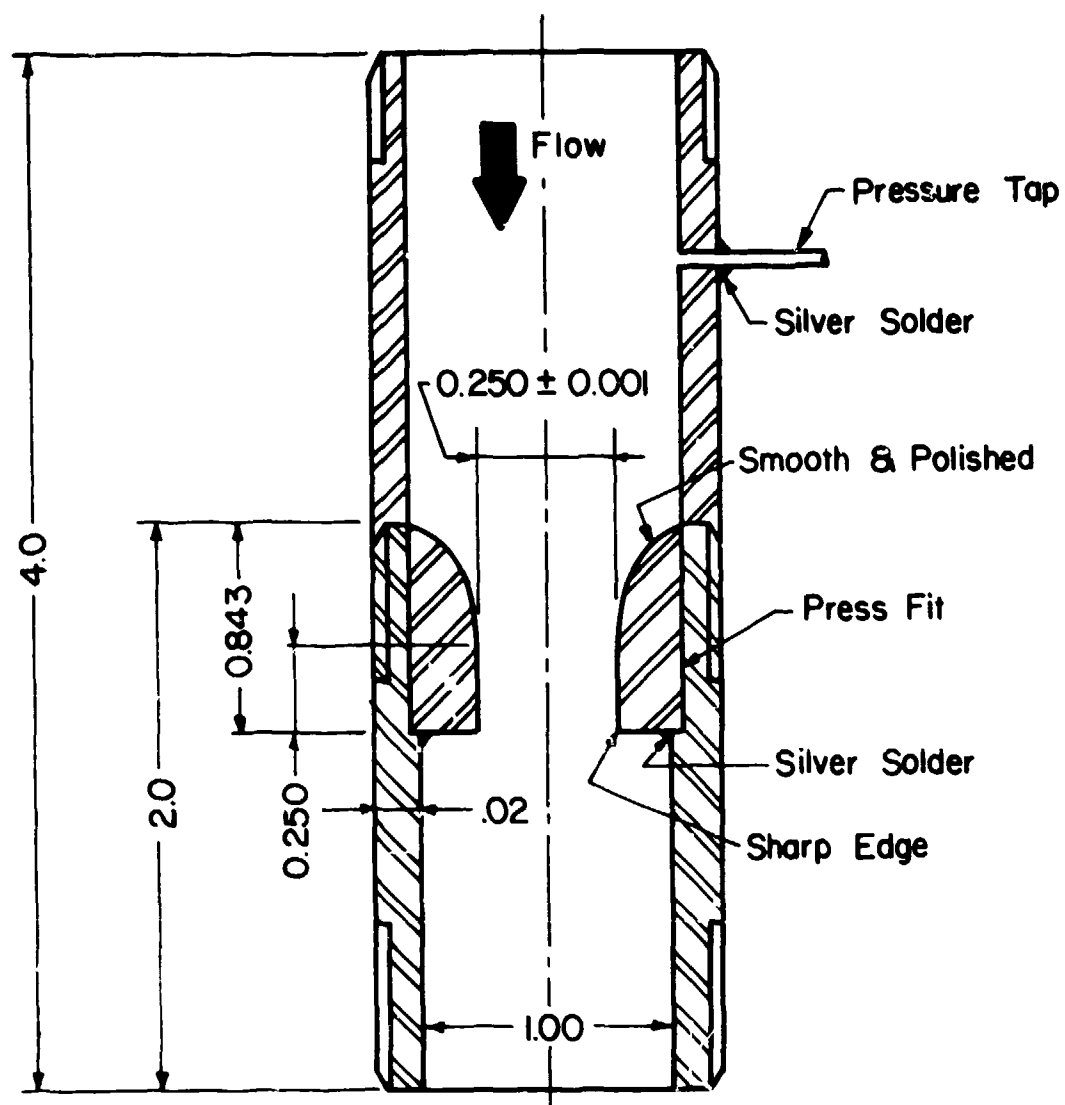
Figure A.5.1 Flow Metering Nozzle for Methane

APPENDIX 6

WATER INJECTION SYSTEM

1. Description

   The water injection system was designed to supply a desired amount of water at a given pressure to the injectors, which injected water (in the injection ring) into the air stream of the Test Compressor.

   The water injection ring, an injector locator, the water supply system and the water distribution system have been shown in Figures 2.9-2.14.

2. Operation of Methane Injection System

2.1 Initial Checks and Operations

   1) The water collection tanks are emptied.

   2) The WSFV1 and WSFV2 are opened.

   3) The SDV2 is closed.

   4) The FRV is fully opened.

   5) The PFTV is fully opened.

   6) The RSOV1 and RSOV2 are closed.

   7) The RBV is opened.

   8) The ABV is closed.

   9) The SDV1 is closed.

   10) The outside drain line to the test cell is installed.

   11) The WMSV is slowly opened.

   12) The SWSV is opened to begin filling the system piping and it it is closed when the system supply pressure gauge shows 15 psig.

   13) The WSFV1 and WSFV2 are closed.

   14) The water pump is started

   15) The RSOV1 and RSOV2 are opened.

   16) The RBV is closed.

   17) Based upon test requirements, the IV1, IV2, IV3, and IV4 are placed in the closed position.

18) The FRV is adjusted until the system supply pressure gauge shows the desired pressure. This pressure is based upon calibration data of spray characteristics with system supply pressure.

2.2. Operational Procedure

19) All other necessary check lists for operating the Drive Engine, the Test Compressor and the instrumentation are completed.

20) A clock is started to determine the duration of water injection at the end of the desired injection period.

21) At the time water injection is to begin, the valve master switch is put in the open position.

22) The valve master switch is placed in the closed position.

23) The water pump is turned off.

24) After the Drive Engine is stopped, the water drained from the bell-mouth and the Test Compressor exit in the two tanks is measured and then discarded.

25) The WMSV is closed.

3. Calibration Tests

The water injection system was calibrated during a series of system tests to ensure that the desired rates of water flow were obtained at the required water pressures.

The performance of an injector nozzle, in terms of the quantity of water injected and the droplet size distribution obtained was a function of the pressure at which water was supplied to the injector.

The droplet size distribution obtained from an injector was assumed to be the same as specified by the manufacturer of the nozzle. The manufacturer provided test data that were obtained from representative batches of nozzles of the same classes as employed in the current tests.

4. Injectors

Two types of injectors were selected for use during the water injection tests, both manufactured by Spraying Systems Company of Illinois:

(i) Model $\frac{1}{4}$ LN6-$\frac{1}{4}$ LNN6 nozzles that were of the "small" droplet, hollow-cone type; and

(ii)　　Model ¼ G1-¼ GG1 nozzles that were of the "large" droplet, full-cone type.

The characteristics of the "small" droplet injector have been presented in Tables A.6.1 and A.6.2; and the "large" droplet characteristics in Tables A.6.3 and A.6.5.

The injectors were operated under choking flow conditions during all of the tests. The spray characteristics were thus only a function of the pressure of water supplied to an injector.

The injectors were calibrated for droplet size distribution by the manufacturer. The calibration data provided by the manufacturer for the two types of nozzles are shown in Figures A.6.1 and A.6.2.

TABLE A.6.1

¼ LNN6 ATOMIZING (HOLLOW CONE PATTERN) NOZZLES

INJECTOR CHARACTERISTICS

Pressure		Capacity (gallons per minute)	$(\frac{m^3}{sec})$	Spray Angle (degree)
(psig)	(N/m²)			
30	3.08×10^5	5.2	5.46×10^{-6}	----
40	3.77×10^5	6.0	6.30×10^{-6}	73
60	5.15×10^5	7.3	7.67×10^{-6}	----
80	6.53×10^5	---	------	79
100	7.91×10^5	9.5	9.98×10^{-6}	----

TABLE A.6.2

¼ LNN6 ATOMIZING (HOLLOW CONE PATTERN) NOZZLES

SPRAY CHARACTERISTICS

Droplet Size (μm)	At 25 psig (2.74 × 10⁵ N/m²)	Pressure 40 psig (3.77 × 10⁵ N/m²)	Of 100 psig (7.91 × 10⁵ N/m²)
$D_{no.5}$ (number median diameter)	80	71	62
D_{10} (number mean diameter)	91	81	58
D_{20} (area mean diameter)	104	92	77
D_{30} (volume mean diameter)	117	103	85
D_{21} (area-number mean diameter)	119	105	86
D_{31} (volume-number mean diameter)	132	117	95
D_{32} (sauter mean diameter)	147	130	105
$D_{vo.5}$ (volume median diameter)	169	148	118

TABLE A.6.3
⅛ TTG1 (FULL CONE SPRAY PATTERN) NOZZLES
INJECTOR CHARACTERISTICS

Pressure		Capacity		Spray Angle
(psig)	(N/m^2)	(gallons per minute)	$(\frac{m^3}{sec})$	(degree)
15	2.05×10^5	0.12	7.56×10^{-6}	----
20	2.39×10^5	0.14	8.82×10^{-6}	58
30	3.08×10^5	0.17	10.71×10^{-6}	----
40	3.77×10^5	0.19	11.97×10^{-6}	59
60	5.15×10^5	0.23	14.49×10^{-6}	----
80	6.53×10^5	0.26	16.38×10^{-6}	----
100	7.91×10^5	0.30	18.90×10^{-6}	53

TABLE A.6.4
⅛ TTG1 (FULL CONE SPRAY PATTERN) NOZZLES
SPRAY CHARACTERISTICS

Droplet Size (μm)	At 10 psig $(1.70 \times 10^5$ $N/m^2)$	Pressure 40 psig $(3.77 \times 10^5$ $N/m^2)$	Of 100 psig $(7.91 \times 10^5$ $N/m^2)$
$D_{no.5}$ (number median diamter)	498	421	276
D_{10} (number mean diameter)	581	472	300
D_{20} (area mean diameter)	683	535	332
D_{30} (volume mean diameter)	781	598	362
D_{21} (area-number mean diameter)	802	607	367
D_{31} (volume-number mean diameter)	904	672	398
D_{32} (sauter mean diameter)	1020	744	432
$D_{vo.5}$ (volume median diameter)	1190	847	481
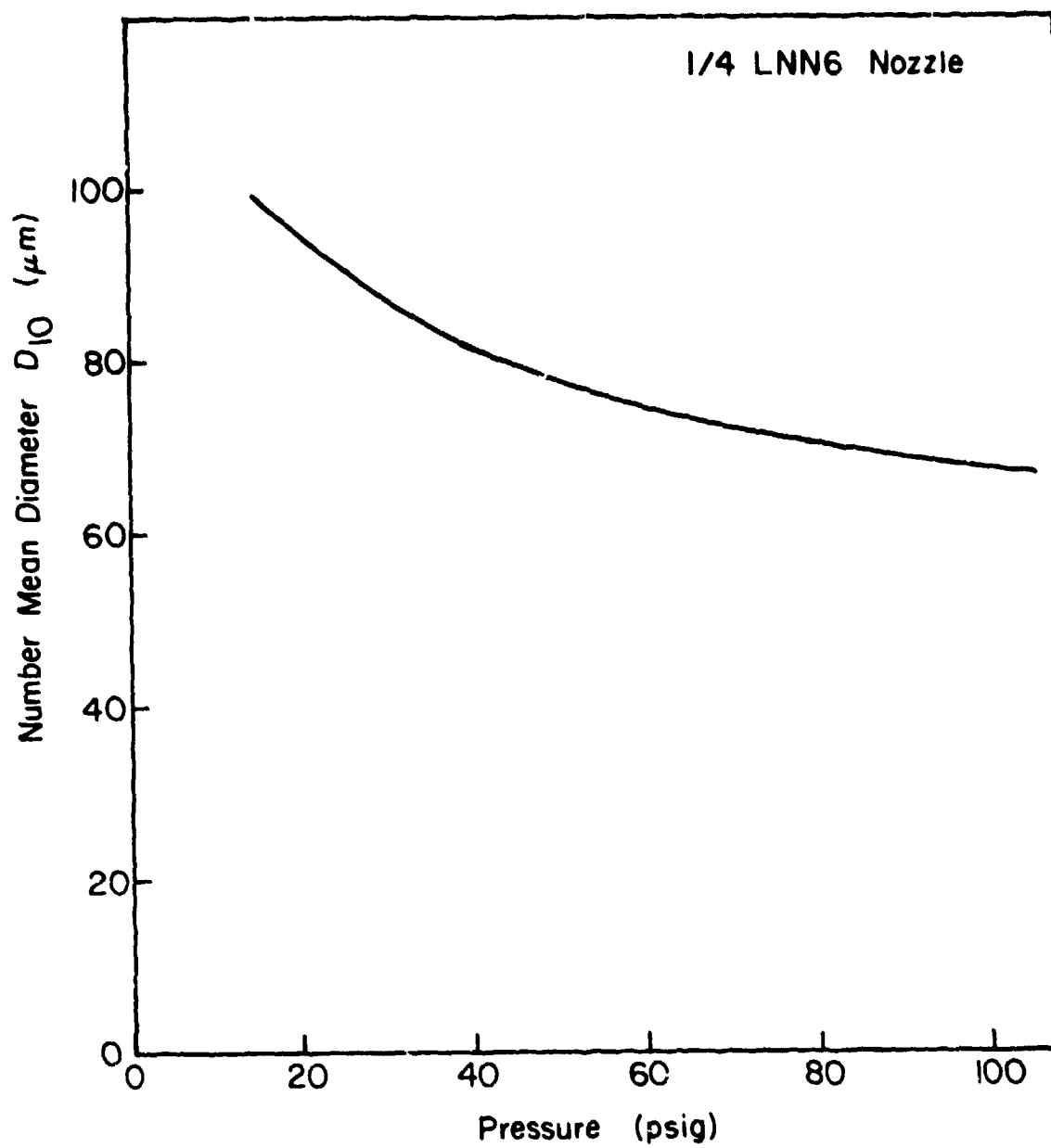
Figure A.6.1   Calibration Data of Water Injector Provided by
Manufacturer (¼ LNN6 Nozzle)
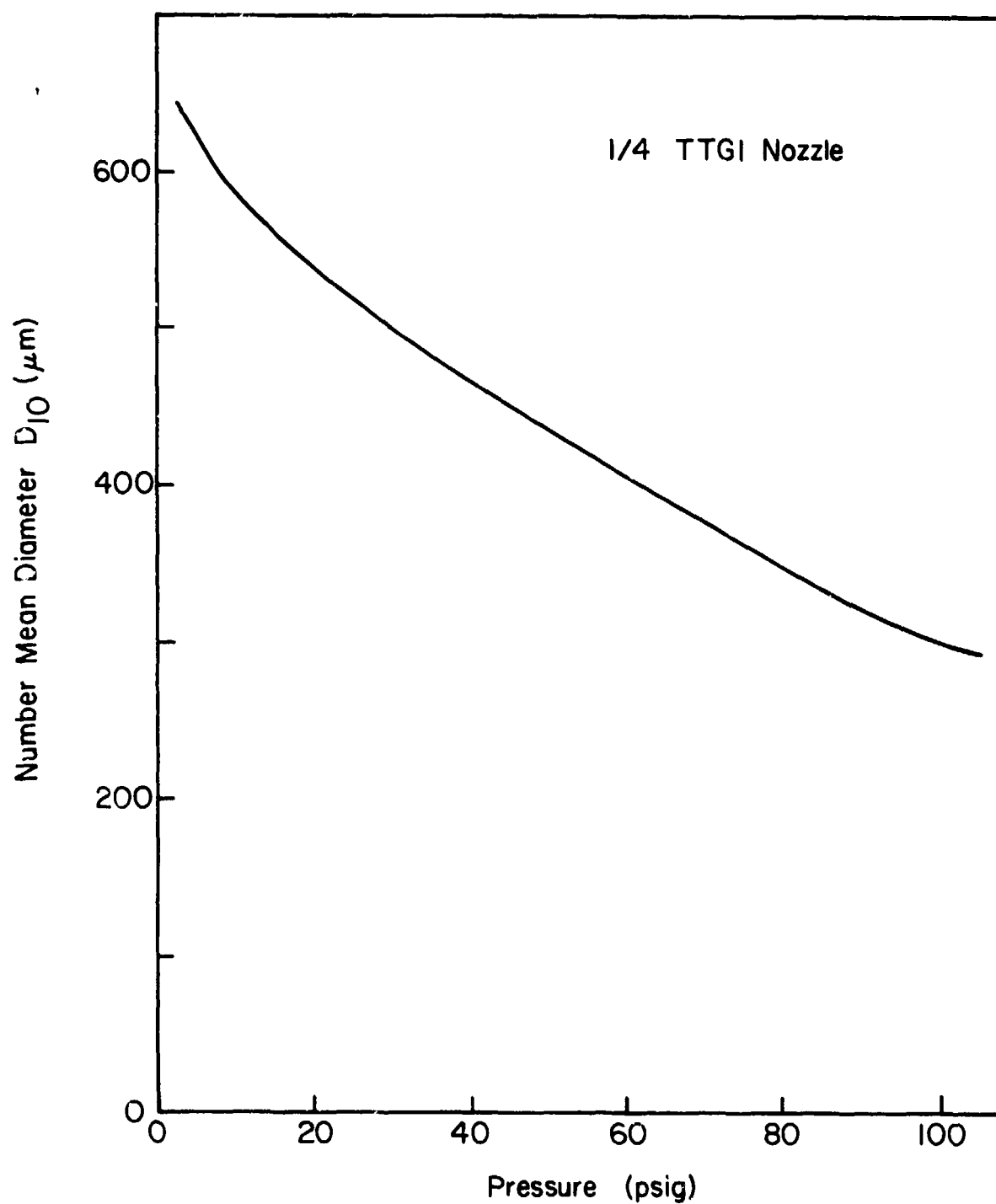
Figure A.6.2 Calibration Data of Water Injector Provided by
Manufacturer (¼ TTGl Nozzle)

APPENDIX 7

TWO PHASE FLOW PRESSURE PROBE

The two-phase (air-water droplet mixture) flow pressure probe is intended for use in water ingestion test. The probe has been built for Purdue University by E.G. & G. Idaho, Inc. The probe needs detailed calibration before use. Since the probe calibration was not accomplished under the current project, the probe has not been used in the testing program.

1. Description

The probe design is shown schematically in Figure A.7.1. The manner in which the probe and its associated hardware can be mounted on the compressor ducting is shown in Figure A.7.2.

The probe is designed for the measurement of the following.

(1) Stagnation pressure of the gas phase; and

(2) Combined stagnation pressure of the air-water droplet mixture.

No provision exists for static pressure measurement.

The combined stagnation pressure of the air-water droplet mixture is the sum of the stagnation pressures of the gas and liquid phases.

The pressure measurements are carried out using pressure transducers. In particular, it is proposed to measure the following utilizing Validyne DP15 differential pressure transducer along with Validyne signal conditioning, consisting of a MC1-10 module case with mating connectors, CD-19 carrier demodulators and, possibly, a PM212-1 3-½ digit digital display.

1) The differential pressure between the gas phase stagnation pressure and the static pressure from a wall tap on the compressor ducting.

2) The differential pressure between the combined stagnation pressure
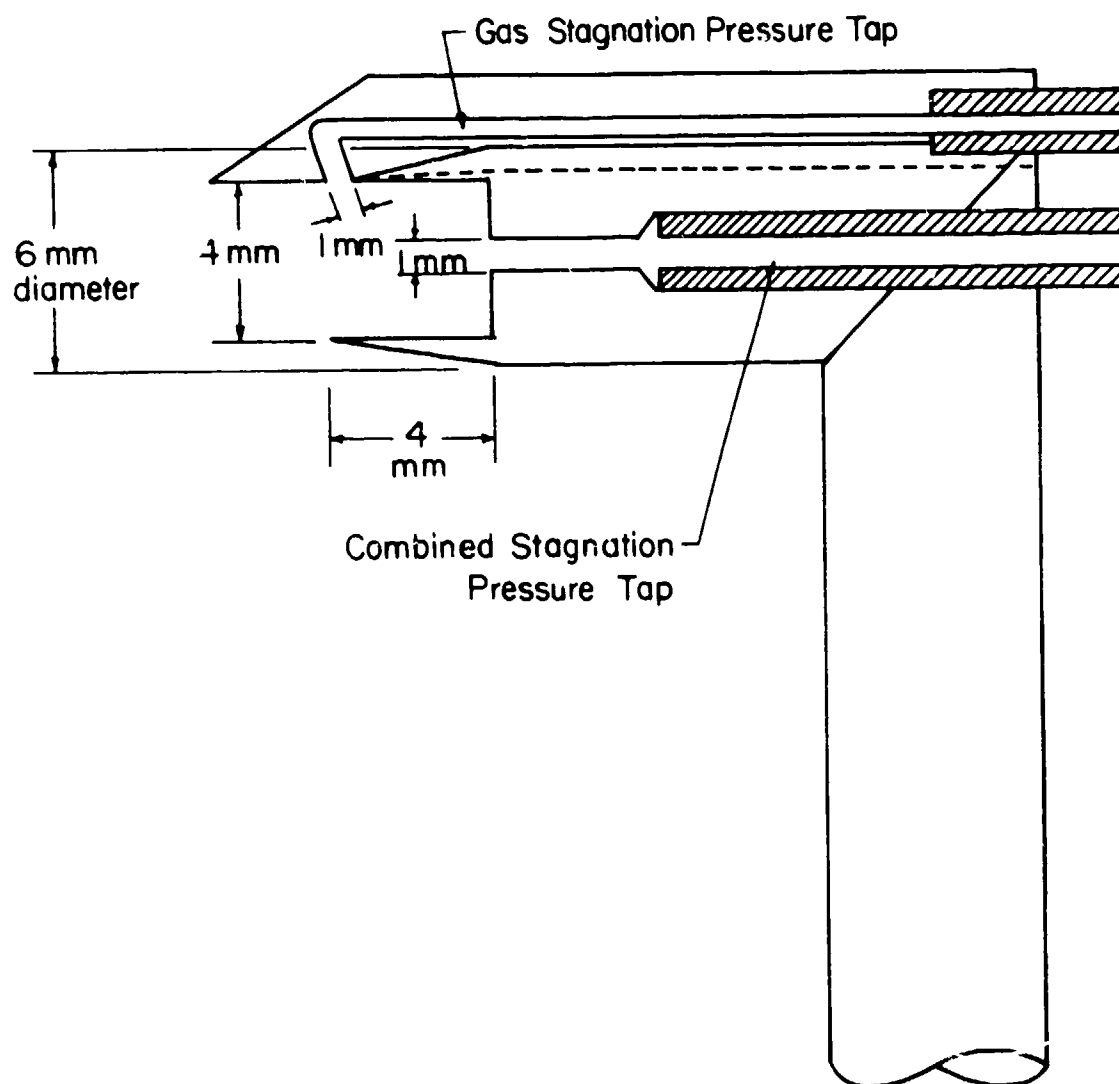
Figure A.7.1 Schematic View of Two Phase Flow Probe Design
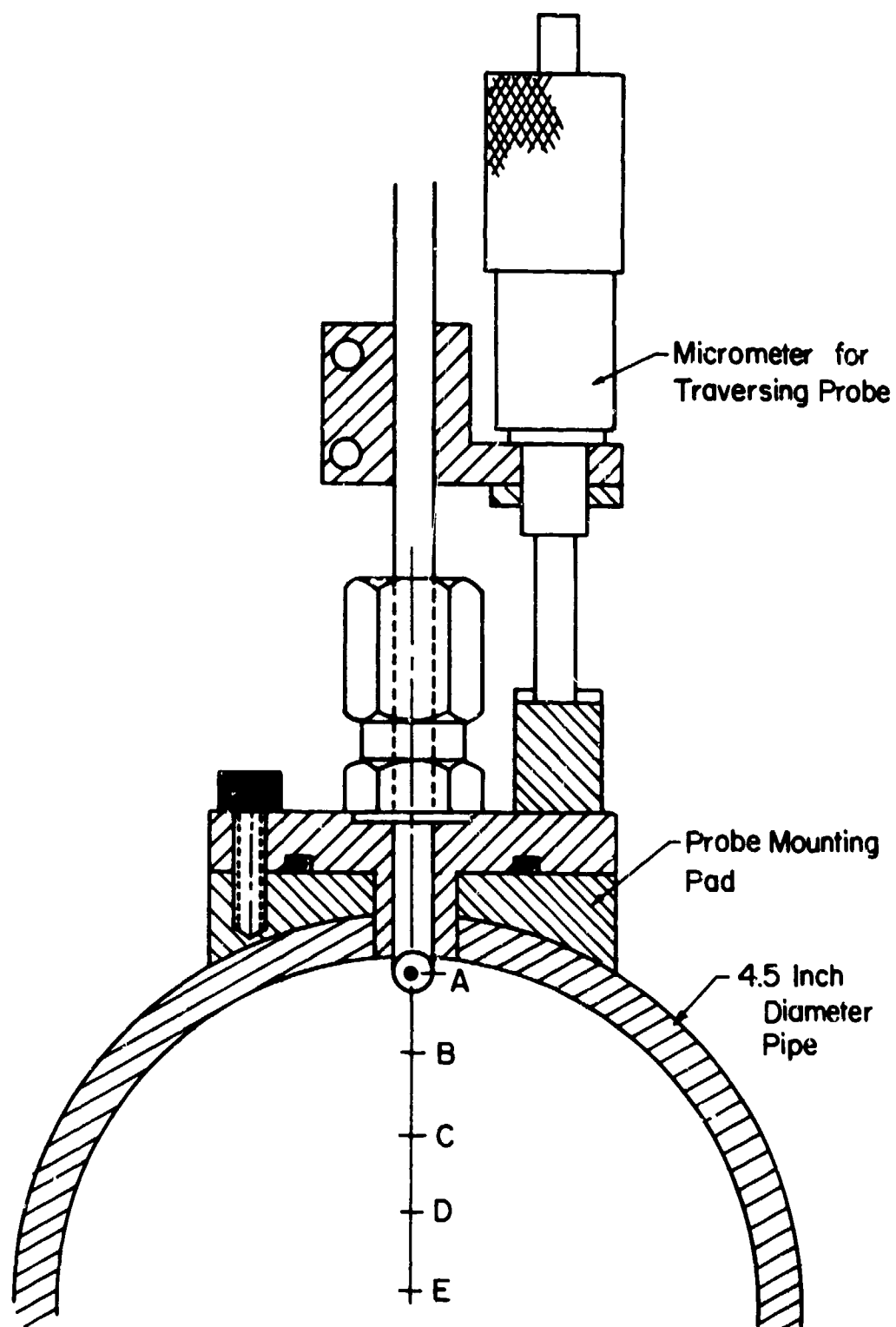
Figure A.7.2   Mounting of Two Phase Flow Probe on Test Compressor

of the mixture (air and water together) and the static pressure from a wall tap on the compressor ducting; and

3) The differential pressure between the wall static pressure and a known reference pressure.

The measured differential pressures from the transducers are recorded on a strip chart recorder.

The general principles based upon which the probe performance can be established are given in References 28-30. Some aspects of the design of the current probe may be found in Reference 31.

2. Scheme for Calibration

The basic principle of operation of the probe is the same as that of any stagnation pressure probe. However, a number of uncertainties arise in the two phase flow probe.

(1) Capture efficiency of the probe in respect of droplets and their momentum: The capture or collection of droplets and the transfer of droplet momentum during stagnation depend upon the droplet trajectories in relation to the gas phase streamlines in the vicinity and inside the mouth of the probe. Figure A.7.3 shows the nature of the flow at entry to the probe. The geometry of the probe mouth (in particular, its diameter) and the external shape of the probe (including the lip geometry) are critical design parameters. Methods of optimization of these parameters need further investigation.

(2) Gas phase pressure change due to the deceleration of droplets: While droplet deceleration and eventual stagnation should, ideally, only increase the stagnation pressure of the liquid phase, some transfer of momentum can occur between the two phase. Thus the gas phase stagnation pressure recorded may have an "over pressure" content. The gas stagnation pressure tap should therefore be placed close to the entry of the probe. A method of optimizing the location of the tap needs further investigation.

(3) Droplet size effects: A general two phase (droplet-laden) flow consists of a distribution of droplet sizes. The droplet motion in a given probe depends upon the distribution as well as on the "density" of droplets. In particular, the flow and therefore the pressure gradient at entry to the probe mouth are affected by the droplet size distribution
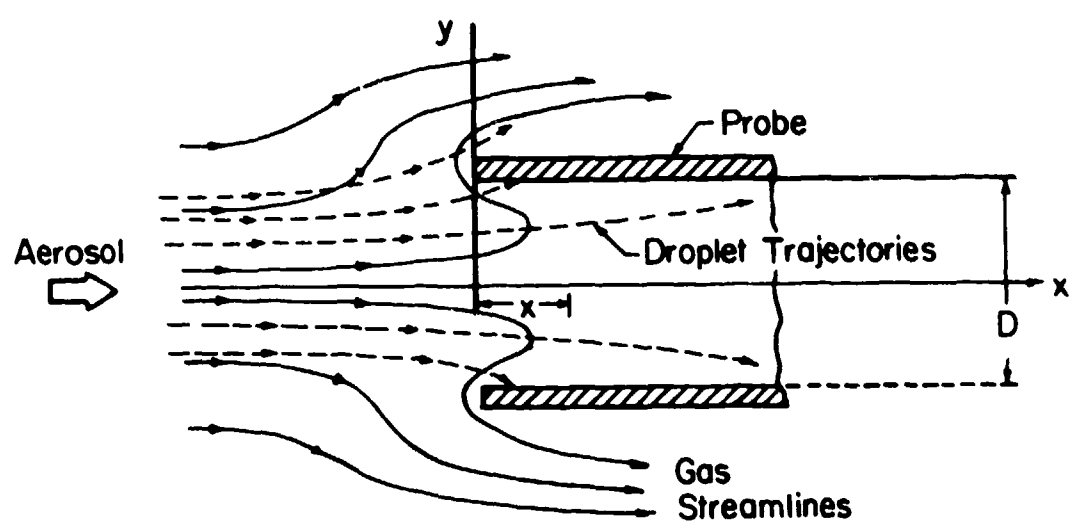
Figure A.7.3 Nature of Flow at Entry to Probe

and water content.

(4) Effects of connecting lines to the pressure taps: The
pressure taps need to be purged and the connecting lines need to be filled
with the appropriate fluids, air in the gas phase line and water in the
liquid phase line. While these can be arranged through appropriate design,
uncertainties exist.

In view of the foregoing, it is felt that it is essential to calibrate
the probe in "known" or reasonable characterized flows. A well-characterized
flow is one which the water content, droplet size, gas phase pressure, and
flow velocities are known at the location (in a duct, say) where the two
phase pressure probe is located.

2.1   The Calibration Rig

A calibration rig was designed and some of the components of the
rig were manufactured.

A schematic drawing of the calibration rig is presented in Figure
A.7.4. It consists basically of the same system as illustrated in Figure 2
with the Test Compressor and its connecting duct replaced by the Test
Duct employed to conduct the pressure probe calibration tests.

The Test Duct is a constant diameter (4.25 in.) duct of length
15.0 in., that has been smooth finished. It has flanges at the ends by
means of which it can be connected to the bell-mouth section on the one
side and to the discharge plenum on the other.

As the Test Duct is connected to the same air supply and water
injection systems as the Test Compressor is during tests on the compressor
the fluid supplied to the Test Duct can be fully characterized.

The Test Duct has provision to locate the pressure probe at the
axis of the duct.

The dynamic pressure of the mixture (air and water) can be calculated
from the foregoing.

$$P_c = 1/2\alpha\rho_g V_g^2 + (1-\alpha)\rho_\ell V_\ell^2$$

$$\dot{m}_\ell = (1-\alpha)\rho_\ell V_\ell A$$

$$\alpha = \frac{\dot{m}_g}{\rho_g V_g A}$$
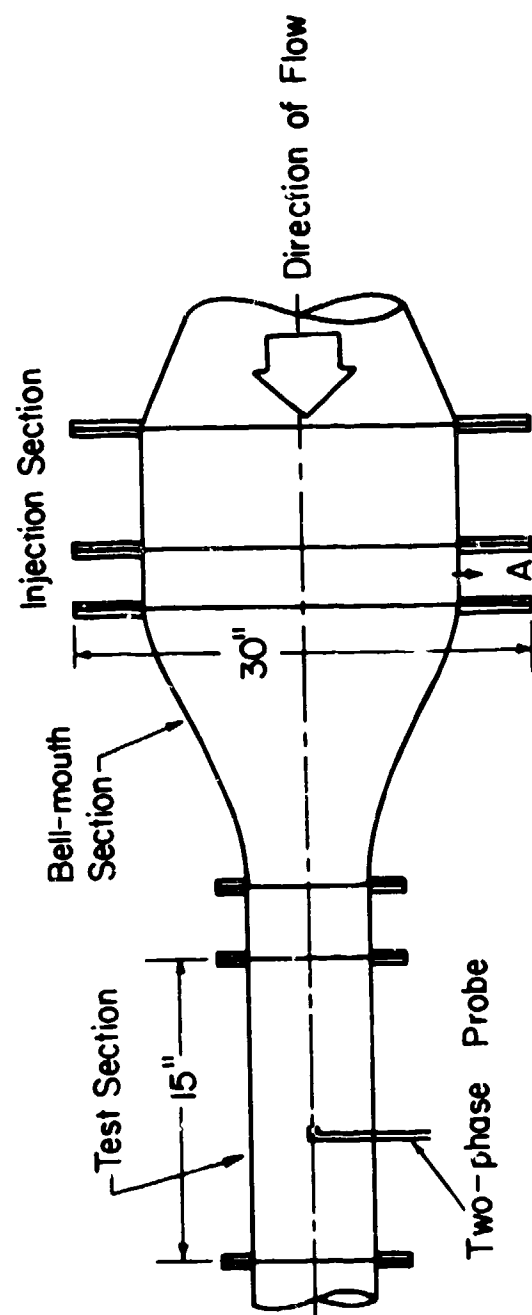
Figure A.7.4   Schematic Drawing of Calibration Rig for Two Phase Flow Probe

In the foregoing, α represents the correction for the nonuniform velocity profile in the duct. The density of the gas phase can be determined from a knowledge of the supply pressure of the gas phase and the temperature of the gas as determined, for example, by the use of a standard aspirated thermocoupie probe.

The measure value of the dynamic pressure is given by the following,

$$\Delta P_{meas} = 1/2 \alpha \rho_g V_g^2 + CV_g \frac{\dot{m}_\ell}{A}$$

where C represents the nondimensional over-pressure ratio given by the relation namely,

$$C = \frac{\Delta P_{meas} - \Delta P_g}{1/2 \rho_g V_g^2 \frac{\dot{m}_\ell}{\dot{m}_g}}$$

The effect of probe mouth diameter on the value of C may be observed in Figure A.7.5 (Reference 28).

$$\frac{P_{meas} - P_0}{\frac{1}{2} \rho_a V_{a\infty}^2 \left(\frac{w_w}{w_a}\right)_\infty}$$
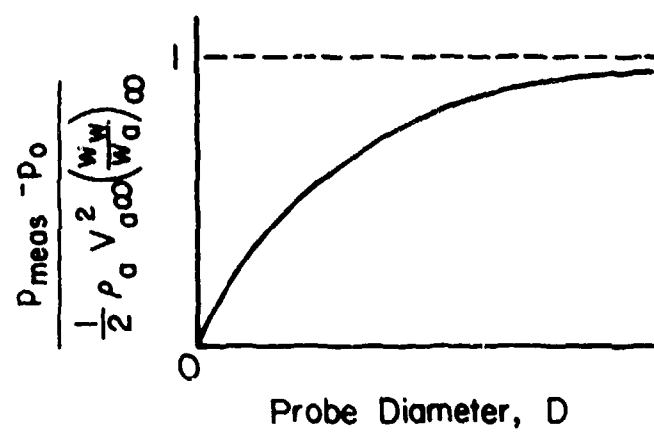
Probe Diameter, D

Figure A.7.5 Effect of Probe Mouth Diameter on the
Valve of Over-Pressure Ratio

APPENDIX 8

CALIBRATION OF THERMOCOUPLES AND TRANSDUCERS;
AND UNCERTAINTY IN PERFORMANCE PARAMETERS

The specifications for the thermocouples and transducers employed during the test were as follows:

1) Pressure at entry to air flow metering nozzle: Gould model PA822-100 thin film strain gauge pressure transducer.

2) Differential pressure across air flow metering nozzle: Gould model PM822 differential pressure transducer.

3) Pressure at entry to methane flow metering nozzles: Gould model PM822-50 thin film strain gauge differential pressure transducer.

4) Static and total pressure at Test Compressor inlet: Gould model PL121TC-10 differential pressure transducer.

5) Static and total pressure at Test Compressor outlet: Gould model PL131TC-50 differential pressure transducer.

6) Ambient barometric pressure: Princo Standard Mercurial Barometer.

7) Laboratory ambient temperature and relative humidity: Edmund Scientific model 61151 Lufft Outdoor Window Weather Station.

8) Temperature at Test Compressor inlet and outlet during air flow and air-methane mixture flow: Omega Type K, model TJ96-CASS-116U-6.

9) Temperature at Test Compressor inlet and outlet during air-water mixture flow:

The thermocouples and the pressure transducers were calibrated according to standard practice at the beginning of each series of tests.

The stagnation pressure probes and the aspirated thermocouples were calibrated by the manufacturer and no additional calibration was carried out as part of the test sequence.

1.   Calibration of Thermocouples

In order to determine the Test Compressor performance, five temperatures at the following locations were measured: the laboratory, air supply station, the compressor inlet section, the compressor outlet section, upstream of air flow metering nozzle and upstream of methane flow metering nozzle. The ambient temperature was read off a standard digital thermomenter. All of the other temperature measurements were obtained utilizing the same type of thermocouple whose output was fed into a recording system. The temperature measurement system has been shown in Figure A.8.1.

Calibration of the system was carried out at two selected conditions: the freezing point of distilled water and the boiling point of distilled water. The calibration scheme consisted in obtaining not less than ten data points at each condition. The calibration was repeated after each series of tests.

2.   Calibration of Transducers

All of the pressures with the exception of the barometric pressure were measured with transducers. The Test Compressor inlet and outlet pressures were measured with a 0-10 psig and a 0-50 psig range pressure transducer respectively. The other two transducers measured the differential pressure at the air measurement flow nozzle and the pressure upstream of the methane measurement flow nozzle.

The pressure measurement system has been shown in Figure A.8.2. Each transducer was calibrated by applying a "known" pressure in five equal incremental steps over the expected range of operation. The "known" pressure was applied by utilizing the shop air supply and a 0-60 psig Heise Gauge connected the outlet of the pressure regulating valve.

3.   Results of Calibration of Thermocouples and Transducers

The output signal from the thermocouples and pressure transducers is linearized by the instrumentation; therefore, the calibration curves were assummed to be straight lines. The calibration data were reduced

Figure A.8.1   TEMPERATURE MEASUREMENT SYSTEM


```
THERMOCOUPLE ---> | THERMOCOUPLE |    | THERMOCOUPLE |    | DIGITAL   |
                  | CHANNEL      |    | SIGNAL       |    | INDICATOR |
                  | CALLER       |    | CONDITIONER  |    |           |
```

Thermocouple - Omega Engineering, Inc.
              part # TJ96-CASS-116U-6

Thermocouple Channel Caller - Daytronic Corporation
                                            model # 9328

Thermocouple Signal Conditioner -
              Daytronic Corp.
              model # 9110

Digital Indicator - Daytronic Corporation
                             model # 9515
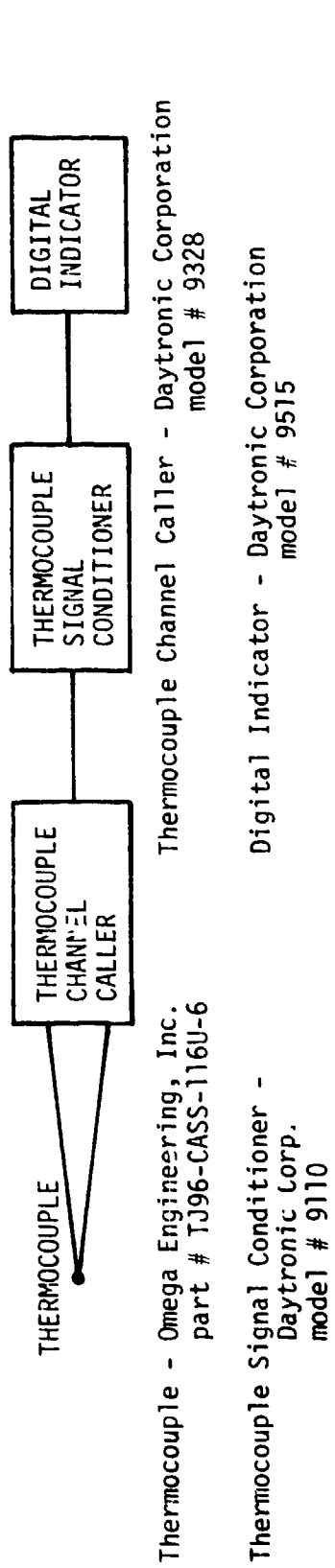
SPECIFICATIONS

Thermocouple types and ranges:
(Specify one when ordering)

Type: Material   Range

K   Chromel-Alumel   -100 to +1260C
K   Chromel-Alumel   -148 to +2300F

Output: standard Five Volt Data Signal
         (see System Handbook)

Accuracy: ±0.1% of scale, ±1 degree

Input Impedance: greater than one megohm

Common Mode Range: ±150 volts

Common Mode Rejection: Less than 1 degree
     error, ±150 volts, DC to 100 Hz

SPECIFICATIONS

Input: standard Five Volt Data Signal

Selectable Scales:

±1500 (by "1's"), with overrange to 1999
±3000 (by "2's"), with overrange to 3998
±7500 (by "5's"), with overrange to 9995
Plus selectable decade multipliers of .0001, .001, .01,
     0.1, 1.0 and 10

Display: seven segment, planar, plasma discharge,
0.375" character height, compatible in color and font
with Model 9530

Sample Rate: five per second

Accuracy: worst case error from combined effects of
non-linearity, internal randomness, line voltage vari-
ation from 105 v to 130 v, ambient temperature vari-
ation of ±30 degree F, and six months drift of zero
and span will not exceed ±0.02% of full scale, ±one
digit

Figure A.3.2 PRESSURE MEASUREMENT SYSTEM
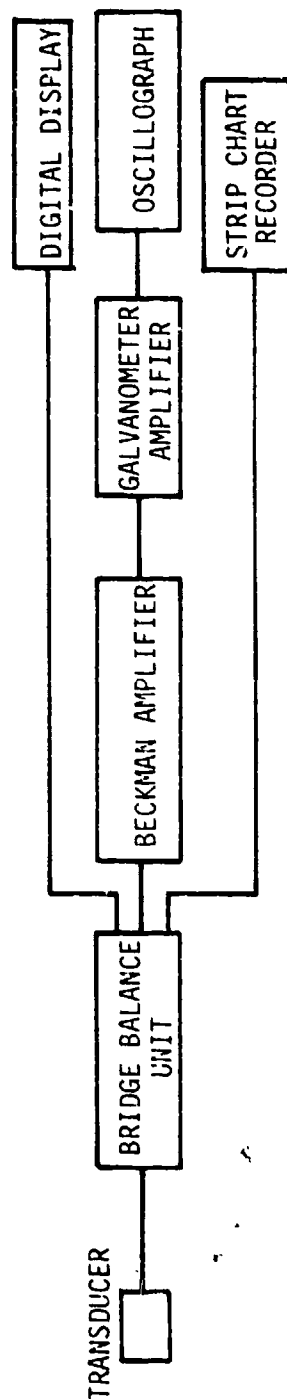
Transducer Systems

1) 0-10 psig, TRANSDUCER-BRIDGE BALANCE UNIT-BECKMAN AMPLIFIER-GALVANOMETER AMPLIFIER-OSCILLOGRAPH

2) 0-50 psig, Same system is used for the 0-10 psig transducer (see 1 above)

3) Air measurement flow nozzle differential pressure, TRANSDUCER-BRIDGE BALANCE UNIT-STRIP CHART RECORDER

4) Methane measurement flow nozzle upstream pressure, TRANSDUCER-BRIDGE BALANCE UNIT-DIGITAL DISPLAY

Bridge Balance Unit - Accudata
    model # 105

Beckman Amplifier - Beckman

Galvanometer Amplifier - Honeywell
    model # T6GA-500

Oscillograph - Honeywell
    model # 1614

Transducers - Gould
    0-10 psig, model PL131TC-10
    0-50 psig, model PL131TC-50
    Δp nozzle, model PM822
    upstream pressure, model PM822-50

Digital Display - Data Tech
    model # 73-100, one digit
    resolution

Strip Chart Recorder - Leeds and Northrup Co.
    model # R-820-1

using the least-squares criterion to obtain an average calibration curve. The least-squares method minimizes the sum of the squares of the vertical differences of the calibration data points from a fitted line, known as the average calibration curve. The bias of each system is removed by the calibration, thus leaving only errors due to imprecision. The imprecision errors, commonly called random errors, are determined to one sigma based upon the least squares method. The equations for reducing the calibration data are as follows:

$$q_o = mq_i + b$$

where q_o: output quantity (dependent variable)

q_i: input quantity (independent variable)

m: slope of line

b: intercept of line on vertical axis

$$m = \frac{N\Sigma q_i q_o - (\Sigma q_i)(\Sigma q_o)}{N\Sigma q_i^2 - (\Sigma q_i)^2}$$

$$b = \frac{(\Sigma q_o)(\Sigma q_i^2) - (\Sigma q_i q_o)(\Sigma q_i)}{N\Sigma q_i^2 - (\Sigma q_i)^2}$$

where N: total number of data points

$$s_{qi}^2 = \frac{1}{N}\sum\left[\left(\frac{q_o - b}{m}\right) - q_i\right]^2$$

where s_{qi} is the random error of the measured quantity.

The random errors or imprecision of various measured quantities have been listed below. The ambient temperature and barometric pressure errors have been based upon specifications supplied by the manufacturer.

Test compressor inlet static pressure, $P_1 \pm 0.04$ psi

Test compressor inlet stagnation pressure, $P_{o1} \pm 0.04$ psi

Test compressor outlet static pressure, $P_2 \pm 0.24$ psi

Test compressor outlet stagnation pressure, $P_{o2} \pm 0.24$ psi

Test compressor inlet temperature, $T_1 \pm 0.55^{\circ}C$

Test compressor outlet temperature, $T_2 \pm 0.55^{\circ}C$

Ambient pressure, $P_{amb} \pm 0.01$ inches of mercury

Ambient temperature, $T_{amb} \pm 0.60^\circ C$

Air flow measurement nozzle differential pressure, $\Delta p \pm 0.04$ psi

Temperature at air flow measurement nozzle, $T_{FN} \pm 0.55^\circ C$

Methane flow measurement nozzle upstream pressure, $P_{met} \pm 0.45$ psi

Temperature at methane flow measurement nozzle, $T_{met} \pm 0.55^\circ C$

4. Uncertainty in Performance Parameters

The uncertainty in performance parameters was calculated utilizing the results of the calibration tests based on the root-sum square formula.

When a quantity N is computed from a set of measured quantities u_1, u_2, u_3,..., one can write as follows:

$$N = f(u_1, u_2, u_3,..., u_n)$$

Since u's are the measured quantities, they are in error by $\pm \Delta u_1$, $\pm \Delta u_2$,..., $\pm \Delta u_n$, respectively. These errors cause an error ΔN in the computed results N. When the Δu's are statistical bounds, such as $\pm 3\sigma$ limits where σ is standard deviation, the method of combining such errors is according to the root-sum square formula as follows:

$$\Delta N = \sqrt{\left[\Delta u_1 \frac{\partial f}{\partial u_1}\right]^2 + \left[\Delta u_2 \frac{\partial f}{\partial u_2}\right]^2 + \dots \left[\Delta u_n \frac{\partial f}{\partial u_n}\right]^2}$$

The overall error ΔN then has the same meaning as the individual errors. That is, if Δu_i represents a $\pm 3\sigma$ limit on u_i, then ΔN represents a $\pm 3\sigma$ limit on N.

Based on the root-sum square formula, the errors in Test Compressor operational parameters were expressed as follows:

1) Corrected Speed: CRPM

$$\frac{\Delta(CRPM)}{CRPM} = \sqrt{\frac{1}{4}\left[\frac{\Delta T_{o1}}{T_{o1}}\right]^2 + \left[\frac{\Delta N}{N}\right]^2}$$

2) Overall Total Pressure Ratio: PR

$$\frac{\Delta(PR)}{PR} = \sqrt{\left[\frac{\Delta P_{o1}}{P_{o1}}\right]^2 + \left[\frac{\Delta P_{o2}}{P_{o2}}\right]^2}$$

3) Overall Total Temperature Ratio: TR

$$\frac{\Delta(TR)}{TR} = \sqrt{\left(\frac{\Delta T_{o1}}{T_{o1}}\right)^2 + \left(\frac{\Delta T_{o2}}{T_{o2}}\right)^2}$$

4) Mass Flow Rate of Air: $\dot{m}_a$

$$\frac{\Delta \dot{m}_a}{\dot{m}_a} = \frac{1}{2}\sqrt{\left(\frac{\Delta P_n}{P_n}\right)^2 + \left(\frac{\Delta(DELP)}{DELP}\right)^2 + \left(\frac{\Delta T_n}{T_n}\right)^2}$$

5) Mass Flow Rate of Methane: $\dot{m}_{CH4}$

$$\frac{\Delta \dot{m}_{CH4}}{\dot{m}_{CH4}} = \sqrt{\left(\frac{\Delta P_{CH4}}{P_{CH4}}\right)^2 + \frac{1}{4}\left(\frac{\Delta T_{CH4}}{T_{CH4}}\right)^2}$$

6) Corrected Mass Flow Rate of Air: CMFR1

$$\frac{\Delta(CMRF1)}{CMFR1} = \sqrt{\left(\frac{\Delta \dot{m}_a}{\dot{m}_a}\right)^2 + \frac{1}{4}\left(\frac{\Delta T_{o1}}{T_{o1}}\right)^2 + \left(\frac{\Delta P_{o1}}{P_{o1}}\right)^2}$$

7) Corrected Mass Flow Rate of Air-Methane Mixture: CMFR2

$$\frac{\Delta(CMFR2)}{CMFR2} = \sqrt{\left(\frac{\Delta \dot{m}_a}{\dot{m}_a}(1-X_{CH4}) + \frac{\Delta \dot{m}_{CH4}}{\dot{m}_{CH4}}X_{CH4}\right)^2 + \frac{1}{4}\left(\frac{\Delta T_{o1}}{T_{o1}}\right)^2 + \left(\frac{\Delta P_{o1}}{P_{o1}}\right)^2}$$

8) Corrected Mass Flow Rate of Air-Water Droplet Mixture: CMFR3

$$\frac{\Delta(CMFR3)}{CMFR3} = \sqrt{\left(\frac{\Delta \dot{m}_a}{\dot{m}_a}(1-X_w) + \frac{\Delta \dot{m}_w}{\dot{m}_w}X_w\right)^2 + \frac{1}{4}\left(\frac{\Delta T_{o1}}{T_{o1}}\right)^2 + \left(\frac{\Delta P_{o1}}{P_{o1}}\right)^2}$$

9) Flow Coefficient: ϕ

$$\frac{\Delta \phi}{\phi} = \sqrt{\left(\frac{\Delta \dot{m}_a}{\dot{m}_a}\right)^2 + \left(\frac{\Delta T_1}{T_1}\right)^2 + \left(\frac{\Delta P_1}{P_1}\right)^2 \left(\frac{\Delta N}{N}\right)^2}$$

where T_{o1} : total temperature at compressor inlet

T_1 : static temperature at compressor inlet

P_{o1} : total pressure at compressor inlet

P_1 : static temperature at compressor inlet

T_{o2} : total temperature at compressor inlet

P_{o2} : total pressure at compressor outlet

P_n : air flow metering nozzle upstream pressure

T_n : air flow metering nozzle upstream temperature

DELP : differential pressure across flow metering nozzle

N : compressor rotational speed

P_{CH4} : methane flow metering nozzle upstream pressure

T_{CH4} : methane flow metering nozzle upstream temperature

$\dot{m}_a$: mass flow rate of air

$\dot{m}_{CH4}$: mass flow rate of methane

$\dot{m}_w$: mass flow rate of water

X_{CH4} : methane content (mass fraction)

X_w : water content (mass fraction)

Based on the root-sum square formula derived earlier and the uncertainty of each measurement, the uncertainty in performance parameters was estimated at each test point. The extent of the uncertainty in various performance parameters, has been given in the following at the design point for illustrative purposes.

1) Corrected Speed: CRPM

$$\frac{\Delta(CRPM)}{CRPM} \sim 3.3 \times 10^{-3}$$

2) Overall Total Pressure Ratio: PR

$$\frac{\Delta(PR)}{PR} \sim 6.1 \times 10^{-3}$$

3) Overall Total Temperature Ratio: TR

$$\frac{\Delta(TR)}{TR} \sim 2.3 \times 10^{-3}$$

4) Mass Flow Rate of Air: $\dot{m}_a$

$$\frac{\Delta \dot{m}_a}{\dot{m}_a} \sim 6.7 \times 10^{-3}$$

5) Mass Flow Rate of Methane: $\dot{m}_{CH4}$

$$\frac{\Delta \dot{m}_{CH4}}{\dot{m}_{CH4}} \sim 9.1 \times 10^{-3}$$

6) Corrected Mass Flow Rate of Air: CMFR1

$$\frac{\Delta(\text{CMFR1})}{\text{CMFR1}} \sim 7.3 \times 10^{-3}$$

7) Corrected Mass Flow Rate of Air-Methane Mixture: CMFR2

$$\frac{\Delta(\text{CMFR2})}{\text{CMFR2}} \sim 7.4 \times 10^{-3}$$

8) Corrected Mass Flow Rate of Air-Water Mixture: CMFR3

$$\frac{\Delta(\text{CMFR3})}{\text{CMFR3}} \sim 7.4 \times 10^{-3}$$

9) Flow Coefficient: ϕ

$$\frac{\Delta\phi}{\phi} \sim 8.1 \times 10^{-3}$$

APPENDIX 9

DETAILS OF THE TEST SERIES

1.   Tests with Air Flow

The tests with air flow were divided into two groups.

(i)   Tests for establishing uniformity or air flow velocity in the bell-mouth and at the entry to the Test Compressor; and

(ii)   Tests for obtaining performance data on the Test Compressor.

1.1   Tests for Establishing Uniformity of Flow into the Test Compressor

The uniformity of flow into the Test Compressor was tested by means of pressure rakes (details of which are provided in Appendix 4 located (a) at entry to the bell-mouth section and (b) in the straight duct located between the bell-mouth and the Test Compressor.

The rakes extended up to the center line of the ducting and consisted of a set of six probes. The rakes were fixed at one circumferential location in the ducting. It was assumed that so long as it was established that the flow was uniform radially at one circumferential location, the flow would be nearly uniform circumferentially; in other words, there would be no rotational component of flow velocity. It may be noted that the pressure probes, according to specification, were insensitive to flow direction to the extent of $\pm 20^{0}$.

1.1.1   Test Procedure

The procedure for conducting these tests was as follows:

(1) The Drive Engine starting procedure and the Test Compressor operation procedure, as described in Appendix 1, were adopted.

(2) The throttle valve was set at the desired point for regulating the air flow through the Test Compressor.

(3) A particular corrected speed of operation of the Test Compressor was chosen, and the corresponding power turbine sneed was determined.

(4) The Test Compressor was operated at the desired corrected speed and throttle setting. The pressure data from the two pressure rakes were recorded after allowing about 2.0 minutes for the operation to become stabilized.

(5) The power turbine speed was slightly changed and readjusted so as to obtain the same corrected speed value for the Test Compressor. The pressure data from the two pressure rakes were recorded. This procedure was repeated six times.

(6) The Test Compressor was operated at the same corrected speed value but with a different throttle setting. The pressure rake data were recorded as described under (4) and (5) above.

(7) The Test Compressor was operated at a total of four corrected speed values (60, 70, 80 and 90 per cent) and at four throttle settings at each value of corrected speed.

In view of the fact that the pressure rake data were found to be uniform within acceptable limits in all cases, no changes were introduced in the flow configuration.

At the end of this series of tests, the pressure rakes were removed from the bell-mouth and the Test Compressor entry duct sections.

1.2.   Test Compressor Tests with Air Flow

The performance of the Test Compressor was obtained with the variables as listed in Table 3.1. The measurements made were as given in Table 3.2.

The test procedure was generally the same as described in Section 1.1 of this Appendix.

It may be pointed out that after every change it was necessary

to allow up to 3.0 minutes before a set of data could be obtained to allow for the stabilization of performance and to account for the time constants associated with temperature sensors.

2.0 Tests with Air-Methane Mixture Flow

The performance of the Test Compressor was obtained with the variables as listed in Table 3.3. The measurements made were as given in Table 3.4.

The test procedure adopted was as follows:

(1) The Drive Engine starting procedure and the Test Compressor operating procedure, as described in Appendix 1, were adopted.

(2) The methane injection procedure, as described in Appendix 5, was adopted.

(3) The throttle valve was set at the desired opening for regulating the air flow through the compressor.

(4) A particular corrected speed of operation of the Test Compressor was chosen, and the corresponding power turbine speed was determined.

(5) The Test Compressor was operated at the desired corrected speed and throttle setting. The desired measurements were carried out after allowing about 3.0 minutes for the performance to become stabilized.

(6) The power turbine speed was changed slightly and readjusted so as to obtain the same corrected speed value for the Test Compressor. The desired measurements were carried out after allowing about 3.0 minutes for the performance to become stabilized.

(7) The value of air mass flow into the compressor during the tests described under (5) and (6) was calculated. The injection rate of methane was calculated in order to obtain the desired air-methane mixture ratio for operation of the Test Compressor. The methane flow rate was metered, as stated in Appendix 5, by means of a choking nozzle. Accordingly, the supply pressure of methane for the desired injection

rate was determined and set in the methane supply line by means of the pressure regulating valve.

(8) The nitrogen purging line was activated. The methane supply valve was opened to supply methane to the injectors. The Test Compressor operated with the air-methane mixture flow.

(9) The desired measurements were carried out on the Test Compressor after allowing about 3.0 minutes to lapse for the Drive Engine and the Test Compressor performance to become stabilized.

It may be pointed out that the throttle valve regulating the flow of gas through the Test Compressor was left at the same position as during the air flow test described under items (5) and (6). However, the air flow into the Test Compressor was determined in each test run by means of measurements made in the air flow metering nozzle. The flow rate of methane was obtained in each test run from the measurements made in the methane flow metering nozzle.

In view of the small amounts of methane and nitrogen introduced during the tests, there was little change in the temperature at the inlet to the Test Compressor compared to the temperature in the immediately preceding air flow test. However, the power turbine speed was adjusted so as to operate the Test Compressor at the same corrected speed as the one at which the preceding air flow test was conducted.

(10) The methane injection was turned off after obtaining all of the data. The nitogen supply line for purging was left open. The Test Compressor thus continued to operate at the same compressor throttle setting but with air flow only. The power turbine speed was adjusted as necessary in order that the Test Compressor corrected speed remained the same. The desired measurements were obtained on the Test Compressor after allowing approximately 3.0 minutes to elapse for the stabilization of the test unit and instrumentation.

It was found in every test that the compressor mass flow and temperature rise became the same during the last part of a test with air

flow (after turning off the methane injection) as during the first part of the test with air flow. In other words, while the methane injection affected the Test Compressor performance, the recovery of the Test Compressor performance on turning off methane injection was invariably complete.

(11) The power turbine speed was changed slightly and then readjusted so as to obtain the same corrected speed value for the Test Compressor. The desired measurements were carried out on the Test Compressor after allowing about 3.0 minutes to lapse for the Drive Engine and the Test Compressor performance to become stabilized. This procedure was repeated six times.

The Drive Engine was usually shut down at the end of a test series as described above, for about 30 minutes in order that the oil, and often the test cell environment, might cool down to an acceptable temperature.

(12) The Test Compressor was operated at the same corrected speed value but with a different setting of the throttle valve employed to regulate the compressor flow. The desired measurements were carried out following the same procedure as described under items (5) through (11).

(13) The Test Compressor was operated at a total of four values of corrected speed (60, 70, 80 and 90 per cent design speed), at four throttle settings at each value of corrected speed, and at two different rates of methane injection (2.0 and 4.0 per cent by weight of air flow) at each speed and throttle setting. In each case, the performance of the Test Compressor was established with (a) air flow, (b) air-methane mixture flow and (c) methane turned off and hence, again, with air flow only.

3.   Tests with Air-Water Droplet Mixture Flow

The performance of the Test Compressor was obtained with the variables as listed in Table 3.5. The measurements made were as given in Table 3.6.

The test procedure adopted was as follows:

(1) The Drive Engine starting procedure and the Test Compressor operating procedure, as described in Appendix 1, were adopted.

(2) The water injection procedure, as described in Appendix 6, was adopted.

(3) The throttle valve was set at the desired opening for regulating the air flow through the compressor.

(4) A particular corrected speed of operation of the Test Compressor was chosen, and the corresponding power turbine speed was determined.

(5) Tests with air flow.

(6) Tests with air-water mixture flow.

(7) The value of air mass flow into the compressor during the tests described under (5) and (6) was calculated. The injection rate of water was calculated in order to obtain the desired air-water droplet mixture ratio for operation of the Test Compressor. The water flow rate was measured as stated in Appendix 6, by means of a flow meter. The water flow lines were activated so as to supply water to the injectors.

(8) The desired measurements were carried out on the Test Compressor after allowing about 4.0 minutes to lapse for the test unit and the instrumentation to become stabilized.

It may be pointed out that, while the Test Compressor throttle was left in the same position as during the preceding air flow test, the air flow and the injected water flow were measured during each test run by means of the air metering nozzle and the water flow meter, respectively.

When water was injected into the air stream entering the Test Compressor, there occurred a substantial change in all parts of the Test

Compressor exit flow ducting, including the air flow controlling throttle valve. In addition, when the amount of water injected was large, some of the water would flow right through the throttle valve and the Test Compressor exhaust ducting. Thus, adequate time had to be provided during each test for the throttle valve and ducting temperature to become stabilized and thus for the air flow metering nozzle pressure drop to become stabilized.

It may be recalled that a drain was provided in the bell-mouth in order to collect any water that may impact the bell-mouth wall and thus not enter the Test Compressor. This drain was opened after each test in order to determine the quantity of water collected in the bell-mouth. The amount of water that entered the Test Compressor was assumed to be the difference between the amount of water injected and the amount drained out of the bell-mouth.

Two drains for water were also provided, as described earlier, one at the exit of the Test Compressor and another further downstream in the air turning section (Figure 14). These drains were connected to a water collection tank which was suitably pressurized (with a connection to the Test Compressor exhaust ducting). The water collection tank was drained at the end of each water injection test to examine if any water had become collected.

Finally, during water injection there was invariably a drop in the compressor inlet temperature. This necessitated a resetting of the power turbine speed in order to operate the Test Compressor at the same corrected speed. The power turbine speed was adjusted accordingly.

(9) The power turbine speed was then altered slightly and then readjusted so as to obtain the same corrected speed value for the Test Compressor. The desired measurements were carried out on the Test Compressor after allowing about 3.0 minutes to elapse for the test unit and the instrumentation to become stabilized. This procedure was repeated six times.

(10) The water injection was then turned off. The engine con-
tinued to operate with air flow at the same compressor throttle setting
as originally. The power turbine speed was adjusted once again to ob-
tain the same corrected speed for the Test Compressor. The desired
measurements were carried out on the Test Compressor after allowing
about 3.0 minutes to elapse for the stabilization of the test unit and
the instrumentation.

It was necessary to allow adequate time for the temperature of
the throttle valve and exhaust ducting of the Test Compressor to become
stabilized, and thereby for the measurements on the air flow metering
nozzle to become stabilized.

(11) The Test Compressor was operated at the same corrected
speed value but with a different setting of the throttle valve employed
to regulate the compressor flow. The desired measurements were carried
out following the same procedure as described under items (5) through
(10).

(12) The Test Compressor was operated at two values of
corrected speed (80 and 90 per cent of design speed), at four throttle
settings at each value of corrected speed and at two rates of water
injection (2.0 and 4.0 per cent by weight of air flow) with two types of
droplets (generally small and generally large) at each speed and throttle
setting. In each case the performance of the Test Compressor was es-
tablished with (a) air flow, (b) air-water droplet mixture flow and (c)
water injection turned off and hence, again, with air flow only.

LIST OF REFERENCES

1. Willenborg, J.A., et al., "F-111 Engine Water Ingestion Review," F-111 System Program Office, Wright-Patterson Air Force Base, Dayton, Ohio, October 31-November 10, 1972.

2. Useller, J.W., et al., "Effect of Heavy Rainfall on Turbojet Aircraft Operation," Aeronautical Engineering Review, February, 1955.

3. MacGregor, C.A. and Bremer, R.J., "An Analytical Investigation of Water Ingestion in the B-1 Inlet," Rockwell International, NA-73-181, June 1973.

4. (a) "Concorde Complete Flooded Runway Tests," Aviation Week and Space Technology, p. 22, October 4, 1971.

    (b) "Board Assays Crash of DC-9 in Storm," Ibid, pp. 63-67, July 24, 1978.

    (c) "Storm Traced in Southern DC-9 Crash," Ibid, pp. 59-61, July 31, 1978.

    (d) "Damage Assessed in Southern Crash," Ibid, pp. 59-63, August 7, 1978.

    (e) "Thrust Loss Cited in Southern Accident," Ibid, pp. 55-58, August 21, 1978.

    (f) "Board Urges Improved Thunderstorm Reporting," Ibid, pp. 63-64, August 28, 1978.

5. Papadaes, B.S. and Taylor, D.W., "A Review of Sea Loiter Aircraft Technology," AIAA Paper No. 76-876, September, 1976.

6. Pfeifer, G.D. and Maier, G.P., "Engineering Summary of Powerplant Icing Technical Data," Federal Aviation Administration Report No. FAA-RD-77-76, July, 1977.

7. Danielson, K. and Huggins, A.W., "Raindrop Size Distribution Measurement of High Elevation Continental Cumuli," Conference on Cloud Physics, pp. 305-310, October, 1974.

8. Fowler, M.G., et al., "Cloud Droplet Measurements in Cumuliform and Stratiform Clouds," Ibid, pp. 296-299, October, 1974.

9. Kissel, G.J., "Rain and Hail Extremes at Altitude," AIAA Paper No. 79-0539, February, 1979.

10. Hearsey, R.M., "A Revised Computer Program for Axial Compressor Design," Wright-Patterson Air Force Base Aerospace Research Laboratories, ARL TR 75-0001, Volume I and II.

11. (a) Murthy, S.N.B., et al., "Water Ingestion Into Axial Flow Compressors," Report No. AFAPL-TR-76-77, Air Force Systems Command, Wright-Patterson Air Force Base, August, 1976.

    (b) Murthy, S.N.B., et al., "Analysis of Water Ingestion Effects in Axial Flow Compressors," Report No. AFAPL-TR-78-35, Air Force Systems Command, Wright-Patterson Air Force Base, June, 1978.

12. Grant, G. and Tabakoff, W., "Erosion Prediction in Turbomachinery Resulting from Environmental Solid Particles," Jr. of Aircraft, Volume 12, No. 5, pp. 471-478, May, 1975.

13. Tabakoff, W., et al., "Effect of Solid Particles on Turbine Performance," Transaction of the ASME, Jr. of Engineering for Power, pp. 47-52, January, 1976.

14. Marble, F.E., "Nozzle Contours for Minimum Particle-Lag Loss," AIAA Journal, Volume 1, No. 12, pp. 2793-2801, December, 1963.

15. Korkan, K.D., et al., "Particle Concentrations in High Mach Number Two-Phase Flows," AIAA Paper No. 74-606, July, 1974.

16. Hoffman, J.D., "An Analysis of the Effects of Gas-Particle Mixtures on the Performance of Rocket Nozzles," Ph.D. Thesis, Purdue University, January, 1963.

17. Moore, M.J. and Sieverding, C.H., Two Phase Steam Flow in Turbines and Separators, McGraw-Hill, New York, 1976.

18. Gardner, G.O., "Events Leading to Turbine Blade Erosion," Proc. Inst. Mech. Eng., Vol. 178, Pt. 1, No. 23, pp. 593-624, 1964.

19. Keller, H., Erosionskorrosion on Heissdampfturbinen VGB Kraftwekstechnik, 1974, Heft 5.

20. Diagnostics and Engine Condition Monitoring, AGARD-CP-165, June, 1975.

21. "Distortion Induced Engine Instability," Advisory Group for Aerospace Research and Development, Lecture Series, AGARD-LS-72, December, 1974.

22. Tsuchiya, T. and Murthy, S.N.B., "Effect of Water on Axial Flow Compressors," Part I; Analysis and Predictions, Technical Report AFWAL-TR-80-2090, Air Force Systems Command, Wright-Patterson Air Force Base, October, 1980.

23. Tsuchiya, T. and Murthy, S.N.B., "Effect of Water on Axial Flow Compressors," Part II: Computer Program, Technical Report AFWAL-TR-80-2090, Air Force Systems Command, Wright-Patterson Air Force Base, December, 1980.

24. Tsuchiya, T., "Water Ingestion into Jet Engine Axial Flow Compressors," Ph.D. dissertation at Purdue University, December, 1981.

25. Hearsey, R.M., "A Revised Computer Program for Axial Compressor Design," Wright-Patterson Air Force Base, Aerospace Research Laboratories, Technical Report ARL-TR-75-0001, Volume I and II, January, 1975.

26. Thwaites, B., "The Design of Contractions for Wind Tunnels," (British) Aeronautical Research Council Reports and Memorandum No. 2278, March, 1946.

27. ASME Power Test Codes, Supplement on Instruments and Apparatus, Part 5, Measurement of Quantity of Materials, Chapter 4, Flow Measurement by Means of Thin Plate Orifices, Flow Nozzles and Venturi Tubes, The American Society of Mechanical Engineers, New York, 1959.

28. Anderson, G.H. and Mantzouranis, B.G.,"Two-Phase (Gas/Liquid) Flow Phenomena II, Liquid Entrainment," Chemical Engineering Science, 12, 9 (1960).

29. Crane, R.I. and Moore, M.J., "Interpretation of Pitot Pressure in Compressible Two-Phase Flow," Journal of Mechanical Engineering Engineering Science, 14, 2 (1972), pp. 128-133.

30. Dussourd, J.L. and Shapiro, A.H., "A Deceleration Probe for Measuring Stagnation Pressure and Velocity of a Particle-Laden Gas Stream," Jet Propulsion, 28, 24 (January, 1958).

31. Fincke, J.R. and Deason, V.A., "The Measurements of Phase Velocities in Mist Flows Using Stagnation Probes," NUREG/CR-0648 TREE-1350, (March, 1979).